

INVESTIGATION OF ASPHALT ADDITIVES

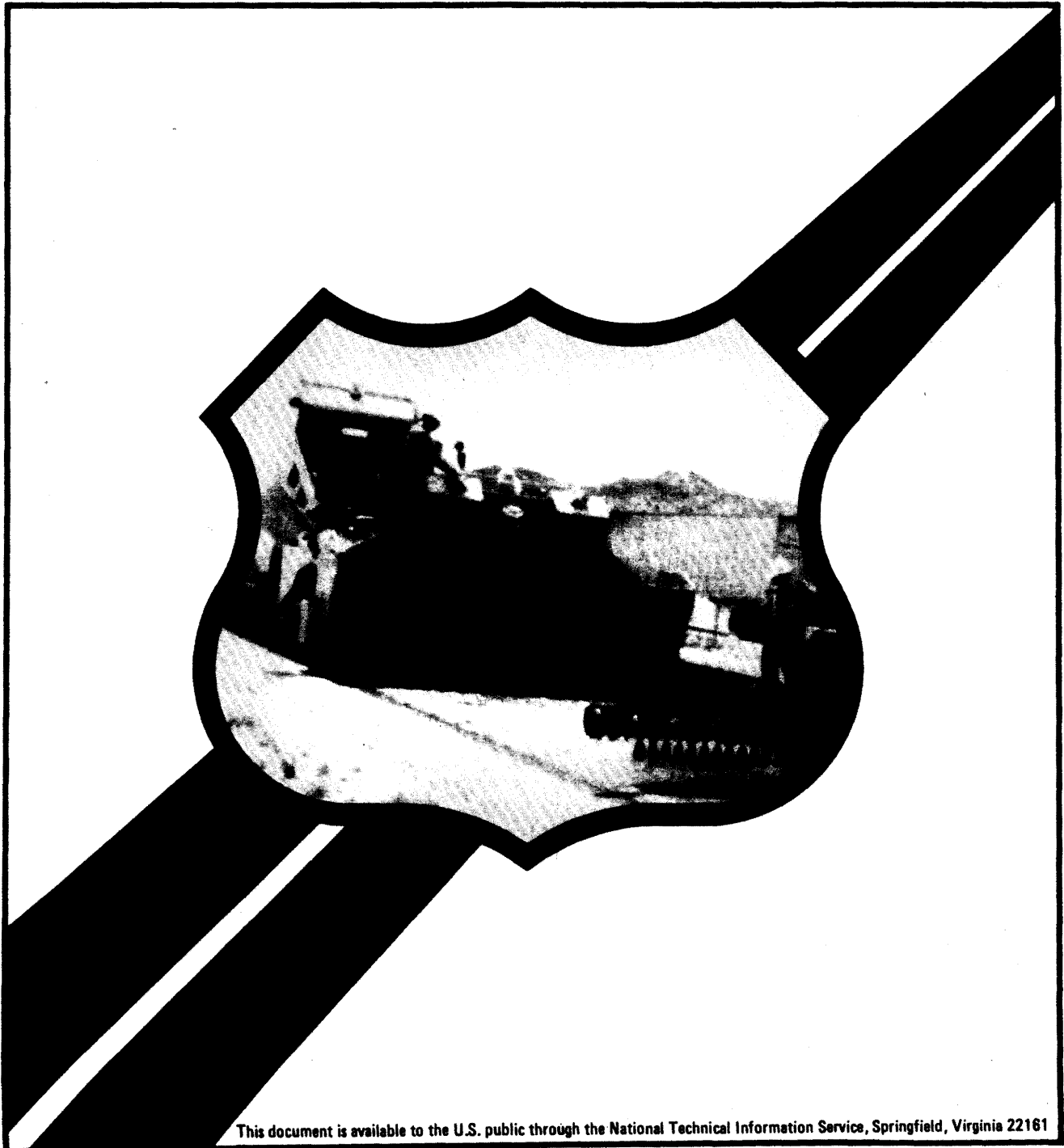
Research, Development,
and Technology
Turner-Fairbank Highway
Research Center
6300 Georgetown Pike
McLean, Virginia 22101-2296

Report No.
FHWA/RD-87/001



U.S. Department
of Transportation
**Federal Highway
Administration**

Final Report
October 1987



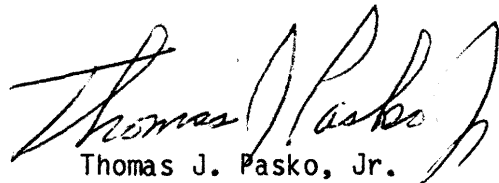
This document is available to the U.S. public through the National Technical Information Service, Springfield, Virginia 22161

FOREWORD

This report presents the findings of a research study to evaluate asphalt additives, or modifiers, used to reduce rutting or cracking in asphalt concrete pavements. Five additive types were chosen and tested in the laboratory using the most current testing procedures and analyses. Both standard and nonstandard sophisticated tests, such as fatigue, creep, and permanent deformation of mixtures, were performed. This study was initiated in order to investigate the degree to which modifiers can affect binder and mixture properties, and as a first step toward the development of better test procedures for evaluating modifiers in general.

This report will be of interest to individuals concerned with the design and quality of asphalt concrete mixtures and with the use of asphalt modifiers to improve performance.

Sufficient copies of the report are being distributed by FHWA Bulletin to provide one copy to each FHWA regional office and division office and two copies to each State highway agency. Direct distribution is being made to the division offices. Additional copies for the public are available from the National Technical Information Service (NTIS), U.S. Department of Commerce, 5285 Port Royal Road, Springfield, Virginia 22161.



Thomas J. Pasko, Jr.
Director, Office of Engineering
and Highway Operations Research
and Development

NOTICE

This document is disseminated under the sponsorship of the Department of Transportation in the interest of information exchange. The United States Government assumes no liability for its contents or use thereof.

The contents of this report reflect the views of the authors, who are responsible for the facts and accuracy of the data presented herein. The contents do not necessarily reflect the official policy of the Department of Transportation. This report does not constitute a standard, specification, or regulation.

The United States Government does not endorse products or manufacturers. Trademarks or manufacturers' names appear herein only because they are considered essential to the object of this document.

1. Report No. FHWA/RD-87/001		2. Government Accession No.		3. Recipient's Catalog No.	
4. Title and Subtitle INVESTIGATION OF ASPHALT ADDITIVES				5. Report Date October 1987	
				6. Performing Organization Code RF 7017	
7. Author(s) D. N. Little, J. W. Button, R. M. White, E. K. Ensley, Y. Kim, S. J. Ahmed				8. Performing Organization Report No. RF 7017-1F	
9. Performing Organization Name and Address Texas Transportation Institute Texas A&M University College Station, Texas 77843				10. Work Unit No. (TRAIS) FCP34C5-014	
				11. Contract or Grant No. DTFH-61-84-C-00066	
12. Sponsoring Agency Name and Address Office of Engineering and Highway Operations R&D Federal Highway Administration 6300 Georgetown Pike McLean, Virginia 22101-2296				13. Type of Report and Period Covered Final Report August 1984-November 1986	
				14. Sponsoring Agency Code	
15. Supplementary Notes FHWA Contract Manager (COTR): Kevin D. Stuart (HNR-20)					
16. Abstract The overall objectives of this research were to (1) identify through laboratory testing, the most promising types of additives or admixtures for reducing rutting and cracking in hot-mixed asphalt pavements, (2) develop guidelines showing how the additives can be incorporated into actual pavements and (3) develop procedures for evaluating additives. Additives selected for evaluation included latex, block copolymer rubber, ethylene vinylacetate, polyethylene, and carbon black. The additives were combined with asphalt cements from two sources with widely differing chemical composition and rheological properties. Asphalts two grades softer than that normally used in hot-mixed asphalt concrete were used with the additives. Binder tests included penetration at two temperatures, viscosity at various temperatures and by various methods, softening point, flash point, specific gravity, rolling thin film oven test, ductility, heat stability, infrared analysis before and after artificial aging, nuclear magnetic resonance, viscoelastic analysis, stress relaxation, and Rostler-Sternberg and Corbett analyses. Energies of interaction between selected asphalts and additives were measured using a microcalorimeter. Paving mixture tests included Hveem and Marshall stabilities, resilient modulus vs. temperature, indirect tension vs. temperature and loading rate, resistance to moisture damage, flexural fatigue, creep/permanent deformation, fracture resistance and fracture healing. The mixture test results were used with the VESYS IV structural subsystem to predict the effects of the additives on pavement performance, cracking, rutting, and roughness. All additives demonstrated the ability to substantially alter the temperature susceptibility of asphalt concrete mixtures.					
17. Key Words Asphalt, asphalt concrete, pavement, asphalt additives, rutting, cracking, fracture mechanics, VESYS			18. Distribution Statement No restrictions. This document is available to the public through the National Technical Information Service, Springfield, Virginia 22161.		
19. Security Classif. (of this report) Unclassified		20. Security Classif. (of this page) Unclassified		21. No. of Pages 330	22. Price

METRIC (SI*) CONVERSION FACTORS

APPROXIMATE CONVERSIONS TO SI UNITS

Symbol	When You Know	Multiply By	To Find	Symbol
LENGTH				
in	inches	2.54	millimetres	mm
ft	feet	0.3048	metres	m
yd	yards	0.914	metres	m
mi	miles	1.61	kilometres	km

Symbol	When You Know	Multiply By	To Find	Symbol
AREA				
in ²	square inches	645.2	millimetres squared	mm ²
ft ²	square feet	0.0929	metres squared	m ²
yd ²	square yards	0.836	metres squared	m ²
mi ²	square miles	2.59	kilometres squared	km ²
ac	acres	0.395	hectares	ha

Symbol	When You Know	Multiply By	To Find	Symbol
MASS (weight)				
oz	ounces	28.35	grams	g
lb	pounds	0.454	kilograms	kg
T	short tons (2000 lb)	0.907	megagrams	Mg

Symbol	When You Know	Multiply By	To Find	Symbol
VOLUME				
fl oz	fluid ounces	29.57	millilitres	mL
gal	gallons	3.785	litres	L
ft ³	cubic feet	0.0328	metres cubed	m ³
yd ³	cubic yards	0.0765	metres cubed	m ³

NOTE: Volumes greater than 1000 L shall be shown in m³.

°F	Fahrenheit temperature	5/9 (after subtracting 32)	Celsius temperature	°C
TEMPERATURE (exact)				

APPROXIMATE CONVERSIONS TO SI UNITS

Symbol	When You Know	Multiply By	To Find	Symbol
LENGTH				
mm	millimetres	0.039	inches	in
m	metres	3.28	feet	ft
m	metres	1.09	yards	yd
km	kilometres	0.621	miles	mi

Symbol	When You Know	Multiply By	To Find	Symbol
AREA				
mm ²	millimetres squared	0.0016	square inches	in ²
m ²	metres squared	10.764	square feet	ft ²
km ²	kilometres squared	0.39	square miles	mi ²
ha	hectares (10 000 m ²)	2.53	acres	ac

Symbol	When You Know	Multiply By	To Find	Symbol
MASS (weight)				
g	grams	0.0353	ounces	oz
kg	kilograms	2.205	pounds	lb
Mg	megagrams (1 000 kg)	1.103	short tons	T

Symbol	When You Know	Multiply By	To Find	Symbol
VOLUME				
mL	millilitres	0.034	fluid ounces	fl oz
L	litres	0.264	gallons	gal
m ³	metres cubed	35.315	cubic feet	ft ³
m ³	metres cubed	1.308	cubic yards	yd ³

°C	Celsius temperature	9/5 (then add 32)	Fahrenheit temperature	°F
TEMPERATURE (exact)				
-40	-40	32	32	32
0	0	40	40	40
32	32	98.6	98.6	98.6
100	100	212	212	212

These factors conform to the requirement of FHWA Order 5190.1A.

* SI is the symbol for the International System of Measurements

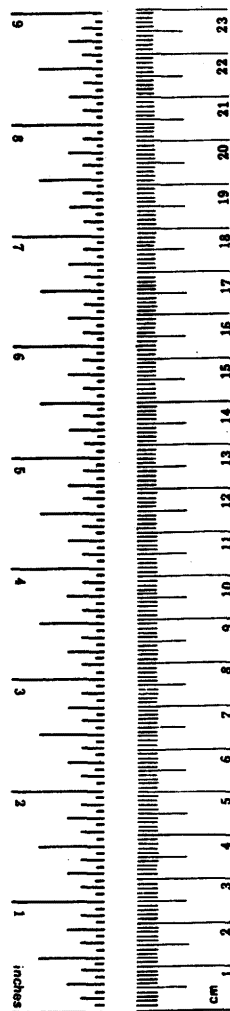


TABLE OF CONTENTS

Section	Page
CHAPTER I - SUMMARY	1
CHAPTER II - INTRODUCTION	6
CHAPTER III - RHEOLOGICAL AND CHEMICAL EVALUATION OF ASPHALT-ADDITIVE BLENDS	9
SELECTION OF ADDITIVES	9
SELECTION OF ASPHALTS	10
BLENDS OF ASPHALTS AND ADDITIVES.	13
1. Asphalt Carbon Black Blends	13
2. Dispersion of SBR in Asphalts	17
3. Dispersion of SBS/SB Copolymers in Asphalts	21
4. Dispersion of Polyethylene in Asphalts	23
5. Dispersion of EVA in Asphalts	26
MISCELLANEOUS TESTING ON SELECTED ADDITIVE-ASPHALT BLENDS	30
1. Flash Point Testing	30
2. Ductility Testing	33
3. Rolling Thin Film Oven Aging	33
4. Sliding Plate Viscosity at 77 F	35
5. Summary of Traditional Tests on Other Modified Binders	35
6. Low Temperature Fracture Susceptibility	35
7. Heat Stability Study	41
CHANGES IN COMPOSITION WITH AGING - AN INFRARED STUDY	41
1. Procedures for Analysis by Infrared Spectroscopy.	41
2. Thin Film Accelerated Aging Test.	43
3. Infrared Analysis of Neat Asphalts.	44
4. Infrared Analysis of Asphalts Modified with Carbon Black.	47
5. Infrared Analysis of Asphalts Modified with EVA	49
6. Infrared Analysis of Asphalts Modified with Polyethylene.	51
7. Infrared Analysis of Asphalts Modified with SBR	52
8. Infrared Analysis of Asphalts Modified with SBS	55
NUCLEAR MAGNETIC RESONANCE (NMR) OF ORIGINAL ASPHALTS	58
ENERGIES OF INTERACTIONS BETWEEN ASPHALTS AND MODIFIERS	58
VISCOELASTIC PROPERTIES OF UNAGED AND AGED BINDERS.	62
1. Introduction to Viscoelasticity	62
2. Viscosity and Elasticity Temperature Susceptibilities	63
3. Viscoelastic Measurements	64
4. Effects of Additives on Viscosities at Four Temperatures.	65

TABLE OF CONTENTS (continued)

Section	Page
5. Influence of Aging on Viscosity	67
6. Viscosity Temperature Susceptibilities of Aged and Unaged Asphalts	68
7. Elastic Component of Aged and Unaged Asphalts at Four Temperatures.	71
8. Influence of Aging on Elastic Components.	74
STRESS RELAXATION OF ASPHALTS WITH ADDITIVES.	79
1. Basis for Test.	79
2. Discussion of Relaxation Results.	83
SUMMARY	83
CHAPTER IV: EVALUATION OF ASPHALT CONCRETE MIXTURES CONTAINING ADDITIVES	85
MIXTURE DESIGN.	85
PREPARATION OF SPECIMENS FOR MIXTURE TESTING.	86
MARSHALL STABILITY.	88
HVEEM STABILITY	88
RESILIENT MODULUS	90
INDIRECT TENSION.	93
MOISTURE RESISTANCE	104
EXTRACTION AND RECOVERY WITH ADDITIVES.	109
1. Extraction of Asphalt Concrete Containing Carbon Black.	109
2. Extraction of Asphalt Concrete Containing SBR	112
3. Extraction of Asphalt Concrete Containing Polyethylene.	113
4. Extraction of Asphalt Concrete Containing EVA and SBS	113
EVALUATION OF FATIGUE CRACKING POTENTIAL.	114
1. Approach.	114
2. Sample Fabrication.	115

TABLE OF CONTENTS (continued)

Section	Page
CONTROLLED STRESS FLEXURAL FATIGUE.	118
1. Experiment Design	118
2. Results of Testing.	118
3. Effects of Accelerated Aging on Controlled Stress Flexural Fatigue.	123
4. General Discussion of Flexural Fatigue Results.	127
CONTROLLED DISPLACEMENT FATIGUE TESTING	128
1. General	128
2. Sample Fabrication.	131
3. Experiment Design	131
4. Results of Testing.	131
5. Discussion of Results	143
HEALING STUDY	144
1. Background.	144
2. Purpose of Healing Study.	147
3. Healing Evaluation Procedure.	147
DEFORMATION CHARACTERISTICS	150
1. General	150
2. Experimental Design	150
3. Fabrication of Specimens.	152
4. Creep Compliance Testing.	154
5. VESYS Deformation Parameters.	156
6. Measuring ALPHA and GNU	159
7. Results	160
EVALUATION OF THERMAL CRACKING POTENTIAL.	186
1. Approach.	186
2. Thermal Fatigue Analysis.	186
3. Thermal Cracking Analysis Based on Mixture Properties	187
4. Discussion of Thermal Cracking Analysis	189
MODULUS PROPERTIES OF ASPHALT MIXTURES MODIFIED WITH ADDITIVES.	192
1. General	192
2. Resilient Modulus	195
3. Creep Stiffness	195
4. Dynamic Modulus	196
5. Flexural Modulus.	196
6. Discussion of Results of Modulus Testing.	196

TABLE OF CONTENTS (continued)

Section	Page
CHAPTER V: STRUCTURAL EVALUATION	201
GENERAL	201
VESYS ANALYSIS.	201
TRAFFIC	202
SYSTEM GEOMETRY	202
ENVIRONMENT	205
MATERIAL CHARACTERIZATION	207
SYSTEM PERFORMANCE BOUNDS	207
VESYS STRUCTURAL SYSTEM	207
RESULTS OF VESYS ANALYSIS	208
AASHTO STRUCTURAL COEFFICIENTS.	215
THICKNESS EQUIVALENCY FACTORS	222
1. General	222
2. Determination of Thickness Equivalencies Based on Stiffness	222
MECHANO-LATTICE ANALYSIS.	226
1. General	226
2. Material Characterization	227
3. Pavement Simulation	227
4. Mechano-Lattice Results	228
CHAPTER VI - EVALUATION AND IMPLEMENTATION OF RESULTS	231
MIXTURE DESIGN AND CHARACTERIZATION	231
1. General	231
2. Suggested Mixture Design/Evaluation Approach.	233
METHODS OF ADDITION	237
MIXING AND COMPACTION TEMPERATURES.	238
SPECIAL REQUIREMENTS ASSOCIATED WITH ADDITIVES.	238

TABLE OF CONTENTS (continued)

Section	Page
APPROXIMATE COSTS FOR ADDITIVES	239
CHAPTER VII - CONCLUSIONS AND RECOMMENDATIONS	241
CONCLUSIONS	241
RECOMMENDATIONS	244
REFERENCES.	246
APPENDIX A: Penetration-Viscosity Data and Photomicrographs for Asphalt-Additive Blends.	251
APPENDIX B: Relation Between Viscosity and Cohesive Energy Density.	268
APPENDIX C: Elasticity Temperature Susceptibility.	270
APPENDIX D: Miscellaneous Mixture Material Properties.	271
APPENDIX E: Background Information on Fracture and Fatigue	275
APPENDIX F: Deformation Parameters	296
APPENDIX G: Resilient Modulus Data	310

LIST OF TABLES

Table		Page
1	Properties of asphalts	11
2	Component composition of asphalts.	12
3	Blends of carbon black with Texaco asphalts.	15
4	Blends of carbon black with San Joaquin Valley asphalts.	16
5	Blends of SBR (as latex) with asphalt.	18
6	Blends of SBR (as latex) with AC-5 and AR-1000 asphalts	20
7	Blends of asphalts with thermoplastic block polymers (Kraton).	22
8	Dispersions of polyethylenes in Texaco AC-10 asphalt . . .	25
9	Replicate dispersions of a low-density polyethylene in asphalts.	27
10	Dispersions of polyethylene in asphalts	28
11	Dispersion of ethylene-vinyl acetate copolymers in AC-10 and AR-2000 asphalts	29
12	Blends of ethylene-vinyl acetate copolymers in AC-5 and AR-1000 asphalts.	31
13	Flash point and ductility of asphalts and selected blends with additives	32
14	Change in properties of asphalts and selected blends exposed to rolling thin film oven aging	34
15	Viscosity data at 275, 140 and 77°F for selected asphalts and asphalt-additive blends	36
16	Summary of properties of control crumb rubber and sulfur-extended asphalt blends	37
17	Summary of predicted cracking temperatures for selected asphalt-additive blends	39

LIST OF TABLES (continued)

Table		Page
18	Summary of data from Texaco AC-5 and selected additive blends before and after heat stability testing.	42
19	Composition and aging characteristics of neat asphalts as determined by infrared functional group analysis . . .	45
20	Composition and aging characteristics of asphalts containing carbon black as determined by infrared functional group analysis	48
21	Composition and aging characteristics of asphalts containing ethylene-vinyl acetate polymer as determined by infrared functional group analysis.	50
22	Composition and aging characteristics of asphalts containing polyethylene as determined by infrared functional group analysis	53
23	Composition and aging characteristics of asphalts containing styrene-butadiene as determined by infrared functional group analysis	54
24	Composition and aging characteristics of asphalts containing styrene-butadiene-styrene thermoplastic block copolymer	57
25	^1H and ^{13}C aromaticity values and n-alkane carbon chainlength for asphalt samples	59
26	Solvent effects on the hydrogen and carbon aromaticity values.	59
27	Heats of interaction between additives and asphalt ¹ . . .	61
28	Viscosities of unaged and aged asphalts, with and without additives	66
29	Viscosity temperature susceptibilities, E, of unaged and aged asphalts	70
30	Viscosity temperature susceptibilities, S, from log η vs. $^{\circ}\text{C}^*$	70
31	Elastic contribution to flow in unaged binders	72
32	Elastic contribution to flow in aged binders	73

LIST OF TABLES (continued)

Table	Page
33 Elastic component temperature susceptibilities of aged and unaged binders	78
34 Viscoelastic data on unaged asphalts at 25°C.	80
35 Viscoelastic data on unaged asphalts at 0°C	81
36 Viscoelastic data on unaged asphalts at -20°C	82
37 Viscoelastic data on aged asphalts at 25°C.	82
38 Resilient modulus and stability of mixtures containing Texaco asphalt and river gravel.	89
39 Resilient modulus and stability of mixtures containing California Valley asphalt and river gravel.	89
40 Tensile properties at 77°F of mixtures made using Texaco asphalt and river gravel	94
41 Tensile properties at 33°F of mixtures made using Texaco asphalt and river gravel	95
42 Tensile properties at -10 or -18°F of mixtures made using Texaco asphalt and river gravel.	96
43 Tensile properties and resilient modulus of mixtures (California Valley asphalt and river gravel)	97
44a Properties of mixtures before and after exposure to moisture (Texaco asphalt and river gravel)	105
44b Properties of mixtures after exposure to moisture (San Joaquin Valley asphalt and river gravel)	106
45 Extraction of asphalt concrete specimens containing Texaco asphalts.	110
46 Extraction of asphalt concrete specimens containing San Joaquin Valley asphalts.	111
47 Adjusted mixing and compaction temperatures for different binders	117

LIST OF TABLES (continued)

Table		Page
48	Summary of K_1 and K_2 values for beam fatigue testing at 34°F and 68°F (normal curing)	120
49	Summary of fatigue parameters K_1 and K_2 computed from unaged and aged (accelerated aging at 140°F) samples	125
50	Factorial test matrix for controlled displacement fatigue testing	132
51	Summary of controlled displacement fatigue results at 77°F	133
52	Summary of controlled displacement fatigue results at 33°F	134
53	Percents by weight additives and binders used in fabrication of cylinders	153
54	Mixing and molding temperatures	153
55	Relative resistance to permanent deformation at long term load durations	179
56	Summary of VESYS permanent deformation parameters: ALPHA and GNU.	183
57	Time-temperature shift factors (BETA) selected for VESYS analysis.	185
58	Summary of average dynamic moduli, creep stiffness (0.1 sec) and resilient moduli from all mixtures fabricated with Texaco asphalt.	197
59	Summary of resilient moduli and creep stiffnesses (0.1 sec - 1000 sec) for all mixtures fabricated with California Valley asphalt	199
60	Summary of pavement geometrics established by FPS-BISTRO for VESYS pavement evaluation.	204
61	Average monthly air temperatures for the cool and warm climates used in the structural analysis	206

LIST OF TABLES (continued)

Table	Page
62 Pavement performance summary from VESYS IV analysis for 8-inch full-depth asphalt concrete pavements over moderate strength subgrade in both cool and warm climates	209
63 Pavement performance summary from VESYS IV analysis for 10-inch full-depth asphalt concrete pavements over moderate strength subgrade in both cool and warm climates	210

LIST OF TABLES (continued)

Table	Page
F5 Average permanent strain from the incremental static compression test at 70°F. All tests at 20 psi applied stress except for latex. Results of only one test are shown for latex at 10 psi applied stress.	300
F6 Average permanent strain from the incremental static compression test at 100°F. All tests at 10 psi applied stress except for latex, which was tested at 5 psi. Results of only one test each for AC-20 and carbon black are shown	301
F7 Average permanent strain from the incremental static test at 70°F after specimens were subjected to one cycle Lottman moisture conditioning. All tests at 20 psi applied stress.	302
F8 Average permanent strain from the incremental static test at 70°F after specimens were heat aged at 140°F for 7 days. All tests at 20 psi.	303
F9 Average permanent strain from the incremental static test at 70°F (California Valley asphalt).	304
F10 Average accumulated strain for repeated load tests at 70°F (California Valley asphalt).	305
F11 GNU μ values for hot climate VESYS analysis	306
F12 Alpha values for hot climate VESYS analysis	307
F13 GNU μ values for cool climate VESYS analysis.	308
F14 Alpha values for cold climate VESYS analysis.	309

LIST OF FIGURES

Figure		Page
1	Plots of log viscosity as a function of K° and $1/K^\circ \times 10^3$ for Texaco AC-5 asphalt (unaged)	69
2	Temperature susceptibility curve of elastic component of AC-5 asphalt, unaged, with and without additives	75
3	Temperature susceptibility curve of elastic component for unaged AR-1000 asphalt, with and without additives	76
4	Test program to evaluate asphalt concrete mixtures.	87
5	Resilient modulus as a function of temperature for river gravel mixtures containing Texaco asphalts with and without additives.	91
6	Resilient modulus as a function of temperature for mixtures containing San Joaquin Valley asphalts with and without additives.	92
7	Tensile strength as a function of temperature for displacement rate of 0.02 in/min for Texaco asphalt mixtures.	98
8	Tensile strength as a function of temperature for displacement rate of 0.2 in/min for Texaco asphalt mixtures.	99
9	Tensile strength as a function of temperature for displacement rate of 2 in/min for Texaco asphalt mixtures.	100
10	Tensile strain at failure as a function of temperature for a displacement rate of 0.02 in/min for Texaco asphalt mixtures	101
11	Tensile strain at failure as a function of temperature for a displacement rate of 0.2 in/min for Texaco asphalt mixtures	102
12	Tensile strain at failure as a function of temperature for a displacement rate of 2 in/min for Texaco asphalt mixtures	103
13	Tensile strength ratios for mixtures.	107

LIST OF FIGURES (continued)

Figure		Page
14	Test matrix for flexural beam fatigue testing °C = (°F-32)/1.8.	119
15	Controlled stress flexural beam fatigue results at 68°F (20°C).	121
16	Controlled stress flexural beam fatigue results at 32°F (0°C)	122
17	Controlled stress flexural fatigue results at 68°F (20°C) following 7-day aging at 140°F (60°C).	126
18	Log-log plot of crack speed versus J-integral at 77°F (25°C) for Texaco asphalts.	135
19	Log-log plot of crack speed versus J-integral at 77°F (25°C) for California Valley asphalts	136
20	Log-log plot of crack speed versus J-integral at 33°F (1°C) for Texaco asphalts	137
21	Log-log plot of crack speed versus J-integral at 33°F (1°C) for California Valley asphalts.	138
22	Log A* from J* analysis vs. Log A ^K from K analysis. . . .	140
23	n* from J* analysis vs. n ^K from K analysis	141
24	Comparison of crack growth rates at crack lengths of 1 in (25.4 mm) and 2 in (50.8 mm) from J* analysis and K analysis.	142
25	Illustration of the hypothesized laboratory to field shift process	146
26	Effects of additives on healing energy.	149
27	Factorial design of deformation experiments	151
28a	The principle of the creep test procedure	155
28b	Qualitative diagram of the stress and total deformation during the creep test	155
29	Creep compliance curves at 70°F (21°C) for mixtures containing Texaco asphalts	161

LIST OF FIGURES (continued)

Figure		Page
30	Creep compliance curves at 40°F (4°C) and 100°F (38°C) for mixtures containing Texaco asphalts.	162
31	Creep compliance curves at 70°F (21°C) after Lottman moisture conditioning for mixtures containing Texaco asphalt	163
32	Creep compliance curves at 70°F (21°C) after 7 days at 140°F (60°C) for mixtures containing Texaco asphalt.	164
33	Creep compliance data at 70°F (21°C) for mixtures using California Valley asphalts	167
34	Permanent strain from incremental static loading tests at 40°F (4°C) and 70°F (21°C) for mixtures using Texaco asphalts	169
35	Permanent strain from incremental static loading tests at 100°F (38°C) for mixtures using Texaco asphalts.	170
36	Permanent strain from incremental static loading tests at 70°F (21°C) after 7 days at 140°F (60°C) (all tests at 20 psi) for mixtures using Texaco asphalts.	171
37	Permanent strain from incremental static loading tests at 70°F (21°C) after one-cycle Lottman for mixtures using Texaco asphalts	172
38	Accumulated strain versus cycles at 100°F (38°C) for additive modified Texaco AC-5	173
39	Accumulated strain versus incremental loading time at 70°F (21°C) for additive modified California Valley AR-1000	174
40	Accumulated strain versus loading cycles at 70°F (21°C) for additive modified California Valley Ak-1000.	175
41	Comparison of creep compliance of mixtures containing 4.5 and 5.0 percent of blends of latex and AC-5	180
42	Comparison of incremental loading derived permanent deformation plots for mixtures containing AC-5 and latex (5% binder versus 4.5% binder).	181

LIST OF FIGURES (continued)

Figure		Page
43	Induced stresses for modified Texaco asphalt mixtures. . .	190
44	Induced stresses for modified California Valley asphalt mixtures	191
45	Simplified illustration of components of stiffness: elastic, viscoelastic, and viscous	194
A1	Blends of Texaco AC-5 and Microfil 8	251
A2	Blends of San Joaquin Valley AR-1000 and Microfil 8. . . .	252
A3	Penetration and viscosity versus temperature for Texaco AC-5, and dispersions of SBR latex	253
A4	Penetration and viscosity versus temperature for San Joaquin Valley AR-1000, and dispersions of SBR latex . . .	254
A5	Penetration and viscosity versus temperature for Texaco AC-5, and solutions of S-B-S thermoplastic rubber.	255
A6	Penetration and viscosity versus temperature for San Joaquin Valley AR-1000, and solutions of S-B-S thermoplastic rubber	256
A7	Penetration and viscosity versus temperature for Texaco AC-5, and dispersion containing 5% LDPE 526	257
A8	Penetration and viscosity versus temperature for San Joaquin Valley AR-1000, and dispersion containing 5% LDPE 526.	258
A9	Penetration and viscosity versus temperature for Texaco AC-5, and blends with EVA resin EX042	259
A10	Penetration and viscosity versus temperature for San Joaquin Valley AR-1000, and blends with EVA resin EX042.	260
A11	Penetration and viscosity versus temperature for Texaco AC-5, and blends with EVA resin ELVAX 150	261
A12	Penetration and viscosity versus temperature for San Joaquin Valley AR-1000, and blends with EVA resin ELVAX 150.	262

LIST OF FIGURES (continued)

Figure	Page
A13 Photomicrographs of Serial No. 49 laboratory dispersion of 5% Dow low-density polyethylene 526 (density 0.919, Melt Index 1.0) in Texaco AC-10 asphalt. One scale division = 10 μ m or 0.0004 in	263
A14 Photomicrographs of Serial No. 50 laboratory dispersion of 5% Dow low-density polyethylene 527 (density 0.921, Melt Index 2.9) in Texaco AC-10 asphalt. One scale division = 10 μ m or 0.0004 in	264
A15 Photomicrographs of Serial No. 51 laboratory dispersion of 5% Dow high-density polyethylene 69065P (density 0.961, Melt Index 0.60) in Texaco AC-10 asphalt. One scale division = 10 μ m or 0.0004 in	265
A16 Photomicrographs of Serial No. 52 laboratory dispersion of 5% Dow linear-low-density polyethylene 2045 (density 0.920, Melt Index 1.0) in Texaco AC-10 asphalt. One scale division = 10 μ m or 0.0004 in	266
A17 Photomicrographs of Serial No. 53 laboratory dispersion of 5% Dow high-molecular-weight-low-density polyethylene 880 (density 0.932, Melt Index 0.45, contains 2.6% carbon black) in Texaco AC-10 asphalt. One scale division = 10 μ m or 0.0004 in.	267
D1 Design gradation specification limits for pea gravel aggregate	274
E1 Schematic of overlay tester	281
E2 Displacement response in overlay tester recorded on X-Y plotter	281
E3 da/dN versus J*, general trend for a controlled displacement test	282
E4 Crack length, a, versus displacement cycle number, N, for brittle and ductile mixtures.	282



CHAPTER I

SUMMARY

The overall objectives of this research were to (1) identify through laboratory testing, the most promising types of additives or admixtures for reducing rutting and cracking in hot-mixed asphalt pavements, (2) develop guidelines showing how the additives can be incorporated into actual pavements and (3) develop procedures for evaluating additives. This work was accomplished for the Federal Highway Administration by the prime contractor, the Texas Transportation Institute and the subcontractors, Matrecon, Inc. and the Western Research Institute.

The additives selected for evaluation in the experimental program included:

1. Latex (styrene-butadiene rubber)
2. Block Copolymer Rubber (styrene-butadiene-styrene)
3. Ethylene Vinylacetate
4. Polyethylene - finely dispersed
5. Carbon Black

Based on current prices, these additives will add about 5 to 10 dollars to the cost of a ton of hot mixed asphalt concrete. The additives were combined with asphalt cements from two sources with widely differing chemical composition and rheological properties. Preliminary testing showed that incorporation of these additives into asphalt had little effect on penetration at 39°F (4°C) but significantly increased viscosity at 140°F (60°C) thus producing a binder with lower temperature susceptibility. Using this rheological information, asphalt cements two grades softer (AC-5 and AR-1000) than that normally used in hot mixed asphalt concrete (HMAC) and additive dosages were selected such that when the additive was incorporated into the asphalt cement, the resulting binder exhibited a viscosity at 140°F (60°C) near 2,000 poise and a penetration at 39°F (4°C) essentially the same as the unmodified asphalt.

Physical binder tests included penetration at two temperatures, viscosity at various temperatures and by various methods, softening point, flash point, specific gravity, rolling thin film oven test, thin film accelerated aging, ductility, heat stability, viscoelastic analysis and stress relaxation. Component analysis of the original asphalts was determined using the Rostler-Sternberg and Corbett analysis techniques. Chemical characterization included infrared analysis before and after artificial aging and nuclear magnetic resonance. Energies of interaction between selected asphalts and additives were measured using a microcalorimeter.

Paving mixtures were tested in the laboratory using primarily a river gravel and sand aggregate with the modified binders. This material produced a relatively binder-sensitive mixture which was designed to be realistic but yet reveal subtle differences in the modified and unmodified asphalts. Limited tests were performed using mixtures made from crushed limestone to address possible differences in mixture properties associated with high stability mixtures. Mixture tests included:

- Hveem Stability.

- Marshall Stability.

- Resilient Modulus at 5 temperatures.

- Indirect Tension at 3 temperatures and 3 loading rates.

- Resistance to Moisture Damage.

- Extraction and Recovery of asphalts.

- Flexural Fatigue at 2 temperatures.

- Creep/Permanent Deformation at 3 temperatures.

- Fracture Resistance at 2 temperatures.

- Fracture Healing.

The mixture test results were used with the VESYS IV structural subsystem to predict the effects of the additives on pavement performance, cracking, rutting and roughness. AASHTO structural layer coefficients and pavement thickness equivalencies were estimated for the modified mixtures. Fracture mechanics theory was applied to selected

mixture test data to compute resistance to crack propagation and crack healing capacity imparted by the additives.

Conclusions from the study are summarized below:

1. Traditional mixture design procedures, such as the Marshall, Hveem and Texas methods are acceptable for determining target binder contents for asphalt mixtures.
2. Each additive studied demonstrated the ability to substantially alter the temperature susceptibility of asphalt concrete mixtures. The degree of alteration is highly dependent upon the chemical composition of the asphalt cement.
3. The ability of additives to alter the mechanical properties of asphalt concrete is reflected in the predicted performance of the pavement systems which incorporate modified asphalt concrete layers. Although each additive tested showed a potential to reduce temperature susceptibility of the base asphalt, no additive appeared to be a panacea. The task of selecting the best additive for a specific combination of climatic, pavement structure and traffic condition is formidable.
4. Although certain binder and mixture properties appeared to be sensitive to compatibility between the asphalt and the additives, overall, the mixture properties demonstrated an ability for each additive to alter temperature susceptibility in a generally favorable manner.
5. Flexural fatigue response at 68°F (20°C) of mixtures containing AC-5 plus an additive was superior to the control mixture which contained AC-20 with no additive. Accelerated aging of test specimens containing additives resulted in a significant decrease in fatigue life; the control specimens, however, exhibited better fatigue properties after aging.
6. Controlled displacement fatigue testing at 34°F (1°C) demonstrated that mixtures containing AC-5 plus an additive gave better resistance to crack propagation than control mixtures containing AC-20. The "solubilized" additives, EVA, SBR and SBS, showed evidence of improving the distribution of tensile stresses within the mixture. Practically, this could result in retarding crack propagation as manifested by resistance to cracking in asphalt concrete overlays.

7. In a limited study of crack healing, the mixtures containing the soft asphalt (AC-5) plus an additive gave better responses than those containing the control asphalt (AC-20). The practical significance of improved healing potential could be substantially improved flexural fatigue lives of asphalt concrete pavements.

8. Creep/permanent deformation testing showed that, at high temperatures, all the additives except latex produced equal or better performance than the AC-20 control mixture. (The binder content of the latex mixture was apparently in excess of the true optimum.) At low temperature, all the additives in AC-5 except polyethylene produced equal or better performance than the AC-20 control mixture.

9. Indirect tension test results showed that, at the lower temperatures and higher loading rates, the additives increased mixture tensile strength over that of the control mixtures. Elongation to failure was generally increased by the additives. This is indicative of improved resistance to traffic induced cracking at low temperatures. At the higher temperatures and lower loading rates, the additives did not appreciably affect the mixture tensile properties as measured by the indirect tension test.

10. The additives increased Marshall stability of mixtures when added to AC-5 (or AR-1000) but not up to that of mixtures containing AC-20 (or AR-4000) with no additive. This should not discourage the use of these additives with asphalts softer than the usual paving grade, particularly if low temperature cracking is a concern.

11. Hveem stability of mixtures was not significantly altered by the additives. Although Hveem stability is quite sensitive to changes in binder quantity, it is not very sensitive to changes in rheological properties of the binder properties.

12. At low temperatures (less than 32°F or 0°C), the additives had little effect on consistency of the asphalt cements. This was reflected in the diametral resilient moduli (stiffness) of the mixtures. Resilient moduli of AC-5 (or AR-1000) mixtures above 60°F (16°C) were generally increased by the additives but not up to that of the AC-20 (or AR-4000) mixtures without additives. Although the load spreading ability of

asphalt concrete containing a soft asphalt is increased when these additives are employed, the pavement thickness should not be reduced.

13. The additives had little effect on moisture susceptibility of the mixtures made using the materials included in this study.

14. Standard asphalt extraction methods to determine binder content of paving mixtures are unsuitable when polymers or carbon black are used as these materials are insoluble or only partly soluble in standard solvents.

15. Long term aging characteristics of modified binders are substantially different, physically as well as chemically, from the unmodified asphalts. Short term aging characteristics, as measured by standard tests, do not manifest an appreciable difference.

16. The five additives studied were selected because of their potential to reduce rutting and cracking. Each additive proved to be successful to some degree in improving properties on at least one end of the performance spectrum. The need for an additive selection procedure based on traffic conditions, pavement structure and traffic conditions is again emphasized. To rank the additives according to relative capabilities is a difficult task as sensitivity to the base asphalt played a significant role. In general, the most effective additives in reducing rutting were EVA, polyethylene and SBS (Kraton) for the Texaco (AC-5) asphalt. For the California Valley asphalt carbon black, polyethylene, and EVA performed most effectively and without significant difference. In terms of reduction of flexural fatigue cracking the most successful additives were, in order, EVA, SBS (Kraton) and SBR (latex) and polyethylene which demonstrated essentially equal performance.

CHAPTER II

INTRODUCTION

Highway engineering is a field which requires the judicious use of materials manufactured by nature. Naturally occurring soils serve as the foundation for highway pavements. Some serve faithfully and well. Others cause problems at every opportunity. Nature's products are used in pavement bases and asphalt mixtures, often with relatively minor refinements. Many of these products are remarkably well suited to meet our needs. It is the duty and responsibility of paving engineers to optimize the use of these materials to the maximum benefit of the taxpayers and the driving public. A host of man-made products are now available which can be used to improve the rheological and/or adhesive properties of nature's own asphalt cement. The laboratory evaluation of five of these asphalt additives is the subject of this report.

Initially, all known asphalt additives were considered for inclusion in the study. Funding and time constraints permitted testing of only five additives. The interest lay primarily in products that would, immediately, upon addition to asphalt concrete, alter the mechanical properties. Materials marketed as purely anti-stripping or antioxidant additives were, therefore, eliminated from the study. Synthetic fibers, sulfur and hydrated lime were also eventually eliminated. The products finally selected for evaluation in the study include:

1. Latex (emulsified styrene-butadiene-rubber),
2. Block Copolymer Rubber (styrene-butadiene-styrene),
3. Ethylene Vinylacetate,
4. Finely dispersed Polyethylene, and
5. Carbon Black

These decisions were made by the prime contractor, Texas Transportation Institute, the subcontractors, Matrecon, Inc. and Western Research Institute and sponsor, the Federal Highway Administration.

The objectives of this research study were to (1) identify, through laboratory testing, the most promising types of additives or admixtures

for reducing rutting and cracking in hot-mixed asphalt pavements, (2) develop guidelines showing how the additives can be incorporated into actual pavements and (3) develop procedures for evaluating additive performance.

In this study, an asphalt cement additive is defined as a material which would normally be added to/or mixed with the asphalt before mix production, or during mix production, to improve the properties and/or performance of the resulting binder and/or mix.

Design of the perfect asphalt additive is a difficult (impossible) task. An additive that will increase mixture stability or reduce rutting will most likely decrease mixture flexibility or increase the probability of cracking. An additive capable of lowering the temperature susceptibility of the binder or, more importantly, the mixture, may be expected to control both rutting and cracking. In addition, the perfect additive should also control age hardening and moisture susceptibility of paving mixtures and be compatible with all asphalts.

The research consisted of a systematic identification of promising types of asphalt additives designed to reduce plastic deformation (rutting, shoving, corrugations) and cracking (thermal, fatigue, reflective) in asphalt concrete pavements. Asphalt cements with and without additives were tested in the laboratory to determine chemical, rheological, elastic, fracture and thermal properties as well as sensitivity to heat and oxidation and compatibility between asphalts and additives. Asphalt concrete mixtures were tested to determine stability, compactibility and water susceptibility as well as stiffness, tensile, fatigue and creep/permanent deformation properties as functions of temperature. State-of-the-art analytical techniques were used in predicting the ability of the additives to reduce pavement distress and prolong pavement service life. Procedures were developed which can be utilized to implement the results of this research on actual paving projects.

Chapter III presents findings of laboratory experiments on the binders; whereas, Chapter IV gives results of laboratory tests on binder-aggregate mixtures. Forecasts, using these data with mathematical

models and other analytical techniques to predict the mechanical effects of the additives on hot-mixed asphalt concrete and determine their influence on pavement service life, are given in Chapter V. Methods for implementation of the findings in paving applications are discussed in Chapter VI. Detailed data and technical discussions of theory and analytical techniques are given in the Appendices.

Findings from this study clearly show that, to date, no asphalt additive is a panacea. However, for certain conditions of traffic, pavement substrate, asphalt paving materials and climate, the data indicate that certain carefully selected and properly applied asphalt additives have the potential to provide cost-effective extensions to pavement service life.

CHAPTER III

RHEOLOGICAL AND CHEMICAL EVALUATION OF ASPHALT-ADDITIVE BLENDS

SELECTION OF ADDITIVES

Five types of additives which appear likely to improve resistance to rutting and cracking were selected for study. The five types were:

1. Carbon black microfiller,
2. Styrene-butadiene rubber (SBR), added as latex,
3. Thermoplastic block copolymer rubber,
4. Polyethylene finely dispersed in asphalt, and
5. Copolymers of ethylene and vinyl acetate (EVA).

Only one carbon black preparation was evaluated since there is presently only one product produced particularly for asphalt modification, Microfil-8, supplied by Cabot Corporation. Microfil-8 is a mixture of approximately 92 percent high-structure HAF grade carbon black plus approximately 8 percent oil similar to the maltenes portion of asphalts, formed into soft pellets dispersible in asphalt.

Styrene-butadiene latexes are available in a wide variety of monomer proportions, molecular weight ranges, emulsifier types and other variables. Two products specifically recommended for use in hot-mixed asphalt concrete were included in the investigation, Latex XUS 40052.00 from Dow Chemical USA and Ultra Pave 70 from Textile Rubber and Chemical Co. Both are anionic and contain about 70 percent solids.

Thermoplastic block copolymer rubber was obtained from Shell Development Company in two preparations, dry crumbs of Kraton TR60-8774 (a blend of equal parts Kraton D-1101 3-block styrene-butadiene-styrene polymer and Kraton DX-1118 2-block styrene-butadiene polymer), and a rubbery solution of equal parts Kraton D-1101 and Dutrex 739 rubber extender oil. Only the TR60-8774 was used in the mixture study. The styrene-butadiene polymers do not have permanent polarization, but the presence of the aromatic rings and double bonds allow for induced polarization from the polar asphalt molecules.

Information on the Novophalt process indicated that almost any polyolefin was satisfactory for processing. Dispersions containing six polyethylene resins which varied in density, molecular weight and melt index were prepared. These included Rexene PE109, Dow 526, Dow 527, Dowlex 880, Dowlex 2045 and Dow 69065P. Polyethylene is a linear nonpolar polymer.

Four EVA resins differing in monomer ratio, solubility, softening point and melt index were studied. These included Elvax grades 40-W, 150, and 250 from DuPont Company and EX 042 from Exxon Chemical Americas. EVA has permanent polarity associated with the acetate group.

SELECTION OF ASPHALTS

Asphalts for this study were obtained from two sources known to produce asphalt of substantially different composition and temperature susceptibility. Three grades of paving asphalt were obtained from each source: AC-5, AC-10 and AC-20 grades from the Texaco refinery at Port Neches, Texas, which processes a blend of crude oils from East Texas, Mexico, South America and Wyoming, and AR-1000, AR-2000 and AR-4000 grades from a California refinery which processes crude oil originating in the San Joaquin Valley. Additional supplies of the AC-5 and AR-1000 grades were obtained later from the same refineries.

Table 1 presents the test results obtained on the asphalts, and several parameters calculated from them which indicate susceptibility of their physical properties to temperature change. Temperature susceptibility is greater for the San Joaquin Valley asphalts than for the Texaco asphalts. Temperature susceptibility of the three grades from each source is similar.

Component composition of the Texaco AC-5 and AC-10 and San Joaquin Valley AR-1000 and AR-2000 grade asphalts is shown in table 2. The San Joaquin Valley asphalts have a relatively low asphaltenes content and a high content of nitrogen bases (table 2); the latter component is a solvent for asphaltenes and makes asphaltenes compatible with the other maltenes fractions. This composition yields a sol-type asphalt with Newtonian behavior. Asphalts with higher asphaltenes content and lower

Table 1. Properties of asphalts.

Asphalt source Grade Serial No.	Texaco				San Joaquin Valley			
	AC-5 7	AC-8 86	AC-10 11	AC-20 17	AR-1000 19	AR-2000 101	AR-4000 25	AR-4000 31
Specific gravity at 77°F ^a	1.019	1.029	1.017	1.017
Flash point ^b , COC, °F	...	565	595	530	595	...
Viscosity at 140°F ^c , P	506	537	1080	2040	498	423	1100	2170
Viscosity at 275°F ^d , cSt	224	217	332	398	128	150	185	256
Penetration at 77°F ^e , 100 g, 5 s	194	186	118	75	146	164	86	57
Penetration at 39.2°F, 100 g, 5 s	20	17	12	8	10	12	5	4
Penetration at 39.2°F, 200 g, 60 s	63	66	41	28	46	59	25	16
Softening point ^f , °C	40.4	41.4	46.6	51.8	41.6	41.2	47.8	51.2
Softening point, °F	104.5	106.5	116	125	107	106	118	124
Temperature suscepti- bility ^g , 140° to 275°F	-3.42	-3.42	-3.40	-3.52	-3.94	-3.71	-3.93	-3.92
PVNH ^h	-0.3	-0.4	-0.3	-0.6	-1.6	-1.2	-1.6	-1.4
P.I. ⁱ from penetration at 39.2°F and 77°F	-1.0	-1.4	-1.1	-1.0	-2.0	-1.9	-2.4	-2.0
P.I. from penetration at 77°F and soften- ing point	0.0	+0.2	+0.3	+0.3	-0.7	-0.4	-0.4	-0.6
Penetration ratio ^j	32	35	35	37	32	36	29	28
After Rolling Thin Film Oven Test ^k								
Weight change, %	...	-0.07	-0.03	-1.08	-0.39	...
Viscosity at 140°F ^c , P	...	1190	2770	893	1900	...
Viscosity at 275°F ^d , cSt	...	311	500	180	276	...
Penetration at 77°F ^e	...	112	71	104	57	...
% of original	...	60	60	63	66	...

^aDetermined at TTI.

^j100 (Pen 39.2°F, 200 g, 60 s) / (Pen 77°F, 100 g, 5 s).

^bAASHTO T48.

^cAASHTO T202.

^kAASHTO T240.

^dAASHTO T201.

^eAASHTO T49.

^fAASHTO T53.

^gTemperature susceptibility = $(\log \log \eta_2 - \log \log \eta_1) / (\log T_2 - \log T_1)$
where η = viscosity in cP, T = absolute temperature.

^hDetermined from penetration at 77°F and viscosity at 275°F (McLeod, 1976).

ⁱP.I. = $(20 - 500\alpha) / (1 + 50\alpha)$:

$\alpha = [\log(\text{pen}_2) - \log(\text{pen}_1)] / (T_2 - T_1)$, or

$[\log 800 - \log(\text{pen}_{25^\circ\text{C}})] / (T_{5p} - 25)$, where T = temperature, °C.

Table 2. Component composition of asphalts.

Property	Texaco Asphalts			San Joaquin Valley Asphalts		
	AC-5	AC-10	AC-20	AR-1000	AR-2000	AR-4000
Corbett Analysis^a						
Asphaltenes, %	14.6	-	14.8	5.0	-	6.0
Saturates, %	13.4	-	10.1	13.7	-	10.0
Naphthene Aromatics, %	41.5	-	30.3	36.1	-	33.5
Polar Aromatics, %	30.5	-	44.8	45.1	-	50.6
Rostler Analysis^b						
Asphaltenes, %	19.1	22.4	-	9.2	10.3	-
Nitrogen bases, %	21.0	18.6	-	37.7	42.0	-
First Acidaffins, %	22.0	14.1	-	16.8	9.0	-
Second Acidaffins, %	25.0	33.5	-	22.2	28.3	-
Paraffins, %	12.9	11.4	-	14.1	10.4	-
Refractive index of paraffins, n_D^{25}	1.4812	1.4820	-	1.4862	1.4907	-
Durability rating $(N+A_1)/(P+A_2)$	1.13	0.73	-	1.50	1.32	-
Sulfur, %	-	5.08	-	-	1.34	-

^aASTM D4124 (Precipitates asphaltenes using n-heptane)

^bASTM D2006 (Discontinued) (Precipitates asphaltenes using n-pentane)

^cDurability decreases with increasing parameter value; 0.4 - 1.0 = Group I, "superior" durability; 1.0 - 1.2 = Group II, "good" durability; 1.2 - 1.5 = Group III; "satisfactory" durability, Rostler and White (1970).

content of nitrogen bases, as in the Texaco asphalts, are more likely to exhibit non-Newtonian behavior as the asphaltenes component is not completely solvated, so a gel structure can develop. These properties of the asphalt binders are related to the resistance of paving mixtures to deformation. They are also related to the relative compatibility with, or solvent power for, polymers such as the rubbers and resins suggested as additives. Table 2 shows only minor differences in the functional groups other than asphaltenes.

When this study was initiated, it was expected that additives would be incorporated into the medium-viscosity AC-10/AR-2000 grade asphalts which would improve the temperature susceptibility so that the viscosity at high temperatures would equal or exceed that of the higher-viscosity AC-20/AR-4000 grades while the stiffness at low temperatures would be decreased to the levels of the low-viscosity AC-5/AR-1000 grades. After it became apparent that additives of the types selected were much more effective at increasing high-temperature viscosity than in decreasing low-temperature stiffness, emphasis was shifted to incorporating the additives into the low-viscosity AC-5/AR-1000 grade asphalts, to increase their viscosity at high temperatures and improve resistance to rutting, while maintaining the cracking resistance of the low-viscosity base asphalts at low temperatures.

BLENDS OF ASPHALTS AND ADDITIVES

1. Asphalt Carbon Black Blends

Dispersions of carbon black in the Texaco AC-5 and AC-10 grade asphalts and the San Joaquin Valley AR-1000 and AR-2000 grade asphalts were prepared to determine the effect of the carbon black on the properties of the asphalts. Three hundred gram dispersions were prepared by adding preweighed pellets to preheated asphalt in Waring Blender jars. The dispersibility of the pellets was checked by dissolving a 10 g portion of each mix in VM&P naphtha, pouring the solution through a No. 325 sieve, washing the sieve with additional naphtha, and weighing the

residue remaining on the sieve after drying. More than 99 percent of the added carbon black passed through the No. 325 sieve.

Values determined for penetration at 39.2^oF (4^oC) and 77^oF (25^oC), and for viscosity at 140 (60^oC) and 275^oF (135^oC) are shown in table 3 for the blends of Microfil-8 with the Texaco AC-5 and AC-10 grade asphalts, and in table 4 for the blends of Microfil-8 with San Joaquin Valley AR-1000 and AR-2000. The temperature susceptibility of all the asphalt:carbon black blends was lower than that of the base asphalt from which each was made. The principal effect of incorporation of Microfil-8 was to increase the viscosity at 140^oF (60^oC) and 275^oF (135^oC). The penetration at 77^oF (25^oC) was decreased by addition of Microfil-8, but the penetration at 39.2^oF (4^oC) remained essentially unchanged. The changes in temperature susceptibility are depicted graphically in appendix A. The 85 percent AC-5:15 percent Microfil-8 blend has approximately the same viscosity at 140^oF as the AC-20 grade asphalt; whereas, the 90:10 blend is equivalent to AC-10 at 140^oF. The 90 percent AC-10:10 percent Microfil-8 blend had approximately the same viscosity at 140^oF as the AC-20; whereas, the 85:15 blend containing AC-10 was equivalent to an AC-40 grade asphalt at 140^oF. The addition of 10 percent Microfil-8 in San Joaquin Valley AR-1000 or AR-2000 also increased the viscosity at 140^oF by about one grade level. The addition of 15 percent Microfil-8 in the San Joaquin Valley asphalts increased the 140^oF viscosity by almost two grade levels. The effect at the 85:15 level was not quite as great for the San Joaquin Valley asphalts as for the Texaco asphalts.

Because the oils used to facilitate the pelletizing of the carbon black in Microfil-8 might affect the asphalt properties, these oils were isolated and characterized. A weighed sample of Microfil-8 was placed in toluene and allowed to stand for several hours. The carbon black was filtered out and washed with additional toluene. The combined toluene fractions were filtered to clarify the solution. The toluene was

Table 3. Blends of carbon black with Texaco asphalts.

	Base Asphalt									
	Texaco AC-5				Texaco AC-10				Texaco AC-20	
	100	100	90	85	100	100	90	85	100	
Asphalt, % ^a	100	100	90	85	100	100	90	85	100	
Microfil 8 ^a , %	10	15	10	15	...	
Serial No.	7	33	34	35	11	36	37	38	17	
Mixing, Blender	No	Yes	Yes	Yes	No	Yes	Yes	Yes	No	
Undispersed Carbon Black, % of added Black ^b	0.34	0.05	0.06	0.10	...	
Viscosity at 140°F ^c , P	506	583	871	1850	1080	1210	1950	3540	2040	
Viscosity at 275°F ^d , cSt	224	...	504	740	332	398	
Penetration at 77°F ^e , 100 g, 5 s	194	189	179	152	118	112	106	92	75	
Penetration at 39.2°F, 100 g, 5 s	20	21	23	21	12	15	16	15	8	
Penetration at 39.2°F, 200 g, 60 s	63	65	65	66	41	48	46	48	28	
Specific Gravity	1.019	1.075	1.029	
Temperature Suscep- tibility ^f , 140 to 275°F	-3.42	...	-2.97	-2.99	-3.40	-3.52	
PVN ^g	-0.3	...	1.0	1.44	-0.3	0.6	
P.I. ^h from Penetration at 39.2°F and 77°F	-1.0	-0.8	-0.4	-0.2	-1.1	-0.3	+0.2	+0.4	-0.9	
Penetration Ratio ⁱ	32	34	36	43	35	43	43	52	37	

^aCabot Corporation, Lot CS-4632.

^bRetained when solution of asphalt:black blend in VM&P naptha was washed on #325 sieve.

^cAASHTO T202.

^dAASHTO T201.

^eAASHTO T49.

^fTemperature susceptibility = $(\log \log \eta_2 - \log \log \eta_1) / (\log T_2 - \log T_1)$
where η = viscosity in cP, T = absolute temperature.

^gDetermined from penetration at 77°F and viscosity at 275°F (McLeod, 1976).

^hP.I. = $(20 - 500\alpha) / (1 + 50\alpha)$:
where $\alpha = [\log(\text{pen}_2) - \log(\text{pen}_1)] / (T_2 - T_1)$ and T = temperature, °C.

ⁱ100 (Pen 39.2°F, 200 g, 60 s) / (Pen 77°F, 100 g, 5 s).

Table 4. Blends of carbon black with San Joaquin Valley asphalts.

	Base asphalt								
	Valley AR-1000				Valley AR-2000				Valley AR-4000
Asphalt, %	100	100	90	85	100	100	90	85	100
Microfil 8 ^a , %	10	15	10	15	...
Serial No.	19	39	40	41	25	42	43	44	31
Mixing, blender	No	Yes	Yes	Yes	No	Yes	Yes	Yes	No
Undispersed carbon black, % of added black ^b	0.27	0.10	...
Viscosity at 140°F ^c , P	498	549	942	1640	1100	1160	1940	3110	2170
Viscosity at 275°F ^d , cSt	128	...	199	398	185	256
Penetration at 77°F ^e , 100 g, 5 s	146	137	123	109	86	75	75	72	57
Penetration at 39.2°F, 100 g, 5 s	10	11	10	10	5	6	6	5	4
Penetration at 39.2°F, 200 g, 60 s	46	49	46	43	25	26	24	24	16
Temperature susceptibility ^f 140 to 275°F	-3.94	...	-3.80	-3.43	-3.93	-3.92
PVNG	-1.6	...	-1.1	-0.1	-1.6	-1.4
P.I. ^h from penetration at 39.2°F and 77°F	-2.0	-1.7	-1.7	-1.4	-2.4	-1.7	-1.7	-2.0	-2.0
Penetration ratio ⁱ	32	36	37	39	29	35	32	33	28

^aCabot Corporation, Lot CS-4632.

^bRetained when solution of asphalt:black blend in VM&P naphtha was washed on #325 sieve. CAASHTU T202.

^dAASHTO T201.

^eAASHTO T49.

^fTemperature susceptibility = $(\log \log \eta_2 - \log \log \eta_1) / (\log T_2 - \log T_1)$
where η = viscosity in cP, T = absolute temperature.

^gDetermined from penetration at 77°F and viscosity at 275°F (McLeod, 1976).

^hP.I. = $(20 - 500\alpha) / (1 + 50\alpha)$:

where $\alpha = [\log(\text{pen}_2) - \log(\text{pen}_1)] / (T_2 - T_1)$ and T = temperature, °C.

ⁱ $100(\text{Pen } 39.2^\circ\text{F}, 200 \text{ g}, 60 \text{ s}) / (\text{Pen } 77^\circ\text{F}, 100 \text{ g}, 5 \text{ s})$.

evaporated to yield 5.9 weight percent of a light amber oil with a consistency similar to that of motor oil.

Infrared spectra were obtained for a film of the oil on a salt plate. The ketone, phenolic OH, and sulfoxides are characteristic of a high-boiling petroleum hydrocarbon fraction that has been oxidized by atmospheric oxygen. Such oxidation might be expected since the oil has been exposed as a thin film on the carbon black surface. The recovered oil showed hydrocarbon spectra with no oxygenated chemical functionality except ketones, a trace of phenolic OH, and a low level of sulfoxides. Ketone and sulfoxide concentration are estimated at about 0.25 and 0.005 mole L⁻¹, respectively. The oil has an aromatic fingerprint region (700-900 cm⁻¹) and an aromatic C=C stretching band similar to those found in heavy petroleum distillation fractions. The evidence is strong that a high-boiling petroleum fraction is used to pelletize Microfil-8.

2. Dispersion of SBR in Asphalts

The recommendation of both manufacturers for incorporation into asphalt concrete is to add the latex in the plant a few seconds after the aggregate has been coated with asphalt. Dispersions of both latexes were prepared at levels of 3 percent and 5 percent solids in Texaco AC-10 and AC-5 and San Joaquin Valley AR-2000 and AR-1000 grade asphalts. Each 300 g batch was prepared by preheating the asphalt in a Waring Blender jar, then adding the latex slowly while blending to flash off the water and disperse the rubber.

Table 5 shows the penetration and viscosity of the blends of styrene-butadiene rubber (SBR) in Texaco AC-10 and San Joaquin Valley AR-2000 asphalts. Observations made under the microscope show that the SBR from both latexes is soluble in the San Joaquin Valley asphalt, but is not completely soluble in the Texaco asphalt.

Three percent SBR increased the 140°F (60°C) viscosity of the Texaco AC-10 asphalt into the AC-30 range for the Dow XUS 40052.00 latex, and the AC-40 range for the Ultra Pave 70. Five percent of either latex increased the 140°F viscosity well beyond the AC-40 range. Penetration

Table 5. Blends of SBR (as latex) with asphalt.

Serial No.	11	54	55	56	57	58	25	59	60	61	62
Asphalt		Texaco AC-10						San Joaquin Valley AR-2000			
Latex	None	XUS 40052.00 ^a ----->					None	XUS 40052.00		Ultra Pave 70	
Proportions asphalt: rubber ^c	...	97:3	97:3	95:5	97:3	95:5	...	97:3	95:5	97:3	95:5
Viscosity at 140°F ^d , P	1080	3210	2940	7280	3840	7620	1100	2230	4700	2350	5250
Viscosity at 275°F ^e , cSt	332	...	1240	3110	185	966	3830
Penetration ^f at 77°F, 100 g, 5 s	118	91	96	78	90	78	86	73	75	69	74
Penetration ^f at 39.2°F, 100 g, 5 s	12	10	11	11	20	11	5	4	3	4	3
Penetration ^f at 39.2°F, 200 g, 60 s	41	40	42	45	70	44	25	17	18	17	20
Temperature susceptibility ^g	-3.40	...	-2.81	-2.55	-3.93	-2.88	-2.26
PVN ^h	-0.3	...	1.4	2.5			-1.6	0.7	2.8
Penetration index ⁱ	-1.1	-0.9	-0.7	-0.1	+1.7	-0.8	-2.4	-2.5	-3.1	-2.4	-3.1
Penetration ratio ^j	35	44	44	58	78	56	29	23	24	25	27

^aAnionic SBR latex from Dow Chemical USA, 69.7% solids.

^bAnionic SBR latex from Textile Rubber and Chemical Company, 70.1% solids.

^cProportions of asphalt to dry solids from latex; 300 g batches prepared by preheating asphalt in a Waring Blendor jar to 135-155°C (275-310°F), then adding latex slowly while operating the Blendor to flash off the water and disperse the rubber.

^dAASHTO T202.

^eAASHTO T201.

^fAASHTO T49.

^gTemperature susceptibility = $(\log \log \eta_2 - \log \log \eta_1) / (\log T_2 - \log T_1)$
where η = viscosity in cP, T = absolute temperature.

^hDetermined from penetration at 77°F and viscosity at 275°F (McLeod, 1976).

ⁱP.I. = $(20 - 500\alpha) / (1 + 50\alpha)$:

α $[\log(\text{pen}_2) - \log(\text{pen}_1)] / (T_2 - T_1)$, where T = temperature, °C.

^j $100(\text{Pen } 39.2^\circ\text{F, } 200 \text{ g, } 60 \text{ s}) / (\text{Pen } 77^\circ\text{F, } 100 \text{ g, } 5 \text{ s})$.

at 77°F (25°C) was reduced by addition of SBR, but the penetration at 39.2°F (4°C) was affected only slightly, except for high values obtained for penetration at 39.2°F for a blend of 3 percent SBR from Ultra Pave 70 in Texaco AC-10. Repeated tests of that blend confirmed the high penetration values, but a second preparation of the same composition did not yield high values for penetration at 39.2°F.

In the San Joaquin Valley AR-2000, which appeared to be the better solvent for SBR, addition of 3 percent SBR increased viscosity to the AC-20 level, while 5 percent increased the viscosity to approximately the high end of the AC-40 level. Penetration was reduced at both 77°F and 39.2°F. The temperature susceptibility of the San Joaquin Valley AR-2000, in the range between 39.2° (4°C) and 140°F (60°C), was not changed significantly by addition of SBR; the values for penetration index and penetration ratio were decreased slightly from the values for the control.

Dispersions of Dow SBR Latex XUS 40052.00 at 3 percent and 5 percent latex solids in Texaco AC-5 grade and San Joaquin Valley AR-1000 grade asphalts were prepared (table 6) at higher temperatures (376-390°F, 191-199°C). The higher temperatures reduced an earlier problem of stalling the Waring Blender during incorporation of the latex.

The addition of 3 percent SBR increased the 140°F viscosity from about 500 P to about 2000 P (i.e. AC-20 range) for the Texaco AC-5 and to about 4000 P (i.e. AC-40 range) for the San Joaquin Valley AC-1000. Addition of 5 percent SBR increased the 140°F viscosity to beyond 5000 P for the AC-5 and to 10,000 P for the AR-1000. The 275°F (135°C) viscosity also was increased to quite high levels. Since, in plant practice, the latex is added after about 90 percent of the aggregate surfaces are coated by asphalt, the high levels of 275°F viscosity may not cause difficulty in mixing and coating the aggregate, but asphalt concrete containing such high-viscosity binders may be difficult to place and compact. The temperature susceptibility of both base asphalts was

Table 6. Blends of SBR (as latex) with AC-5 and AR-1000 asphalts.

Serial No. Asphalt Latex	86	131	132	101	133	134
	None	Texaco AC-5 XUS-40052.00 ^a		None	San Joaquin Valley AR-1000 XUS-40052.00	
Proportions asphalt: rubber ^b	97:3	95:5	97:3	95:5
Viscosity at 140°F ^c , P	537	1960	5460	423	4020	10,100
Viscosity at 275°F ^d , cSt	217	1020	2780	150	1190	3600
Penetration ^e at 77°F, 100 g, 5 s	186	140	114	164	83	72
Penetration ^e at 39.2°F, 100 g, 5 s	17	15	14	12	6	6
Penetration ^e at 39.2°F, 200 g, 50 s	66	57	54	59	28	29
Softening point ^f , °C	41.4	51.6	62.5	41.2	54.2	66.8
Softening point ^f , °F	106.5	125	144.5	106	129.5	152
Specific Gravity	1.019	1.014	1.012	1.017	1.014	1.015
Temperature suscepti- bility ^g	-3.42	-2.78	-2.52	-3.71	-2.96	-2.58
PVN ^h	-0.4	1.8	3.0	-1.2	1.2	2.5
P.I. ⁱ from penetration at 39.2 and 77°F	-1.4	-0.9	-0.5	-1.9	-1.9	-1.6
P.I. from penetration at 77°F and softening point	0.2	2.4	4.1	-0.4	1.2	3.3
Penetration ratio ^j	35	41	47	36	34	40

^aAnionic SBR latex from Dow Chemical USA, 69.7% solids.

^bProportions of asphalt to dry solids from latex; 300 g batches prepared by preheating asphalt in a Waring Blender jar to 191-199°C (376-390°F), then adding latex slowly while operating the Blender to flash off the water and disperse the rubber.

^cAASHTO T202.

^dAASHTO T201.

^eAASHTO T49.

^fAASHTO T53.

^gTemperature susceptibility = $(\log \log \eta_2 - \log \log \eta_1) / (\log T_2 - \log T_1)$
where η = viscosity in cP, T = absolute temperature.

^hDetermined from penetration at 77°F and viscosity at 275°F (McLeod, 1976).

ⁱP.I. = $(20 - 500\alpha) / (1 + 50\alpha)$: $\alpha = [\log(\text{pen}_2) - \log(\text{pen}_1)] / (T_2 - T_1)$, or
 $[\log 800 - \log(\text{pen}_{25^\circ\text{C}})] / (T_{\text{SP}} - 25)$ where T = temperature, °C.

^j100 (Pen 39.2°F, 200 g, 60 s) / (Pen 77°F, 100 g, 5 s).

substantially decreased by incorporation of SBR. The decrease in temperature susceptibility is also shown by increased values for penetration index, PVN, and penetration ratio. Plots of the penetration and viscosity against temperature are presented in appendix A.

3. Dispersion of SBS/SB Copolymers in Asphalts

Since Shell had supplied to TTI the dispersions of 5 percent Kraton TR60-8774 in the AC-5 and AR-1000 asphalt, additional dispersions were not prepared. Samples from the 5-gal lots prepared by Shell were tested by Matrecon. The values determined for the Texaco AC-5/Kraton TR60-8774 blend did not agree with the values reported by Shell. The differences were attributed to nonhomogeneity of the blend, which appeared to have "zones" with a gelled consistency. After discussions with Shell personnel, the blend was reheated to a higher temperature 356⁰F (180⁰C) and the determinations repeated. The gelled zones were less evident at the higher temperature, however, there still seemed to be some variability within material poured from the same well-stirred beaker. This variability was demonstrated by an abnormal variation in softening point of two specimens tested side by side.

Subsequently, Shell recommended an additive composed of equal parts Kraton D-1101 and Dutrex 739 rubber extender oil. Since the polystyrene "domains" of the SBS block polymer are plasticized by the extender oil, the concentrate can be incorporated into asphalt without the high-shear mixing which is necessary for incorporating the block polymer directly into asphalt. Shell supplied a sample of a 50:50 blend of Kraton D-1101 and Dutrex 739, which was used to prepare four blends. Data for these blends in Texaco AC-5 and San Joaquin Valley AR-1000 are shown in table 7. Even after being dissolved in the rubber extender oil, the SBS block polymer did not readily form homogeneous blends in the Texaco asphalt, but seemed to have strings of gel throughout when melted. The 140⁰F (60⁰C) viscosity was increased from the 500 P level to the 1000-1200 P level by addition of 6 percent of the SBS/oil blend. The addition of 12 percent of the blend increased the 140⁰F viscosity of the San Joaquin

Table 7. Blends of asphalts with thermoplastic block polymers (Kraton).

Serial No.	86	102(1)	128	126	101	130	129	127
Texaco AC-5	100	95	94	88	-	-	-	-
San Joaquin Valley AR-1000	-	-	-	-	100	95	94	88
Kraton TR-60-8774 ^a	-	5	-	-	-	5	-	-
Kraton/Dutrex Blend 10 FBP 1000 ^b	-	-	6	12	-	-	6	12
Viscosity at 140°F ^c , P	537	6720	1160	gel	423	1720	1040	15,500
Viscosity at 275°F ^d , cSt	217	873	493	1350	150	431	305	752
Penetration at 77°F ^e , 100g, 5s	186	103	145	111	164	134	154	132
Penetration at 39.2°F, 100g, 5s	17	14	17	21	12	11	12	13
Penetration at 39.2°F, 200g, 60s	66	49	61	58	59	43	49	56
Softening point ^f , °C	41.4	58.6	47.2	79.0	41.2	52.2	49.6	71.0
Softening point, °F	106.5	137.5	117	174	106	126	121	152
Specific Gravity	1.019	1.014	1.017	1.015
Temperature susceptibility ^g , 140 to 275°F	3.42	2.44	3.11	-	3.71	3.38	3.46	-3/78
PVN ^h	-0.4	1.0	0.6	1.8	-1.2	0.3	-0.1	1.2
P.I. ⁱ from penetration at 39.2°F and 79°F	-1.4	-0.2	0.7	1.0	-1.9	-1.6	-1.8	-1.2
P.I. from penetration at 77°F and softening point	0.2	2.9	1.2	6.7	-0.4	2.4	2.2	6.2
Penetration ratio ^j	35	48	42	52	36	32	32	42

^aBlend supplied by Shell Development Co. Kraton TR-60-8774 is 50% Kraton D-1101 S-B-S, 50% Kraton DX-1118 S-B.

^bBlend 10 FBP 1000 is 50% Kraton D-1101 S-B-S, 50% Dutrex 739 Rubber Extender Oil ASTM D2226, type 101.

^cAASHTO T202.

^dAASHTO T201.

^eAASHTO T49.

^fAASHTO T53.

^gTemperature susceptibility = $(\log \log \eta_2 - \log \log \eta_1) / (\log T_2 - \log T_1)$, where η = viscosity in cP, T = absolute temperature.

^hDetermined from penetration at 77°F and viscosity at 275°F (McLeod, 1976).

ⁱP.I. = $(20 - 50\alpha) / (1 + 50\alpha)$: $\alpha = [\log(\text{pen}_2) - \log(\text{pen}_1)] / (T_2 - T_1)$ or $[\log 800 - \log(\text{pen}_{25^\circ\text{C}})] / (T_{\text{Sp}} - 25)$, where T = temperature, °C.

^j $100(\text{Pen } 39.2^\circ\text{F}, 200 \text{ g}, 60 \text{ s}) / (\text{Pen } 77^\circ\text{F}, 100 \text{ g}, 5 \text{ s})$.

Valley AR-1000 to more than 15,000 P. The Texaco AC-5 containing 12 percent of the SBS/oil blend was a gel at 140°F and could not be tested in the capillary viscometer. Penetration at 77°F was decreased, but penetration at 39.2°F was unaffected or slightly increased by addition of the SBS/oil blend. Plots of the penetration and viscosity as a function of temperature are provided in appendix A.

4. Dispersion of Polyethylene in Asphalts

Polyethylene resins are semicrystalline polymers which are not soluble, or only slightly soluble, at temperatures below the melting point of the resin. The Novophalt process, developed by the Felsing Company in Austria, consists of dispersing polyethylene (4 to 7 percent by weight) in asphalt at temperatures of approximately 300 to 355°F (150 to 180°C) by high-speed, high-shear mixing in equipment similar to a colloid mill with very close spacing between the stationary and rotating members. The gap between rotor and stator in the laboratory equipment is 0.03 mm (0.001 in); while the gap in production equipment is 0.1 mm (0.004 in). When it is properly dispersed, the polyethylene will still separate during hot storage, i.e., float to the top of the stored asphalt, but the particles do not coalesce and can be readily redispersed by low-shear stirring, according to the information supplied by the Felsing Company.

Scrap or recycled polyethylene is used in the production of Novophalt. While it is claimed that almost any polyethylene can be used, a desirable range of properties was suggested, i.e. a melt index between 0.7 and 1.2, and a density about 0.93. Low-molecular weight polyethylenes such as used for wax additives do not contribute much strength. Requirements for the bitumen also are either not very critical or not well defined.

All the polyethylene dispersions for this study were prepared in a Model 60 Vicosator high-speed dispersing mill supplied by the Felsing Company, following their procedure, which requires several passes of the

asphalt-polyethylene mixture through the mill. Novophalt is usually produced at the site (hot plant) and used immediately, to avoid settling during storage. In laboratory testing, it is necessary to reheat to about 356⁰F (180⁰C) and stir thoroughly to redisperse the "creamed" polyethylene phase each time a specimen is withdrawn for testing.

Five polyethylene resins differing in density, molecular weight and melt index were dispersed in Texaco AC-10. Table 8 shows data collected during the runs and the penetration and viscosity values measured. One or two passes through the mill were sufficient to disperse these LDPE resins to small spherical particles, which generally became irregular in shape, though not much smaller, with additional passes through the mill. The difficulty in determining viscosity at 140⁰F (60⁰C), and examination of microscope slides of the preparations, show that three of the polyethylene resins were not dispersed to the standards recommended for Novophalt. The appearance of the particles indicates that the high density polyethylene, linear low density polyethylene, and high molecular weight low density polyethylene resins probably were not liquid, but retained a strong gel structure, at the 355⁰F (180⁰C) temperature reached during blending. Photomicrographs of the dispersions of the Dow resins in Texaco AC-10 are given in appendix A.

Addition of 5 percent polyethylene increased the stiffness of the asphalt over the whole range of temperatures tested. The viscosity at 140⁰F (60⁰C) was increased about four-fold by the two low-density polyethylenes, and much more by the high-density, linear-low-density, and high-molecular-weight low-density polyethylenes, which produced blends having gel-like consistency and did not flow through the capillary viscometers. Since the reduction of penetration at 39.2⁰F (4⁰C) was less than the reduction at 77⁰F (25⁰C), the overall effect of polyethylene was a reduction of temperature susceptibility.

Dispersions of one of the low-density resins, Dow LDPE 526, were also prepared in the Texaco AC-5 and in the San Joaquin Valley AR-1000 and AR-2000. The particle size of the dispersed LDPE in these asphalts was similar to that obtained in the Texaco AC-10 asphalt.

Table 8. Dispersions of polyethylenes in Texaco AC-10 asphalt.

Serial No.	11	49	50	51	52	53
Polyethylene ^a	None	Dow 526	Dow 527	Dow 69065P	Dow 2045	Dow 880
Type	...	LDPE	LDPE	HDPE	LLDPE	HMWLDPE
Density (manufacturer's data)	...	0.919	0.921	0.920	0.961	0.932
Melt Index (manufacturer's data)	...	1.0	2.9	1.0	0.60	0.45
No. of passes through mill ^b	None	5	5	6	5	5
Temperature after 1 pass, °C	...	152	158	162	162	166
Temperature after 2 passes, °C	...	162	163	172	170	169
Temperature after 3 passes, °C	...	164	168	178	173	173
Temperature after 4 passes, °C	...	168	172	184	178	179
Temperature after 5 passes, °C	...	170	172	186	181	183
Temperature after 6 passes, °C	186
Volume of settled layer of swollen polyethylene ^c , %	...	20	19	19	29	20
Viscosity at 140°F ^d , P	1080	4740	4640
Penetration ^e at 77°F, 100 g, 5 s	118	60	58	36	38	59
Penetration ^e at 39.2°F, 100 g, 5 s	12	7	8	6	5	9
Penetration ^e at 39.2°F, 200 g, 60 s	41	31	33	21	22	27
Penetration index ^f	-1.1	-0.7	-0.2	+0.5	-0.3	+0.2
Penetration ratio ^g	35	52	57	58	58	46

^aAll blends contained 95% asphalt, 5% polyethylene. Additional data for the polyethylenes was presented in Table 1 of Progress Report 3, February 5, 1985.

^bProbst and Class Vicosator, Model 60.

^cSpecimen in 3-oz tin kept in 150°C oven 3 h, then chilled. Thickness of layers measured under ultraviolet illumination after stripping off the tin.

^dASTM D2171, modified Koppers capillary viscometers. Reliable values were not obtained for the blends containing HDPE, LLDPE, and HMWLDPE.

^eASTM D5.

^fP.I. = $(20 - 500\alpha)/(1 + 50\alpha)$:

$\alpha = [\log(\text{pen}_2) - \log(\text{pen}_1)] / (T_2 - T_1)$, where T = temperature, °C.

^g100(pen 39.2°F, 200 g, 60 s) / (pen 77°F, 100 g, 5 s).

In the Texaco AC-5, the effect was similar to that for the same resin in Texaco AC-10 (see Serial No. 49 in table 8). In the San Joaquin Valley asphalts, the effect was less dramatic than in the Texaco asphalts. Table 9 shows that fairly consistent results were obtained in replicate preparations of Novophalts using LDPE 526 in the AC-5, AC-10, AR-1000 and AR-2000 asphalts.

Five gallon lots of Novophalt needed for preparation of asphalt concrete specimen specimen at TTI, were prepared by Matrecon using 5 percent LDPE 526 in Texaco AC-5 and San Joaquin Valley AR-1000. Properties of these blends are shown in table 10, and plots of the rheological data are provided in appendix A.

5. Dispersion of EVA in Asphalts

Dispersion of three ethylene-vinyl acetate copolymer resins, Elvax 40-W, 150 and 250, in San Joaquin Valley AR-2000 and Texaco AC-10 asphalts were prepared as 300 g batches in the Waring Blender. Examination under the microscope showed differences in compatibility with the two asphalts. There were also differences in compatibility between the three resins, which differed in melt index, which affects viscosity of solutions, and in ratio of the two monomers, which affects solubility.

Table 11 shows the properties of the blends in San Joaquin Valley AR-2000 and Texaco AC-10. Addition of the EVA polymers at the 3 percent level increased the 140°F (60°C) viscosity of each asphalt from the AC-10 level to the AC-20 range. Penetration at 77°F (25°C) was decreased by the addition of EVA to Texaco AC-10 but was not changed much by the addition of EVA to San Joaquin Valley AR-2000. Overall, the penetration at 39.2°F (4°C) exhibited only a slight increase. Of the three EVA resins tested, Elvax 150 appeared to be the most compatible with the asphalts and Elvax 250 the least compatible.

Preliminary trails of a lower-melting EVA resin, Exxon EX042, indicated that this copolymer is more readily incorporated into asphalt than the Elvax resins. Dispersions of Exxon EX042 and Elvax 150 in the Texaco AC-5 and San Joaquin Valley AR-1000 asphalts were prepared. These

Table 9. Replicate dispersions of a low-density polyethylene^a in asphalts.

Asphalt Serial No. Polyethylene ^a , %	Texaco AC-5					Texaco AC-10			San Joaquin Valley AR-1000					San Joaquin Valley AR-2000		
	7	86	65	84	97	11	49	82	19	101	64	83	113	25	63	81
No. of batches prepared in mill ^b	1	1	10	...	1	6	1	1	10	...	1	6
Volume of settled layer of swollen poly- ethylene ^c , %	18	33	21	...	20	8	29	38	38	...	9-19	4
Viscosity at 140°F ^d , P	506	537	1990	2410	2200	1080	4740	3410	498	423	1660	1620	1295	1100	2920	2580
Penetration ^e at 77°F, 100 g, 5 s	194	186	95	104	105	118	60	64	146	164	74	104	98	86	44	54
Penetration ^e at 39.2°F, 100 g, 5 s	20	17	11	16	13	12	7	9	10	12	7	9	8	5	3	4
Penetration ^e at 39.2°F, 200 g, 60 s	63	66	42	55	49	41	31	32	46	59	26	38	41	25	15	19
Penetration index ^f	-1.0	-1.4	-0.7	+0.2	-0.5	-1.1	-0.7	-0.1	-0.2	-1.9	-1.3	-1.5	-1.6	-2.4	-2.1	-1.9
Penetration ratio ^g	32	35	44	53	47	35	52	50	32	36	35	37	42	29	34	35

^aBlends contained 95% asphalt, 5% Dow LDPE 526 (density 0.919, Melt Index 1.0). Blends No. 65 and 84 were made from base asphalt No. 7; blend 97 from base asphalt No. 86; blends 49 and 82 from base asphalt No. 11.

^bProbst and Class Vicosator, Model 60.

^cSpecimen in 3-oz tin kept in 150°C oven 3 h, then chilled. Thickness of layers measured under ultraviolet illumination after stripping off the tin.

^dAASHTO T202, modified Koppers capillary viscometers.

^eAASHTO T49.

^fP.I. = $(20 - 500\alpha)/(1 + 50\alpha)$: $\alpha = [\log(\text{pen}_2) - \log(\text{pen}_1)]/(T_2 - T_1)$, where T = temperature, °C.

^g100 (Pen 39.2°F, 200 g, 60 s)/(Pen 77°F, 100 g, 5 s).

Table 10. Dispersions of polyethylene^a in asphalts.

Asphalt	Texaco AC-5		San Joaquin Valley AR-1000	
	86	97	101	113
Serial No.	86	97	101	113
Polyethylene ^a , %	None	5	None	5
No. of batches prepared in mill ^b	...	10	...	10
Volume of settled layer of swollen polyethylene ^c , %	...	28	...	38
Viscosity at 140°F ^d , P	537	2200	423	1295
Viscosity at 275°F ^e , cSt	217	843	150	399
Penetration ^f at 77°F, 100 g, 5 s	186	105	164	98
Penetration ^f at 39.2°F, 100 g, 5 s	17	13	12	8
Penetration ^f at 39.2°F, 200 g, 60 s	66	49	59	41
Softening point ^g , °C	41.4	52.2	41.2	47.2
Softening point ^g , °F	106.5	126	106	117
Temperature susceptibility ^h , 140 to 275°F	-3.42	-2.98	-3.71	-3.33
PVN ⁱ	-0.4	1.0	-1.2	-0.2
Penetration index ^j from penetration at 39.2°F and 77°F	-1.4	-0.5	-1.9	-1.6
Penetration index from penetration at 77°F and softening point	0.2	1.5	-0.4	-0.2
Penetration ratio ^k	35	47	36	37
After rolling thin film oven test weight change, %	-0.07	-0.06	-1.08	-0.97
viscosity at 140°F, P	1190	6040	893	3840
viscosity at 275°F, cSt	311	1280	180	532
penetration at 77°F, 100g, 5s	112	65	104	59
% of original	60	62	63	60

^aBlends contained 95% asphalt, 5% Dow LDPE 526 (density 0.919, Melt Index 1.0).

^bProbst and Class Vicosator, Model 60.

^cSpecimen in 3-oz tin kept in 150°C oven 3 h, then chilled. Thickness of layers measured under ultraviolet illumination after stripping off the tin.

^dAASHTO T202, modified Koppers capillary viscometers.

^eAASHTO T201.

^fAASHTO T49.

^gAASHTO T53.

^hTemperature susceptibility = $(\log \log \eta_2 - \log \log \eta_1) / (\log T_2 - \log T_1)$ where η = viscosity in cP, T = absolute temperature.

ⁱDetermined from penetration at 77°F and viscosity at 275°F (McLeod, 1976).

$J.P.I. = (20 - 500\alpha) / (1 + 50\alpha)$:

$\alpha = [\log(\text{pen}_2) - \log(\text{pen}_1)] / (T_2 - T_1)$, or $[\log 800 - \log(\text{pen}_{25^\circ\text{C}})] / [T_{\text{sp}} - 25]$ where T = temperature, °C.

^k $100(\text{pen}_{39.2^\circ\text{F}, 200\text{g}, 60\text{s}}) / (\text{pen}_{77^\circ\text{F}, 100\text{g}, 5\text{s}})$.

Table 11. Dispersion of ethylene-vinyl acetate copolymers in AC-10 and AR-2000 asphalts.

Serial No. Asphalt EVA Resin ^a	11	70	72	68	67	25	71	73	69	66
		Texaco AC-10				San Joaquin Valley AR-2000				
	None	Elvax 40-W	Elvax 150	Elvax 250	Elvax	None	Elvax 40-W	Elvax 150	Elvax 250	Elvax
Proportion asphalt:EVA	...	97:3	95:5	97:3	97:3	...	97:3	95:5	97:3	97:3
Viscosity ^b at 140°F, P	1080	1670	2520	1750	f	1100	1780	2320	1640	1640
Penetration ^c at 77°F, 100 g, 5 s	118	101	92	91	82	86	84	91	89	93
Penetration ^c at 39.2°F, 100 g, 5 s	12	13	12	14	13	5	5	7	5	5
Penetration ^c at 39.2°F, 200 g, 60 s	41	44	43	49	42	25	29	30	30	23
Penetration index ^d	-1.1	-0.4	-0.3	0.0	+0.3	-2.4	-2.3	-1.8	-2.5	-2.5
Penetration ratio ^e	35	44	47	54	51	29	34	33	34	25

^aEVA pellets added to asphalt preheated to 275°F (135°C) in Waring Blendor. Typical properties of resins from manufacturer (DuPont Company):

Elvax 40-W, 39-42% vinyl acetate, softening point 220°F, (104°C), specific gravity 0.965.

Elvax 150, 32-34% vinyl acetate, softening point 230°F (110°C), specific gravity 0.957.

Elvax 250, 27-29% vinyl acetate, softening point 260°F (127°C), specific gravity 0.951.

^bAASHTO T202.

^cAASHTO T49.

^dp.I. = $(20 - 50\alpha)/(1 + 50\alpha)$:

$\alpha = [\log(\text{pen}_2) - \log(\text{pen}_1)]/(T_2 - T_1)$, where T = temperature, °C.

^e $100(\text{Pen } 39.2^\circ\text{F, } 200 \text{ g, } 60 \text{ s})/(\text{Pen } 77^\circ\text{F, } 100 \text{ g, } 5 \text{ s})$.

^fSerial No. 67 blend contained undispersed resin and could not be tested in the capillary viscometer.

blends were prepared by stirring with a low-shear Jiffy mixer instead of by high-shear mixing in a Waring Blender. The Exxon EX042 resin appeared to dissolve completely while being stirred at 325°F (163°C). It was necessary to increase the temperature to 347°F (175°C) to completely dissolve the Elvax 150. The data obtained on these blends are presented in table 12.

The EX042 did not change the properties of the asphalt as much as an equivalent amount of Elvax 150. The viscosity at 275°F (135°C) was increased by addition of the EVA resins, but not to the very high levels of the SBR latex blends. EX042 at 3 percent and 5 percent increased the 140°F viscosity of Texaco AC-5 slightly, but did not affect the 140°F viscosity of San Joaquin Valley AR-1000. Elvax 150 at 3 percent increased the 140°F viscosity to about 800 P and 5 percent to near 1200 P (i.e. AC-10 range) for both asphalts. Effect on penetration at 77°F appeared inconsistent. Penetration at 39.2°F (4°C) was not appreciably affected by incorporation of EVA. Plots of penetration and viscosity vs temperature are given in appendix A. Since the changes achieved with 5 percent EVA are comparatively modest, it appears appropriate to incorporate higher levels of EVA.

MISCELLANEOUS TESTING ON SELECTED ADDITIVE-ASPHALT BLENDS

Flash point, ductility testing and physical property changes following rolling thin film oven aging were determined for selected additive-asphalts combinations.

1. Flash Point Testing

Flash points were determined for one blend containing each of five types of additives (table 13). The flash points of the blends are lower than for the base asphalts, but still well above standard specification limits.

Table 12. Blends of ethylene-vinyl acetate copolymers in AC-5 and AR-1000 asphalts.

Serial No. Asphalt EVA Resin ^a	86	120	121	124	125	101	116	117	118	119
	None	Texaco AC-5			San Joaquin Valley AR-1000			None	EX 042	Elvax 150
	None	EX 042	Elvax 150	Elvax 150	Elvax 150	None	EX 042	Elvax 150	Elvax 150	Elvax 150
Proportion asphalt:EVA	...	97:3	95:5	97:3	95:5	...	97:3	95:5	97:3	97:5
Viscosity ^b at 140°F, P	537	634	742	785	1160	423	433	419	852	1180
Viscosity ^c at 275°F, cSt	217	278	368	380	618	150	170	264	281	434
Penetration ^d at 77°F, 100 g, 5 s	186	133	113	202	176	164	176	132	155	161
Penetration ^d at 39.2°F, 100 g, 5 s	17	16	15	20	17	12	10	10	11	12
Penetration ^d at 39.2°F, 200 g, 60 s	66	49	47	63	54	59	40	38	45	50
Softening point ^e , °C	41.4	44.8	53.4	42.0	49.0	41.2	42.2	48.0	44.0	44.8
Softening point ^e , °F	106.5	112.5	128	107.5	120	106	108	118.5	111	112.5
Temperature suscepti- bility ^f ,	3.42	3.33	3.16	3.16	2.94	3.71	3.60	3.19	3.45	3.22
PVN ^g	-0.4	-0.5	-0.2	-0.6	1.3	-1.2	-0.9	-0.6	-0.2	0.5
Penetration index ^h from penetration at 77°F and 39.2°F	-1.4	-0.6	-0.3	-1.2	1.2	-1.9	-2.4	-1.8	-2.0	-1.9
Penetration index ^h from penetration at 77°F and softening point	0.2	0.1	2.0	0.9	2.6	-0.4	0.3	1.1	0.4	0.8
Penetration ratio ⁱ	35	37	42	31	31	36	23	29	29	31

^aEVA pellets added to asphalt while stirring with Jiffy mixer at 200 rpm. EX 042 dissolved at 325°F(163°C). Elvax 150 dissolved at 347-356°F(175-180°C). Typical properties of resins from manufacturers:

Exxon EX 042 softening point 230°F, specific gravity 0.92.

DuPont Elvax 150, 32-34% vinyl acetate, softening point 230°F (110°C), specific gravity 0.957.

^bAASHTO T202.

^cAASHTO T201.

^dAASHTO T49.

^eAASHTO T53.

^fTemperature susceptibility = $(\log \log n_2 - \log \log n_1) / (\log T_2 - \log T_1)$ where n = viscosity in cP, T = absolute temperature.

^gDetermined from penetration at 77°F and viscosity at 275°F (McLeod, 1976).

^hP.I. = $(20 - 500\alpha) / (1 + 50\alpha)$: $\alpha = [\log(\text{pen}_{77})] / (T_2 - T_1)$, or $[\log 800 - \log(\text{pen}_{25})] / (T_{sp} - 25)$, where T = temperature, °C.

ⁱ $100(\text{Pen}_{39.2^\circ\text{F}, 200\text{ g, 60 s}}) / (\text{Pen}_{77^\circ\text{F}, 100\text{ g, 5 s}})$.

Table 13. Flash point and ductility of asphalts and selected blends with additives.

Serial No.	86	101	102	130	131	132	133	134	135	136	137	113
Composition, %												
Texaco AC-5	100	...	95	...	97	95	95
San Joaquin Valley AR-1000	...	100	...	95	97	95	...	90	95	95
S-B-S/S-B block polymer ^a	5	5
SBR ^b	3	5	3	5	5	...
EVAC ^c	5
Microfil-8	10
LDPE 526 (Novophalt)	5
Flash Point, °F, AASHTO T48 (COC)	565	530	...	500	560	495	510	495
Ductility, cm, AASHTO T51												
At 39.2°F, 1 cm/min	>150	>150
At 39.2°F, 5 cm/min	>150	>150	68 ^d	141 ^d	>150	>150	36 ^f	>150	24 ^d
At 77°F, 5 cm/min	>150	130	98 ^d	83 ^e	>150	>150	131 ^f	144 ^g	45 ^d

^aKraton TR60-8774, blend of equal parts Kraton D-1101 three-block S-B-S polymer and Kraton DX-1118 two-block S-B (styrene-butadiene) polymer.

^bStyrene-butadiene rubber from Dow XUS 40052.00 latex.

^cElvax 150, 32-24% vinyl acetate, softening point 230°F, specific gravity 0.957.

^dPulled out as much thicker threads than unmodified asphalts.

^eBroke by "necking", i.e. one point of the thick threads pulled out to very thin threads, which then broke.

^fOne specimen >150 cm.

^gTwo specimens >150 cm.

2. Ductility Testing

Ductilities were determined in accordance with ASTM T51 for AC-5 and AR-1000 asphalts and selected blends of them with additives. Novophalt and Microfil-8 blends were not included as previous experience has shown that the ductility test is not appropriate for testing asphalts containing fillers or undissolved particles. The presence of such particles results in low ductility values. The same appeared to apply to the AC-5/EVA blends tested.

The ductility test results are presented in table 13. Both base asphalts had very good ductility at both 39.2^oF (5^oC) and 77^oF (25^oC). The specimens of the blend containing Elvax 150 broke at relatively short elongations, probably due to the presence of undissolved resin particles as discussed above. The blends containing thermoplastic block polymer (SBS) rubber formed thick threads, obviously much stronger than the threads of unmodified asphalts, with some of the material within the end holders actually pulled out into the thread. The behavior of the block-polymer blends could probably be characterized in more detail by the force-ductility test (1) or the toughness-tenacity test (2) both of which measure stress-strain properties of asphalt cement binders.

3. Rolling Thin Film Oven Aging

Table 14 presents results after exposure of the modified binders to the Rolling Thin Film Oven Test. Generally, the test results are inconsistent and difficult to analyze. AASHTO specifications allow a four-fold increase in viscosity at 140^oF (60^oC); all of the materials meet this criterion.

Viscosity at 275^oF (135^oC) for the blends containing SBR decreased during the RTFO test, probably indicating thermal degradation of the polymer during the 325^oF (163^oC) exposure. Binders containing the LDPE 526 and EVA yielded the largest increase in consistency.

Table 14. Change in properties of asphalts and selected blends exposed to rolling thin film oven aging.

Serial No.	86	101	102	130	131	132	133	134	135	97	113	136
Composition, %												
Texaco AC-5	100	...	95	...	97	95	95	95
San Joaquin Valley AR-1000	...	100	...	95	97	95	95	90
S-B-S/S-B block polymer ^a	5	5
SBR ^b	3	5	3	5
EVAC	5
LDPE 526 ^d	5	5	...
Microfil-8 ^e	10
Viscosity at 140°F ^f , P	537	423	6720	1720	1960	5480	4020	10,100	1170	2200	1295	889
Viscosity at 275°F ^g , cSt	217	150	873	431	1020	2780	1190	3600	634	843	399	257
Penetration at 77°F ^h , 100 g, 5 s	186	164	103	134	140	114	83	72	156	105	98	121
After Rolling thin Film Oven Test ⁱ												
Weight change, %	-0.07	-1.08	-0.05	-0.95	-0.19	-0.19	-0.76	-0.63	-0.11	-0.05	-0.91	-0.81
Viscosity at 140°F, P	1190	983	15,900	2940	4110	9230	8250	19,600	2740	5060	4170	1890
η_a/η_o	2.22	2.11	2.37	1.71	2.10	1.68	2.05	1.94	2.34	2.30	3.22	2.13
Viscosity at 275°F, cSt	311	180	2680	486	877	2400	1170	2710	1040	1320	431	324
η_a/η_o	1.43	1.20	3.28	1.13	0.86	0.86	0.98	0.75	1.64	1.57	1.08	1.26
Penetration at 77°F	112	104	80	87	85	103	49	46	73	65	57	78
% of original penetration	60	63	78	65	61	90	59	64	47	62	58	64

^aKraton TR60-8774, blend of equal parts Kraton D-1101 three-block S-B-S polymer and Kraton DX-1118 two-block S-B (styrene-butadiene) polymer.

^bStyrene-butadiene rubber from Dow XUS 40052.00 latex.

^cElvax 150, 32-24% vinyl acetate, softening point 230°F, specific gravity 0.957.

^dDow low-density polyethylene, density 0.919, melt index 1.0.

^eLot CS-4632, 93.3% high-structure HAF carbon black, 6.7% oil.

^fAASHTO T202.

^gAASHTO T201.

^hAASHTO T49.

ⁱAASHTO T240.

4. Sliding Plate Viscosity at 77⁰F

The sliding glass plate microviscometer (ASTM D3570-77) was used to determine binder viscosities at 77⁰F (25⁰C). For purposes of comparison, viscosities determined at three temperatures for selected asphalts and asphalt-additive blends are presented in table 15.

The sliding plate test is inappropriate for binders containing granular materials with particle sizes approaching the binder film thickness. As a result, data from the binder containing LDPE 526 is questionable.

Viscosity at 77⁰F of the AC-5 is increased significantly by the addition of the SBS/SB block polymer and the EVA. However, only slight increases in viscosity at 77⁰F are exhibited upon addition of the SBR and the Microfil-8. Microfil-8 is composed of carbon black with 8 percent oil. This oil may be at least partly responsible for retention of the low viscosity at 77⁰F.

5. Summary of Traditional Tests on Other Modified Binders

Results from "traditional" tests on four sulfur extended asphalt (SEA) blends and two crumb rubber blends are included (table 16) for comparison with the other modified asphalt binders. To produce the SEA blends, the asphalt was heated to 285⁰F (140⁰C), then molten sulfur was added and blended for five minutes. The blends were then poured into small containers and cooled rapidly and avoid separation. The crumb rubber blends were produced using a Genstar rubber product. Asphalt was heated to 375⁰F (190⁰C), then the rubber was added and blended for two hours at 375⁰F, which is typical for pavement construction.

6. Low Temperature Fracture Susceptibility

The low temperature fracture susceptibility of additive-asphalt blends was evaluated on the basis of two approaches: (1) sophisticated rheometrics mechanical spectrometer analysis and (2) traditional

Table 15. Viscosity data at 275, 140 and 77°F for selected asphalts and asphalt-additive blends.

Asphalt	Additive	% Asphalt: % Additive	275°F, ^f cst.	140°F, ^g P	77°F ^h P x 10 ⁶
Texaco AC-5	224	506	0.25
Texaco AC-20	398	2040	0.31
Texaco AC-5	S-B-S/S-B Block Polymer ^a	95:5	873	1170-6720	0.42
	SBR ^b	97:3	1020	1960	0.28
	EVA ^c	95:5	618	1160	0:32
	LDPE 526 ^d	95:5	843	2200	1.5
	Microfil-8 ^e	85:15	740	1850	0.26

^aKraton TR60-8774, blend of equal parts Kraton D-1101 three-block S-B-S polymer and Kraton DX-1118 two-block S-B (styrene-butadiene) polymer.

^bStyrene-butadiene rubber from Dow XUS 40052.00 latex.

^cElvax 150, 32-34% vinyl acetate, softening point 230°F, specific gravity 0.957.

^dDow low-density polyethylene, density 0.919, melt index 1.0.

^eLot CS-4632, 93.3% high-structure HAF carbon black, 6.7% oil.

^fAASHTO T201.

^gAASHTO T202.

^hASTM D-3570.

ⁱNot determined.

Table 16. Summary of properties of control crumb rubber and sulfur-extended asphalt blends.

Asphalt Source Grade	Texaco					
	AC-10			AC-20		
Additive in Blend	12%CR ^k	22%CR	20%S ^l	35%S	20%S	35%S
Specific gravity at 77°F ^a			1.229	1.383	1.233	1.386
Flash point ^b , COC, °F	* ^m	* ^m	375	385	365	370
Sliding Plate Viscosity, ^c 77°F, P	3.53x10 ⁶	3.00x10 ⁶	1.46x10 ⁵	2.90x10 ⁵	8.9x10 ⁵	9.9x10 ⁵
Viscosity at 140°F ^d , P	840	2000	796	807	833	1010
Viscosity at 275°F, cSt	250	175	148	145	176	115
Penetration at 77°F ^f , 100 g, 5s	56	49	144	151	84	93
Penetration at 39.2°F, 100 g, 5 s	24	23	20	25	20	18
Softening point, g °C	53	66	45	46	47	47
Softening point, °F	128	151	113	114	117	116
Ductility, ^h cm						
77°F	13 ⁱ	10 ⁱ	75	35	51	26
39.2°F	6 ⁱ	10 ⁱ	14	15	5	1
PVN (77-215°F)	-1.49	-2.08	-1.40	-1.36	-1.64	-2.20
P.I. from penetration at 77°F and softening point	0.9	1.4	0.2	0.3	0.2	0.6
After Rolling Thin Film Oven Test ^j weight change, %	* ^m	* ^m	3.19	3.53	3.70	4.03
Penetration at 77°F % of original	65	70	60	60	70	65

^aAASHTO T228.

^bAASHTO T48.

^cASTM D3570.

^dAASHTO T202.

^eAASHTO T201.

^fAASHTO T49.

^gAASHTO T53.

^hASTM D113

ⁱThe particulate nature of the rubber-asphalt probably affected these values.

^jAASHTO T240.

^kCrumb rubber (Genstar)

^lElemental sulfur.

^mUnable to perform due to foaming.

techniques based on limiting stiffnesses of the binder. The latter approach will be discussed in this section while the rheometrics based approach will be discussed in detail later in this chapter.

In this section, the selected asphalts and blends will be evaluated based on predicted cracking temperatures using two methods: (1) limiting asphalt stiffness and (2) critical asphalt stress.

a. Limiting Stiffness Method

One of the simplest means of determining a predicted cracking temperature is to estimate the temperature at which the asphalts reach a critical value of "limiting stiffness." Developments by Canadian researchers and others have led to a proposed asphalt stiffness of approximately 145,000 psi at a 1/2-hour loading time as the limiting stiffness (3,4,5). Thus the critical temperature at which the asphalt stiffness reaches 145,000 psi (1×10^9 MPa) at 1/2-hour loading time is considered to be the predicted cracking temperature. Stiffnesses can be determined using the van der Poel nomograph. Predicted cracking temperatures based on this method for selected asphalts and blends are presented in table 17.

b. Critical Stress Method

Hills introduced a procedure for determining predicted cracking temperatures of pavements based on an estimation of thermal stresses developed in the asphalt phase (6). In this procedure, it is assumed that the thermal stress, σ_t , developed in asphalt as it cools can be calculated from:

$$\sigma_t = (S_i \times \alpha_A \times \Delta T) \quad \text{Equation 1}$$

where S_i is the asphalt stiffness at a one hour loading time at a series of temperature intervals, ΔT . The coefficient of linear thermal contraction, α_A , is assumed to be 2×10^{-4} in/in/°C.

Table 17. Summary of predicted cracking temperatures for selected asphalt-additive blends.

Asphalt Type	Additive Type	Blend of Asphalt and Additive % Asphalt: % Additive	Cracking Temperature, °C		
			Limiting Stiffness Method	Critical Stress Method	
Texaco AC-20	None	-	-38	-36	
Texaco AC-10	None	-	-40	-40	
Texaco AC-5	None	-	-49	-44	
SJV AR-4000	None	-	-23	-23	
SJV AR-2000	None	-	-29	-27	
SJV AR-1000	None	-	-38	-34	
Texaco AC-10	Microfil-8	90:10	-40	-40	
		85:15	-38	-34	
Texaco AC-5	Microfil-8	90:10	-50	-45	
		85:15	-45	-45	
SJV AR-1000	Microfil-8	90:10	-38	-40	
		85:15	-35	-36	
SJV AR-2000	Microfil-8	90:10	-34	-32	
		85:15	-32	-30	
Texaco AC-5	Dow Latex (SBR)	97:3	-37	-40	
		95:5	-36	-39	
SJV AR-1000	Dow Latex (SBR)	97:3	-22	-30	
		95:5	-14	-13	
Texaco AC-5	Kraton TR-60-8774	95:5	-65	-50	
		Kraton/Dutrex Blend	94:6	-53	-42
		Kraton/Dutrex Blend	88:12	-40	-42
SJV AR-1000	Kraton/Dutrex Blend	94:6	-39	-32	
		88:12	-36	-32	
Texaco AC-5	Novophalt	95:5	-45	-50	
SJV AR-1000	Novophalt	95:5	-35	-32	
Texaco AC-5	EVA (Elvax 150)	97:3	-52	-40	
		95:5	-72	-36	
	EVA (Exxon EX042)	97:3	---	-40	
		95:5	-55	-45	
SJV AR-1000	EVA (Elvax 150)	95:5	-33	---	
SJV AR-1000	EVA (Exxon EX042)	97:3	-30	-30	
		95:5	-32	-35	
Texaco AC-10	Crumb Tire Rubber	88:12	-70	-55	
		78:22	-67	-60	
	Sulfur	80:20	-52	-44	
Texaco AC-20	Sulfur	65:35	-40	-46	
		80:20	-40	---	
		65:35	-35	---	

Using asphalt penetration data, asphalt stiffnesses at 18°F (10°C) intervals from, say, 32°F (0°C) down to -58°F (-50°C) are determined. When required, the temperature range can be modified to accommodate various asphalt grades. The thermal stress, σ_t , is calculated by summing the individual stress increments.

Hills concluded from semi-theoretical considerations and from mix cracking observations that pavement cracking occurred at a temperature corresponding to a calculated thermal stress, σ_t , of about 73 psi (5×10^5 MPa). The calculated cracking temperature is taken as the temperature at which a stress of 73 psi is induced. These critical temperatures are tabulated in table 17.

c. Discussion of Low Temperature Fracture Analysis

The data from table 17 must be viewed with caution. This is because the limiting stiffness and critical stress levels established for asphalt cement may not be acceptable failure criteria for additive modified binders. However, without established failure criteria for additive-modified asphalts, the criteria traditionally used for unmodified asphalts may be used as a guide (and only as a guide.) On this basis, the following observations are presented:

1. Microfil-8, Elvax (EVA), and Novophalt do not appear to significantly alter the temperature at which thermally induced cracking occurs in the AC-5 and AR-1000 asphalts tested.
2. The addition of the Dow latex appears to increase the temperature at which low temperature cracking occurs for both the Texaco AC-5 and San Joaquin AC-1000 asphalt blends; this may be anomalous.
3. Crumb tire rubber appears to be very effective in lowering the predicted pavement cracking temperature when used with Texaco AC-10. Shell Kraton TR-60-8774 performs almost as well with Texaco AC-5.
4. In every case, the softer grade asphalts or the soft asphalt-additive blends exhibit lower cracking temperatures than do the stiffer grades from the respective sources (i.e., AC-20 or AR-4000).

7. Heat Stability Study

Heat stability of Texaco AC-5 and selected additive blends with Texaco AC-5 was evaluated by exposing the binders to 500°F (260°C) for two hours in a covered penetration can. (Note: this is not an oxidative hardening test.) Viscosity and penetration data were obtained after the heating procedure and compared to data that was obtained before heating. Results show primarily that no hardening occurs in these materials when exposed to 500°F for two hours while protected from exposure to significant oxygen. The apparent decreases in consistency after heating may be due to interlaboratory differences. Two exceptions to this are SBR latex and Kraton SBS/SB in Texaco AC-5, both of which exhibited a significant decrease in consistency. This test is nonstandard and was first used in testing Solar Laglugel (7).

Obviously, the interpretation of results is quite subjective. Test results are presented in table 18. Unpublished data from Shell and California DOT show that prolonged exposure of SBR and SBS modified asphalts to temperatures above 350°F (176°C) for significant periods will cause a reduction in viscosity.

CHANGES IN COMPOSITION WITH AGING - AN INFRARED STUDY

1. Procedures for Analysis by Infrared Spectroscopy

Specific chemical functionality in asphalt and changes in chemical functionality with aging were examined by functional group analyses procedures developed at Western Research Institute (WRI) (8-10). When possible, important chemical functionalities present in the asphalt modifiers were identified by infrared (IR) spectroscopy.

In the infrared procedure, the qualitative and quantitative identification of important functionalities in asphalt having overlapping and interfering infrared absorption bands is made possible by the simultaneous application of three special techniques: 1) the use of the polar spectral solvent, tetrahydrofuran (THF), to break up hydrogen bonding and simplify the absorption spectrum; 2) the use of selective

Table 18. Summary of data from Texaco AC-5 and selected additive blends before and after heat stability testing.

Composition	Viscosity				Penetration	
	140°F, cSt		275°F, P		@ 77°F	
	Before Heat Testing	After Heat Testing	Before Heat Testing	After Heat Testing	Before Heat Testing	After Heat Testing
95% Texaco AC-5 + 5% LDPE 526 ^a	2200	1796	843	833	60	68
95% Texaco AC-5 + 5% SBS ^b	2100	1420	873	465	82	120
97% Texaco AC-5 + 3% EVA ^c	490	410	380	300	107	106
85% Texaco AC-5 + 15% Microfil-8 ^d	1850	1900	740	*f	75	98
95% Texaco AC-5 + 5% SBR ^e	3900	904	2780	*f	116	147
Texaco AC-5	510	500	211	190	155	145

^aDow low-density polyethylene, density 0.919, melt index 1.0.

^bKraton TR60-8774, blend of equal parts Kraton D-1101 three-block S-B-S polymer and Kraton DX-1118 two-block S-B (styrene-butadiene) polymer.

^cElvax 150, 32-24% vinyl acetate, softening point 230°F, specific gravity 0.957.

^dLot CS-4632, 93.3% high-structure HAF carbon black, 6.7% oil.

^eStyrene-butadiene rubber from Dow XUS 40052.00 latex.

^fUnable to obtain data due to repeated clogging of viscometer.

chemical reactions to shift or eliminate the absorption bands of the chemical functionality of interest; and 3) the use of differential infrared spectrometry, using a double-beam spectrophotometer, with which the samples before and after selective chemical reaction are compared to reveal only the absorption bands affected by the selective reaction. Since THF has absorption bands in the regions of interest, solvent compensation must be used.

Carboxylic acids are determined using triphenyltin hydroxide as the selective reagent. Reaction with sodium hydroxide converts carboxylic acids, anhydrides and phenolics to their salts. To calculate the ketone concentration, background and sodium hydroxide-reactive material contributions must be subtracted from the total carbonyl absorption. The remaining carbonyl band then is attributed to ketones. Two-quinolone types and acid salts are determined using a silylation reaction. In addition to the differential spectra in THF, a solvent-compensated spectrum in carbon disulfide (CS_2) is also obtained to determine sulfoxides and provide a complete infrared spectrum of the sample except for a small region ($1600\text{-}1400\text{ cm}^{-1}$) which is masked by the CS_2 .

All spectra are determined on 50 mg samples in 1.00 ml of solvent and with 1.00 mm sealed cells. Concentrations of the chemical functional groups of interest are calculated by measuring the area under their infrared absorption bands and using the molar absorptivities of corresponding functional groups in model compounds.

2. Thin Film Accelerated Aging Test

The thin film accelerated aging test (TFAAT) was used to age all samples of modified and unmodified asphalts evaluated in the IR study. The TFAAT simulates the average level of oxidative aging in asphalt that occurs in the field during 10-15 years of service. The test is a modification of the rolling-microfilm test developed by R. J. Schmidt of Chevron (11) in which a 0.5-g sample is aged at 210°F (98.9°C) for 48 hours. Schmidt's test was designed to simulate field aging. In the modified test, 4.0 gm of asphalt is aged 72 hours at (235°F) 113°C .

These conditions produce an oxidation level in asphalts that corresponds with the typical oxidation level found in a series of ten 13-year-old pavements. In preparation for aging, the asphalts dissolved in toluene, are cast as thin films (0.16 mm) on the inner surface of RTFO (rolling thin-film oven) bottles. During aging, the bottle opening is restricted with a capillary tube (3 mm diameter) to provide approximately the same loss of volatile asphalt components as occurs in normal pavement. The sample is aged in a rolling thin film oven.

3. Infrared Analysis of Neat Asphalts

Functional group analyses were performed on San Joaquin AR-1000 and Texaco AC-5 asphalts (table 19). The two asphalts are significantly different with regard to their functional group content. The San Joaquin asphalt has a higher content of all heteroatoms. The phenolic functionality and pyrrolic functionality are about four times greater in the San Joaquin asphalt than the Texaco asphalt with their combined content being 0.32 and 0.085 mol L⁻¹, respectively. The acid content of the San Joaquin is 0.045 mol L⁻¹ which is relatively high for asphalts. All acids in this asphalt are present as acid salts, probably produced during caustic treatment of the crude. No significant amounts of acids were found in the Texaco asphalt. The aromaticity of the asphalts differs greatly. The aromatic C=C stretching band in asphalt is a measure of the asphalt aromaticity. Based on the data in table 19, the aromaticity of the San Joaquin asphalt appears to be considerably greater than that of the Texaco asphalt.

The higher aromaticity of the San Joaquin asphalt is important with regard to the solvency characteristic of this asphalt, and should have a significant effect on its molecular interactions, sensitivity to oxidative hardening, and its interaction with polymers. The high carboxylic acid salt content of the San Joaquin asphalt is probably beneficial in acting as a dispersant for polar asphalt components that are produced by long-term oxidation. Good dispersion of components is beneficial in reducing age hardening and may reduce molecular

Table 19. Composition and aging characteristics of neat asphalts as determined by infrared functional group analysis.

Asphalts	Treatment	Concentration, mol·L ⁻¹								Aromatic C=C relative peak height at 1600 cm ⁻¹	Aging index ^b
		Ketones	Anhydrides	Carboxylic acids		Sulfoxides	2-Quinolones	Phenolics	Pyrrololics		
				Free	Salts						
San Joaquin Valley AR-1000	Unaged	Trace	0	0	0.046	0.15	0.019	0.07	0.25	50.5	
	aged ^a	0.34	0.027	0.021	0.024	0.23	0.019	0.07	0.25	52.5	8
45 Texaco AC-5	Unaged	Trace	0	0	0	0.14	0.012	0.15	0.07	32.5	
	aged	0.21	0.007	0.016	0	0.34	0.013	0.15	0.07	36.0	41

^a Aged by thin film accelerated aging test, 3 days, 113°C (235.4°F)

^b Ratio of 60°C (140°F) viscosity after and before aging

structuring. However, this dispersion reduces the micellar interactions which may contribute to poor mix setting characteristics which, in turn, may lead to rutting and permanent deformation. In addition, the carboxylic acid salt content may be detrimental to the moisture resistance of the asphalt mixture. The above compositional characteristics should be considered when interpreting physical property data on the modified asphalts and the corresponding laboratory pavement design mixtures.

Ketone and anhydride formation (table 19) indicate the San Joaquin asphalt is more reactive with atmospheric oxygen than the Texaco asphalt. However, oxidation of sulfides to sulfoxides was more prevalent in the Texaco asphalt. Ketones and sulfoxides are the major oxygen-containing functionalities produced in asphalts during oxidative aging. Ketones are not naturally occurring in petroleum but are easily formed upon exposure to atmospheric oxygen and, further, are unstable at high temperatures and may decompose.

Although the acids in the San Joaquin asphalt were initially present in their acid salt form, the salts were partially converted to free acids during aging (table 19). Only a small amount of carboxylic acid was formed during oxidative aging. The concentration of 2-quinolone types, phenolics, and pyrrolics were not changed significantly with aging. These polar functionalities are important chemical parameters affecting the association of asphalt molecular agglomerates, asphalt-aggregate bonding, and interaction between asphalt components and modifiers.

It is instructive to compare the rate of chemical oxidation in the two asphalts (as indicated by ketone and sulfoxide formation) with the aging indexes determined from the 140°F (60°C) viscosities before and after aging. The ketone content was considerably higher in the San Joaquin asphalt than in the Texaco asphalt and the sulfoxide content was lower. The combined concentrations of these two chemical functionalities produced on oxidation, however, was 0.57 and 0.55 mol L⁻¹ for the San Joaquin and Texaco asphalt, respectively. This concentration represents, on the average, about one functionality for every two asphalt molecules. Although the combined concentrations of the ketones and sulfoxides

produced with aging were nearly the same in both asphalts, the increase in viscosity with aging, as indicated by the TFAA aging index, was much higher for the Texaco asphalt (41) than for the San Joaquin asphalt (8) (table 19). The low aging index of the San Joaquin asphalt is believed to result from its ability to disperse the polar functionality and reduce the degree of molecular association on aging. Significant chemical compositional factors contributing to the low aging index are probably the comparatively high aromaticity and concentration of acid salts (natural dispersants) previously discussed.

4. Infrared Analysis of Asphalts Modified with Carbon Black

Functional group analyses were performed on asphalts containing Microfil-8 before and after the TFAA test. Examination of these samples required special handling techniques because carbon black was not soluble in the infrared spectral solvents. Results of the analyses are shown on table 20 together with the analyses of the unmodified asphalts for comparison.

In order to determine functional group concentrations in the asphalts containing Microfil-8, the carbon black had to be removed to permit reactions with the selective chemical reagents and to permit infrared spectra to be obtained. This was accomplished by dissolving the asphalt in toluene, filtering twice and finally centrifuging. After centrifugation the toluene-asphalt solution was decanted from residual carbon black and the toluene was removed from the solution using a rotary evaporator.

The purpose of examining the asphalt recovered from the carbon black was to determine the tendency for the additive to adsorb polar functionality in the original asphalt or formed with aging. This tendency could affect the aging characteristics and the physical properties of the asphalt. The data should be useful in the interpretation of physical property measurements on the asphalts and asphalt-aggregate mixtures.

Addition of Microfil-8 to the San Joaquin asphalt resulted in adsorption of free carboxylic acids but did not result in strong

Table 20. Composition and aging characteristics of asphalts containing carbon black as determined by infrared functional group analysis.

Asphalt	Treatment		Concentration, mol·L ⁻¹						Aging Index ^b
	Carbon Black, ^a %	Aged ^b	Ketones	Anhyd- rides	Carboxylic acids		Sulfox- ides	2-Quinolones	
					Free	Salts			
San Joaquin AR-1000	0	No	Trace	0	0	0.046	0.15	0.019	--
	0	Yes	0.34	0.027	0.021	0.024	0.23	0.019	8
	15 ^c	No	Trace	0	0	0.044	0.11	0.014	--
	10 ^c	Yes	0.26	0	0	Trace	0.33	-- ^d	--
	15 ^c	Yes	0.12	0	0	0	0.33	-- ^d	6
Texaco AC-5	0	No	Trace	0	0	0	0.14	0.012	--
	0	Yes	0.21	0.007	0.016	0	0.34	0.013	44
	15 ^c	No	N.D. ^e	N.D.	N.D.	N.D.	N.D.	N.D.	--
	10 ^c	Yes	0.12	0	0	0	0.29	-- ^d	--
	15 ^c	Yes	0.10	0	0	0	0.32	-- ^d	49

^a Microfil-8

^b Aged by thin film accelerated aging test, 3 days, 113°C (235.4°F)

^c Asphalts containing Microfil-8 were dissolved in toluene, the additive filtered off, and the asphalt recovered before functional group analysis

^d Value uncertain because of interfering absorption

^e Not determined.

adsorption of the carboxylic acid salts. This is evidenced by the complete recovery of the acid salts in the asphalt separated from the carbon black by toluene. However, when the asphalt containing the Microfil-8 was aged, virtually all of the acid salts were adsorbed by the carbon black. A possible explanation for these results is that the acid salts were converted to free acids during the aging and the free acids have a strong affinity for the surface of the carbon black; whereas, their acid salts do not.

The ketone concentration in the aged asphalts containing Microfil-8 was considerably lower than in the neat aged asphalts, and anhydrides were absent. This could be caused by adsorption of the ketones and anhydrides on the carbon black or by inhibited oxidation of the asphalt.

If the latter effect is prevalent, then the additive has a significant effect on the aging mechanism. The higher-than-normal sulfoxide content of the aged asphalt containing Microfil-8 suggests that the oxidation mechanism may have been altered. The aging index, however, was not significantly affected by Microfil-8.

Examination of the infrared spectra of the asphalts before and after aging showed that molecules containing the pyrrolic NH and phenolic OH functional groups were not adsorbed by the carbon black. However, after aging, most of the materials with carbonyl functionality remained with the carbon black after toluene extraction. Why oxidative aging caused the irreversible adsorption of these chemical functionalities is not known. The sulfoxides did not appear to be strongly adsorbed on the carbon black after aging.

5. Infrared Analysis of Asphalts Modified with EVA

The San Joaquin and Texaco asphalts were evaluated by infrared analyses after being modified with 3 percent and 5 percent Dupont Elvax 150 and Exxon EX042 (table 21). The EVA resin concentration was monitored by following the peak intensity (height) of the carbonyl band of its acetate functionality, which absorbs at 1735 cm^{-1} . Comparison of the acetate band peak intensities of the EX042 and Elvax 150 resins in

Table 21. Composition and aging characteristics of asphalts containing ethylene-vinyl acetate polymer as determined by infrared functional group analysis.

Asphalt	Treatment		Concentration, Mol·L ⁻¹		Carbonyl band of EVA at 1735 cm ⁻¹ absorbance ^c	Phase separation in aged film	Aging Index ^a
	Modifier	Aged	Ketones ^e	Sulfoxides			
San Joaquin AR-1000	None	No	Trace	0.15	--	--	--
	None	Yes	0.29(0.34)	0.25	--	None	8
	3% EVA ^e	No	Trace	Trace	0.105	None	--
	3% EVA ^e	Yes	0.43	0.17	No loss on aging	None	--
	5% EVA ^e	No	Trace	Trace	0.175	None	--
	5% EVA ^e	Yes	0.39	0.19	No loss on aging	None	--
	3% EVA ^g	No	Trace	Trace	0.270	None	--
	3% EVA ^g	Yes	0.38	0.21	No loss on aging	None	--
	5% EVA ^g	No	Trace	Trace	0.420	None	--
	5% EVA ^g	Yes	0.34	0.25	No loss on aging	None	4
Texaco AC-5	None	No	Trace	0.14	--	--	--
	None	Yes	0.21	0.34	--	None	44
	3% EVA ^e	No	Trace	Trace	0.105	--	--
	3% EVA ^e	Yes	0.23	0.30	No loss on aging	Small-sized globules	--
	5% EVA ^e	No	Trace	Trace	0.180	--	--
	5% EVA ^e	Yes	0.24	0.32	No loss on aging	Small-sized globules	--
	3% EVA ^g	No	Trace	Trace	0.255	--	--
	3% EVA ^g	Yes	0.27	0.35	No loss on aging	Medium-sized globules	--
	5% EVA ^g	No	Trace	Trace	0.435	--	--
	5% EVA ^g	Yes	0.26	0.38	No loss on aging	Medium-sized globules	17

- ^a Aged by thin film accelerated aging test, 3 days, 113°C (235.4°F)
^b Calculated from differential spectra of aged versus unaged asphalts after subtracting anhydride band area
^c Determined from CS₂ spectra
^d Calculated from spectrum of aged, modified asphalt after subtracting background absorption and using standard band boundary procedures
^e Exxon EX042 ethylene-vinylacetate polymer
^f Confirmed by differential spectra of aged versus unaged asphalts
^g Dupont Elvax 150 ethylene-vinylacetate polymer

the unaged samples showed that the Elvax 150 resin contained about 2.5 times the acetate functionality of the EX042 resin. The effect of this difference in functionality should be considered when comparing physical property data of asphalts modified by these resins. Also, a comparison of the acetate peaks agreed with the relative concentration of resins. This confirmed that there had been no stratification of the resin in the asphalt and that the resin dispersion was homogeneous.

A significant difference in solubility or compatibility of the resins in the two different asphalts was observed. A separation of EVA from the asphalt phase was noted after aging Texaco AC-5 that contained both EVA polymers. Further the EX042 separated into smaller particles than the Elvax 150. This may relate to its lower acetate functionality. Visually, both the EX042 and Elvax 150 resins appeared completely soluble or compatible in the San Joaquin AR-1000 asphalt.

The superior solvent power of the San Joaquin asphalt for the EVA resins is not entirely unexpected when the chemical functionality of the two asphalts is considered. The San Joaquin asphalt has a higher concentration of polar functional groups and higher aromaticity than the Texaco asphalt.

Because of EVA acetate absorption which interfered with the normal determination of ketones in the functional group analysis, an alternate method of ketone determination was employed. Differential infrared spectra of THF solutions of the modified asphalts, before and after aging, were obtained; thus, the EVA bands were cancelled and the band area of the carbonyl functionality formed with oxidation was displayed. Since this band area contains absorption of both ketones and anhydrides, the area contributed by the anhydrides (determined from analysis of aged, unmodified samples) was subtracted from the total carbonyl band area to give the band area of ketone absorption.

6. Infrared Analysis of Asphalts Modified with Polyethylene

Infrared techniques were used to evaluate both the San Joaquin and Texaco asphalts modified with 5 percent Dow 526 low-density polyethylene

before and after oxidative aging (table 22). The mixtures were prepared by the patented Novophalt process.

The polyethylene (PE) separated from the asphalt as discrete, transparent globules in the asphalt film during the TFAA test. The polyethylene globules were larger in the aged San Joaquin asphalt than in the Texaco asphalt.

Ketone content of the PE-modified San Joaquin asphalt was lower after aging than the unmodified control. The significance of the lower ketone value is uncertain since the polyethylene is not expected to reduce the reactivity of the asphalt with atmospheric oxygen. The lower ketone content in the modified San Joaquin asphalt together with the lower sulfoxide content for both asphalts may result from antioxidants, which are often added to polyethylene. Ketone content was nearly the same for the control and for the PE-modified Texaco asphalt.

7. Infrared Analysis of Asphalts Modified with SBR

Styrene-butadiene rubber (SBR) has olefinic double bonds in its structure that could lead to instability in a modified asphalt system, either through reaction with atmospheric oxygen or through crosslinking. Crosslinking could lead to high viscosity and rigidity in the modified asphalt. Since the crosslinking reaction would be promoted by high temperatures, crosslinking may be a potential problem during high-temperature storage of asphalt and during processing in a hot-mix plant. To follow the potential loss of the double bond through SBR crosslinking, the absorbance of the C=C at 965 cm^{-1} was monitored before and after oxidative aging. In addition to changes in the double-bond absorbance, the ketone and anhydride concentrations after aging were also monitored for increases that might result from SBR oxidation. The above analysis is possible since SBR is soluble in the solvents required for infrared analysis. Hydroperoxide-free THF was used to deposit a thin film of modified asphalt for aging in the TFAA test. Analyses of asphalts modified with Dow XUS 40052.00 SBR latex are shown in table 23.

Ketone and anhydride contents in both SBR-modified asphalts were higher than in the control asphalts. These results suggest possible

Table 22. Composition and aging characteristics of asphalts containing polyethylene as determined by infrared functional group analysis.

Asphalt	Treatment		Concentration, Mol·L ⁻¹				Sulfox- ides	Phase separation in aged film	Aging ^a Index
	Modifier	Aged ^a	Ketones	Anhydrides	Carboxylic acids				
					Free	Salts			
San Joaquin Valley AR-1000	None	No	Trace	0	0	0.046	0.15	--	--
	None	Yes	0.34	0.027	0.021	0.024	0.23	None	8
	5% PE ^b	No	Trace	0	0	0.051	Trace	--	--
	5% PE ^b	Yes	0.27	0.022	0.016	0.023	0.12	PE globules	56
Texaco AC-5	None	No	Trace	0	0	0	0.14	--	--
	None	Yes	0.21	0.007	0.016	0	0.34	None	44
	5% PE ^b	No	Trace	0	0.005	0	Trace	--	--
	5% PE ^b	Yes	0.22	0.013	0.011	0	0.30	PE globules	197

^a Aged by thin film accelerated aging test, 3 days, 113°C (235.4°F)

^b Dow 525 low-density polyethylene (Novophalt process)

Table 23. Composition and aging characteristics of asphalts containing styrene-butadiene as determined by infrared functional group analysis.

Asphalt	Treatment		Concentrations, Mol·L ⁻¹					Olenfinic C=C at 965 cm ⁻¹ , absorbance	Phase separation in aged film	Aging Index ^a
	Modifier	Aged ^a	Ketones	Anhydrides	Carboxylic acids		Sulfoxides			
					Free	Salts				
San Joaquin AR-1000	None	No	Trace	0	0	0.046	0.15	--	--	--
	None	Yes	0.34	0.027	0.021	0.024	0.23	--	None	8
	5% SBR ^c	No	Trace	0	0.022	0.024	Trace	0.255	--	--
	5% SBR ^c	Yes	0.48	0.038	0.034	0.014	0.24	0.240 ^b	Cracks	23
54 Texaco AC-5	None	No	Trace	0	0	0	0.14	--	--	--
	None	Yes	0.21	0.007	0.016	0	0.34	--	None	44
	5% SBR ^c	No	Trace	0	0.016	0	Trace	0.215	--	--
	5% SBR ^c	Yes	0.24	0.008	0.014	0	0.26	0.250 ^b	Cracks	28

^a Aged by thin film accelerated aging test, 3 days, 113°C (235.4°F)

^b Sulfoxide band produced minor interference with this band

^c Dow XUS 40052.00 SBR latex

oxidation of the SBR, although the differences seen for the Texaco system are within the single-determination repeatability of the TFAA test. Significant changes in the concentrations of the C=C after aging were not apparent. The shoulder of the sulfoxide band formed upon oxidation produced a minor interference with the determination of the C=C peak height, which could account for the differences seen. If oxidation of the SBR does occur, forming ketones, it may be due to the oxidation of the benzylic carbon of the styrene moiety, which would not affect the concentration of the olefinic double bond. However, since oxidation of the styrene moiety would produce only ketones and not anhydrides, the corresponding increase in anhydride concentration in the modified asphalt compared with the control suggests that the increased oxidation results from asphalt oxidation, possibly promoted by components in the SBR. The significant decrease in sulfoxide content of the aged, modified Texaco asphalt may result from materials in the SBR that act as antioxidants with regard to sulfoxide formation. Finally, it should be noted that the acid salts in the unaged San Joaquin Valley asphalt containing SBR were partially converted to free acids, suggesting some inherent acidity in the SBR latex.

In summary, it is possible that the addition of SBR might increase the oxidation of asphalt in some SBR-modified systems. The possibility of SBR crosslinking via reaction of the double bond should not be overlooked in considering the behavior of this system in high-temperature storage or in a hot-mix plant. After aging in the TFAA test, the SBR-modified system showed a network of fine cracks in the thin asphalt film. However, the SBR appeared to remain dispersed in the asphalt. Since the aging test temperature is considerably higher than that experienced by pavements, the correlation between cracking in the aged film to the behavior of the SBR systems in pavements is uncertain.

8. Infrared Analysis of Asphalts Modified with SBS

Although the SBS polymer is a thermoplastic rather than an elastomer, it has chemical functionalities in common with the SBR system such as the potentially reactive olefinic double bond. Thus, similar chemical

changes were expected for SBS and SBR polymers with aging. One SBS system was further modified by the addition of equal amounts of an extender oil, which in addition to modifying the SBS, could partially offset the effect of the absorption of asphalt components by the SBS. Infrared analysis of the two asphalts modified with Shell Kraton D-1101 SBS containing Dutrex 739 extender are shown in table 24. An increase in ketones with aging is seen for both asphalt systems. No acid salts were converted to free acids by the SBS in the unaged asphalt in contrast to the SBR-modified San Joaquin Valley asphalt.

Evaluation of changes in the SBS double bond (C=C) showed slight decreases in infrared absorption intensity with aging for both modified asphalts; however, these differences are within the error limits allowed for interference from sulfoxide absorption in the aged samples. The SBS appears to be relatively stable during the aging test.

The relative solubilities or compatibilities of the SBS resin in the two asphalts are dependent on the asphalt source or composition, as they were with the EVA resin. The SBS is much more soluble, or compatible, with the San Joaquin Valley asphalt than with the Texaco asphalt. The aged film of the modified San Joaquin Valley asphalts showed no phase separation, i.e., the asphalt film appeared clear and homogeneous. On the other hand, SBS separated from the Texaco asphalt in small globules during the TFAA test.

The San Joaquin Valley asphalt was also modified with a 50:50 mixture of Kraton D-1101 and Kraton D-1118 (table 24). The slight increase in ketone content seen for the SBS-Dutrex system was also observed for the mixed SBS system. Partial conversion of the acid salts to free acids occurred in the San Joaquin Valley asphalt with and without the modifiers. These results indicate that the aging mechanism of the asphalt was not significantly altered by the presence of the SBS. This conclusion is further supported by the similar ketone and anhydride ratios exhibited by both modified and unmodified aged systems. The consistently lower sulfoxide content after aging in SBS-modified asphalts from both crude sources suggests that components in the SBS might be acting as antioxidants with regard to sulfoxide formation.

Table 24. Composition and aging characteristics of asphalts containing styrene-butadiene-styrene thermoplastic block copolymer.

Asphalt	Modifier	Aged ^a	Concentration, mol·L ⁻¹					Olefinic C=C at 965 cm ⁻¹ , absorbance	Phase separation in aged film	Aged Index ^a
			Ketones	Anhydrides	Carboxylic acids		Sulfoxides			
					Free	Salts				
	None	No	Trace	0	0	0.046	0.15	--	--	--
San Joaquin Valley	None	Yes	0.34	0.027	0.021	0.024	0.23	--	None	8
	3% SBS ^b + 3% oil ^c	No	Trace	0	0	0.048	Trace ^d	0.11	--	--
AR-1000	3% SBS ^b + 3% oil ^c	Yes	0.38	0.028	0.021	0.020	0.14	0.10	None	--
	5% Mixed SBS ^d	No	Trace	0	Trace	0.046	Trace	0.17	--	--
	5% Mixed SBS ^d	Yes	0.39	0.027	0.018	0.028	0.19	0.15	None	--
	None	No	Trace	0	0	0	0.14	--	--	--
Texaco AC-5	None	Yes	0.21	0.007	0.016	0	0.34	--	None	44
	3% SBS ^b + 3% oil ^c	No	Trace	0	0.014	0	Trace	0.11	--	--
	3% SBS ^b + 3% oil ^c	Yes	0.18	0.009	0.016	0	0.27	0.10	SBS globules	--

^a Aged by thin film accelerated aging test, 3 days, 113°C (235.4°F)

^b Shell Kraton D-1101 SBS thermoplastic block copolymer

^c Dutrex 739 rubber extender oil, ASTM D2226 type 101, serial 123

^d 2.5% Kraton D-1101 plus 2.5% Kraton D-1118 SBS thermoplastic block copolymer

NUCLEAR MAGNETIC RESONANCE (NMR) OF ORIGINAL ASPHALTS

The hydrogen and carbon aromaticity values were determined for Texaco AC-5, AC-10 and AC-20 and for San Joaquin AR1000 and AR2000 (table 25). Both the hydrogen and carbon spectra were obtained on a JEOL FX-270 NMR spectrometer. All samples were dissolved in mono-deuterated carbon trichloride (CDCl_3). Texaco AC-5 and San Joaquin AR2000 were also dissolved in benzene- d_6 (a better solvent) and the hydrogen and carbon NMR spectra obtained. Calculations of the aromaticity values in C_6D_6 after correcting for solvent interference resonances are within experimental error of the samples dissolved in CDCl_3 (table 26). The results indicated that no appreciable loss of material was observed because of insolubility when using CDCl_3 as a solvent. The weight percentage of aromatic carbons (or hydrogens) in a sample can be obtained by multiplying the total weight percentage of carbon (or hydrogen) by the aromaticity value.

The results given in table 25 for the hydrogen and carbon aromaticity values indicate little differences between the asphalt samples. The San Joaquin AR-1000 and AR-2000 samples appear to be slightly more aromatic than the Texaco samples. Differences in these values are near the experimental error of the NMR technique. Further experiments are needed to determine the actual limits of error for these samples.

All samples contain appreciable amounts of n-alkane. The average carbon chainlength for the n-alkane in each of the samples is given in table 25. The carbon chainlength of the n-alkane in San Joaquin asphalt samples seems to be slightly smaller than that of the Texaco samples.

ENERGIES OF INTERACTIONS BETWEEN ASPHALTS AND MODIFIERS

Thermodynamic measurements of interacting systems can often shed light on the mechanism by which they interact. Knowing whether the interaction is endothermic or exothermic, or knowing the rate at which the reaction takes place can help in a mechanistic interpretation (7). For that reason, limited thermodynamic measurements were made on the

Table 25. ^1H and ^{13}C aromaticity values and n-alkane carbon chainlength for asphalt samples.

Sample	Aromaticity Value ^a		Average n-alkane Carbon Chainlength
	^1H	^{13}C	
Texaco AC-5	0.066	0.306	18.0
Texaco AC-10	0.070	0.314	19.6
Texaco AC-20	0.068	0.319	18.5 (18.3) ^b
AR-1000	0.081	0.315	16.5
AR-2000	0.077	0.322	17.8

^a ^1H and ^{13}C values are ratios of aromatic hydrogen to total hydrogen and ratios of aromatic carbon to total carbon, respectively.

^bRephasing of carbon-13 spectrum

Table 26. Solvent effects on the hydrogen and carbon aromaticity values.

Sample	Aromaticity Value		Solvent
	^1H	^{13}C	
Texaco AC-5	0.060	0.332	C_6D_6
	0.066	0.306	CDCl_3
AR-2000	0.077	---	C_6D_6
	0.077	0.322	CDCl_3

interaction between a few additives and two selected asphalts. The heats of interaction were measured using a microcalorimeter at 328°F (150°C).

The interaction between the additive and the asphalt was measured for two or three hours. An initial energy peak representing maximum energy flow rate usually occurred within the first half hour. This was considered peak height. Following the peak energy release, a long energy curve tail usually occurred, often parallel to the zero base line. This was considered as tail height. The energy release at two hours was selected as a representative value, and is probably more representative of an interaction phenomenon than the peak height.

Polyethylene (LDPE 526) and latex (SBR) absorbed energy upon interacting (table 27). Carbon black (Microfil-8) and the ethylene vinylacetate polymers (Elvax 150 and EX042) released energy. The energies of interaction are also shown to be asphalt dependent.

The interaction between the polyethylene and SBR were highly endothermic, indicating a breaking of bonds probably occurred. This may be attributed to the swelling of the outer surface of the polymer particles. The polar ethylene vinylacetate polymers, Elvax 150 and EX042, interacted exothermically with the asphalts indicating the formation of bonds. Endothermic swelling could have still been occurring but was masked by the strong interaction possibly between the polar acetate group of the polymer and the polar asphalt molecules. Some dissolution at the ends of the polymer molecules may have occurred. Aging studies (TFAAT) showed that a very thin homogeneous film developed in the aging cell. Discrete particles were not detected when the cells were cleaned after measuring the heat of mixing. Perhaps both dissolution and swelling of the polymer by the asphalt occurred. Both phenomena would produce a polymer-asphalt interfacial region that would cause the mixture to behave as a semihomogeneous system.

Table 27. Heats of interaction between additives and asphalt¹.

<u>Asphalt</u>	<u>Additive</u>	<u>ΔHeat of Interaction, mcal/g-2 hr</u>	<u>Tail Height, mcal/g</u>
AC-5	Dow (LDPE) 526	+ 11,200	109
AR-1000	Dow (LDPE) 526	+ 11,800	113
AR-1000	SBR-Latex ²	+ 16,800	153
AC-5	SBR-Latex ²	+ 16,000	103
AC-5	Microfil-8	- 2,100	0.0
AR-1000	Microfil-8	- 3,400	0.0
AC-5	Elvax 150	- 1,211	0.9
AR-1000	Elvax 150	- 621	6.1
AC-5	EX042	- 480	2.0
AR-1000	EX042	- 680	2.1

¹ Particle size of the materials added to the asphalt will influence the rate and duration of the reactions. Since particle size of the additives was not controlled, these data should be viewed with caution.

² Water was removed from latex and SBR was cryogenically ground prior to use in this experiment.

VISCOELASTIC PROPERTIES OF UNAGED AND AGED BINDERS

1. Introduction to Viscoelasticity

Asphalt is considered a viscoelastic material that flows by both Newtonian viscous flow and Hookean elastic displacement. At high temperatures, when asphalt is a fluid, viscous flow is dominant. At low temperatures, near the glass transition temperature, elastic flow is dominant. Between these extremes asphalt flow is considered viscoelastic.

Newtonian flow implies the following equation is obeyed.

$$F/A = \eta \frac{\partial V_x}{\partial y} = \eta \dot{\gamma} \quad \text{Equation 2}$$

where F/A = shear stress or force per unit area,

η = viscosity coefficient,

$\frac{\partial V_x}{\partial y}$ = velocity gradient, and

$\dot{\gamma}$ = rate of shear strain.

Hookean elastic displacement is expressed in the following formula.

$$F/A = E \frac{\Delta L}{L} \quad \text{Equation 3}$$

where F/A = force per unit area,

E = Young's modulus, and

$\Delta L/L$ = strain (unit deformation).

The reader is reminded that for viscoelastic materials, modulus varies with time rate of displacement.

Maxwell combined Newton's viscosity equation and Young's elastic modulus formula and derived an equation to express viscoelastic flow. One result of Maxwell's equation is the stress relaxation equation.

$$\tau = \frac{\eta}{G(t)} \quad \text{Equation 4}$$

where τ = relaxation time or time for stress to decay to 1/e of its maximum value ($e = 2.718\dots$).

Large relaxation times imply either large viscosities and/or small elastic components. Short relaxation times imply either low viscosities and/or large elastic components.

The influence of additives on relaxation times at various temperatures is related to rutting and cracking in the discussion of the data.

2. Viscosity and Elasticity Temperature Susceptibilities

There are numerous formulas for representing viscosity as a function of temperature (12). Two of these formulas are applied in the analysis of the data and are discussed below. The first equation presented is an exponential equation and the second a polynomial equation.

$$\eta = Ae^{E/RT} \quad \text{Equation 5}$$

where η = viscosity,
A = liquid constant,
R = gas constant, and
T = absolute temperature.

$$\log \eta = a + bT + cT^2 + dT^3 \quad \text{Equation 6}$$

where T = temperature in degrees centigrade.

A third way of expressing viscosity-temperature data is an empirical plot of $\log \eta$ as a function of temperature which is useful for engineering purposes.

Equation 5 is referred to as the Arrhenius (or Eyring) (13) equation and has been related to the energy which holds the material together or the cohesive energy density (appendix B).

Equation 6 is an empirical equation that relates viscosity to temperature with no consideration of the physical or molecular properties of the material. However, the polynomial equation and its derivative are useful in extrapolation of properties beyond the temperature range of

experimental data. The derivative with respect to temperature is a measure of temperature susceptibility. The polynomial coefficients a,b,c and d are determined by measuring the viscosity, η , at four different temperatures and solving a set of four equations for the constants. Three of these constants are used to find the temperature susceptibilities applying the following formula.

$$\frac{d \log \eta}{dT} = b + 2cT + 3dT^2 \quad \text{Equation 7}$$

The elastic modulus, $G(t)$, of viscoelastic materials varies with temperature in a way that is equally as complex as viscosity temperature dependency. However, a simplified treatment expresses the elastic component as varying linearly with temperature (see appendix C). The elastic component in this study was observed to vary almost exponentially with temperature. This might be expected in view of the strong interactions in asphalt that are highly temperature dependent. Because of the complexity of elastic component temperature dependency, a polynomial equation was selected to represent the elastic component as a function of temperature.

$$G(t) = a + bT + cT^2 + dT^3 \quad \text{Equation 8}$$

Temperature susceptibilities of the materials were determined by the method discussed for viscosity temperature susceptibilities. That is, the slopes of the curves for $G(t)$ as a function of temperature were computed from the derivative of Equation 8. As seen later, viscosity temperature susceptibilities are reported for two temperature ranges, -4 to 32°F (-20 to 0°C) and 77 to 140°F (25 to 60°C). The slopes of the curves at midpoint between the low and high temperatures were selected as temperature susceptibilities.

3. Viscoelastic Measurements

A Rheometrics Inc. mechanical spectrometer was used to obtain several viscoelastic measurements. This included complex viscosity,

η^* , shear storage (elastic) modulus, G' , and shear loss (viscous flow) modulus, G'' , at four temperatures, -20, 0, 25 and 60°C. From these data, both a viscous and an elastic temperature susceptibility were obtained. Other data that can be calculated from the above viscoelastic parameters include $\tan \delta$, and complex dynamic shear modulus G^* . The relation between these parameters is shown below.

$$\tan \delta = G''/G' \quad \text{Equation 9}$$

$$G^* = [(G'')^2 + (G')^2] \quad \text{Equation 10}$$

$$\eta^* = G^*/\omega \quad \text{Equation 11}$$

The term, ω , is the frequency of the applied force. The relation between the elastic modulus, G' , and elastic modulus, $G(t)$, is discussed under the topic of relaxation times.

4. Effects of Additives on Viscosities at Four Temperatures

Viscosities of the asphalts with and without modifiers at four temperatures are given in table 28. The influence of aging on viscosity is also shown.

Microfil-8 showed the least influence of all the additives on viscosity at 140°F (60°C) of AC-5 and AR-1000 (table 28). Carbon black probably interacts by adsorption only. If asphalt forms an interphase around the carbon black, it is probably a structured system at -20°C similar to the structure of bulk asphalt. Therefore, Microfil-8 could increase the viscosity at 60°C by increasing the structuring of the system, but the structuring would be similar to bulk asphalt at -20°.

Elvax 150 had little influence on viscosity of either the AC-5 or AR-1000 asphalt at -4°F (-20°C), but did increase the viscosity of both asphalts at the higher temperatures. It should be pointed out that, at -20°C, no actual flow occurred in the specimen. Interaction data showed

Table 28. Viscosities of unaged and aged asphalts with and without additives.

Binder Asphalt	Dynamic Viscosity in Poises				Aging Index ^e at 60°C
	-20°C ^a	0°C ^b	25°C ^c	60°C ^d	
AC-5	1.33x10 ¹⁰	5.38x10 ⁷	5.05x10 ⁴	5.38x10 ²	-
+15% Microfil-8	1.85x10 ¹⁰	3.09x10 ⁸	2.37x10 ⁵	6.59x10 ²	-
+5% Elvax 150	1.44x10 ¹⁰	1.62x10 ⁸	2.88x10 ⁵	2.00x10 ³	-
+5% Polyethylene	1.56x10 ¹⁰	2.42x10 ⁸	3.15x10 ⁵	1.77x10 ³	-
+5% SBR	1.23x10 ¹⁰	2.52x10 ⁸	3.87x10 ⁵	3.79x10 ³	-
+6% Kraton/Dutrex	1.46x10 ¹⁰	1.67x10 ⁸	2.39x10 ⁵	1.31x10 ³	-
AR-1000	9.30x10 ¹⁰	3.53x10 ⁸	1.12x10 ⁵	5.18x10 ²	-
+15% Microfil-8	9.37x10 ¹⁰	9.06x10 ⁸	4.75x10 ⁵	1.03x10 ³	-
+5% Elvax 150	5.35x10 ¹⁰	2.34x10 ⁸	2.94x10 ⁵	1.36x10 ³	-
+5% Polyethylene	6.10x10 ¹⁰	5.91x10 ⁸	5.58x10 ⁵	1.62x10 ³	-
+5% SBR	3.52x10 ¹⁰	1.04x10 ⁹	1.09x10 ⁶	7.43x10 ³	-
+6% Kraton/Dutrex	4.23x10 ¹⁰	3.68x10 ⁸	3.00x10 ⁵	7.43x10 ³	-
+5% Kraton TR60-8774	4.46x10 ¹⁰	4.51x10 ⁸	3.35x10 ⁵	2.10x10 ³	-
<u>After Aging^e</u>					
AC-5	1.78x10 ¹⁰	1.10x10 ⁹	1.16x10 ⁷ ^f	1.61x10 ⁴ ^g	29.9
+15% Microfil-8	3.04x10 ¹⁰	1.95x10 ⁹	1.36x10 ⁷	1.62x10 ⁴	24.6
+5% Elvax 150	2.17x10 ¹⁰	6.06x10 ⁸	1.45x10 ⁷	1.78x10 ⁴	8.9
+5% Polyethylene	3.70x10 ¹⁰	4.57x10 ⁹	5.48x10 ⁷	1.43x10 ⁵	80.8
+5% SBR	1.65x10 ¹⁰	1.66x10 ⁹	2.02x10 ⁷	6.27x10 ⁴	16.5
+6% Kraton/Dutrex	2.63x10 ¹⁰	2.00x10 ⁹	2.21x10 ⁷	4.54x10 ⁴	34.7
AR-1000	8.75x10 ¹⁰	2.82x10 ⁹	5.72x10 ⁶	3.89x10 ³	7.51
+15% Microfil-8	1.23x10 ¹¹	4.48x10 ⁹	1.08x10 ⁷	6.59x10 ³	6.40
+5% Elvax 150	6.84x10 ¹⁰	1.62x10 ⁹	3.77x10 ⁶	5.83x10 ³	4.20
+5% Polyethylene	8.97x10 ¹⁰	4.34x10 ⁹	1.95x10 ⁷	3.53x10 ⁴	21.8
+5% SBR	6.39x10 ¹⁰	6.37x10 ⁹	7.36x10 ⁸	1.01x10 ⁵	13.6
+6% Kraton/Dutrex	5.76x10 ¹⁰	2.31x10 ⁹	5.87x10 ⁶	5.71x10 ³	4.3
+5% Kraton TR60-8774	5.78x10 ¹⁰	3.00x10 ⁹	9.59x10 ⁶	9.29x10 ³	4.4

^a0.05 rad/sec strain rate, 0.3% strain.

^b0.05 rad/sec strain rate, 1% strain.

^c5 rad/sec strain rate, 10% strain.

^d5 rad/sec strain rate, 50% strain.

^eThe thin film accelerated aging test (TFAAT) was used to condition these samples (3 days @ 113°C (235°F) in a very thin film).

^f0.10 rad/sec strain rate, 10% strain.

^g2.5 rad/sec strain rate, 50% strain.

that an exothermic interaction occurred between the asphalts and Elvax 150. The presence of an exothermic interaction implies an adsorption process occurred. The acetyl oxygen might be a bonding site for the polar asphalt molecules.

Polyethylene, SBR (Dow XUS 40052100 latex), SBS + extender oil (Kraton D-1101 + Dutrex 739), and SBS block copolymers (Kraton D-1101 + Kraton DX1118) all behaved in a manner similar to the Elvax 150 polymer.

5. Influence of Aging on Viscosity

The influence of asphalt aging by oxidation is often expressed in terms of an aging index. In this section, the aging index is the ratio of the 140°F (60°C) viscosities after and before aging by the TFAA test. The aging index is a relative measure of structuring from age hardening which is caused by a combination of oxidation and the increase in molecular interactions. Comparisons of the unmodified asphalts show that the AC-5 is more susceptible to age hardening than AR-1000.

Additives can influence the aging index by various mechanisms. They can restrict or support oxidation by a catalytic effect. Additives can selectively absorb oxidation products or they may also undergo oxidation.

Carbon black influenced the aging index the least and polyethylene influenced the aging index the most when compared to AC-5 and AR-1000. Polyethylene increased the aging index of both the AC-5 and AR-1000 asphalts several fold. Possibly, the polyethylene is absorbing nonpolar constituents during the aging process, causing the viscosity to increase. Similarly the polar Elvax 150 as well as the SBR and SBS polymers may be absorbing polar and unsaturated ring systems, respectively, to cause a decrease in the aging index. The Kraton/Dutrex with AC-5 is an exception. Each asphalt with each additive should be analyzed separately. Generalizations on the effect of additives on aging are difficult.

6. Viscosity Temperature Susceptibilities of Aged and Unaged Asphalts

Additives are considered beneficial if they can be used to provide a "softer" binder at low temperatures. Asphalts are called soft when they have better flow properties at low temperatures, which can lead to reduced cracking. The benefit of additives at higher temperatures is the reduction of flow under traffic-induced loading on hot summer days. The reduction of viscosity at low temperatures and the increased viscosity at high temperatures imply that additives improve asphalt flow properties by lowering the temperature susceptibility.

There are several methods for representing the viscosity temperature susceptibility data of asphalts. Two examples are seen in figure 1 in which plots of both $\log \eta$ vs K^0 (or centigrade) and $\log \eta$ vs $1/K^0$ are given. A plot is shown for only one asphalt, the unaged Texaco AC-5 asphalt. All other plots are similar. The slope of the curves between 273^0K (0^0) and 253^0K (-20^0C) represent low-temperature susceptibility; whereas, the slope between 298^0K (25^0C) and 333^0K (60^0C) represent high-temperature susceptibility.

Temperature susceptibility, E , represents cohesive energy density. Moavenzadeh and Stander (14) have shown that temperature susceptibility at both the low (E_L) and high temperatures (E_H) are useful in presenting data from $\log \eta$ vs $1/K^0$ plots. The results for the additive systems are tabulated in table 29.

In general, the additives decreased the temperature susceptibilities (E) at low temperatures and increased the temperature susceptibilities at high temperatures for both the AR-1000 and the AC-5 asphalts. However, SBR decreased the temperature susceptibility at high temperatures for both asphalts. The SBR may have been interacting strongly with polar constituents in the asphalts thus eliminating their influence on temperature susceptibility. The SBR polymer, as mentioned previously, can interact with the polar conjugate ring-type molecules in the asphalt by dipole-induced dipole interactions. The Kraton SBS polymers could probably interact in a similar manner, but a similar decrease in the

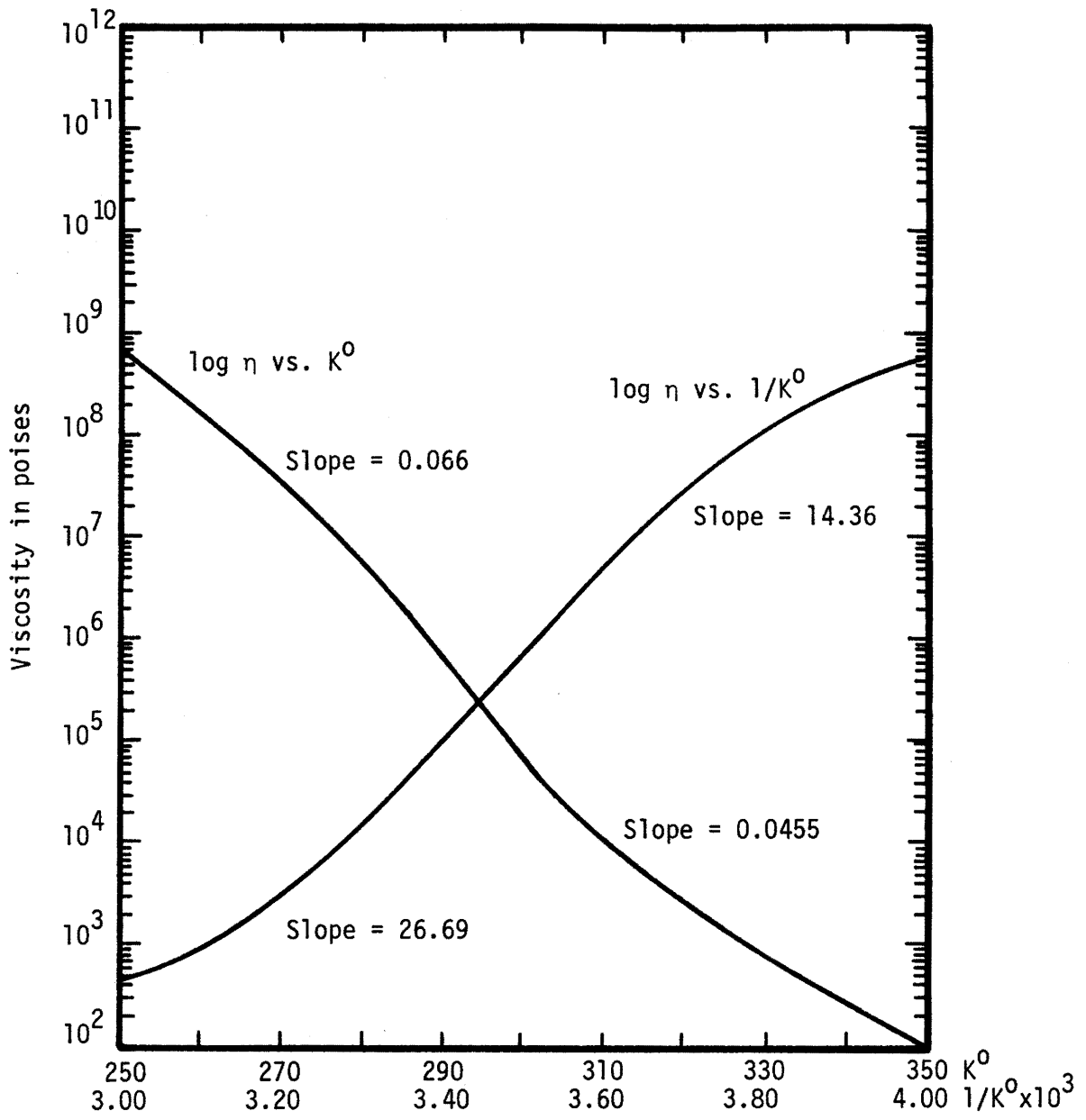


Figure 1. Plots of log viscosity as a function of K^0 and $1/K^0 \times 10^3$ for Texaco AC-5 asphalt (unaged).

Table 29. Viscosity temperature susceptibilities, E, of unaged and aged asphalts.

Binder	Viscosity Temperature Susceptibility (E)			
	Unaged		Aged	
	0° to -20°	25° to 60°	0° to -20°	25° to 60°C
AC-5	37.7	25.8	19.1	37.1
+15% Microfil-8	28.0	33.0	18.8	37.9
+5% Elvax 150	30.8	28.2	24.6	37.8
+5% Polyethylene	28.5	29.4	14.4	33.5
+5% SBR	26.7	23.5	15.8	32.5
+6% Kraton/Dutrex	30.6	29.5	17.7	34.8
AR-1000	38.2	30.6	23.6	41.1
+15% Microfil-8	31.7	34.6	22.8	41.7
+5% Elvax 150	31.9	30.6	25.9	36.4
+5% Polyethylene	31.9	33.2	20.8	35.9
+5% SBR	24.1	28.4	15.9	37.5
+6% Kraton/Dutrex	32.5	30.4	22.1	39.1
+5% Kraton/TR-60-8774	31.5	28.9	20.3	39.1

Table 30. Viscosity temperature susceptibilities, S, from log η vs. °C*

Binder	Viscosity Temperature Susceptibility (Log η vs. °C)			
	Unaged		Aged	
	0° to -20°	25° to 60°	0° to -20°	25° to 60°C
AC-5	0.120	0.056	0.061	0.082
+15% Microfil-8	0.089	0.073	0.059	0.084
+5% Elvax 150	0.098	0.062	0.078	0.083
+5% Polyethylene	0.091	0.064	0.046	0.074
+5% SBR	0.085	0.057	0.050	0.072
+6% Kraton/Dutrex	0.097	0.065	0.056	0.077
AR-1000	0.121	0.067	0.075	0.091
+15% Microfil-8	0.100	0.076	0.072	0.092
+5% Elvax 150	0.118	0.067	0.081	0.080
+5% Polyethylene	0.101	0.073	0.066	0.078
+5% SBR	0.077	0.062	0.050	0.081
+6% Kraton/Dutrex	0.103	0.067	0.070	0.086
+5% Kraton/TR60-8774	0.100	0.063	0.064	0.086

*Computed from slope of viscosity-temperature curves similar to Figure 1. Higher values indicate higher temperature susceptibility.

temperature susceptibility at high temperatures was not observed. The Dutrex 739 may have influenced the systems in which it was present. The Kraton additive containing only SBS plus SB polymers decreased the temperature susceptibility of the AR-1000 appreciably.

The temperature susceptibilities, S , in table 30, were calculated from the average slopes of the curves (similar to figure 1) between two temperatures. Temperature susceptibility at low temperatures represents the average slope of a curve between 0° and -20°C and the temperature susceptibility at high temperatures represents the average slope of a curve between 25° and 60°C . As seen in figure 1, the curve produced by plotting $\log \eta$ vs K° (or C°) is nearly a mirror image of the curve produced by plotting $\log \eta$ vs $1/K^{\circ}$ (or $1/C^{\circ}$). Although the curves are similar, the slopes have opposite signs. Because of the similarities, any discussion of temperature susceptibility, S , would parallel the previous discussion of temperature susceptibility, E . The advantage of using S is that it expresses directly the relation between temperatures and viscosities, which is of primary concern to engineers.

7. Elastic Component of Aged and Unaged Asphalts at Four Temperatures

The influence that the additives have on the elastic behavior of the asphalts at 140°F (60°C), 77°F (25°C), 32°F (0°C), and -4°F (-20°C) before and after TFAAT aging is shown in tables 31 and 32. Discussions are given only on the two extreme temperatures, -20° and 60°C . The additives had little effect on the elastic component at -20°C (table 31). At low temperatures, the asphalt molecules become highly associated and approach the character of a solid. Some trends, however, are apparent in the data and warrant further discussion.

The interaction between polymers and asphalt is probably a result of chain uncoiling, as mentioned in the thermodynamic section. If the interaction between a polymer and an asphalt produces a partial uncoiling of the polymer molecules, then the polar asphalt molecules are likely to

Table 31. Elastic contribution to flow in unaged binders.^a

Binders	Elastic Contribution (G') - Unaged Asphalts			
	-20°C ^b	0°C ^c	25°C ^d	60°C ^e
Texaco AC-5	5.47x10 ⁸	1.09x10 ⁶	5.96x10 ⁴	1.10x10 ²
+15% Microfil-8	7.54x10 ⁸	8.40x10 ⁶	2.82x10 ⁵	1.45x10 ²
+5% Elvax 150	5.63x10 ⁸	4.16x10 ⁶	5.10x10 ⁵	6.10x10 ²
+5% Polyethylene	6.40x10 ⁸	5.61x10 ⁶	4.22x10 ⁵	4.29x10 ²
+5% SBR	5.10x10 ⁸	6.65x10 ⁶	7.84x10 ⁵	4.31x10 ³
+5% Kraton/Dutrex	5.68x10 ⁸	3.39x10 ⁶	6.40x10 ⁵	4.54x10 ²
San Joaquin AR-1000	4.29x10 ⁹	5.62x10 ⁶	5.11x10 ⁴	2.44x10 ¹
+15% Microfil-8	4.23x10 ⁹	1.35x10 ⁷	2.64x10 ⁵	6.32x10 ¹
+5% Elvax 150	2.25x10 ⁸	9.30x10 ⁵	2.59x10 ⁵	6.20x10 ²
+5% Polyethylene	2.64x10 ⁹	1.14x10 ⁷	6.22x10 ⁵	5.77x10 ²
+5% SBR	1.59x10 ⁸	2.92x10 ⁷	2.20x10 ⁶	9.61x10 ³
+5% Kraton/Dutrex	1.82x10 ⁸	5.03x10 ⁶	2.86x10 ⁵	1.65x10 ³
+5% Kraton TR-60-8774	1.94x10 ⁸	6.36x10 ⁶	3.46x10 ⁵	3.42x10 ³

^aLower G' at lower temperatures is indicative of improved resistance to cracking. Higher G' at higher temperatures is indicative of improved resistance to rutting (plastic deformation).

^b0.05 rad/sec strain rate, 0.3% strain.

^c0.05 rad/sec strain rate, 1% strain.

^d5 rad/sec strain rate, 10% strain.

^e5 rad/sec strain rate, 50% strain.

Table 32. Elastic contribution to flow in aged binders.

Binders	Elastic Contribution (G')				Aging Index	
	-20°C	0°C	25°C	60°C	-20°C	60°
Texaco AC-5	7.92x10 ⁸	4.10x10 ⁷	5.74x10 ⁵	9.15x10 ³	1.5	83.2
+15% Microfil-8	1.36x10 ⁹	7.37x10 ⁷	6.30x10 ⁵	7.50x10 ³	1.8	51.7
+5% Elvax 150	9.36x10 ⁸	2.57x10 ⁷	7.91x10 ⁵	7.61x10 ³	1.7	12.5
+5% Polyethylene	1.71x10 ⁹	1.91x10 ⁸	3.23x10 ⁶	1.21x10 ⁵	2.7	28.2
+5% SBR	7.42x10 ⁸	6.52x10 ⁷	1.11x10 ⁶	5.53x10 ⁴	1.6	12.8
+5% Kraton/Dutrex	1.19x10 ⁹	7.98x10 ⁷	1.30x10 ⁶	4.47x10 ⁴	2.1	98.0
San Joaquin AR-1000	4.05x10 ⁹	8.37x10 ⁷	8.82x10 ⁴	1.31x10 ²	0.94	5.3
+15% Microfil-8	5.77x10 ⁹	1.33x10 ⁸	1.51x10 ⁵	5.24x10 ²	1.40	8.3
+5% Elvax 150	3.07x10 ⁹	4.59x10 ⁸	5.29x10 ⁴	1.01x10 ³	13.6	1.6
+5% Polyethylene	4.16x10 ⁹	1.56x10 ⁸	6.81x10 ⁵	3.16x10 ⁴	1.60	54.8
+5% SBR	2.96x10 ⁹	2.70x10 ⁸	4.21x10 ⁶	8.11x10 ⁴	18.6	8.4
+5% Kraton/Dutrex	2.62x10 ⁹	7.31x10 ⁷	1.41x10 ⁵	1.44x10 ³	14.4	0.87
+5% Kraton/TR-60-8774	2.63x10 ⁹	1.00x10 ⁸	2.73x10 ⁵	3.96x10 ³	13.6	1.2

initiate the interaction. They are the molecules that contribute to elasticity, but they may cease this contribution when entering the uncoiled polymer matrix.

The Elvax 150 additive was the only additive that decreased G' in both asphalts at -20°C . Its permanent polarity may make it vulnerable to attack by both asphalts. All the other additives produced an increase in G' with AC-5 and a decrease in G' with AR-1000.

At 60°C , the elastic contribution to flow is minor and the viscous contribution is major. At this temperature, all additives produced a decrease in G' with AC-5 and an increase in G' with AR-1000 (table 31).

The AR-1000 asphalt, being more polar and perhaps a better solvent system than the AC-5 asphalt, should interact more strongly with additives whether by adsorption, partial dissolution of the additive, or by partial uncoiling of the polymer. These polar asphalt molecules probably produced an interphase region of structured polar molecules on the polymer surface and in the coils of the polymers.

8. Influence of Aging on Elastic Components

An aging index was calculated at two temperatures, -4°F (-20°C) and 140°F (60°C), for the elastic component contributions. The aging index is the ratio of the elastic component after aging divided by the elastic component before aging. The data are reported in table 32.

The additives had little influence on the low-temperature elastic component aging index for either asphalt. The additives had a much greater effect on the elastic component aging index at 60°C . Polyethylene had the greatest influence.

The effect of additives on the elastic component of both aged and unaged asphalts is seen in figures 2 and 3 for the AC-5 and AR-1000 asphalts, respectively. The optimum system would have a relatively low G' at lower temperatures that would increase with increasing temperature.

The curves for the unaged asphalts with and without additives converge at -20°C . At this temperature, it appears that elastic flow is

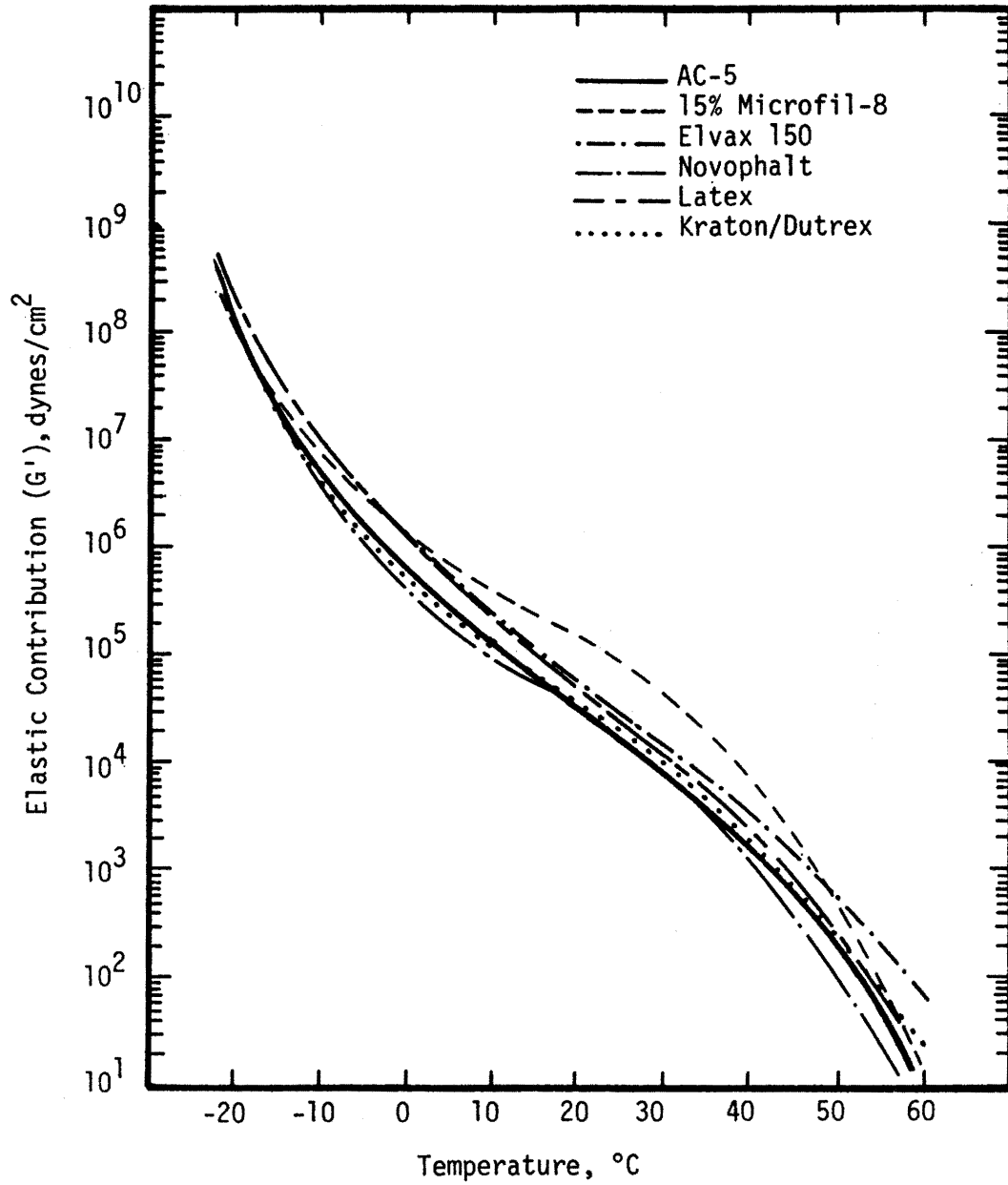


Figure 2. Temperature susceptibility curve of elastic component of AC-5 asphalt, unaged, with and without additives.

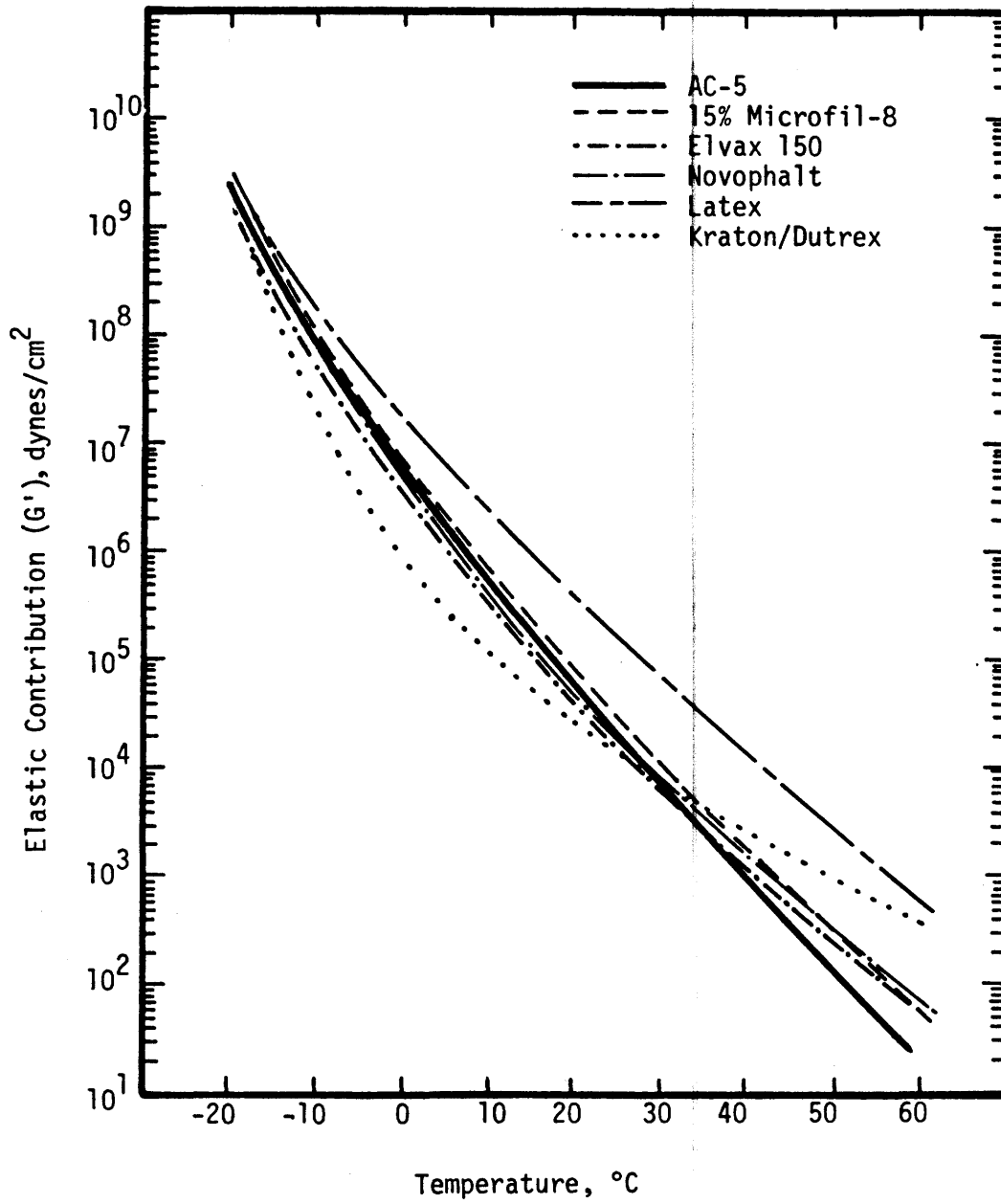


Figure 3. Temperature susceptibility curve of elastic component for unaged AR-1000 asphalt, with and without additives.

influenced little by the additives, which is desirable when using the additives in softer-than-usual asphalts. There are two possible explanations. If carbon black (Microfil-8) interacts with the asphalt by adsorption, then there could be an interphase region between the carbon black and the asphalt that is influenced by the temperature. At low temperatures, the interphase region may have the same solid characteristics as the bulk asphalt. Thus, the G' versus temperature curves for unmodified and carbon black-treated asphalts would merge.

A second possible reason for the merging of the curves assumes that the polymer dispersed in asphalt is a three-dimensional network of polymer branching throughout an asphalt matrix. This three dimensional polymer network may have little mobility at -20°C with flow properties of the mixture being influenced by the asphalt only.

Plots of G' versus temperature have been presented by Nadkaml, et. al. (15) for polymer-asphalt systems. They show a curve peak for G' near -20°C followed by a gradual decrease with decreasing temperature. Data collected by WRI do not go below -20°C . Thus, the peak seen by Nadkaml, et. al. would not be observed. The above authors noted that the greater the peak width on the G' versus temperature curve, the lower the temperature susceptibility.

To facilitate comparisons, elastic component temperature susceptibilities (average slope of the curves) were computed between 22°F (-20°C) and 32°F (0°C) and between 77°F (25°C) and 140°F (60°C) for both aged and unaged binders (table 33). Generally, the additives had little influence on elastic component temperature susceptibility of the unaged materials at low temperatures. The additives decreased the temperature susceptibility of the unaged AC-5 and AR-1000 asphalts. The additives generally caused a decrease in temperature susceptibility at both temperature ranges in the aged materials. Microfil-8 and Elvax 150 in AR-1000 were the exceptions. This indicates that the elastic properties of the AC-5 are less susceptible to aging with the additives present.

Table 33. Elastic component temperature susceptibilities of aged and unaged binders.

Binder	Elastic Component Temperature Susceptibility			
	Unaged		Aged	
	0° to -20°C	25° to 60°C	0° to -20°C	25° to 60°C
Texaco AC-5	0.140	0.078	0.064	0.051
+15% Microfil-8	0.098	0.094	0.063	0.055
+5% Elvax 150	0.167	0.083	0.078	0.078
+5% Polyethylene	0.102	0.086	0.048	0.028
+5% SBR	0.094	0.065	0.053	0.037
+6% Kraton/Dutrex	0.111	0.090	0.059	0.042
San Joaquin AR-1000	0.144	0.095	0.049	0.081
+15% Microfil-8	0.125	0.104	0.082	0.070
+5% Elvax 150	0.121	0.075	0.091	0.049
+5% Polyethylene	0.118	0.087	0.071	0.038
+5% SBR	0.087	0.067	0.022	0.049
+5% Kraton/Dutrex	0.128	0.063	0.060	0.057
+5% Kraton TR-60-8774	0.119	0.057	0.071	0.053

STRESS RELAXATION OF ASPHALTS WITH ADDITIVES

1. Basis for Test

Relaxation time for a Maxwellian liquid is expressed in the following equation (see Equation 4):

$$\tau = \frac{\eta}{G(t)}$$

As stated previously, the relaxation time, τ , is the time for a viscoelastic system to relax to $1/e$ ($e = 2.718\dots$) of the maximum stress value. The dynamic viscosity, η , was found directly from mechanical spectrometer measurements. Elastic modulus, $G(t)$, was calculated from $G'(t)$, elastic modulus contribution, which is also found directly from mechanical spectrometer measurements. The relation between $G(t)$ and $G'(t)$ for a Maxwellian material is shown below.

$$G(t) = \omega^2 \frac{\eta^2 \pm \omega\eta}{2G'} [\omega^2 \eta^2 - 4(G')]^{\frac{1}{2}} \quad \text{Equation 12}$$

where ω is frequency in radians per second.

When stress is applied to a Hookean solid no stress relief occurs. When stress is applied to a Newtonian viscous fluid it flows without stress build-up. When stress is applied to a viscoelastic material, stresses occur but are relieved through viscous flow. A large increase in the viscosity, either due to incorporation of an additive or a decrease in temperature, implies a strong interaction which inhibits molecular movement. On the other hand, two phase system containing SBR, for example, may be comprised of a network of entangled "rubber bands" in a continuous asphalt phase, with the main effect being purely physical.

A large increase in the elastic modulus, again either due to addition of a modifier or a temperature decrease, implies a strong molecular interaction which inhibits large elastic displacements. The data in tables 34-37 are discussed in terms of these concepts.

Table 34. Viscoelastic data on unaged asphalts at 25°C.

Binder	Viscosity(η), poise	G' ^a , dynes/cm ²	$G(t)$ ^b , dynes/cm ²	τ ^c , seconds
Texaco AC-5	5.05×10^4	5.96×10^4	8.69×10^5	0.0205
+15% Microfil-8	2.37×10^5	2.82×10^5	1.02×10^6	0.0215
+5% Elvax 150	2.88×10^5	5.10×10^5	6.00×10^5	0.0195
+5% Polyethylene	3.15×10^5	4.22×10^5	1.58×10^6	0.0215
+5% SBR	3.87×10^5	7.84×10^5	4.58×10^5	0.0234
+6% Kraton/Dutrex	2.39×10^5	6.40×10^5	i^d	0.0195
San Joaquin AR-1000	1.12×10^5	5.11×10^4	3.98×10^6	0.0176
+15% Microfil-8	4.75×10^5	2.64×10^5	4.56×10^6	0.0200
+5% Elvax 150	2.94×10^5	2.59×10^5	9.54×10^5	--
+5% Polyethylene	5.58×10^5	6.22×10^5	1.22×10^6	0.0195
+5% SBR	1.09×10^6	2.20×10^6	1.01×10^6	0.0215
+6% Kraton/Dutrex	3.00×10^5	2.86×10^5	8.19×10^5	0.0195
+5% Kraton/TR-60-8774	3.35×10^5	3.46×10^5	7.86×10^5	--

a G' is elastic modulus contribution

b $G(t)$ is elastic shear modulus

c τ is relaxation times

d No value implies an imaginary value or non-Maxwellian material.
 τ not equal to $\eta/G(t)$ also implies non-Maxwellian flow.

Table 35. Viscoelastic data on unaged asphalts at 0°C.

Binder	Viscosity(η), poise	G' ^a , dynes/cm ²	$G(t)$ ^b , dynes/cm ²	τ ^c , seconds
Texaco AC-5	5.38×10^7	1.09×10^6	5.20×10^8	.072
+15% Microfil-8	3.09×10^8	8.40×10^6	4.94×10^8	.113
+5% Elvax 150	1.62×10^8	4.16×10^6	4.99×10^8	.037
+5% Polyethylene	2.42×10^8	5.61×10^6	6.21×10^8	.105
+5% SBR	2.52×10^8	6.65×10^6	5.30×10^8	.074
+6% Kraton/Dutrex	1.67×10^8	3.39×10^6	5.77×10^8	.045
San Joaquin AR-1000	3.53×10^8	5.62×10^6	1.23×10^9	.291
+15% Microfil-8	9.06×10^8	1.35×10^7	1.18×10^9	.375
+5% Elvax 150	2.34×10^8	9.30×10^5	-- ^d	--
+5% Polyethylene	5.91×10^8	1.14×10^7	1.09×10^9	.227
+5% SBR	1.04×10^9	2.92×10^7	8.28×10^8	.283
+6% Kraton/Dutrex	3.68×10^8	5.03×10^6	9.34×10^8	.133

^a G' is elastic modulus contribution

^b $G(t)$ is elastic shear modulus

^c τ is relaxation times

^d No value implies an imaginary value or non-Maxwellian material.
 τ not equal to $\eta/G(t)$ also implies non-Maxwellian flow.

Table 36. Viscoelastic data on unaged asphalts at -20°C.

Binder	Viscosity(η), poise	G' ^a , dynes/cm ²	$G(t)$ ^b , dynes/cm ²	τ ^c , seconds
Texaco AC-5	1.33x10 ¹⁰	5.47x10 ⁸	1.52x10 ⁹	8.2
+15% Microfil-8	1.85x10 ¹⁰	7.54x10 ⁸	1.55x10 ⁹	12.6
+5% Elvax 150	1.44x10 ¹⁰	5.63x10 ⁸	--	--
+5% Polyethylene	1.56x10 ¹⁰	6.40x10 ⁸	1.93x10 ⁹	12.5
+5% SBR	1.23x10 ¹⁰	5.10x10 ⁸	1.53x10 ⁹	9.09
+6% Kraton/Dutrex	1.46x10 ¹⁰	5.68x10 ⁸	1.66x10 ⁹	8.19
San Joaquin AR-1000	9.30x10 ¹⁰	4.29x10 ⁹	2.82x10 ⁹	233.6
+15% Microfil-8	9.37x10 ¹⁰	4.23x10 ⁹	3.03x10 ⁹	203.9
+5% Elvax 150	5.35x10 ¹⁰	2.25x10 ⁸	--	--
+5% Polyethylene	6.10x10 ¹⁰	2.64x10 ⁹	2.61x10 ⁹	107.9
+5% SBR	3.52x10 ¹⁰	1.59x10 ⁸	2.06x10 ⁹	54.7
+6% Kraton/Dutrex	4.23x10 ¹⁰	1.82x10 ⁸	2.36x10 ⁹	50.7
+5% Kraton/TR-60-8774	4.46x10 ¹⁰	1.94x10 ⁸	--	--

Table 37. Viscoelastic data on aged asphalts at 25°C.

Binder	Viscosity(η), poise	G' ^a , dynes/cm ²	$G(t)$ ^b , dynes/cm ²	τ ^c , seconds
Texaco AC-5	1.16x10 ⁷	5.74x10 ⁵	i	42
+15% Microfil-8	1.36x10 ⁷	6.30x10 ⁵	9.87x10 ⁵	42.4
+5% Elvax 150	1.45x10 ⁷	7.91x10 ⁵	7.92x10 ⁵	91.8
+5% Polyethylene	5.48x10 ⁸	3.23x10 ⁶	1.95x10 ⁶	39.9
+5% SBR	2.02x10 ⁷	1.11x10 ⁶	1.10x10 ⁶	39.9
+6% Kraton/Dutrex	2.21x10 ⁷	1.30x10 ⁶	i	
San Joaquin AR-1000	5.72x10 ⁶	8.82x10 ⁴	3.34x10 ⁶	1.8
+15% Microfil-8	1.08x10 ⁷	1.51x10 ⁵	9.48x10 ⁶	1.38
+5% Elvax 150	3.77x10 ⁶	5.29x10 ⁴	2.93x10 ⁶	1.29
+5% Polyethylene	1.95x10 ⁷	6.81x10 ⁵	2.29x10 ⁶	10.8
+5% SBR	7.36x10 ⁸	4.21x10 ⁶	i	
+6% Kraton/Dutrex	5.87x10 ⁶	1.41x10 ⁵	1.15x10 ⁶	5.7
+5% Kraton/TR-60-8774	9.59x10 ⁶	2.73x10 ⁵	1.61x10 ⁶	7.6

^a G' is elastic modulus contribution

^b $G(t)$ is elastic shear modulus

^c τ is relaxation time

^d i means no value implies an imaginary value or a non-Maxwellian material.

2. Discussion of Relaxation Results

Relaxation data were obtained on the original asphalts with and without additives at 77°F (25°C), 32°F (0°C) and 22°F (-20°C) and on aged asphalt with and without additives at 25°C only. The additives had little influence on the relaxation time of unaged asphalts at 25°C. The aged asphalt relaxation data at 25°C show a large increase in relaxation times over the corresponding relaxation times for unaged asphalt. Large increases were expected because aging increases the polarity of the asphalt thus leading to strong molecular interactions. At 0°C and below, the additives had a significant effect on relaxation times of the asphalts but the effects were not consistent.

An increase in relaxation times with a decrease in temperature (25 to -20°C) occurred for all systems. This reflects the typical exponential increase in viscosity and not quite as rapid an increase in the elastic modulus, $G(t)$ with a decrease in temperature.

Relaxation times for materials containing San Joaquin asphalt were more sensitive to temperature than those containing Texaco asphalt. This is probably due to the AR-1000 having a higher polarity than the AC-5 which leads to greater association for the AR-1000 as the materials cool.

SUMMARY

Chapter III presents a rheological and chemical characterization of the modified asphalt binders. Asphalts from two sources were used; tests showed that the San Joaquin products were lower in asphaltenes (more highly peptized), higher in aromaticity and had a higher concentration of polar functional groups than the Texaco products. As a result, the San Joaquin asphalts were notably more compatible with the polymeric additives. Physical property measurements included penetration and viscosity at various temperatures by various methods. Calculations revealed that all the additives produced marked decreases in temperature susceptibility of the asphalts. Rolling thin film oven tests (RTFOT) showed deviations from normal asphalt behavior. For example, blends

containing SBR exhibited a decrease in viscosity at 275⁰F (135⁰C) after RTFOT.

Infrared spectroscopy was applied before and after artificial aging using a thin-film accelerated aging test (TFAAT) to monitor the formation of oxidation products. None of the additives greatly affected the oxidation of the asphalts. Some of the polymers, particularly the polyethylene, separated from the asphalt during the TFAAT. Addition of SBR showed evidence of increased reactivity with oxygen.

Energies of interaction between the asphalts and the additives were endothermic for polyethylene and SBR (indicating a breaking of chemical bonds) and exothermic for the remaining additives (indicating a formation of chemical bonds, possibly adsorption).

Sophisticated rheological tests were used to describe the viscoelastic properties of the modified binders. Since the results were somewhat inconsistent, the following statements are generalizations. The additives tended to increase the viscosities of the AC-5 and the AR-1000 at 32⁰F (0⁰C) and higher. At -4⁰F (-20⁰C), the additives had little effect on viscosity. Mixtures containing polyethylene showed the greatest increase in viscosity and relaxation time upon artificial long-term aging by the TFAAT; Elvax 150 showed the least increase in viscosity. At temperatures above 32⁰F (0⁰C), the additives produced an increase in the elastic modulus of the asphalts both before and after aging; below 32⁰F, they produced a decrease. This should aid in reducing the potential for pavement cracking at low temperatures. All the additives decreased the temperature susceptibilities of the asphalts at temperatures from -4⁰F (-20⁰C) to 32⁰F (0⁰C), whether computed using viscosity data or elastic modulus data. Relaxation times at 77⁰F (25⁰C) (a typical ambient temperature) were changed little upon addition of the modifiers. Relaxation times at -4⁰F (-20⁰C) were improved more for the AR-1000 than for the AC-5; a comparison of the additives shows that the SBR and Kraton were the most effective in decreasing relaxation time.

Data generated in this portion of the study were used to select additive dosages used in the mixture study.

CHAPTER IV

EVALUATION OF ASPHALT CONCRETE MIXTURES CONTAINING ADDITIVES

MIXTURE DESIGN

Two different aggregates were selected for use in the mixture study to provide a wide variation in mixture properties. The aggregate used in most of the mixture tests consisted of subrounded, silicious river gravel and similar sand with limestone crusher fines added to improve stability. This material was selected as the primary aggregate because it produces a relatively binder-sensitive mixture which accentuates the properties of the binders more than a high-stability mix. The secondary aggregate was composed of crushed limestone with field sand added to improve workability. This relatively absorptive, very angular material produces a high stability mix suitable for high-type roadway systems. Both of these aggregate blends are routinely used for paving construction in Texas. Details of these aggregate blends and gradations are given in appendix D.

The asphalts used in this segment of the study include Texaco and San Joaquin (California) Valley products. Texaco AC-20 (in the control mixtures) and Texaco AC-5 modified with the five additives discussed in Chapter III were used in most of the mixtures. Texaco AC-10 and California Valley AR-1000, AR-2000 and AR-4000 were also used. The additives were incorporated into the mixtures using methods which simulate field conditions as closely as possible. For example, latex and carbon black were added to the hot asphalt-aggregate mixture and stirred for an extra one minute period; whereas, the other three additives were preblended in the asphalt cement before combining with the aggregate. Binder properties are discussed in Chapter III.

Optimum binder content was determined using the Marshall Method with emphasis on uniform air void content (density). Results of the mix design procedures are given in table D4, appendix D. Values in table D4

may have been interpolated if tests were not actually performed at the selected optimum binder content.

Optimum binder content for most of the mixtures including river gravel and crushed limestone was about 4.5 percent. Mixtures containing carbon black require a slightly higher binder content. The primary reason for this is that the carbon black modified binder has a significantly higher specific gravity and the binder is added on approximately an equivalent volume basis. Apparently, the carbon black reduces the lubricating effects of the binder thus producing a slightly higher air void content at a given compaction energy. On the average, mixtures containing the Texaco yielded higher Marshall stabilities than those containing the California Valley asphalt. This is likely due to the resulting rheological properties of the binders. Exposure to heat in the presence of aggregate surfaces during mixing can significantly affect asphalt rheology (16). Mixtures made using crushed limestone, of course, gave higher stabilities than those made using river gravel.

Until additional research is completed, Marshall mix design procedures appear to be suitable for designing paving mixtures containing the types of asphalt additives studied herein.

PREPARATION OF SPECIMENS FOR MIXTURE TESTING

Paving mixtures for the laboratory tests were produced using the river gravel and crushed limestone aggregates with the aforementioned binders. The test program is described in figure 4. Mixing and compaction were performed in accordance with ASTM method D1559. That is, binder viscosity upon mixing was 170 ± 20 cSt and upon compacting was 280 ± 30 cSt. This was an attempt to produce specimens with approximately equivalent air void contents. Mixing and compaction temperatures for each binder are given in appendix D. Test methods included Marshall and Hveem stability, resilient modulus at 5 temperatures, indirect tension at 3 temperatures and 3 loading rates, and an assessment of resistance to damage by moisture. River gravel specimens were prepared using 50-blow Marshall compaction; limestone specimens were prepared using 75-blow compaction. Moisture-treated specimens are typically compacted to

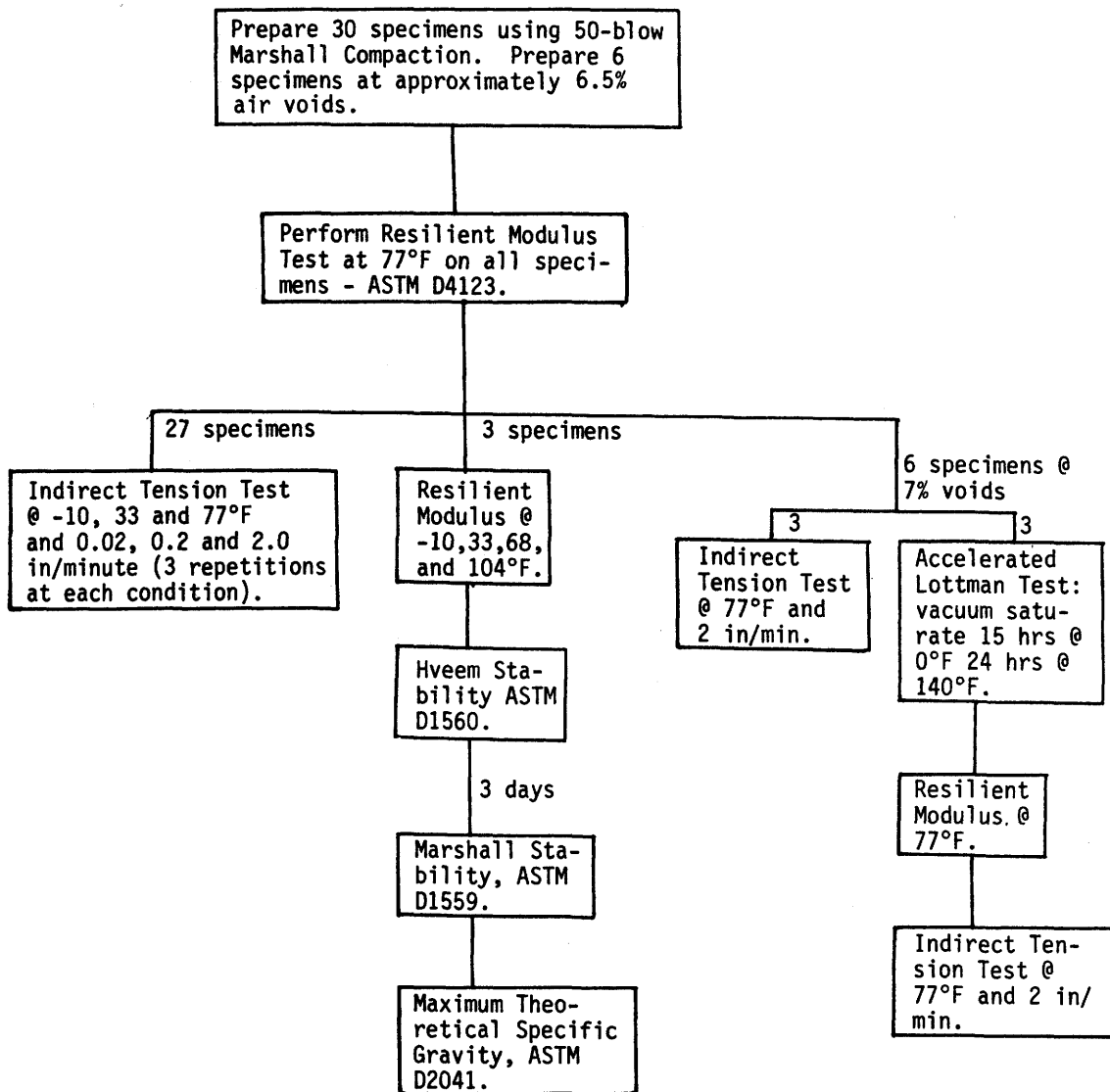


Figure 4. Test program to evaluate asphalt concrete mixtures.

approximately 6.5 percent voids to allow sufficient intrusion of the water.

MARSHALL STABILITY

None of the mixtures containing modified AC-5 or AR-1000 binders exhibited Marshall stabilities greater than the AC-20 or AR-4000 controls (tables 38 and 39). However, all of the modifiers show the capacity to improve stability over that of the AC-5 or AR-1000 control mixtures. No single additive showed the ability to produce mixtures with consistently higher Marshall stabilities than the other additives. Kraton and Novophalt generally exhibited the greatest improvement.

Marshall flows for these laboratory mixtures were often below values specified by most highway agencies. This is the nature of this river gravel mixture which was specifically chosen because of its sensitivity to binder properties and should not be a concern.

After collection of significant data, it is surmised that the design asphalt content selected for the latex modified mixture with Texaco asphalt was slightly higher than it should have been. As a result, the latex mixture probably exhibited lower air void content, stability and stiffness than it should have.

HVEEM STABILITY

Hveem stability (table 38 and 39) is largely dependent upon interparticle friction of the aggregate and does not correlate particularly well with binder properties. However, the test was performed because many State highway agencies employ it in their mix design procedures. As one might expect, there were no strong correlations between Hveem stability and the additives utilized for either of the two mix types. The latex plus Texaco AC-5 mixture exhibited the lowest Hveem stability; this may have been a result of excessive binder content as mentioned earlier.

No particular problems were encountered in determining Hveem stability of these modified mixtures. It appears, therefore, that the

Table 38. Resilient modulus and stability of mixtures containing Texaco asphalt and river gravel.

Type Mixture	Air Void Content, Percent	Hveem Stability	Marshall Test		Resilient Modulus, psi x 10 ³				
			Stability	Flow	0°F	33°F	68°F	77°F	104°F
Control: AC-20	5.0	43	1600	8	2200	1600	700	470	110
Control: AC-5	4.3	43	900	9	1800	1200	270	160	34
AC-5 + 15% Microfil 8	5.5	42	900	8	1700	1100	250	140	36
AC-5 + 5% Elvax 150	4.9	46	1100	9	-	-	300	220	45
AC-5 + 5% Kraton D	4.6	47	1300	7	-	-	380	290	47
AC-5 + 5% Latex	4.1	41	1000	10	1800	1500	250	150	35
AC-5 + 5% Novophalt	5.5	51	1300	8	-	-	470	370	69

68

Table 39. Resilient modulus and stability of mixtures containing California Valley asphalt and river gravel.

Type Mixture	Air Void Content, Percent	Hveem Stability	Marshall Test		Resilient Modulus, psi x 10 ³				
			Stability	Flow	10°F	32°F	68°F	77°F	104°F
Control: AR-4000	4.4	49	1200	7	2000	1700	900	710	93
Control: AR-1000	4.1	48	700	6	2000	1400	250	140	25
AR-1000 + 15% Microfil 8	5.0	50	1200	7	1900	1600	430	250	40
AR-1000 + 5% Elyax 150	5.2	44	600	7	2000	1500	240	120	19
AR-1000 + 5% Kraton D	4.8	46	900	6	2000	1500	370	210	29
AR-1000 + 5% Latex	5.1	48	800	6	1900	1500	370	230	32
AR-1000 + 5% Novophalt	5.3	46	950	5	2000	1600	460	280	39

Hveem design method would be suitable for application when using these types of binders but would not be sensitive to differences in binder properties.

It should be pointed out that all specimens were compacted using the Marshall hammer. However, the Hveem stability values should be valid for comparisons within this study.

RESILIENT MODULUS

Mixture stiffness was measured in accordance with D 4123-82 using the Mark III Resilient Modulus device. Typically, a diametral load of approximately 72 pounds was applied for a duration of 0.1 seconds while monitoring the diametral deformation perpendicular to the loaded plane. The load is normally reduced to about 20 pounds for tests performed at 100°F or higher to prevent damage to specimens. Resilient modulus measured over a range of temperatures is used to estimate mixture temperature susceptibility. Test results are given in tables 38 and 39 and plotted in figures 5 and 6.

The results at the low temperatures (33° to 10°F, 1° to 12°C) are typical; that is, resilient modulus approaches a limiting value of about 2 million pounds per square inch. At the higher temperatures (above 60°F, 16°C), however, the additives exhibit the capacity to increase resilient modulus of the mixtures. The rheological properties of the binders strongly influence the resilient modulus values. Resilient modulus of the AC-20 or AR-4000 mixtures was consistently higher than the other mixtures. Analysis of variance using $\alpha = 0.05$ and Duncan's multiple range test showed that resilient modulus of the additive modified mixtures was significantly different from the control mixtures (AC-20 and AR-4000) at 68°F (20°C) and higher but not at 33°F (1°C) and below. On the average, Novophalt and Kraton showed the greatest increases in mixture stiffness at the higher temperatures.

Although pavement performance data based on resilient modulus has not been established, it appears that the ideal asphalt additive should decrease mixture stiffness at low temperatures to improve flexibility and

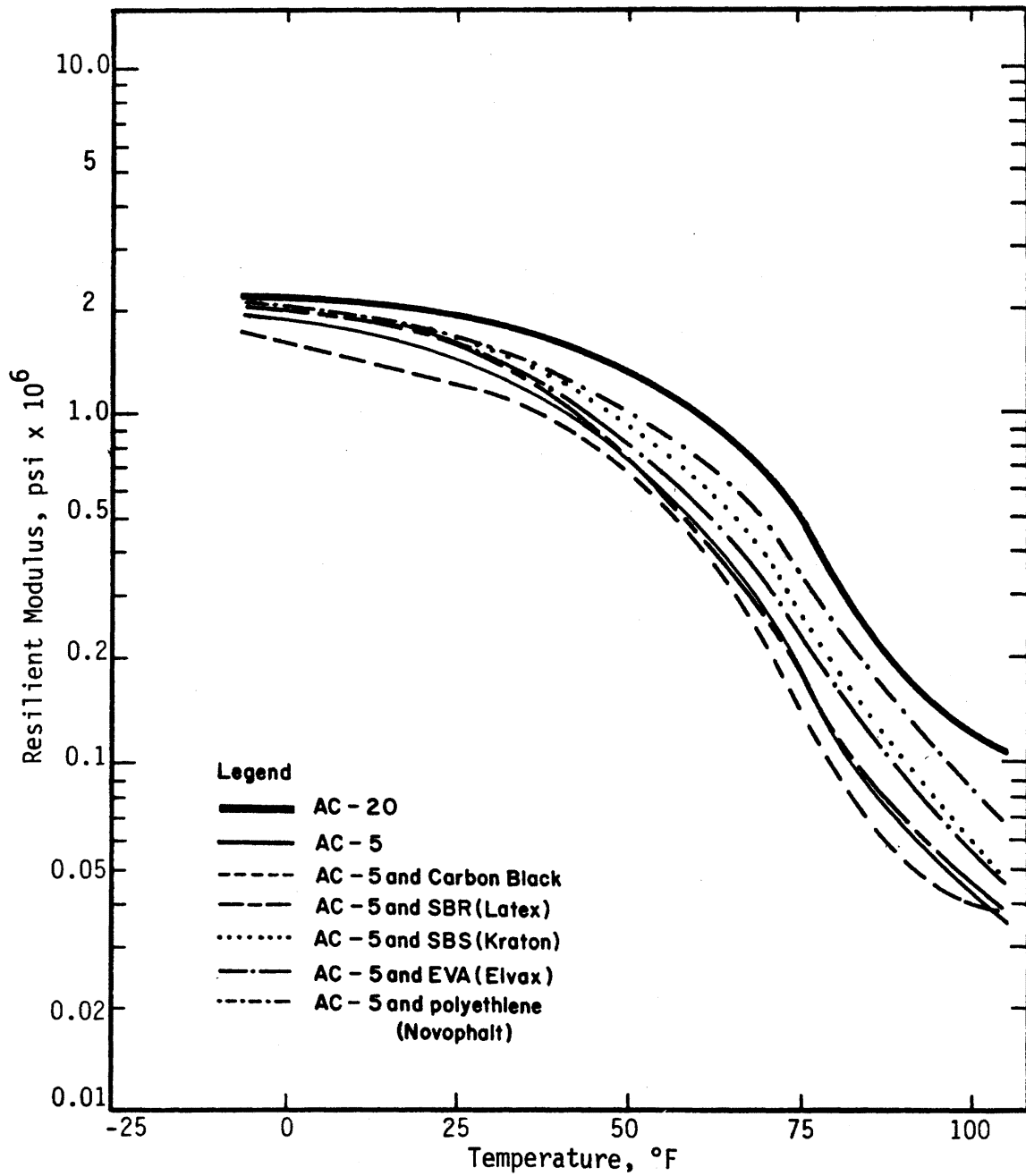


Figure 5. Resilient modulus as a function of temperature for river gravel mixtures containing Texaco asphalts with and without additives.

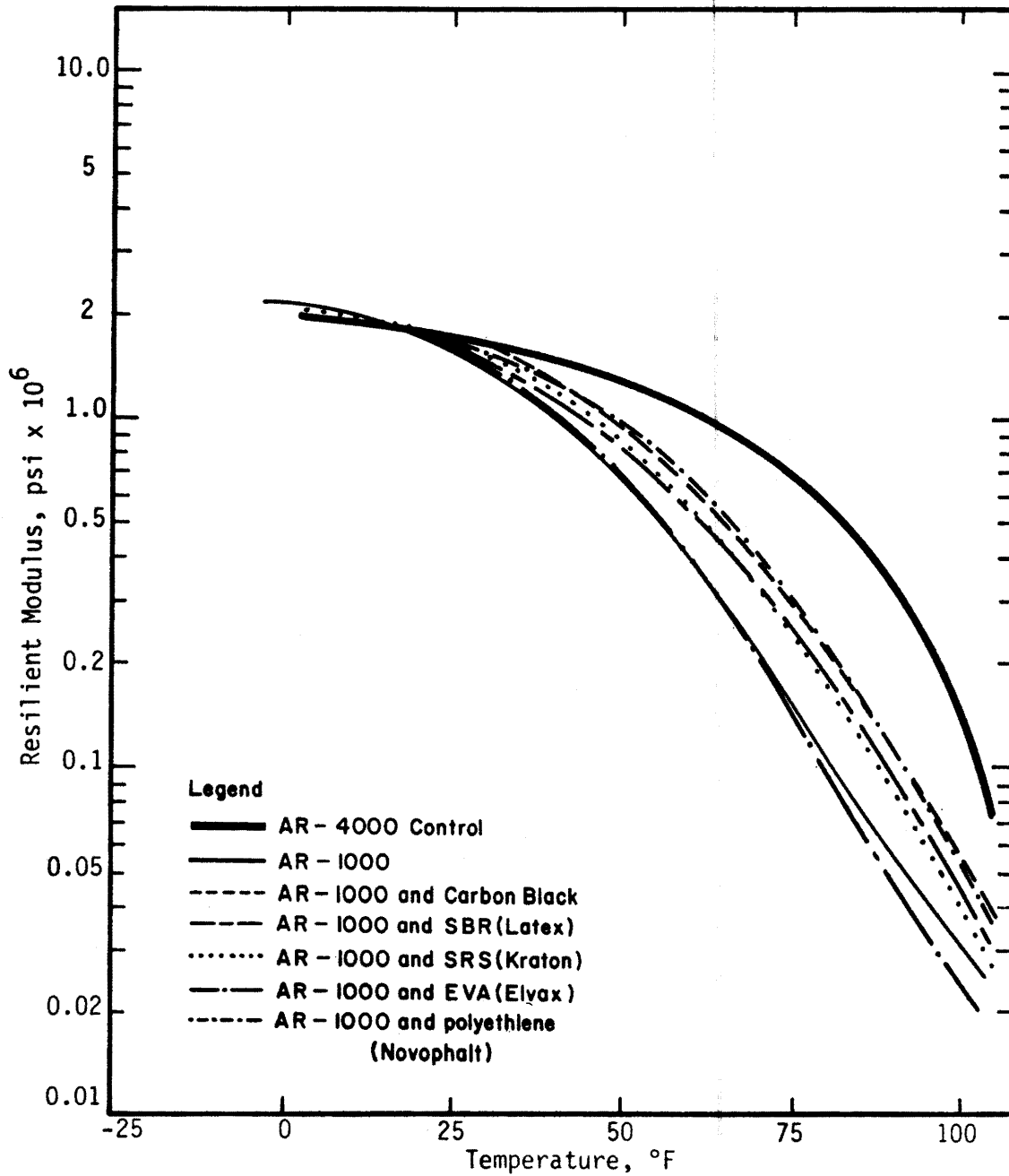


Figure 6. Resilient modulus as a function of temperature for mixtures containing San Joaquin Valley asphalts with and without additives.

reduce cracking and/or increase mixture stiffness at high temperatures in order to reduce permanent deformation.

INDIRECT TENSION

The indirect tension test employs the indirect method of measuring mixture tensile properties. The 2-inch (51 mm) high and 4-inch (102 mm) diameter cylindrical specimens were loaded diametrically at a constant rate of deformation until complete failure occurred. Diametral deformation perpendicular to the loaded plane was monitored in order to quantify mixture stiffness. Tests were conducted at nominal temperatures of 0, 33 and 77°F (-18, 1 and 25°C) and deformation rates of 0.02, 0.2 and 2-inches per minute (0.51, 5.1 and 51 mm/min) on specimens made using the Texaco asphalts (17). Specimens containing the California Valley asphalt were tested only at 77°F (25°C) and 2-inches per minute. Data are tabulated in tables 40 through 43 and plotted in figures 7 through 12. Strain at failure is the total diametral strain in the specimen at the maximum load in the plane perpendicular to the applied load. Secant modulus is the slope of the straight line on the stress strain plot from the origin to the point of maximum stress and corresponding strain, thus the term "secant".

Regarding the Texaco asphalt mixtures, the AC-20 control mixture consistently exhibited the greatest tensile strength at 77°F (25°C) and all loading rates. At lower temperatures, tensile strength of the AC-20 control mixture appeared to reach a maximum of about 400 pounds per square inch (2.76×10^6 MPa). Tensile strengths of the mixtures containing the AC-5 with or without an additive are shown to exceed 400 pounds per square inch by 10 to 25 percent. At low temperatures and the higher loading rates, all of the additives demonstrated the ability to increase mixture tensile strength over that of the AC-5 or AC-20 alone. Furthermore, the mixtures containing AC-5, with and without an additive, generally required significantly more strain at failure at the intermediate temperatures than the mixtures containing AC-20.

Table 40. Tensile properties at 77°F of mixtures made using Texaco asphalt and river gravel.

Type Mixture	Tensile Properties @ 0.02 in/min.			Tensile Properties @ 0.2 in/min.			Tensile Properties @ 2.0 in/min.		
	Tensile Strength, psi	Strain @ Failure, in/in	Secant Modulus, psi	Tensile Strength, psi	Strain @ Failure, in/in	Secant Modulus, psi	Tensile Strength, psi	Strain @ Failure, in/in	Secant Modulus, psi
Control: AC-20	45	0.0028	16,000	83	0.0030	27,700	121	0.0036	34,000
Control: AC-5	16	0.0023	7,100	28	0.0029	9,600	63	0.0031	20,100
AC-5 + 15% Microfil 8	15	0.0030	5,100	33	0.0028	11,900	64	0.0040	17,000
AC-5 + 5% Elvax 150	22	0.0023	9,800	48	0.0023	21,100	87	0.0024	35,300
AC-5 + 5% Kraton D	27	0.0028	9,700	54	0.0025	21,300	112	0.0025	45,700
AC-5 + 5% Latex	15	0.0032	4,900	31	0.0030	10,300	74	0.0031	24,100
AC-5 + 5% Novophalt	28	0.0024	12,100	58	0.0022	26,600	119	0.0025	48,600

Table 41. Tensile properties at 33°F of mixtures made using Texaco asphalt and river gravel.

Type Mixture	Tensile Properties @ 0.02 in/min.			Tensile Properties @ 0.2 in/min.			Tensile Properties @ 2.0 in/min.		
	Tensile Strength, psi	Strain @ Failure, in/in	Secant Modulus, psi	Tensile Strength, psi	Strain @ Failure, in/in	Secant Modulus, psi	Tensile Strength, psi	Strain @ Failure, in/in	Secant Modulus, psi
Control: AC-20	211	0.00112	194,000	342	0.00040	866,000	369	0.00039	996,000
Control: AC-5	128	0.00178	72,000	244	0.00156	157,000	376	0.00165	265,000
AC-5 + 15% Microfil 8	132	0.00163	82,000	217	0.00192	114,000	360	0.00139	267,000
AC-5 + 5% Elvax 150	119	0.00138	87,000	241	0.00160	155,000	444	0.00130	349,000
AC-5 + 5% Kraton D	136	0.00118	117,000	300	0.00118	253,000	428	0.00077	569,000
AC-5 + 5% Latex	121	0.00152	80,000	239	0.00182	189,000	399	0.00166	242,000
AC-5 + 5% Novophalt	167	0.00138	121,000	329	0.00118	278,000	436	0.00040	1,133,000

Table 42. Tensile properties at -10 or -18°F of mixtures made using Texaco asphalt and river gravel.

Type Mixture	Tensile Properties @ 0.02			Tensile Properties @ 0.2			Tensile Properties @ 2.0		
	Tensile Strength, psi	Strain @ Failure, in/in	Secant Modulus, psi	Tensile Strength, psi	Strain @ Failure, in/in	Secant Modulus, psi	Tensile Strength, psi	Strain @ Failure, in/in	Secant Modulus, psi
Control: AC-20	(2)413	0.00013	3.18X10 ⁶	(1)395	*	*	(2)374	0.00008	4.68X10 ⁶
Control: AC-5	(2)327	0.00024	1.50X10 ⁶	(1)440	0.00005	9.17X10 ⁶	(2)522	0.00012	4.20X10 ⁶
AC-5 + 15% Microfil 8	(2)319	0.00053	0.61X10 ⁶	(1)424	0.00005	9.42X10 ⁶	(2)450	*	*
AC-5 + 5% Elvax 150	(1)381	0.00018	2.29X10 ⁶	(1)512	0.00007	7.52X10 ⁶	(1)425	0.00006	9.81X10 ⁶
AC-5 + 5% Kraton D	(1)404	0.00017	2.43X10 ⁶	(1)472	0.00008	5.90X10 ⁶	(1)502	0.00011	4.54X10 ⁶
AC-5 + 5% Latex	(1)348	0.00025	1.38X10 ⁶	(1)352	0.00010	3.70X10 ⁶	(2)437	0.00016	5.60X10 ⁶
AC-5 + 5% Novophalt	(1)393	0.00010	4.16X10 ⁶	(1)444	0.00003	11.59X10 ⁶	(1)387	0.00004	8.98X10 ⁶

Note: * - Difficult to accurately measure due to very small strain.

(1) - Tensile test performed at -10°F.

(2) - Tensile test performed at -18°F.

Table 43. Tensile properties and resilient modulus of mixtures (California Valley asphalt and river gravel).

Type Mixture	Air Void Content, percent	Resilient Modulus @ 77°F, psi x 10 ³	Tensile Properties*		
			Tensile Strength, psi	Strain @ Failure, in/in	Secant Modulus, psi
Control: AR-4000	4.4	720	260	0.0028	95,000
Control: AR-1000	4.2	140	80	0.0032	25,000
AR-1000 + 5% Latex	5.1	220	100	0.0028	35,000
AR-1000 + 15% Microfil 8	5.2	260	130	0.0029	46,000
AR-1000 + 5% Kraton D	4.9	200	110	0.0031	34,000
AR-1000 + 5% Novophalt	5.2	310	130	0.0025	53,000
AR-1000 + 5% Elvax 150	5.0	130	100	0.0042	25,000

* Tensile tests at 2 in/min and 77°F.

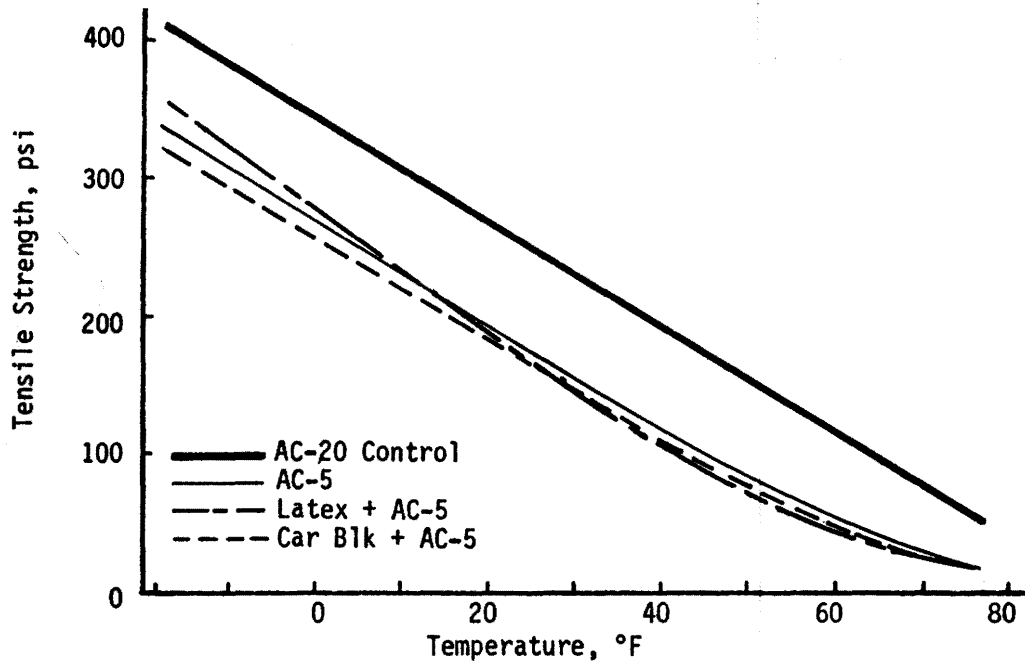


Figure 7a

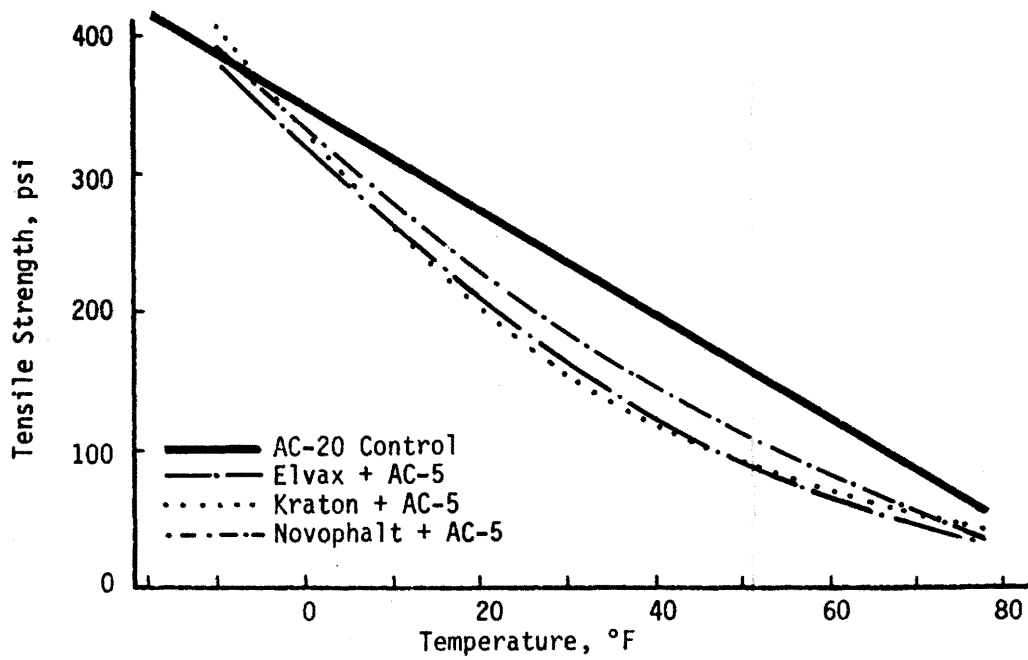


Figure 7b

Figure 7. Tensile strength as a function of temperature for displacement rate of 0.02 in/min for Texaco asphalt mixtures.

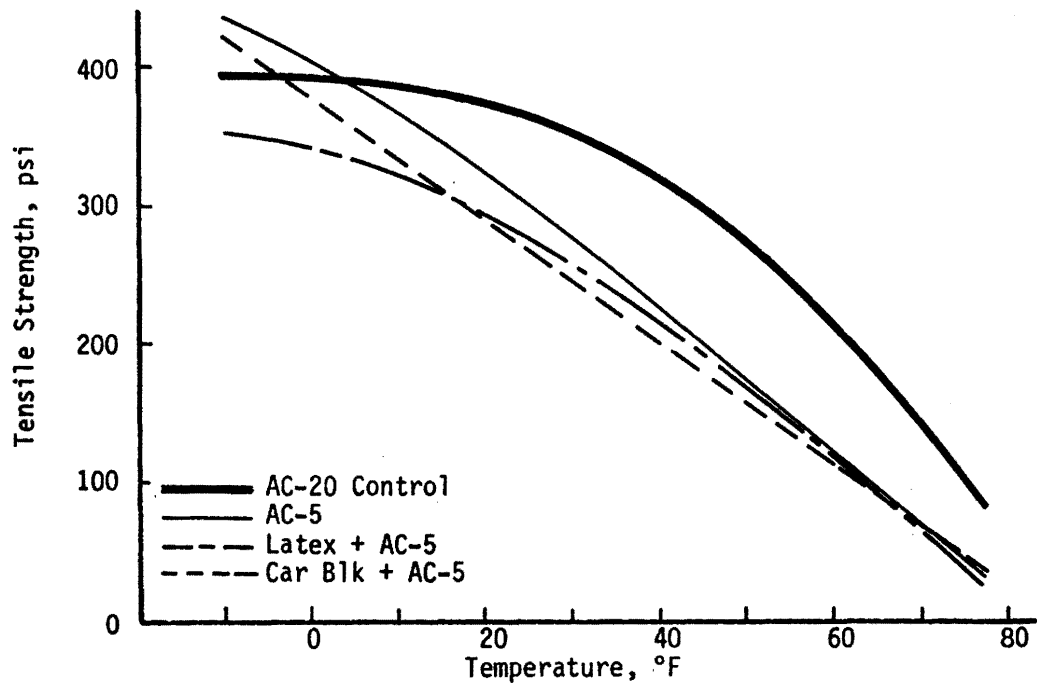


Figure 8a

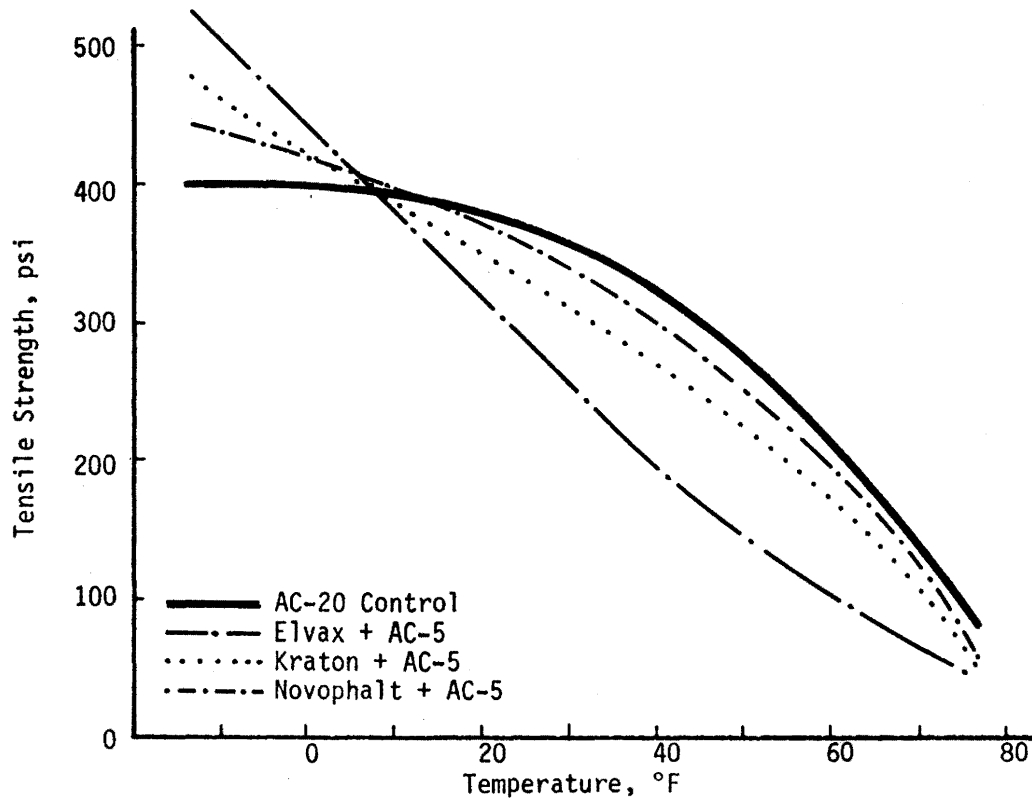


Figure 8b

Figure 8. Tensile strength as a function of temperature for displacement rate of 0.2 in/min for Texaco asphalt mixtures.

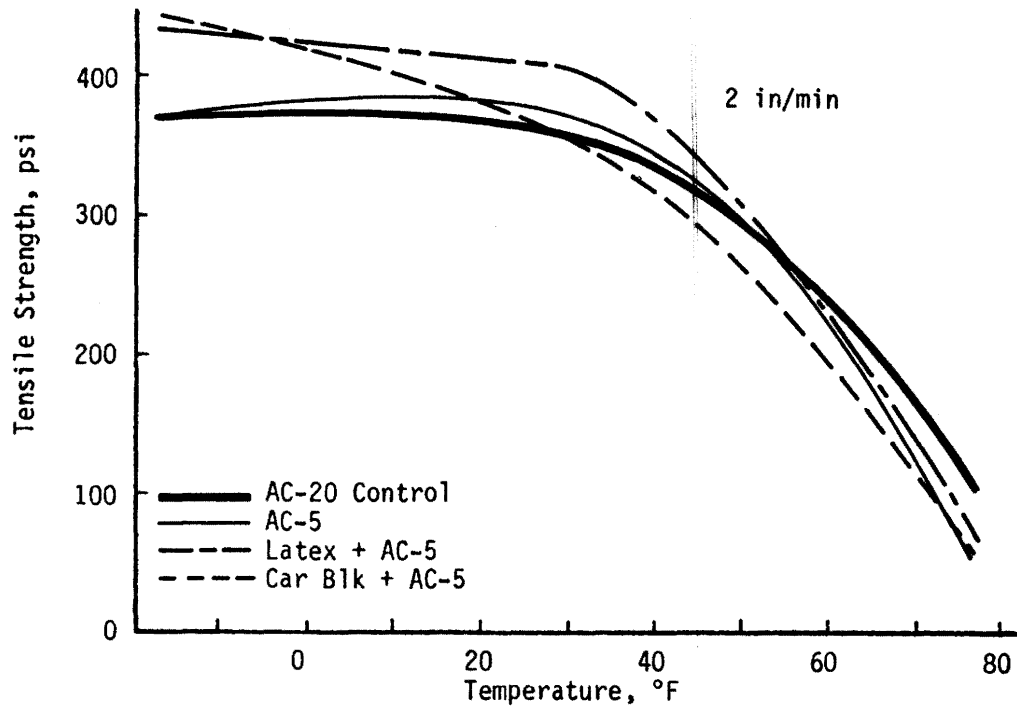


Figure 9a

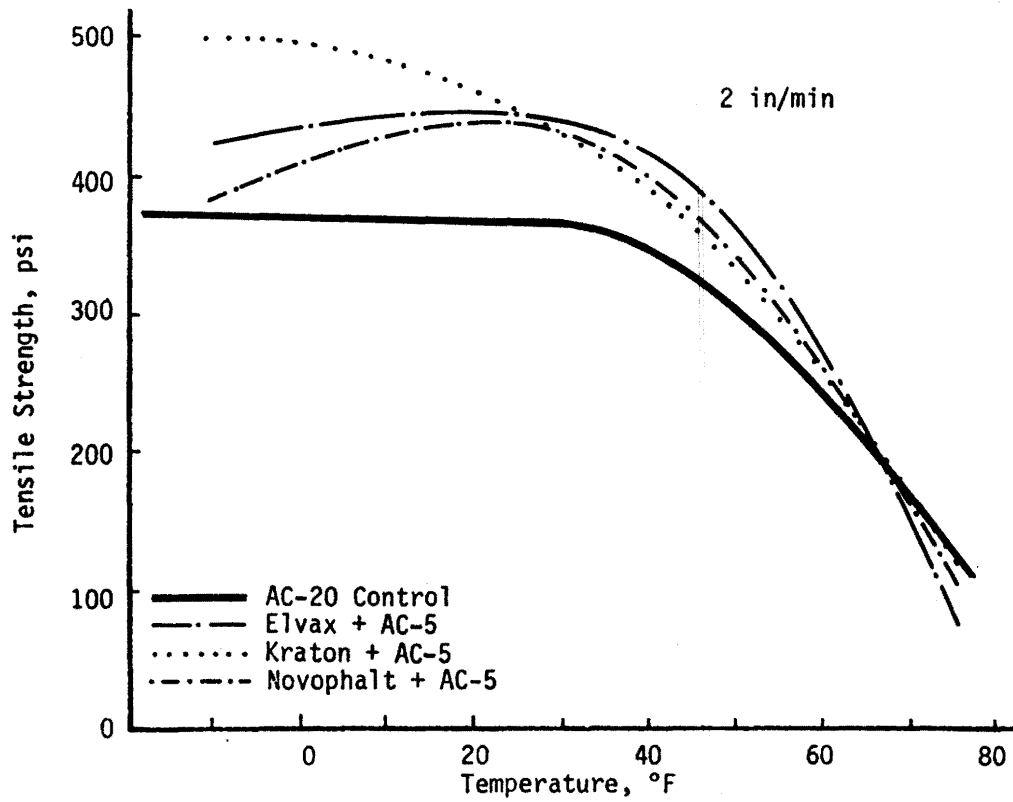


Figure 9b

Figure 9. Tensile strength as a function of temperature for displacement rate of 2 in/min for Texaco asphalt mixtures.

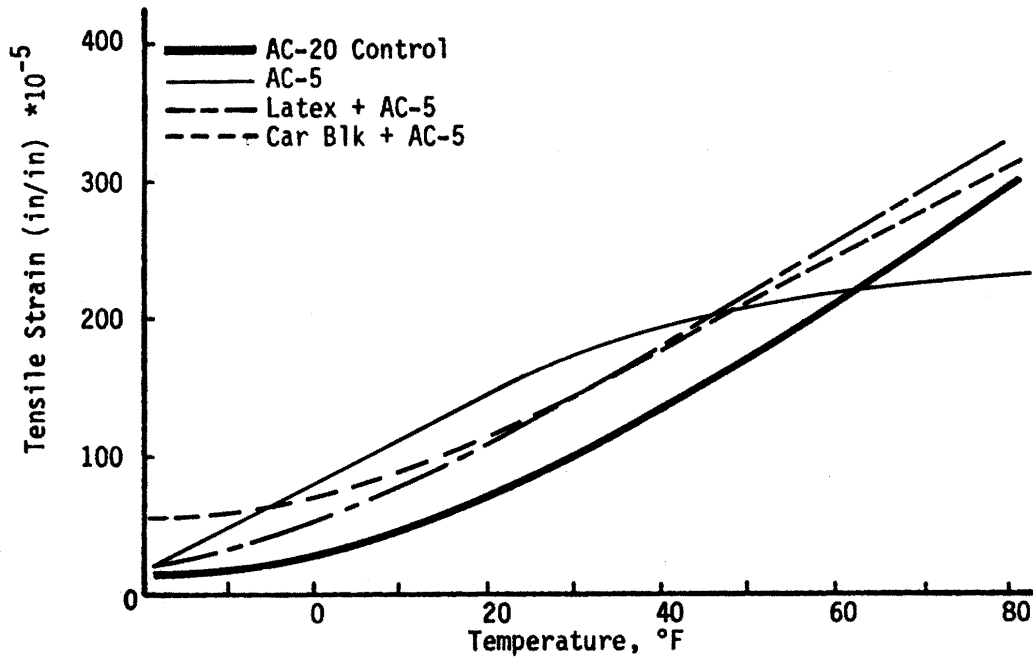


Figure 10a

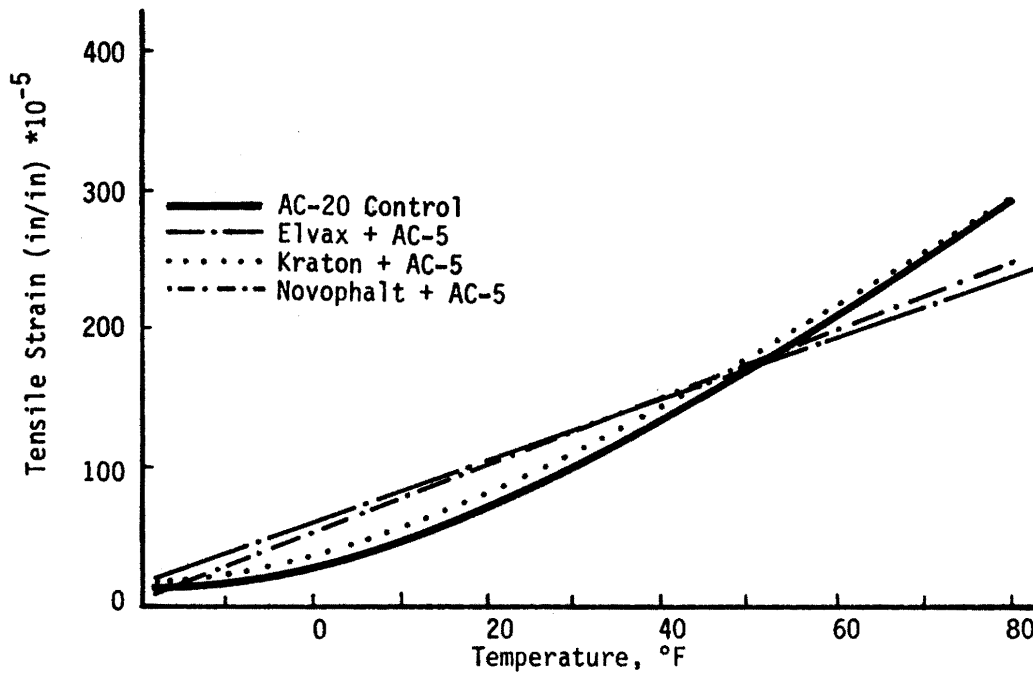


Figure 10b

Figure 10. Tensile strain at failure as a function of temperature for a displacement rate of 0.02 in/min for Texaco asphalt mixtures.

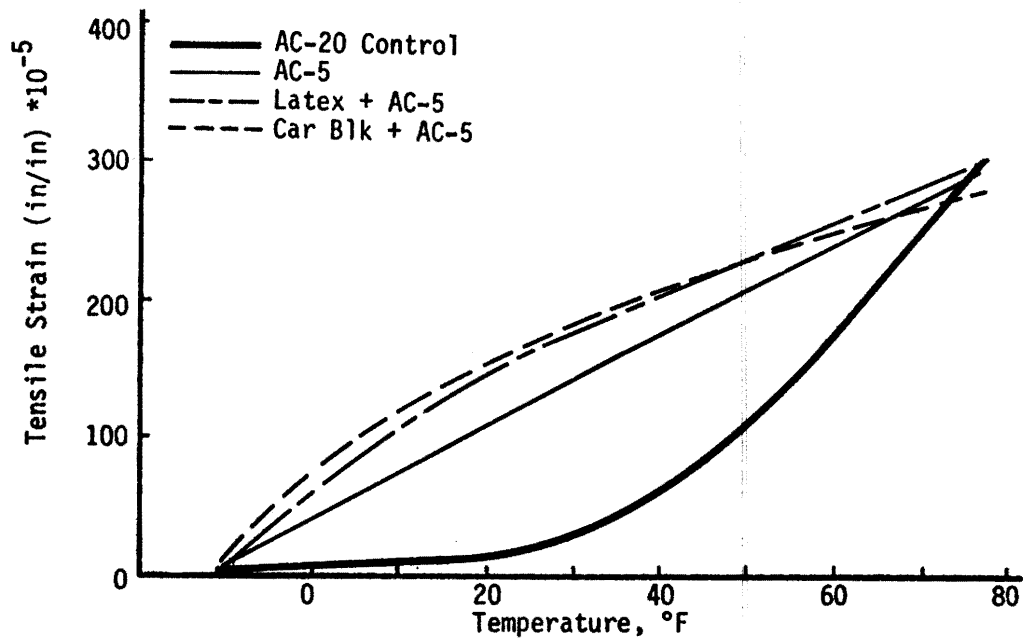


Figure 11a

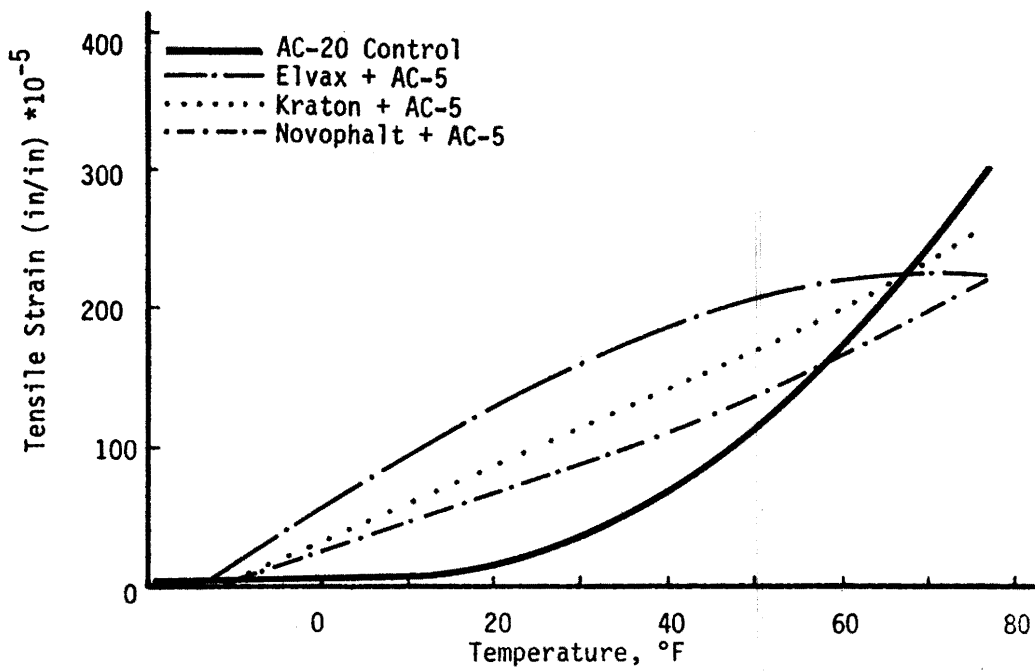


Figure 11b

Figure 11. Tensile strain at failure as a function of temperature for a displacement rate of 0.2 in/min for Texaco asphalt mixtures.

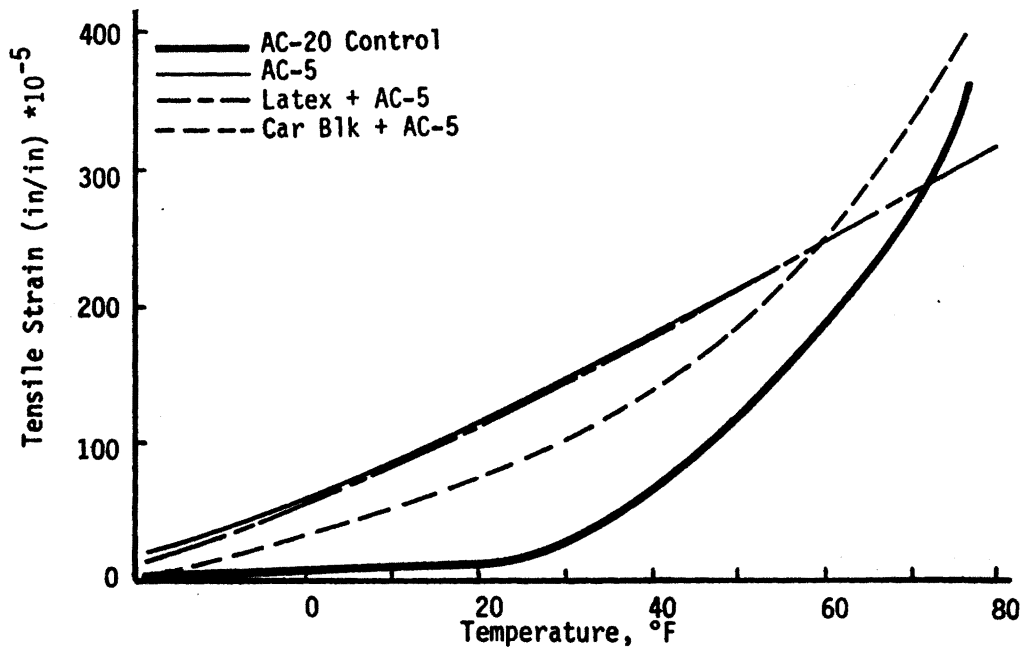


Figure 12a

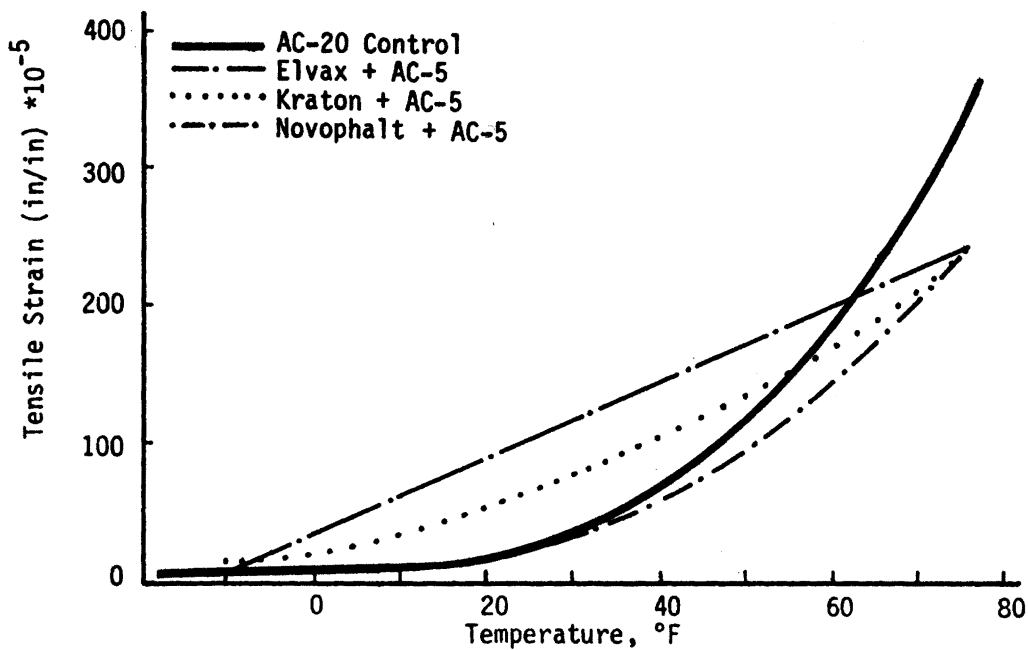


Figure 12b

Figure 12. Tensile strain at failure as a function of temperature for a displacement rate of 2 in/min for Texaco asphalt mixtures.

Tensile strengths at 77⁰F (25⁰C) and 2-inches per minute of the mixtures made using the California Valley asphalt (table 43) are generally greater than those made using the Texaco asphalts (Mixtures containing Kraton are an exception). This may be due to the greater compatibility of the additives with the California Valley material.

At very low temperatures (as those experienced in northern regions of the United States) and high loading rates (as those induced by traffic), soft asphalts modified with the additives studied herein have the potential to increase resistance to traffic induced cracking. This is inferred as a result of the increase in tensile strength and strain at failure (flexibility). However, since neither the tensile strength nor strain at failure is increased by the additives at low loading rates, the additives may not appreciably affect thermally induced cracking. Based solely on the results of these indirect tension tests, any increase in service life would be modest and cost effectiveness would be questionable. Positive statements in this area can only be made upon completion of a significant number of controlled field trials.

MOISTURE RESISTANCE

Indirect tension and resilient modulus tests before and after exposure to moisture were used evaluate the susceptibility of the mixtures to damage by moisture. The modified accelerated Lottman (18) moisture treatment consisted of vacuum saturating the specimens at a vacuum of 4-inches (102 mm) of mercury below atmospheric pressure at room temperature, wrapping them in cellophane to retain the moisture and freezing them at 0⁰F (-18⁰C) for 15 hours followed by a 24-hour period at 140⁰F (60⁰C). The specimens were then brought to 77⁰F (25⁰C) and tested in accordance with the program depicted in figure 4. Test results are given in tables 44a and 44b and figure 13. Normally, samples used in moisture testing are compacted to approximately 6.5 percent air voids; however, to economize and provide direct comparison with data in table 43, the samples containing the California Valley asphalt (table 44b) were

Table 44a. Properties of mixtures before and after exposure to moisture (Texaco asphalt and river gravel).

Type Mixture	Before Treatment					After Treatment					Resilient Modulus Ratio	Tensile Strength Ratio
	Air Void Content, Percent	Resilient Modulus @ 77°F, psiX10 ³	Tensile Properties*			Air Void Content, Percent	Resilient Modulus @ 77°F, psiX10 ³	Tensile Properties*				
			Tensile Strength, psi	Strain @ Failure,	Secant Modulus, psi			Tensile Strength, psi	Strain @ Failure	Secant Modulus, psi		
Control: AC-20	7.4	410	130	0.0032	42,000	7.4	220	110	0.0047	23,000	0.55	0.80
Control: AC-5	5.9	80	50	0.0034	14,000	5.4	100	70	0.0052	13,000	1.30	1.48
AC-5 + 15% Microfil 8	7.0	70	60	0.0040	15,000	7.3	60	50	0.0047	11,000	0.88	0.88
AC-5 + 5% Elvax 150	7.6	190	60	0.0024	28,000	7.0	70	70	0.0037	20,000	0.89	1.09
AC-5 + 5% Kraton D	6.4	270	80	0.0024	35,000	6.1	210	80	0.0031	27,000	0.80	1.00
AC-5 + 5% Latex	5.8	140	70	0.0037	19,000	5.8	100	70	0.0050	15,000	0.74	1.01
AC-5 + 5% Novophalt	6.3	320	90	0.0022	42,000	6.0	230	100	0.0031	33,000	0.73	1.07

*Tensile tests at 2 in/min and 77°F.

Table 44b. Properties of mixtures after exposure to moisture
(San Joaquin Valley asphalt and river gravel).

Type Mixture	After Treatment						
	Air Void Content, percent	Resilient Modulus @ 77°F, psiX10 ³	Tensile Properties*		Secant Modulus, psi	Resilient Modulus Ratio	Tensile Strength Ratio
			Tensile Strength, psi	Strain @ Failure,			
Control: AR-4000	3.8	500	170	0.0031	58,000	0.70	0.66
Control: AR-1000	3.4	100	60	0.0044	14,000	0.73	0.78
AR-1000+ 5% Latex	4.1	130	70	0.0047	16,000	0.60	0.76
AR-1000 + 15% Micro- fil 8	4.2	210	90	0.0040	25,000	0.81	0.73
AR-1000+5% Kraton D	4.4	150	90	0.0055	16,000	0.72	0.84
AR-1000 + 5% Novo- phalt	4.6	180	110	0.0039	28,000	0.59	0.82
AR-1000 + 5% Elvax 150	4.6	60	80	0.0072	11,000	0.47	0.77

*Tensile tests performed at 2 in/min and 77°F.

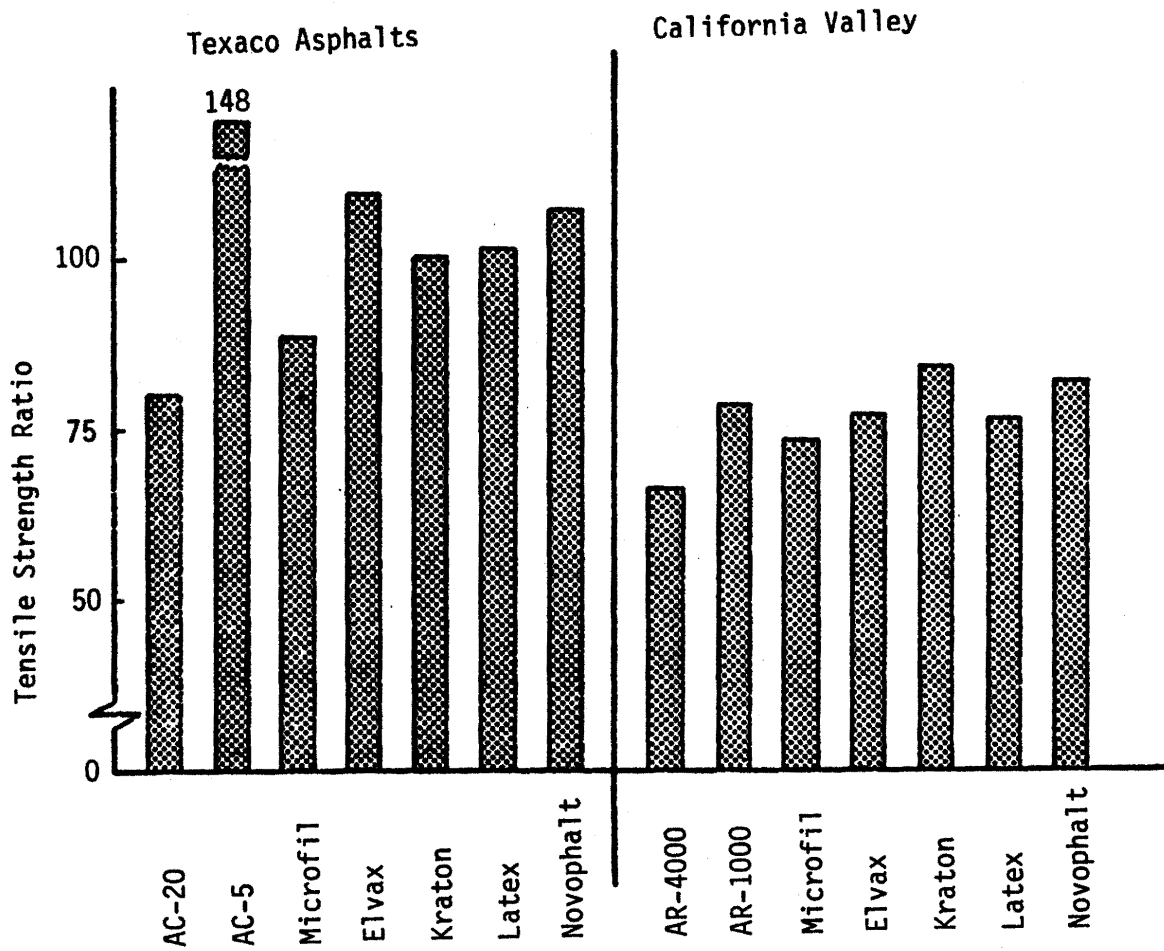


Figure 13. Tensile strength ratios for mixtures.

compacted using standard procedures and the resulting void contents were approximately 4 percent.

Ratios for resilient modulus and indirect tension were calculated by dividing measurements after moisture treatment by those obtained on untreated specimens. These tests were performed to evaluate any changes in moisture sensitivity of the paving mixture effected by the additives.

The most obvious result from these data is that the mixtures made using the San Joaquin Valley asphalts are more susceptible to moisture damage than those made using the Texaco asphalts (figure 13). This is consistent with predictions from the infrared analysis which showed a significantly higher concentration of carboxylic acid salts in the San Joaquin Valley asphalt. When the Texaco and San Joaquin Valley asphalts are considered separately the mixtures containing the softer binders (AC-5 and AR-1000) with or without an additive always exhibited greater tensile strength ratios than the control mixtures containing the AC-20 and AR-4000.

It appears that, generally, the additives have little effect on moisture susceptibility of the mixtures made using the materials included in this study. Mixtures containing Microfil-8 exhibited slightly lower tensile strength ratios with both asphalts. Microfil-8 differs significantly in properties when compared to the polymers utilized. It is basically a granular material with no ability to coat an aggregate with a continuous film. In fact, surfaces of mixtures containing Microfil-8 had a "dry" appearance when compared with mixtures containing the other binders.

Resilient modulus ratios are generally supportive of the results obtained from the tensile strength ratios but showed considerably more scatter. Tensile strength ratios from this procedure are widely accepted as relatively sensitive measures of moisture susceptibility. Resilient modulus ratios were merely measured to add to the data base since the test is fast and inexpensive.

EXTRACTION AND RECOVERY WITH ADDITIVES

Asphalt concrete containing the asphalts and additives studied herein were extracted and the binders were recovered (tables 45 and 46). Some of the recovered binders were analyzed to determine the amount of the additives recovered. There were differences in the relative efficacy of the hot (reflux) and cold (centrifugal) extraction methods. Some of the results with the San Joaquin Valley asphalts were contrary to those found for the Texaco asphalts. The limited number of tests did not establish whether the differences in extractability of the additives were specific to the asphalt used, or were due to other factors in the preparation and history of the asphalt concrete.

Since the conventional extraction methods do not remove all of the additives, data obtained for the amount of extracted binder and for properties of the recovered binders should be used only with the realization that a substantial fraction of the additive may remain in the extracted aggregate.

Analysis of some of the recovered binders showed that the amount of additive in the recovered binder may be determined by using an analytical method specific for the type of additive present. Content of carbon black can be determined by thermogravimetric analysis (TGA), and content of polyethylene in Novophalt can be determined by filtration of the dispersion in toluene or trichlorethylene. Determination of the content of SBR (e.g. from latex) by centrifuging and filtering of the dispersion in methyl isobutyl ketone appeared promising; but further effort would be required to develop a reliable method. The analytical methods must be standardized using the specific asphalt involved, since asphalts from different sources will yield different "blank" values for the analyses.

1. Extraction of Asphalt Concrete Containing Carbon Black

Extraction of asphalt concrete containing carbon black using benzene or trichloroethylene (TCE) removed most of the carbon black from the aggregate, but some of it was lost in the filter or in the "silt"

Table 45. Extraction of asphalt concrete specimens containing Texaco asphalts.

Binder	Design Binder Content, %	Extraction Method ^a	Extraction Solvent ^b	Extracted Aggregate, %	Recovered Binder, %	Unaccounted Loss, %	Tests on Recovered Binder			Comments
							Penetration at 77°F, 100g, bs	Viscosity at 140°F, P	Viscosity at 275°F, cSt	
Texaco AC-5, no additive	4.6	B	Benzene	95.7	4.3	0	51	930	350	Compare to values of 112 pen., 1190 P at 140°F and 311 cSt at 275°F for AC-5 after Rolling Thin Film Oven Test.
	4.6	B	TCE	95.5	4.5	0	100	1540	336	
Texaco AC-20, no additive	4.5	B	Benzene	95.9	3.8	0.3	32	9300	735	...
	4.5	B	TCE	95.8	4.2	0	28	13,200	841	
Texaco AC-5 + 5% Microfil B	4.75	B	Benzene	95.7	4.3	0	92	1710	433	Filter paper stained, but most of carbon black was in the recovered asphalt.
	4.75	B	TCE	95.7	4.3	0	106	1480	364	Filter paper stained, (more than B-7 above) but most of carbon black was in the recovered asphalt.
Texaco AC-5+ 5% Ultrapave Latex	5.0	B	Benzene	96.2	3.8	0	132	1120	439	Extraction very slow due to slow draining through filter. Aggregate obviously still still contained rubber. Recovered asphalt was not tested because extracted was overheated during long extraction time.
	5.0	A	TCE	95.4	4.6	0.0	Aggregate contained trace of rubber, much less than C-10 and C-18. Recovered asphalt was not tested because of long elapsed time between start of extraction and completion of recovery.
Texaco AC-5+ 5% Ultrapave Latex	5.0	A	TCE	95.4	4.6	0	70	6400	960	Aggregate contained trace of rubber.
	5.0	B	TCE	95.6	4.4	0	80	3710	830	Extraction very slow due to slow draining through filter. Aggregate contained rubber and could be lifted from filter as a single, loosely-bound conglomerate.
Texaco AC-5+ 5% Kraton S-B-S	4.5	B	TCE	95.8	4.2	-	61	18,100	1180	Extraction was rapid; aggregate did not appear to contain rubber.
	4.5	B	Benzene	95.9	4.1	0	60	19,200	1180	Extraction was rapid; aggregate did not appear to contain rubber.
Texaco AC-5+ 5% LDPE 526	4.6	B	TCE	95.6	4.4	0	57	8980	1130	Silt separated from extract by centrifuging appeared to contain some polyethylene.
	4.6	N	Benzene	95.8	4.1	0.1	53	6860	761	Silt separated from extract by centrifuging contained some polyethylene.
Texaco AC-5+ 5% Elvax 150	4.5	B	TCE	95.5	4.5	0	71	3090	1100	Extraction very slow due to slow draining through filter.
	4.5	B	Benzene	95.8	4.1	0.1	69	3000	1060	Extraction very slow due to slow draining through filter.

^aAASHTO T164. Method A used centrifugal "Rotarex" extraction; extraction is carried out at room temperature. In Method B, extraction is carried out at the temperature of boiling solvent. Extracts from both methods were centrifuged to remove silt which passed the primary filters, then distilled to recover the binder by AASHTO T170. Because volume of recovered binder was small, a round-bottom flask was substituted for the flat-bottom flask, to obtain better stripping of solvent by the CO₂ inlet tube.

^bReagent-grade benzene or reagent-grade trichloroethylene, as indicated.

Table 46. Extraction of asphalt concrete specimens containing San Joaquin Valley asphalts.

Binder	Design binder content, %	Extraction method ^a	Extraction solvent ^b	Extracted aggregate, %	Recovered binder, %	Unaccounted loss, %	Tests on recovered binder			Comments
							Penetration at 77°F, 100 g, 5 s	Viscosity at 140°F, P	Viscosity at 275°F, cSt	
AR-4000	4.6	B	Benzene	95.7	4.2	0.1	27	5380	387	...
85% AR-1000 15% Microfil 8	4.7	B	Benzene	96.2	3.8	0	150	644	194	No undispersed carbon black pellets were detected, but some carbon black was retained in the filters and some was removed from the asphalt solution by centrifuging.
95% AR-1000 5% SBR from Dow XUS 40052.00	4.5	B	TCE	96.0	4.0	0	62	16,960	6130	Extraction was very slow. A few pieces of aggregate were bound together by unextracted rubber. Recovered binder was very "rubbery".
		A	TCE	95.7	4.3	0	69	4520	946	No evidence of rubber in the extracted aggregate, but recovered binder did not seem very "rubbery".
95% AR-1000 5% Kraton S-B-S	4.5	B	Benzene	95.8	4.2	0	112	27,640	815	Recovered binder was almost a gel. No evidence of rubber in extracted aggregate.
95% AR-1000 5% LDPE 526	4.5	B	TCE	96.0	4.0	0	52	3880	371	Extraction was very slow. Some of the polyethylene remained in the extracted aggregate.
		A	TCE	95.8	4.1	0.1	47	4050	342	Much of the polyethylene remained in the extracted aggregate.
95% AR-1000 5% Elvax 150	4.5	B	Benzene	95.7	4.3	0	131	1410	458	Recovered binder was not very "rubbery", but viscosity at 275°F was relatively high. No obvious signs of EVA in extracted aggregate.

^aAASHTO T164. Method A uses centrifugal "Rotarex" extraction; extraction is carried out at room temperature. In Method B, extraction is carried out at the temperature of boiling solvent. Extracts from both methods were centrifuged to remove silt which passed the primary filters, then distilled to recover the binder by AASHTO T170.

^bReagent-grade benzene or reagent-grade trichlorethylene, as indicated.

centrifuged from the extract, so the recovered binder did not contain all the carbon black.

Previous experience with samples from field trials has shown that the recovery of carbon black is highly dependent on the dispersion achieved during mixing the asphalt concrete. Carbon is not soluble, so only that which is very finely dispersed will be retained in the extract through the filtering and centrifuging steps. More of the carbon black was retained in the benzene extract than in the TCE extract.

The binder present in the asphalt concrete containing Microfil 8 may have been significantly stiffer than indicated by the viscosity and penetration values determined on the recovered binder, as the recovered material probably contained all the oil component of the Microfil (6 to 8 percent), which is a diluent or plasticizer for the asphalt, but contained only about half the carbon black.

2. Extraction of Asphalt Concrete Containing SBR

In the extraction of the five specimens of asphalt concrete containing Texaco AC-5 plus styrene-butadiene rubber added as latex, cold extraction with trichloroethylene (TCE) removed more of the rubber than did hot extraction with refluxing TCE or benzene. The extracted aggregates from the specimens containing the Texaco binder all obviously contained enough rubber to bind some of the aggregate particles together. When portions of the asphalt concrete specimen containing San Joaquin Valley AR-1000 plus SBR added as latex were extracted with TCE by both methods, there were only a few traces of rubber in the aggregate extracted by the reflux method, and no visible rubber in the cold-extracted aggregate. The properties of the binder recovered by the two methods were very different. The binder from the reflux extraction was very "rubbery". Its viscosity was quite high at both 140°F (60°C) and 275°F (135°C). Since portions of a single molded specimen were used in the two extraction runs, the history of the contained binder can be assumed to have been identical until the extraction. This suggests that some crosslinking of the SBR polymer occurred during the long heating

period in the presence of the refluxing TCE, possibly involving reaction with the TCE.

3. Extraction of Asphalt Containing Polyethylene

Reflux extraction of asphalt concrete containing Novophalt made with Texaco AC-5 showed that both benzene and TCE extracted practically all the binder, but that some recrystallized polyethylene was precipitated from the benzene solution during centrifuging of the extract before removing the solvent. The recrystallized polyethylene floated on top of the denser TCE solution, so less was lost during centrifuging. Only two samples of Novophalt made with San Joaquin Valley AR-1000 were extracted. Both portions were extracted with TCE, one using the reflux method and the other using the cold method. There was very little difference in the amount of binder recovered by the two methods, and in the properties of the recovered binders.

4. Extraction of Asphalt Concrete Containing EVA and SBS

Benzene and TCE appeared to be equally effective in extracting asphalt concrete containing S-B-S thermoplastic block copolymer rubber (Kraton) and ethylene-vinyl acetate copolymer resin (Elvax 150). There were no visible signs of S-B-S rubber or EVA resin remaining in the aggregates or filters; however, the non-tacky EVA might be difficult to detect. Since the amount of binder recovered was less than the design content, it is possible that some binder did remain in the aggregate; however, the discrepancy between design content and recovered binder was no larger than that for the control specimens.

In summary, the paving engineer should recognize that standard extraction methods are not totally effective for extracting modified asphalts from paving mixtures.

EVALUATION OF FATIGUE CRACKING POTENTIAL

1. Approach

The potential of mixtures of asphalt concrete modified by asphalt additives to crack due to cyclic fatigue was evaluated using two approaches: (1) the phenomenological, beam fatigue approach and (2) a fracture mechanics based controlled displacement approach.

The phenomenological regression approach is the most common method used in fatigue testing or analysis of highway materials. The very familiar relationship used to represent the fatigue response is of the form:

$$N_f = K_1 (1/\epsilon_t)^{K_2} \quad \text{Equation 13}$$

where N_f is the number of repetitions to failure, ϵ_t is the repeatedly induced tensile strain and K_1 and K_2 are regression constants. These parameters are influenced by several variables including type and rate of load, type of test, mixture properties and temperatures. Hence, K_1 and K_2 are not material properties.

The beam fatigue test may be performed either in a controlled strain or controlled stress mode. The proper test mode depends on the type of pavements being simulated. Epps and Monismith (19) reported that a controlled stress mode of loading is encountered in thick, stiff pavements typically 6-inches (152 mm) thick or thicker. Controlled strain loading is, on the other hand, typically encountered in thin pavement sections (2-inches (50 mm) thick or thinner).

Generally, the phenomenological approach provides a reasonably simple approach which has been almost universally adopted. However, it bears the limitation that it cannot account for both crack initiation and propagation. Such distinctions may be very important in establishing the fatigue life of a new material expected to be used for a wide range of applications. It seems reasonable that a stiff but brittle material may perform well in a controlled-stress laboratory test, but fail rapidly due to immediate crack propagation if the material is used in situ where controlled strain is the mode of cyclic applications.

The fracture mechanics based approach employs a device which applies a controlled displacement to an asphalt concrete beam. The device was developed at Texas A&M and is called the overlay tester as it was initially used to simulate the controlled displacement opening and closing of a crack beneath an asphalt concrete overlay. Fracture mechanics techniques are used to evaluate the energy required to propagate the crack through the material.

In summary, two testing techniques were used to evaluate the potential of asphalt concrete mixtures to fail in fatigue. First, the controlled stress beam fatigue test was used to simulate controlled stress as induced due to repeated applications of a design load. Second, the controlled displacement (overlay) test was used to simulate the controlled cyclic strains imparted to a pavement due to movement of the underlying fractured pavement, such as joint movement in a PCC pavement. These tests should yield a thorough analysis of the fatigue potential of the materials evaluated.

2. Sample Fabrication

Beams 3 in (76 mm) square and 15 in (318 mm) long were prepared using the Cox kneading compactor for both controlled stress (flexural beam fatigue) testing and controlled displacement (overlay) testing. Mixing and compaction temperatures for the various asphalt-additive blends were determined based on viscosity versus temperature data (Chapter 3).

The temperatures required for mixing based on the viscosity data were often quite high. For example, asphalt blends with latex required mixing temperatures of 405^oF (207^oC) and 414^oF (212^oC), respectively, for AC-5 and AR-1000. These temperatures are not practical under field conditions and more realistic mixing temperatures of 340^oF (171^oC) and 315^oF (157^oC), respectively, were used.

The predicted compaction temperatures based on viscosity versus temperature data had to be adjusted downward for each asphalt-additive blend, except carbon black.

It was virtually impossible to compact mixtures at the predicted compaction temperatures due to excessive shoving under the compaction foot. Adjusted mixing and compaction temperatures are listed in table 47.

All additives and asphalts were heated to 300°F (149°C) for 40 minutes and poured into separate cans prior to mixing. Even so, large lumps were observed in the pre-blended additives (Kraton and Elvax). These additives were heated for an additional 40 minutes to completely melt the lumps. The blending procedure should be explicitly identified when such additives are used.

A target air void contents of 6-percent was established for each beam. In order to minimize void content variability among samples, it was necessary to alter the compaction procedures specified by the VESYS User's Manual (20). This problem was magnified because of the poor degree of interlocking among the rounded, smooth river gravel particles resulting in easy shearing and shoving of the mixture.

A second problem was within sample variation in air void content. For example, severe density gradients from top to bottom of the beams were identified. For beams with a 6-percent air void content, it was typical to measure 7.5 to 8-percent air voids in the top, 6-percent in the middle and 4 to 5-percent in the bottom of the beam. To minimize the problem, a stepwise increasing compaction pressure was used. Low pressure at the early stage of compaction was used to stabilize the sample, followed by high pressures to reduce the air void contents.

A trial and error method was used to determine the proper compaction procedure. The procedure resulted in a difference in air void content from top to bottom of the beam of less than 0.5 percent.

The target air voids content was achieved for all mixtures except those containing carbon black. For these beams, it was much more difficult to compact the specimens to the 6-percent air void level. Even when twice the compactive effort was applied, the air void content could only be reduced to about 7-percent. Consequently, the void contents for the samples containing carbon black are from 1/2 to 1-percent higher than for the other samples. This difference in compaction is largely due to

Table 47. Adjusted mixing and compaction temperatures for different binders.

Type of Binder	From Visc.-Temp. Data		Adjusted	
	Mixing Temp.	Compaction Temp.	Mixing Temp.	Compaction Temp.
AC-20	307	287	307	275
Latex+AC-5	405	374	340	290
Carbon Black + AC-5	339	315	339	315
Kraton+AC-5	339	316	339	290
Novophalt+AC-5	345	322	345	290
Elvax+AC-5	335	311	335	290
AR-4000	290	271	290	271
Latex+AR-1000	414	385	315	290
Carbon Black + AR-1000	310	289	310	289
Kraton+AR-1000	316	291	316	291
Novophalt +AR-1000	313	289	313	289
Elvax+AR-1000	316	292	316	292

$$^{\circ}\text{C} = (^{\circ}\text{F} - 32)/1.8$$

the effect of the dry powder (carbon black) to resist the compactive effort.

CONTROLLED STRESS FLEXURAL FATIGUE

1. Experiment Design

Flexural beam fatigue testing was performed as shown in figure 14. All testing was on beams fabricated with a silicious river gravel aggregate of the gradation and specifications shown in appendix D. As previously discussed the production quality of each beam was controlled by assuring an air void content of between 5.5 and 6.5 percent for all beams except those containing carbon black where the range was 6.5 to 7.0 percent.

Nine beam samples were tested at each combination of variables. Three beams were tested at each of three stress levels (low, intermediate and high). The logarithm of the strain, ϵ_t , induced at the 200th repetition of the stress level in question was plotted versus the logarithm of the number of load cycles to failure, N_f . A least squares regression curve was fitted through the data to determine the characteristic parameters K_1 and K_2 .

2. Results of Testing

Table 48 summarizes the flexural beam fatigue data (controlled stress) in terms of the fatigue parameters K_1 and K_2 . In order to more easily evaluate the relative controlled stress fatigue response, the 68°F (20°C) data are plotted in figure 15 and the 32°F (0°C) data are plotted in figure 16.

Based on the $\log \epsilon_t$ versus $\log N_f$ plots the following trends are apparent:

1. At 68°F each additive blend with AC-5 produced a mixture which has statistically superior fatigue properties compared to the control mixture using AC-20 asphalt as the binder. Although the plots of fatigue results from mixtures containing AC-20, AC-5 with Novophalt and AC-5 with

Aggregate	Binder	Test Temperature, °F	Curing Condition	River Gravel (Silicious)					
				AC-20	AC-5 Carb.Blk.	AC-5 Latex	AC-5 Novo.	AC-5 SBS	AC-5 EVA
		Normal	33	9*	9	9	9	9	9
			68	9	9	9	9	9	9
		14 days @ 140°F	33						
			68	9	9	9	9	9	9

* 9 samples were tested for each cell, 3 at each of 3 stress levels.

Figure 14. Test matrix for flexural beam fatigue testing.
 $^{\circ}\text{C} = (^{\circ}\text{F} - 32) / 1.8$

Table 48. Summary of K_1 and K_2 values for beam fatigue testing at 34°F and 68°F (normal curing).

Temp.	Binder	K_1	K_2	R^2 of Regression
34°F	AC-20	1.28×10^{-12}	3.77	0.70
	AC-10*	7.26×10^{-11}	3.90	0.80
	AC-5 + Carbon Black	2.56×10^{-17}	5.78	0.94
	AC-5 + EVA	1.92×10^{-10}	3.99	0.74
	AC-5 + SBS	9.76×10^{-13}	4.73	0.91
	AC-5 + Latex	7.84×10^{-11}	4.16	0.96
	AC-5 + Polyethylene (Novophalt)	7.18×10^{-17}	5.91	0.91
68°	AC-20	4.70×10^{-6}	2.63	0.89
	AC-10*	8.00×10^{-9}	3.74	0.72
	AC-5 + Carbon Black	2.63×10^{-6}	2.84	0.88
	AC-5 + EVA	1.28×10^{-7}	3.91	0.94
	AC-5 + SBS	1.64×10^{-5}	3.12	0.68
	AC-5 + Latex	3.63×10^{-5}	3.04	0.78
	AC-5 + Polyethylene (Novophalt)	2.33×10^{-8}	3.38	0.85

*Mixture of AC-10 and crushed limestone.

$$^{\circ}\text{C} = (^{\circ}\text{F} - 32)/1.8$$

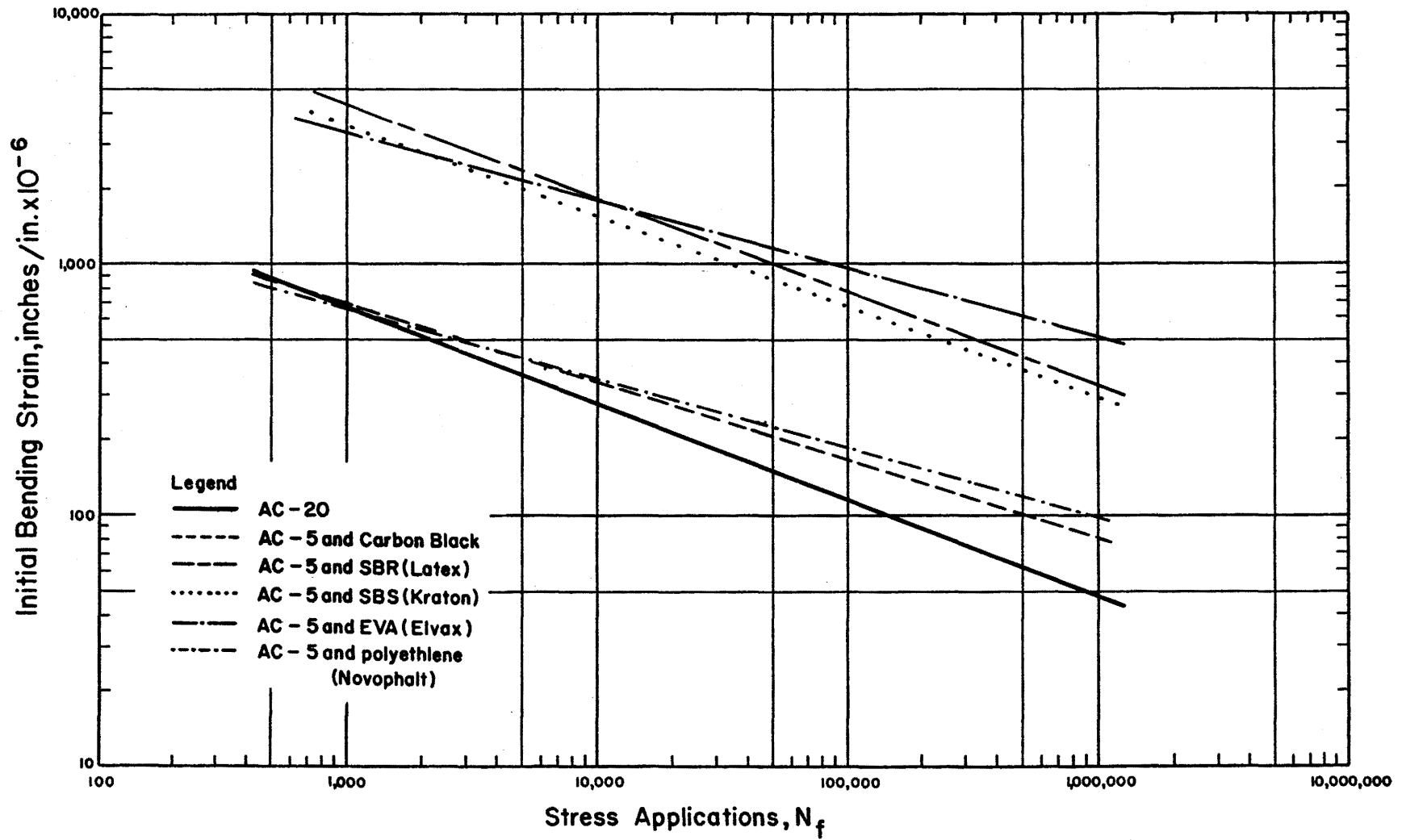


Figure 15. Controlled stress flexural beam fatigue results at 68°F (20°C).

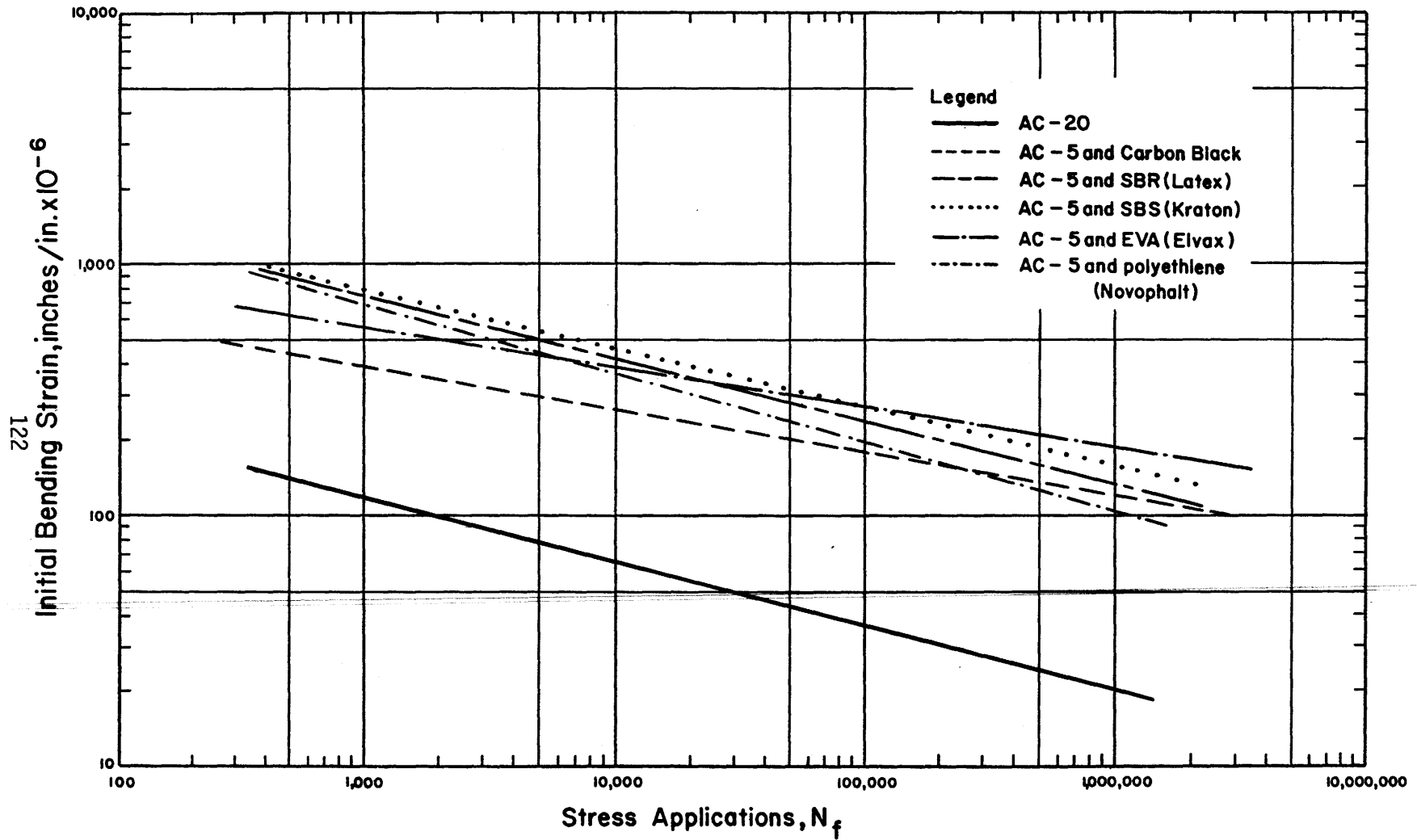


Figure 16. Controlled stress flexural beam fatigue results at 32°F (0°C).

carbon black are closely grouped, they are statistically different ($\alpha = 0.05$). Statistical difference is defined as when either the intercept or slope or both are different.

2. At 68⁰F the mixtures containing blends of AC-5 and EVA (Elvax), AC-5 and SBR (Latex) and AC-5 and SBS (Kraton) performed practically the same, although the fatigue plots are statistically different ($\alpha = 0.05$). These mixtures showed significantly superior fatigue responses to the mixtures containing either blends of AC-5 and carbon black or AC-5 and polyethylene (Novophalt).

3. At 32⁰F (0⁰C) the modified AC-5 asphalt blends once again provided a superior response to the control. Fatigue results among mixtures containing blends of AC-5 and polyethylene (Novophalt), SBS (Kraton), SBR (Latex) and EVA (Elvax) were not significantly different.

4. The levels of applied flexural stress, strain at the 200th load cycle and cycles to failure are documented in tables E7 through E12 of appendix E. Stress levels over the range of approximately 200 psi (1.38×10^6 MPa) to approximately 475 psi (3.27×10^6 MPa) were used for all mixtures. The 200th cycle strains were substantially different among the mixtures tested at 68⁰F (20⁰C) (see tables E7 though E12). The general trend was a substantially softer response for AC-5 blends containing EVA, SBS (Kraton) and SBR (Latex). These effects will be considered in "Discussion of Results".

3. Effects of Accelerated Aging on Controlled Stress Flexural Fatigue

Asphalt concrete mixtures are often subjected to extended periods of accelerated oxidative aging at high temperatures. The laboratory mixture fabrication procedure subjects mixtures to an environment similar to that of the hot mix plants. No standard procedure has been documented to simulate post construction oxidative aging in the field. However, laboratory testing at Texas A&M (21) has revealed that aging at 140⁰F

(60°C) substantially changes material properties such as resilient modulus and indirect tensile strength.

Button (22) has shown that essentially all detectable changes in mixture properties occur within a 14-day period of high temperature aging (140°F). In this study, beams were aged for 14 days and tested in controlled stress flexural fatigue to evaluate the effects of accelerated oxidative aging. This should represent the effects of aging at substantially longer periods of oxidative aging in the field.

Table 49 compares flexural controlled stress fatigue parameters K_1 and K_2 for aged and unaged specimens tested at 68°F (20°C). The high R^2 values associated with each test are indicative of how well the regression curves account for the variance between initial strain and cycles to failure.

The K_1 and K_2 values are substantially different between the aged and unaged samples. The general trend is poorer fatigue response following aging. A more fracture-susceptible response is demonstrated by the generally higher K_1 values coupled with substantially low K_2 values, indicative of a much steeper slope.

Figure 17 illustrates the fatigue curves following accelerated aging.

Based on the data summarized in tables 49 and figure 17, the following trends are identified:

1. The most dramatic effect of accelerated aging on fatigue life occurred in the SBS (Kraton) and EVA (Elvax) mixtures. A significant change in the slope of the fatigue curves revealed a much more rapid fatigue rate as stress-level increases for those mixtures compared to their unaged counterpart mixtures.
2. The aging effects on the SBR (Latex) and polyethylene (Novophalt) mixtures were less pronounced but highly significant and resulted in a substantially decreased fatigue life.
3. The accelerated aging period significantly improved the flexural fatigue response of the AC-20 mixtures in direct contrast to the effects on AC-5 asphalt-additive blends.

It is difficult to assess the results of the heat-aging experiment. The complexities of the binder-additive compatibility no doubt have an

Table 49. Summary of fatigue parameters K_1 and K_2 computed from unaged and aged (accelerated aging at 140°F) samples.

Specimen History	Binder Identification	K_1	K_2	R^2 of Regression
No Accelerated Aging - Tested at 68°F.	AC-20	4.70×10^{-6}	2.63	0.89
	AC-10*	8.00×10^{-9}	3.74	0.72
	AC-5 + Carbon Black	2.63×10^{-6}	2.84	0.88
	AC-5 + EVA	1.28×10^{-7}	3.91	0.94
	AC-5 + SBS	1.64×10^{-5}	3.12	0.68
	AC-5 + Latex	3.63×10^{-5}	3.04	0.78
	AC-5 + Polyethylene (Novophalt)	2.33×10^{-8}	3.38	0.85
Accelerated Aging at 140°F for 14 Days - Tested at 68°F	AC-20	1.57×10^{-9}	3.94	0.97
	AC-5 + Carbon Black	2.23	1.19	0.75
	AC-5 + EVA	2.68×10^{-4}	2.28	0.97
	AC-5 + SBS	1.05×10^{-2}	1.74	0.92
	AC-5 + Latex	3.58×10^{-5}	2.73	0.96
	AC-5 + Polyethylene (Novophalt)	5.09×10^{-3}	1.88	0.93

* Mixture of AC-10 and crushed limestone.

$$^{\circ}\text{C} = (^{\circ}\text{F} - 32)/1.8$$

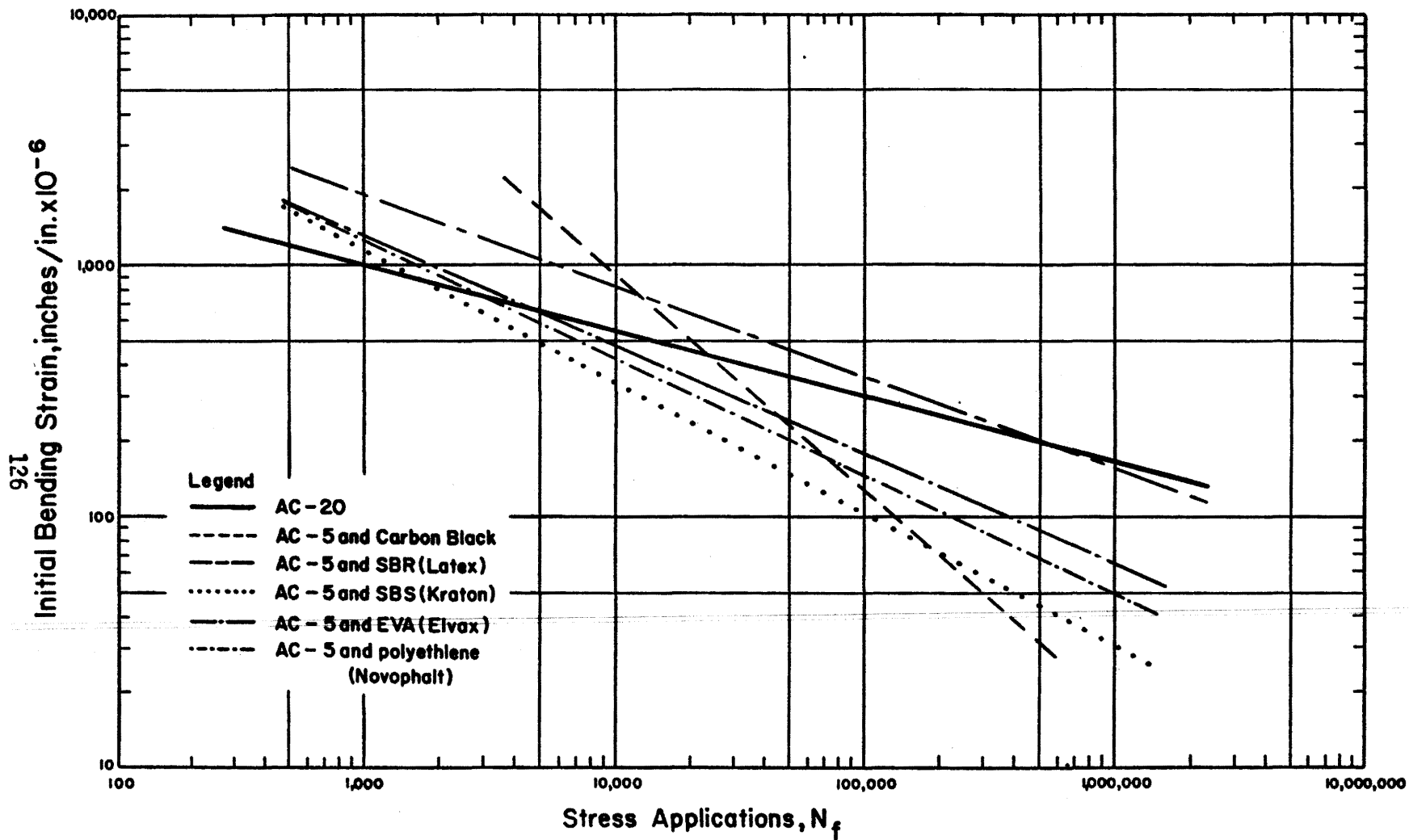


Figure 17. Controlled stress flexural fatigue results at 68°F (20°C) following 7-day aging at 140°F (60°C).

effect. Apparently, the high temperature aging diminishes the effect of the polymeric network on the asphalt-additive blend. However, a similarly deleterious effect of heat aging on the AC-5 and carbon black blends cannot be attributed to a breakdown in the polymeric network.

4. General Discussion of Flexural Fatigue Results

The flexural fatigue data graphically presented in figures 15 and 16 represents the ability of asphalt concrete samples to resist fatigue induced damage when a selected stress level is applied. The magnitude of strain produced by the stress level is, of course, dependent upon the stiffness of the mixture. This must be considered as the plots in figures 15 and 16 and the data in appendix tables E7 through E12 are evaluated.

At 68°F (20°C), the three stress levels used to test each mixture were approximately equal. However, the strains induced at the 200th load cycle were substantially larger for most AC-5 plus additive mixtures due to their lower stiffness values. In fact, mixtures composed of AC-5 blends with SBS and EVA produced strains which were about nine times larger than those produced in the AC-20 control mixture. The mixture containing latex resulted in strains about 15 times larger than those produced in the AC-20 control. A most interesting result is that the AC-5 mixture containing polyethylene was most similar to the AC-20 control in terms of level of induced flexural strain.

At 32°F (0°C) the range of induced strains in all mixtures containing AC-5 and the polymers were quite similar. The mixtures containing polyethylene developed approximately the same level of induced strains as those containing latex, SBS and EVA. The AC-5 and carbon black mixture exhibited a significantly lower range of induced strains over a similar range of applied stresses.

In conclusion, although at 68°F, the mixtures containing AC-5 blends with latex, SBS and EVA exhibit superior fatigue performance based on the N_f versus ϵ_t (at 200th load cycle) criterion, the mixtures containing AC-5 blends with polyethylene and carbon black possess sufficient

stiffness so that higher stress levels are required to induce the critical strains. Based on the total analysis of fatigue data, mixtures containing AC-5 and polyethylene possess attractive fatigue properties as those mixtures combine good fatigue resistance based on the N_f versus ϵ_t (200th load cycle) criterion, higher values of stiffness than other AC-5 and additive blends at 68°F and similar values of stiffness and a similar N_f versus ϵ_t (200th load cycle) relationship at 32°F.

CONTROLLED DISPLACEMENT FATIGUE TESTING

1. General

A mechanistic approach proposed by several researchers (23,24, and 25) considers fatigue as a process of cumulative damage and utilizes fracture mechanics to investigate this property. In this approach, fatigue life, under a given stress state, is defined as the period of time during which damage increases according to a crack propagation law from an initial state to a critical or final level. The method accounts for the changes in state of stress due to cracking, geometry and boundary conditions, material characteristics and variability. The fatigue life can be obtained from both controlled stress and controlled strain tests. The method is independent of the mode of testing.

In order to describe the fatigue process and to predict the fatigue life of any system, it is essential to establish the laws governing the crack growth from the initial stage to the final stage. The process of crack growth in materials like asphalt can basically be described as blunting and sharpening of the crack tip during cyclic loading and can be explained in terms of the energy balance at the crack tip. During the loading stage, the plastic zone at the crack tip becomes larger and, hence, the crack tip becomes blunt. Essentially, blunting occurs when the stresses at the crack tip exceed the yield stress of the material before the stored energy is great enough to propagate the crack. During unloading the crack tip sharpens as a result of the substantial reduction in the size of the plastic zone ahead of the crack tip. The unloading

stage can also leave some permanent deformation that will result in reduction of the amount of available strain energy for the next cycle.

A variety of crack propagation laws have been proposed in the literature, among which the Paris equation is most useful for this research:

$$da/dN = A(\Delta K)^n \quad \text{Equation 14}$$

where da/dN is the change in crack length per cycle, N , and A and n are material constants. The term, K , is the change in stress intensity factor. This factor provides a single parameter characterization of the state of stress at the crack tip including the effects of specimen geometry and configuration, boundary condition and load. The normal stresses and shear stress at a point a distance r from the crack front which makes an angle θ with the crack plane are related to the mode I (tensile) stress intensity factor by:

$$\sigma_y = \frac{K_I}{2\pi r} \cos \frac{\theta}{2} \left(1 + \sin \frac{\theta}{2} \sin \frac{3\theta}{2}\right) \quad \text{Equation 15}$$

$$\sigma_x = \frac{K_I}{2\pi r} \cos \frac{\theta}{2} \left(1 - \sin \frac{\theta}{2} \sin \frac{3\theta}{2}\right) \quad \text{Equation 16}$$

$$\tau_{xy} = \frac{K_I}{2\pi r} \left(\sin \frac{\theta}{2} \cos \frac{\theta}{2} \cos \frac{3\theta}{2}\right) \quad \text{Equation 17}$$

The above relations were derived by Irwin (26). They describe the stress in the vicinity of crack tip subjected to mode I deformation. The stress intensity factor K_I , which describes stress distribution at the crack tip in a linear elastic medium, also provides a means of estimating the size of the plastic region around the crack tip. The critical stress intensity factor, K_{IC} , is the value of K_I which causes the crack to grow at a given value of crack length or level of stress in a specific crack and loading geometry.

Utilizing the Paris law, failure life, N_f , can be expressed as:

$$N_f = \int_{c_0}^{c_f} \frac{1}{A_{\Delta} K_I^n} \quad \text{Equation 18}$$

where c_f is the crack size at failure, and c_0 is the initial crack or flaw size.

The advantages of the mechanistic method are: (1) the critical stress intensity factor, K_{Ic} , is a material property, independent of mode of loading and specimen geometry; and (2) failure is defined realistically to be either rapid brittle crack propagation at the critical crack size or stable crack growth through the entire specimen depth. The disadvantages are: (1) the inherent computational complexity in obtaining K_I for all but the simplest geometries and (2) the inherent assumptions of linear elasticity and an infinitely sharp crack tip at all times. The first disadvantage may be overcome by testing specimens of simplified geometry for which K_I computations have been accomplished. The second disadvantage is prohibitive for virtually every condition with the possible exception of testing at very low temperatures (below T_g).

The fracture energy under plane strain conditions where elastic-plastic conditions exist may be determined by the J integral. The path-independent J integral proposed by Rice (27) characterizes the stress-strain field at the tip of a crack by an integration path taken sufficiently far from the crack tip to be substituted for a path close to the crack-tip region. Thus, even though considerable yielding occurs in the vicinity of the crack tip, if the region away from the crack tip can be analyzed, behavior of the crack tip region can be inferred.

In this research, the J-integral was used to characterize the stress-strain field at the crack tip and hence the energy input to the crack as a result of the controlled displacement. Appendix E presents a more detailed discussion of the J-integral and the way its results are analyzed to evaluate fracture potential in this research. A brief discussion of the overlay tester, used to induce a crack in the asphalt concrete samples, is also found in appendix E.

2. Sample Fabrication

The beam specimens for controlled displacement fatigue testing were fabricated identically to those used in the flexural beam fatigue study. The fabrication process is explained in the previous section.

As was the case for flexural beam fatigue testing, a river gravel aggregate (appendix E) was used in all mixtures with asphalt and asphalt-additive blends.

3. Experiment Design

The experiment design is shown in table 50. The objective of the experiment was to evaluate the response of the various mixtures to controlled displacement fatigue.

4. Results of Testing

Tables 51 and 52 summarize the important controlled displacement fatigue parameters at 33°F (1°C) and 77°F (25°C), respectively.

Log-log plots of da/dN versus J^* are presented in figures 18 through 21. Because the regression lines often cross one another, it is not prudent to evaluate relative performance by the crack speed index (as explained in appendix E) of the form $\log A^* + cn^*$, where c is a logarithm of an arbitrarily selected J^* value. A slightly different approach was used to determine the crack speed index. In this approach, crack speeds at crack length of 1-in and 2-inches (25.4 and 50.8 mm) were compared for the various materials. These results are recorded in table 51 and 52.

The reader is reminded that appendix E discusses the analysis procedure for the da/dN versus J^* results. The plots which produce the higher intercepts, A , and shallower slopes, n , represent superior results, i.e., lower fracture potential. Thus, the more negative the value of crack index, the better the potential of the material to resist fracture (controlled displacement).

Two different approaches were used to analyze the data: the elastic-plastic approach employing the J^* integral and the linear elastic

Table 50. Factorial test matrix for controlled displacement fatigue testing.

Asphalt Type Asphalt Grade Test Temperature, °F Additives	California Valley (AR)				Texaco (AC)			
	AR-4000		AR-1000		AC-20		AC-5	
	32	68	32	68	32	68	32	68
	None	2*	2			2	2	
Carbon Black			2	2			2	2
Latex			2	2			2	2
Kraton			2	2			2	2
Elvax			2	2			2	2
Novo-phalt			2	2			2	2

* 2 replicates were tested for each factorial cell.

Table 51. Summary of controlled displacement fatigue results at 77°F.

Base Asphalt	Type	Sample No.	A*	n*	$\text{Log}(\frac{da}{dN})@ a=1$	$\text{Log}(\frac{da}{dN})@ a=2$	N _f	Air Void(%)
Texaco AC	AC-20	3	0.005110	1.116	-1.476	-2.202	200	5.7
		4	0.004816	0.874	-1.827 -1.652	-2.375 -2.289	300	6.0
	AC-5 + Carbon Black	3	0.031929	1.174	-0.413	-1.328	50	7.1
		4	0.005523	1.596	-1.504 -0.959	-2.640 -1.984	1000	6.3
	AC-5 + Elvax	1	0.528484	0.178	-0.101	-0.214	4	6.5
		3	0.195776	0.502	-0.184	-0.550	7	6.0
		30	0.012785	0.405	-0.610 -0.298	-0.828 -0.531	10	5.6
	AC-5 + Kraton	3	0.001414	1.890	-1.236	-2.466	515	5.1
		4	0.010515	1.408	-1.019 -1.128	-1.971 -2.219	185	6.4
	AC-5 + Latex	7	0.003667	1.763	-1.844	-2.973	980	6.9
		8	0.005577	1.059	-2.124 -1.984	-2.668 -2.821	500	5.4
	AC-5 + Novo-phalt	1	0.024345	0.792	-0.987	-1.554	70	6.0
		2	0.005914	1.088	-1.758 -1.373	-2.451 -2.003	300	6.9
	San Joaquin Valley AR	AR-4000	1	0.008446	0.789	-1.235	-1.770	100
4			0.004751	0.977	-1.184 -1.210	-1.860 -1.815	119	5.6
AR-1000 + Carbon Black		2	0.002628	1.537	-1.858	-2.852	476	6.8
		3	0.002699	1.320	-2.024 -1.941	-2.819 -2.836	500	6.2
AR-1000 + Elvax		2	0.001452	1.727	-2.690	-3.666	>2000	6.2
		3	0.000994	2.118	-2.766 -2.728	-3.940 -3.803	>2000	6.7
AR-1000 + Kraton		2	0.002371	1.709	-2.233	-3.106	1256	6.8
		4	0.000379	2.354	-2.955 -2.594	-4.285 -3.696	>2000	6.8
AR-1000 + Latex		2	0.001493	1.967	-2.268	-3.439	1900	6.8
		6	0.001126	1.738	-2.616 -2.442	-3.588 -3.514	>2000	6.4
AR-1000 + Novo-phalt		1	0.001992	1.826	-1.821	-3.023	764	6.8
		2	0.000855	1.767	-2.390 -2.106	-3.528 -3.276	800	6.0

Table 52. Summary of controlled displacement fatigue results at 33°F.

Base Asphalt	Type	Sample No.	A*	n*	$\text{Log}\left(\frac{da}{dN}\right)@ a=1$	$\text{Log}\left(\frac{da}{dN}\right)@ a=2$	N_f	Air Void(%)
Texaco AC	AC-20	15	0.319806	0.471	-0.474	-0.707	9	5.8
		18	-	-	-	-	2	5.9
	AC-5 + Carbon Black	23	0.025585	0.453	-1.689	-1.894	420	6.8
		32	0.011457	0.501	-2.077	-2.322	766	7.2
					-1.883	-2.108		
	AC-5 + Elvax	12	0.012743	0.649	-1.846	-2.270	295	5.9
		13	0.007318	0.679	-2.294	-2.633	484	5.9
					-2.070	-2.452		
	AC-5 + Kraton	1	0.005222	0.792	-2.423	-2.799	922	5.5
		15	0.005701	0.854	-2.358	-2.802	800	5.7
					-2.391	-2.801		
	AC-5 + Latex	22	0.004590	0.497	-2.499	-2.727	1379	5.9
		23	0.006648	0.679	-2.318	-2.645	1000	6.0
					-2.409	-2.686		
	AC-5 + Novophalt	12	0.006027	1.045	-2.121	-2.759	743	6.1
18		0.003382	0.579	-2.622	-2.896	1952	5.8	
24		0.006325	0.716	-2.296	-2.662	1000	6.0	
				-2.346	-2.772			
San Joaquin Valley AR	AR-4000	5	-	-	-	-	-	6.2
		13	-	-	-	-	-	6.3
	AR-1000 + Carbon Black	4	0.086014	0.402	-1.088	-1.293	95	7.3
		11	0.012573	1.755	-0.963	-2.243	250	6.7
		5	0.009827	0.661	-2.032	-2.381	415	7.3
					-1.361	-1.972		
	AR-1000 + Elvax	4	0.009960	1.158	-1.834	-2.474	650	7.0
		9	0.005762	0.496	-2.298	-2.536	822	6.8
					-2.066	-2.505		
	AR-1000 + Kraton	7	0.016701	0.918	-1.738	-2.232	419	6.5
		8	0.013175	0.964	-1.547	-2.198	322	6.1
					-1.643	-2.215		
	AR-1000 + Latex	10	0.025178	1.225	-0.633	-1.639	131	6.3
		11	0.098267	0.625	-0.628	-1.071	50	6.7
					-0.631	-1.355		
AR-1000 + Novophalt	11	0.016646	1.247	-0.627	-1.719	140	6.8	
	12	0.017599	2.013	-0.709	-2.091	220	6.6	
				-0.668	-1.905			

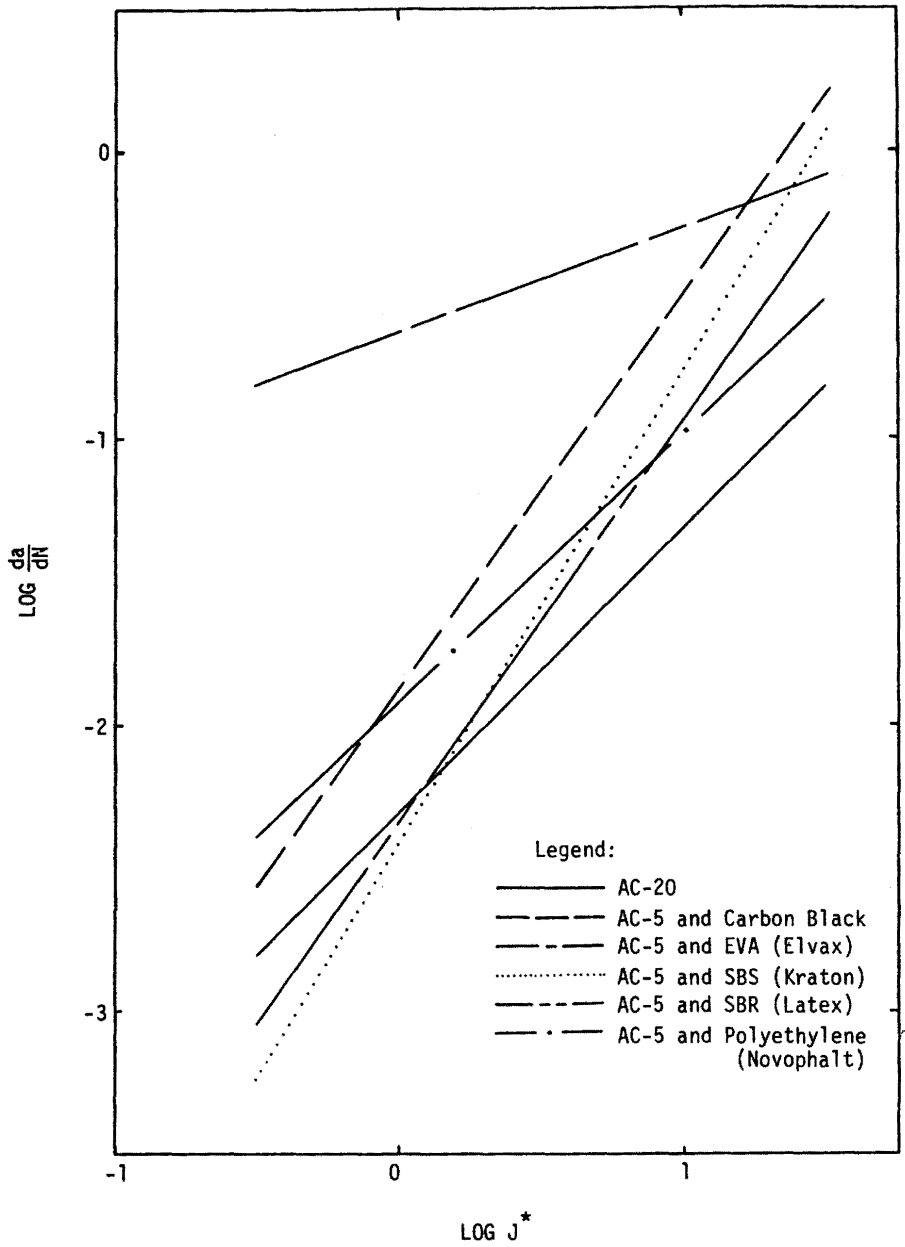


Figure 18. Log-log plot of crack speed versus J-integral at 77°F (25°C) for Texaco asphalts.

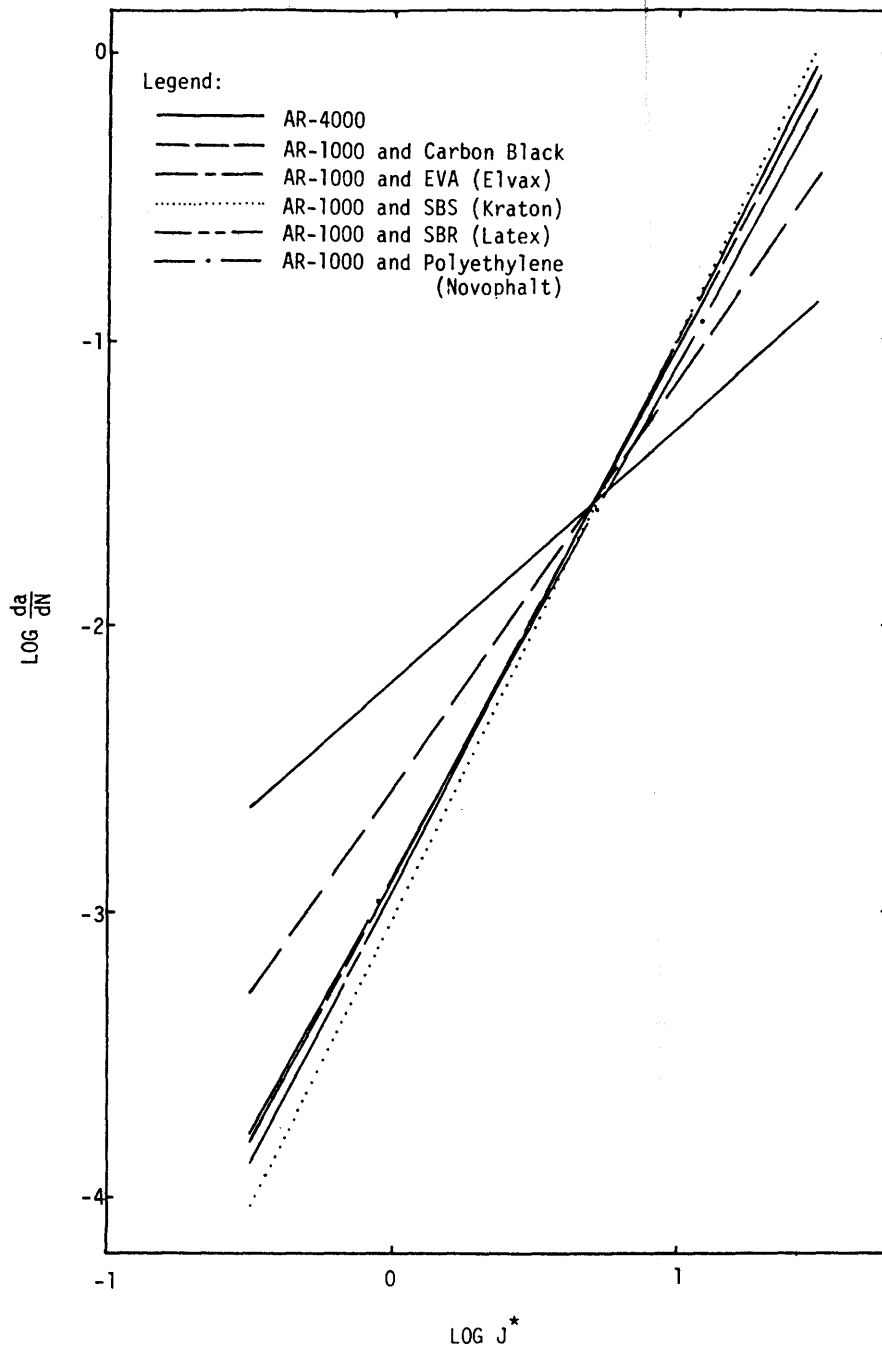


Figure 19. Log-log plot of crack speed versus J-integral at 77°F. (25°C) for California Valley asphalts.

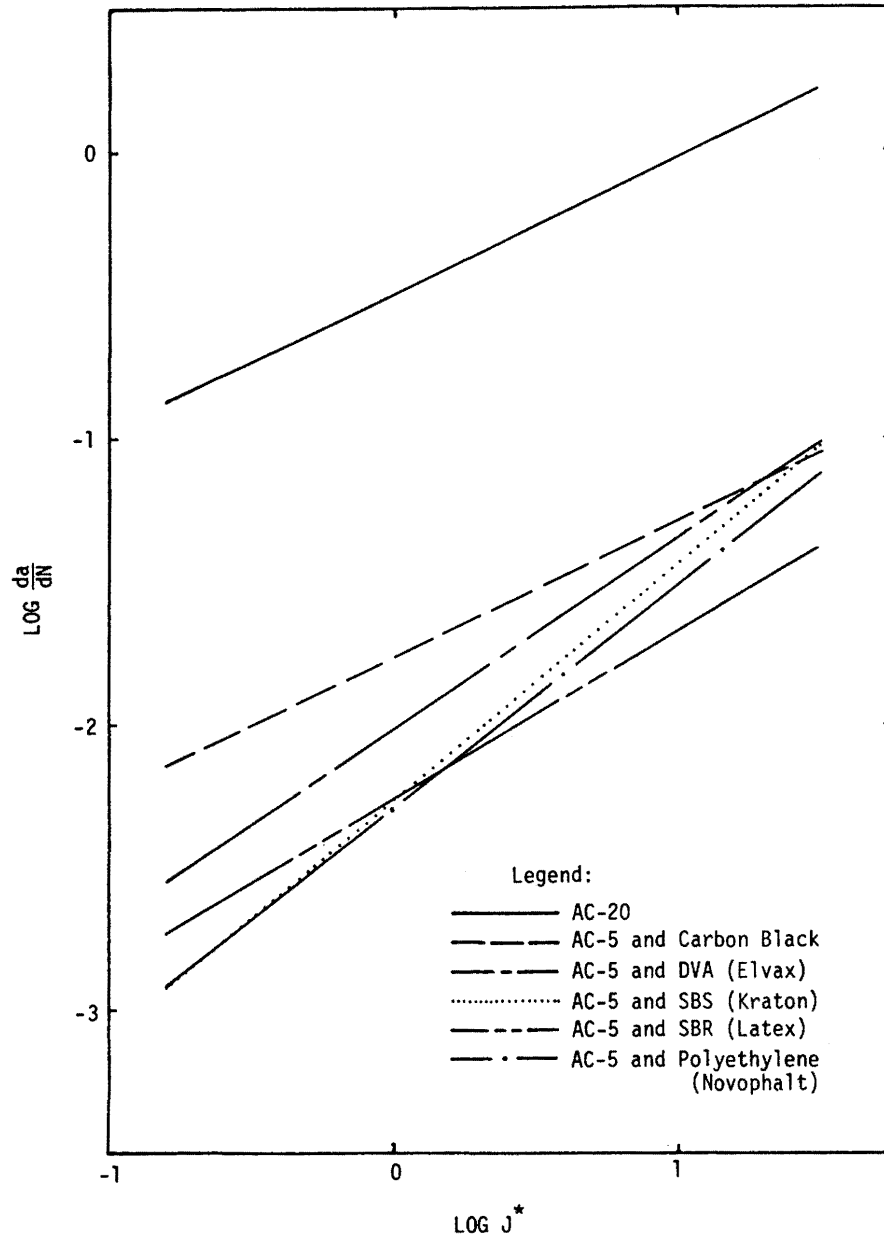


Figure 20. Log-log plot of crack speed versus J-integral at 33°F (1°C) for Texaco asphalts.

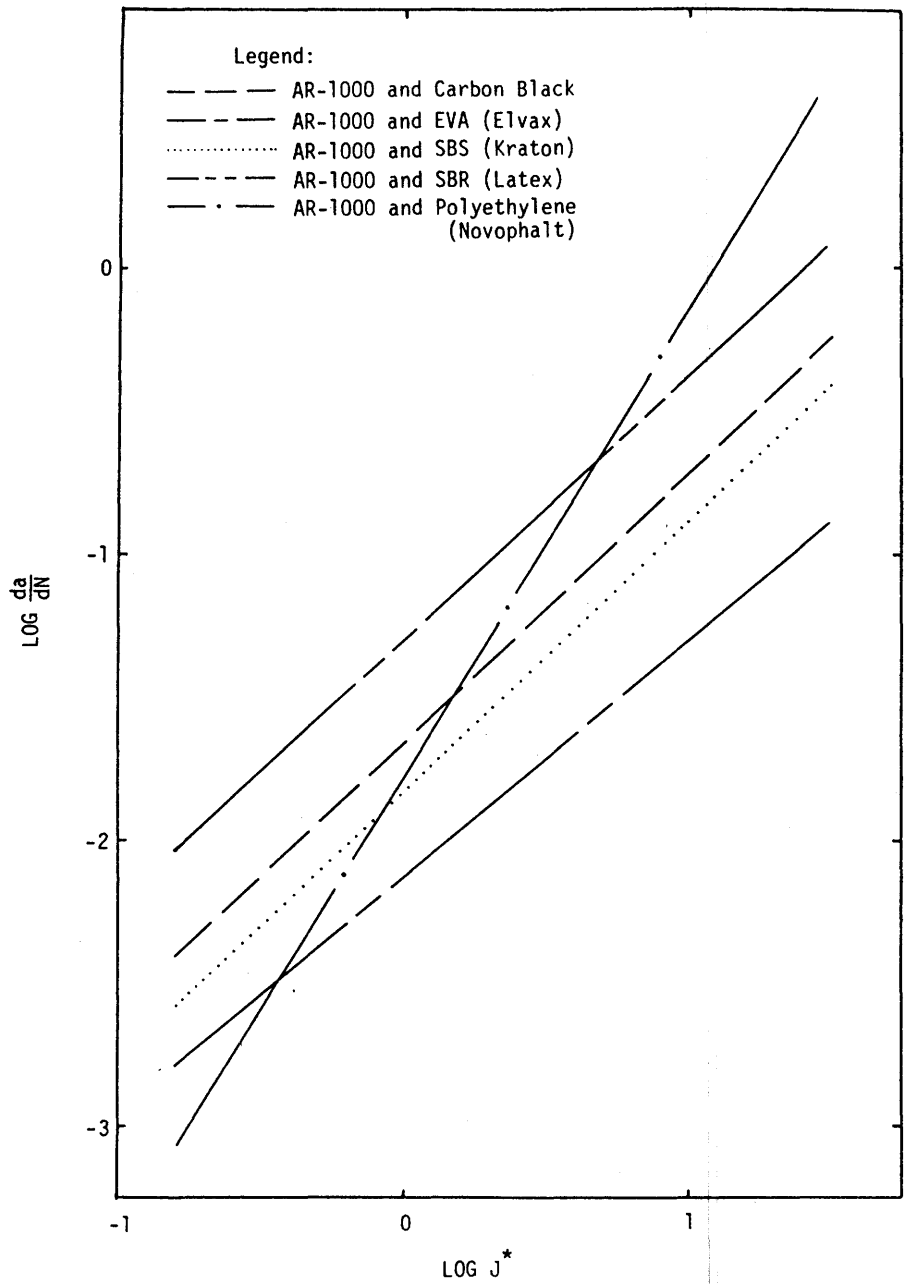


Figure 21. Log-log plot of crack speed versus J-integral at 33°F (1°C) for California Valley asphalts.

approach, as established by Lytton and Jayawickrama (28), employing the stress intensity factor, K. Both approaches are explained in appendix E.

Assuming that the materials exhibit linear elastic behavior,

$$J^* = \frac{K^2}{E} \quad \text{Equation 19}$$

then the constants of the Paris equation (A^* and n^* when written in terms of the J-integral) become $A^* E^{n^*/2}$ and $n^*/2$ when written in terms of the stress intensity factor, K. For clarity the Paris equations are summarized as:

$$da/dN = A^* J^{n^*} \quad \text{Equation 20}$$

$$da/dN = A^* E^{n^*/2} (\Delta K)^{n^*/2} \quad \text{Equation 21}$$

or

$$da/dN = A_K (\Delta K)^{n_K} \quad \text{Equation 22}$$

Figures 22 and 23 compare the A and n parameters derived from the two analysis. The A_K value computed from the elastic analysis is smaller than A^* computed from the viscoelastic analysis, while n_K is larger than n^* .

Schaperly, in 1973 (29), developed a theoretical relationship among the Paris Law parameters and material properties of viscoelastic media. According to his theory, n is inversely proportional to the slope, m, of the log-log plot of creep compliance versus time. Therefore, the smaller n value predicted from the elastic-plastic analysis (employing J^*) is indicative that the elastic-plastic analysis is more sensitive to the time dependent characteristics of the material. However, as can be seen in figure 24, the crack velocities (at crack lengths, equal to 1-inch and 2-inches) are identical when computed from either the linear elastic or elastic-plastic approach. This demonstrates the applicability of either analysis as far as crack-speed determinations are concerned.

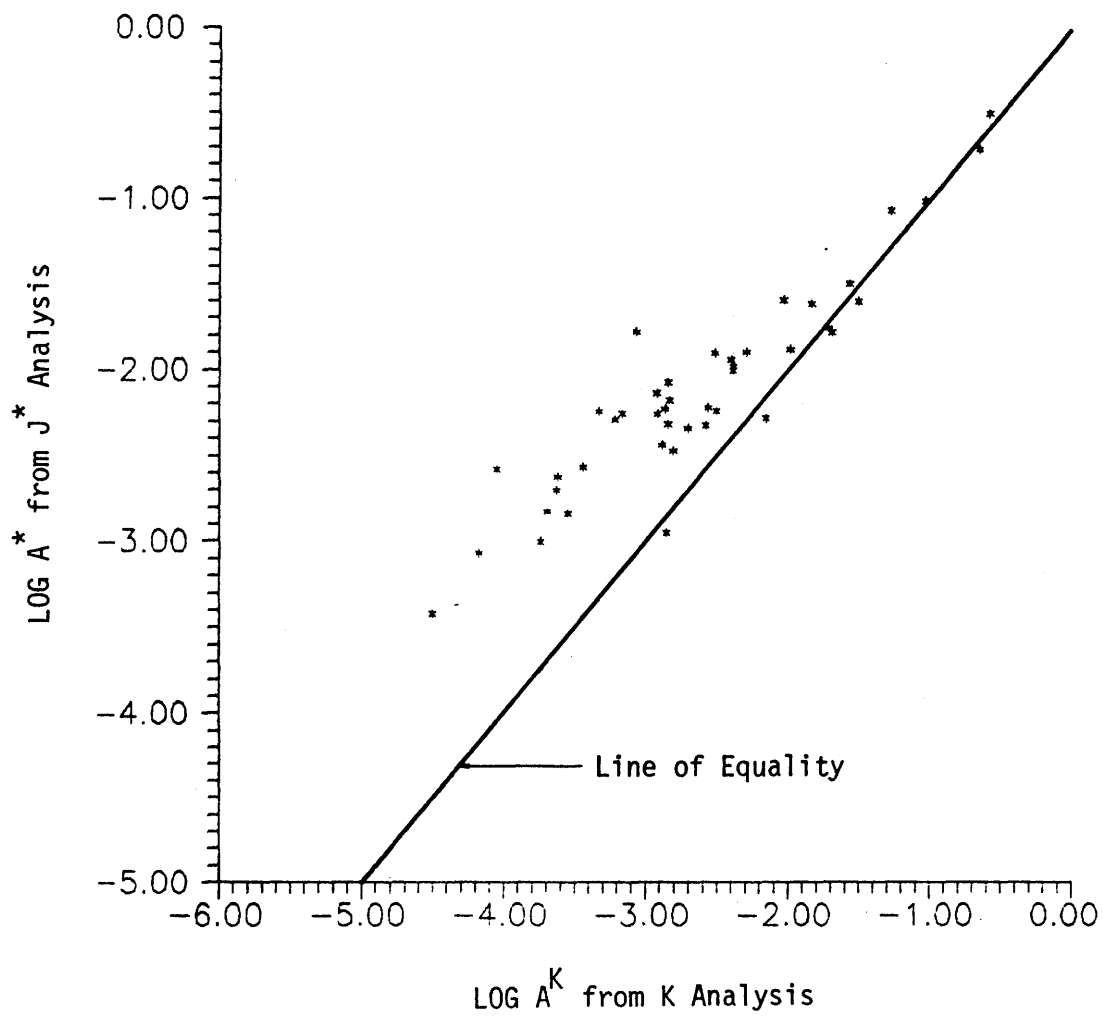


Figure 22. Log A* from J* analysis vs. Log A^K from K analysis.

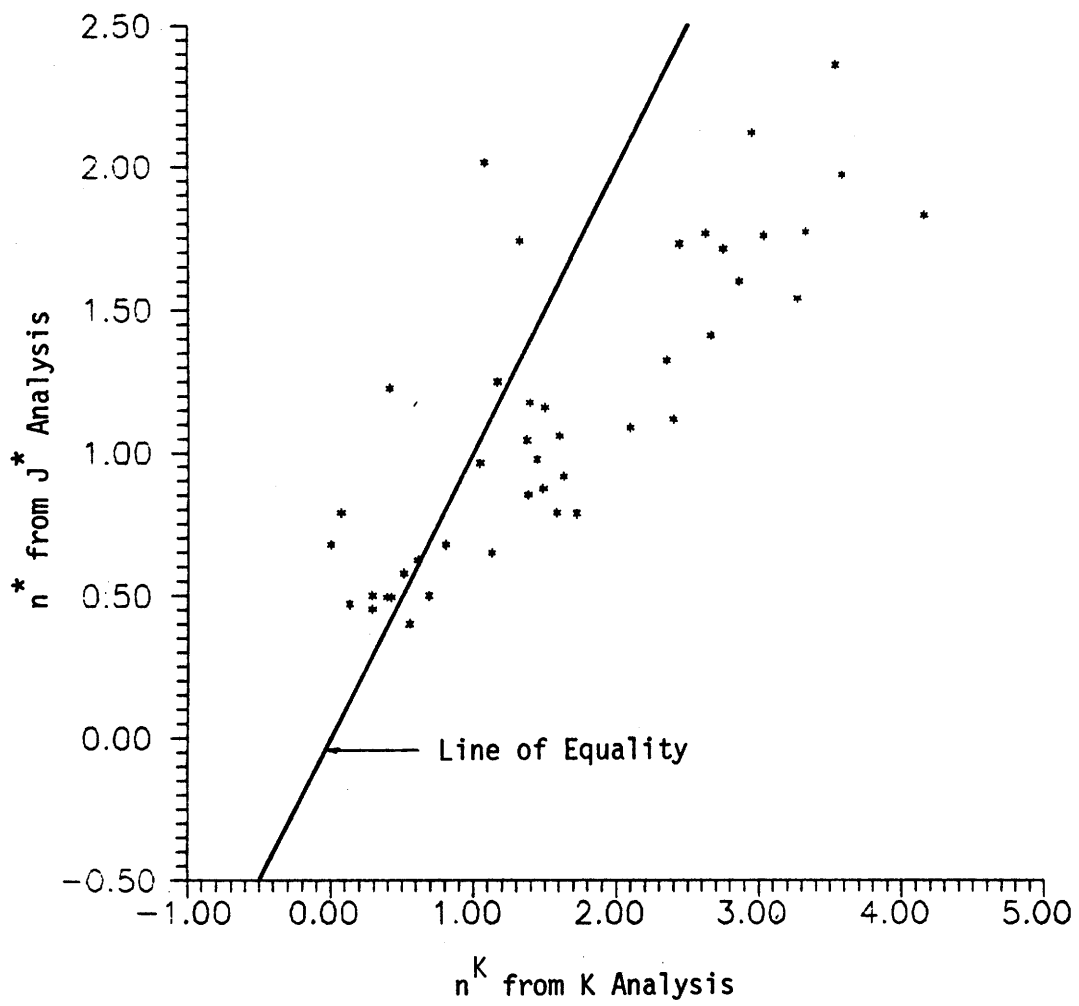


Figure 23. n^* from J^* analysis vs. n^K from K analysis.

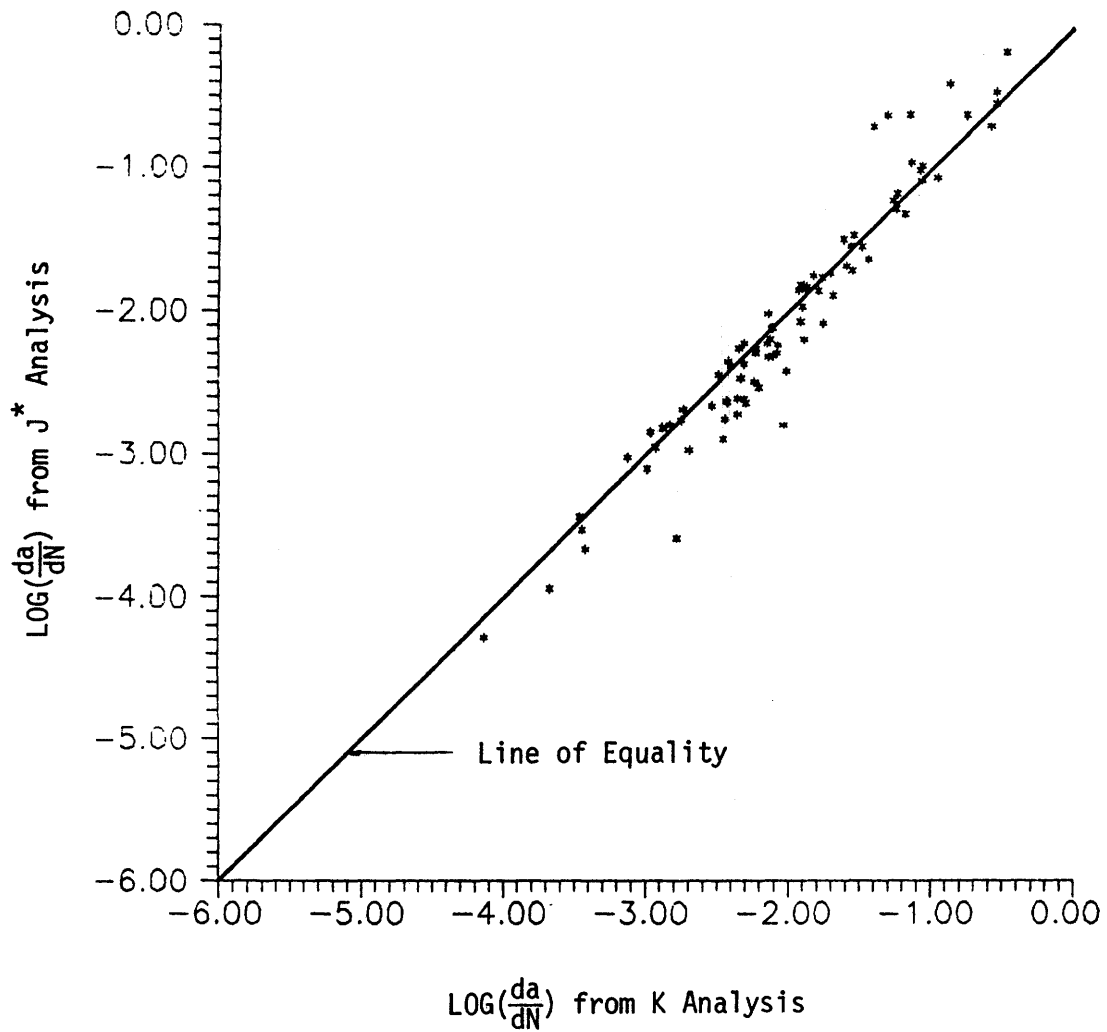


Figure 24. Comparison of crack growth rates at crack lengths of 1 in (25.4 mm) and 2 in (50.8 mm) from J* analysis and K analysis.

5. Discussion of Results

Based on a review of the results presented in tables 51 and 52 and figures 18 through 21, the following trends are noted:

1. At 33⁰F (1⁰C) all additive-soft asphalt blends demonstrated significantly superior crack propagation characteristics compared to the control mixtures which were bound with a harder asphalt without additives. The improvement in the resistance to crack propagation due to the additive-soft asphalt blends was equally dramatic for both asphalts: California Valley and Texaco.

2. At 33⁰F, the EVA (Elvax)-AR-1000 blend gave the best results among the blends of additives and California Valley asphalts, while the SBR (Latex)-AC-5 blend gave the best results among blends of additives and Texaco asphalt.

3. Considering the performance of additives from both asphalt sources at 33⁰F, the SBS (Kraton) - asphalt blends produced the most consistently superior results.

4. At 33⁰F, the additives blended with Texaco AC-5 demonstrated superior performance when compared to California AR-1000 blends. This can be partially explained by the higher penetrations of the AC-5-additive blend at 39.2⁰F (4⁰C) as compared to the AR-1000 blends at 39.2⁰F. Note also that the Texaco AC-20 asphalt performed slightly better than did the California Valley AR-4000 at 33⁰F (see tables 51 and 52).

5. At 77⁰F (25⁰C) the additive blends with the California Valley AR-1000 asphalt generally outperformed the blends of additives and the Texaco AC-5 asphalt. Perhaps this is due to the better compatibility between the additives and the California Valley asphalt than between the additive and the Texaco asphalt. Furthermore, the base asphalt penetrations are very similar at 77⁰F so that compatibility may well be the predominant effect. On the otherhand, at 33⁰F the significant

difference in penetration seems to predominate over relative compatibility.

6. The effect of additive-asphalt compatibility at 77°F is most dramatically illustrated by the mixtures composed of blends of EVA (Elvax) and AC-5 and EVA (Elvax) and AR-1000. The controlled displacement samples fabricated with the EVA (Elvax)-AC-5 blend failed in 4, 7 and 10 cycles (table 51), whereas samples fabricated with EVA (Elvax)-AR-1000 blends failed in excess of 2000 cycles. Apparently EVA (Elvax) blended with AC-5 cannot withstand the 0.045 inch crack opening displacement, but the same EVA (Elvax) AC-5 blend performs quite well in controlled stress fatigue testing at 68°F.

7. At 77°F samples fabricated with EVA (Elvax), SBS (Kraton) and SBR (Latex) blends with AR-1000 demonstrated multiple cracking or "crack branching". This branching of hairline cracks distributes the tensile stresses from the original crack tip and slows the progression of cracks through the sample. As a result cycles to failure for these samples were often greater than 2000.

8. Mixtures fabricated with carbon black asphalt blends generally demonstrated the poorest controlled displacement fatigue performance at 77°F.

HEALING STUDY

1. Background

Without question, laboratory phenomenological fatigue data under-predicts the field fatigue performance of asphalt mixtures. The controlled stress laboratory flexural fatigue tests do not account for healing of the pavement between stress applications, residual stresses, the length of rest periods between load applications and variability of the position of the wheel load.

Data dealing with fatigue shift factors ranges widely. Van Dijk (30), Finn (31), Santucci (32) and Pickett, et al. (33) have specified shift factors ranges from 0.02 to 43 by which to transform the laboratory

fatigue data to field results. The more typically used range is from 3 to 20. Little, et al. present a rather detailed discussion of fatigue curve shift factors in Report No. FWHA/RD-85/032 (34).

Lytton (35) has proposed a laboratory to field fatigue curve shift factor which accounts for the two major phenomena which affect the factor: (1) residual stresses and (2) healing. Figure 25 is a representation of the shift factor. In one process (labeled 1), the material relaxes and loses some of its residual compressive strain. The material is, in effect, losing, through relaxation, some of the prestressing developed by the previous wheel load.

In the second process (labeled 2), the material is allowed to heal from its distressed state. During this period, the plastic zone size ahead of the crack tip is reduced, and the existing crack may even be closed upon removal of the applied load due to compression resulting from bending forces within the material. The intersection of laboratory and field fatigue curves at approximately 10^7 load repetitions is based on the efforts of several researchers (35).

Lytton postulated that the two components of the shift factor, that due to the residual stresses (SF_R) and that due to the healing phenomenon (SF_H), are multiplicative factors which form the total shift factor:

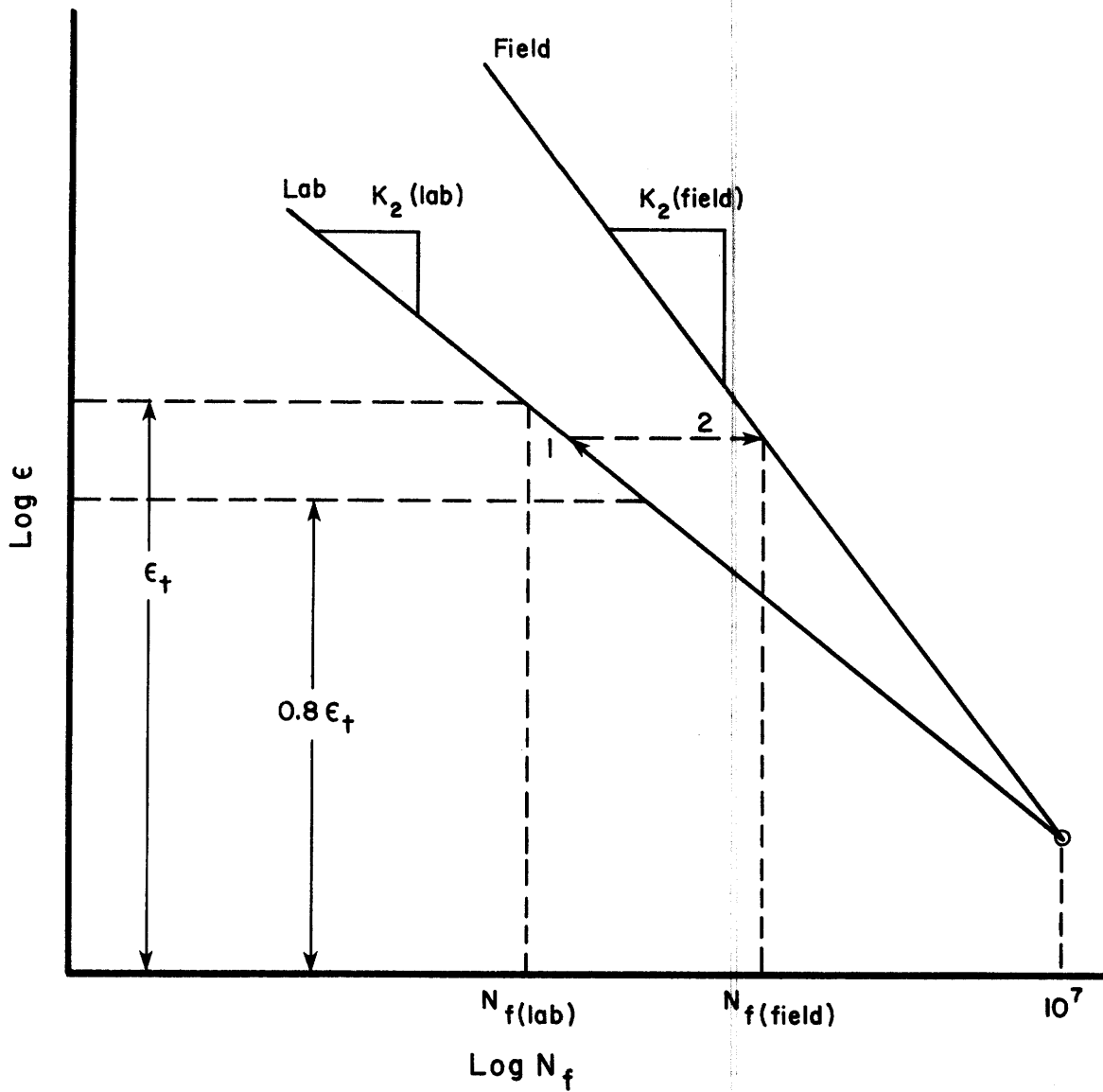
$$SF = (SF_R) \times (SF_H) \quad \text{Equation 23}$$

Little, et al. (34) developed a shift factor composed of the effects of residual stresses and healing:

$$SF = \underbrace{\left[\frac{1}{1 - (\epsilon_0)^m} \right]}_{SF_R} \left[1 + \underbrace{5.685 \times 10^{-3} e^{1.965 \log t - n_r}}_{SF_H} \right]^{K_2} \quad \text{Equation 24}$$

where ϵ_0 is the induced strain per load cycle,
 t is the duration of the rest period,
 m is the slope of the relaxation curve and
 n_r is the number of rest periods.

Based on the model and on the results of extensive stress relaxation testing and controlled displacement crack propagation studies (accounting



- (1) Shift due to loss of residual stress through relaxation of asphalt concrete ($0.8 \epsilon_t$ represents the strain actually induced due to residual stresses. ϵ_t is the tensile strain induced after full relaxation of compressive prestresses).
- (2) Shift due to crack healing tensile and plastic zone reduction.

Figure 25. Illustration of the hypothesized laboratory to field shift process.

for the effect rest periods), Little (34) found that for asphalt concrete and for a specific plasticized sulfur binder the SF ranged from 3 to 20, typical of the values predicted by other researchers. Furthermore, the SF is shown to be a function of (1) the duration of the rest period, t , (2) the magnitude of the induced tensile strain, ϵ_0 , and (3) the number of rest periods.

2. Purpose of Healing Study

Report FHWA/RD-85/032 (34) showed that in the controlled displacement fatigue mode the energy required to initiate crack propagation is affected by rest periods as follows:

$$\Delta u = e^h \log t \quad \text{Equation 25}$$

The term Δu is the increase in energy required to initiate a selected magnitude of crack opening displacement between loading cycles N and $N + 1$, where a rest period, t , intervenes. The term h represents a constant equal to 0.45. This is based on test data in report FHWA/RD-85/032.

Since asphalt additives have been shown to substantially affect the creep and relaxation properties of asphalt mixtures, it was assumed that additives could dramatically affect the healing characteristics of asphalt mixtures as reflected by Δu . The purpose of this study was to evaluate the relative effect on healing of the five additives studied in this research by comparing the relative effects of the additives on healing.

3. Healing Evaluation Procedure

All beams used in the healing experiments were fabricated identically to the beams used in the flexural beam fatigue and controlled displacement fatigue (overlay simulation) testing. The beams were fabricated using river gravel aggregate and California Valley Asphalt. The control beam was fabricated with river gravel and AR-4000 while other beams were fabricated with river gravel and additive modified AR-1000 asphalt. The specimens were subjected to controlled displacement cycling

using the overlay tester as previously explained. All testing was accomplished at 77°F (25°C). The experiment was performed identically to previous controlled displacement experiments at 77°F except that 45 minute rest periods were introduced after 3, 6, 10, 20, 30, 50, 100 and 200 cycles. Healing energies were calculated as follows:

$$\Delta u = u' - u_0 \quad \text{Equation 26}$$

where Δu is the healing energy, u' is the energy required to induce the prescribed displacement following a 45 minute rest period, and u_0 is the energy required to induce the prescribed displacement prior to the rest period.

The cause of the higher energy level necessary to develop the prescribed displacement after healing occurs is now being studied by Little, et al. under a grant from the National Science Foundation. Several reasons have been hypothesized for the healing phenomenon including diffusion phenomena, adhesion between rough surfaces and flow. Jud, et al. (36) have related the diffusion constant for polymers to viscoelastic and structural parameters of the polymer. Since additives unequivocally affect the dynamic modulus-temperature relationship of asphalt mixtures, one must expect that they affect the diffusion related healing aspects of asphalt mixtures.

Precisely speaking, the healing energy is slightly larger than the u value recorded using the overlay tester by the amount of energy required to propagate the crack during the cycle immediately following the rest period. However, it is difficult to quantify the difference.

Figure 26 shows the relationships between healing energy normalized by u_0 and crack length. The energy at 77°F (25°C) required to propagate a crack in the control AR-4000 sample is much larger than for mixtures containing blends of AR-1000 and additives. Thus, the healing energies were normalized by dividing by the energy required to cause the prescribed displacement before the rest period. The relatively low R^2 's indicate large data scatter. However, the general trends are evident.

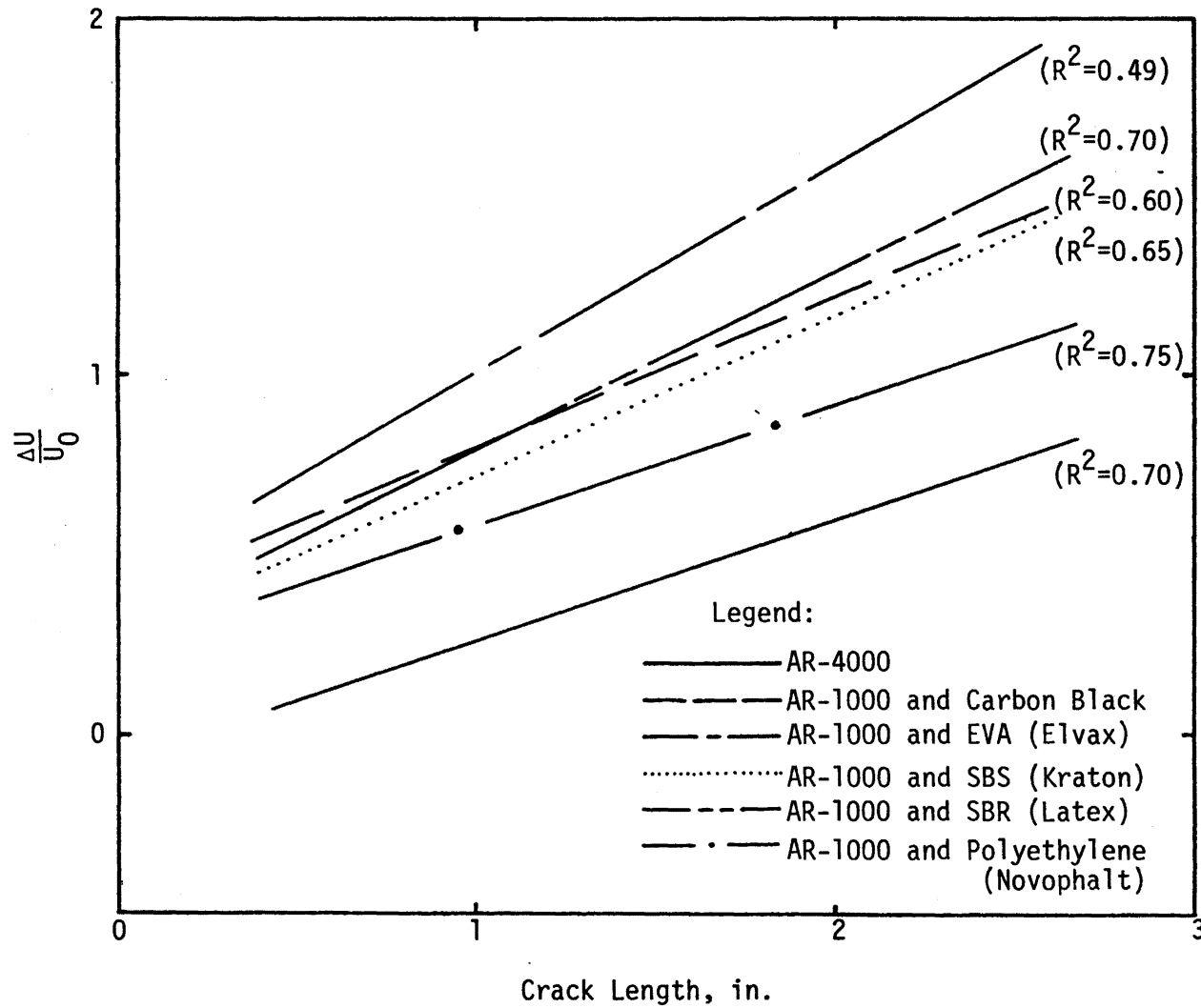


Figure 26. Effects of additives on healing energy.

Using the criteria of normalized healing energy, Δ^u/u_0 , the ability of the binders to heal during rest periods is ranked as follows:

1. AR-1000 and EVA (Elvax)
2. AR-1000 and SBR (Latex)
3. AR-1000 and Carbon Black
4. AR-1000 and SBS (Kraton)
5. AR-1000 and polyethylene (Novophalt)
6. AR-4000 control.

Unfortunately, no samples of AR-1000 were tested for comparison.

DEFORMATION CHARACTERISTICS

1. General

Asphalt concrete mixtures are commonly characterized as viscoelastic materials. The assumption that asphalt concrete behaves in a viscoelastic manner is subject to considerable dispute. However, substantial research in this area has provided credibility to the approach and has developed guidelines to be carefully considered by those evaluating deformation characteristics of asphalt concrete mixtures.

2. Experimental Design

Figure 27 represents the experimental design for all deformation testing. The silicious river gravel aggregate described in appendix D was selected as the basic aggregate because it has proven to be much more sensitive to binder properties than the crushed stone aggregates (crushed limestone, crushed sandstone or crushed basalt).

The Texaco AC-5 was selected as the primary base asphalt for all deformation testing, and the California Valley AR-1000 was selected as the secondary asphalt.

This is not a factorial experiment. The purpose of the experiment was not to statistically account for a variety of variables affecting compliance and other deformation responses, but instead, to orderly evaluate the rheological response of the asphalt-additive blends over a temperature range normally encountered by asphalt concrete pavements.

Asphalt Aggregate Temperature, °F		Texaco						California Valley					
		Control	Carbon Black	SBR	SBS	EVA	PE	Control	Carbon Black	SBR	SBS	EVA	PE
		40	RG	●	●	●	●	●	●				
70	RG	○	○	○	○	○	○						
		●	●	●	●	●	●	●	●	●	●	●	●
		△	△	△	△	△	△						
100	RG	●	●	●	●	●	●						

- Normally conditioned specimens.
- Specimens conditioned by Lottman procedure prior to testing.
- △ Specimens aged for 14 days at 140°F prior to testing.

Figure 27. Factorial design of deformation experiments. (Each symbol represents three replicate samples used to determine an average value for each cell. The tests included in the experiments are: creep compliance, accumulated permanent strain as a function of both load duration and cycles of loading, and dynamic moduli.)
OC(0F-32)/1.8

3. Fabrication of Specimens

A total of seventy-two cylinders 8-inches (204 mm) high and 4-inches (102 mm) in diameter were fabricated using the standard California kneading compactor for the creep testing program. Two replicate specimens for each of the cells shown in figure 27 were fabricated at their respective optimum binder contents as determined by Marshall mixture designs (ASTM D1559-82 and AASHTO T245-82). Table 53 reports the optimum binder contents for the Texaco asphalts as percent by weight of the aggregate, also percent by weight of binder of the additives is shown.

During the fabrication of cylinders for creep compliance testing, temperatures were selected from viscosity-temperature relationships such that the viscosities were 170 centistokes and 280 centistokes, respectively, for mixing and compaction of specimens. These values for the Texaco asphalts are presented in table 54.

Every effort was made to keep the air voids in the cylinders between six and seven percent. Also, care was taken that the air voids should be distributed equally in the cylinders and that a vertical density gradient would not develop. In order to achieve this, trial cylinders were prepared and then cut into three equal portions and the air void content was determined for each. The compactive effort for the three layers was adjusted based on the results of the previous trial cylinder. The tamping foot pressure was kept constant at 250 psi (1.72×10^6 MPa) and only the number of blows was adjusted for the compaction of the three layers. Once a compactive effort was determined for each mixture, it was used for the fabrication of the six cylinders for each binder. The ends of the cylinders were capped using a sulphur capping compound to obtain a smooth and level surface.

The mixing and molding methods used to fabricate the cylinders are outlined in ASTM Method D 1560 and ASTM D 1561, respectively.

Table 53. Percents by weight additives and binders used in fabrication of cylinders.

Binder	Percent Additive by Weight of Binder	Percent Total Binder by Weight of Aggregate
AC-20	-	4.5
AC-5 + SBR (Latex)	5	5.0
AC-5 + Carbon Black	15	4.75
AC-5 + SBS (Kraton)	5	4.5
AC-5 + Polyethylene (Novophalt)	5	4.5
AC-5 + EVA (Elvax)	5	4.5

Table 54. Mixing and molding temperatures.

Binder	Mixing Temperature (°F)	Molding Temperature (°F)
AC-20	305	275
AC-5 + Carbon Black	341	317
AC-5 + SBR (Latex)	340	320
AC-5 + SBS (Kraton)	340	290
AC-5 + EVA (Elvax)	335	290
AC-5 + Polyethylene (Novophalt)	345	290

$$^{\circ}\text{C} = (^{\circ}\text{F} - 32)/1.8$$

4. Creep Compliance Testing

All creep tests were performed on a Material Test System 810 closed-loop, feedback control hydraulic tester with a controlled-environment chamber. The creep tests were performed in accordance with the Alternate Procedure II described in the Federal Highway Administration VESYS Users Manual (20). Tests on two specimens each at temperatures of 40°F (4°C), 70°F (21°C) and 100°F (38°C) were performed. Permanent deformation properties were calculated from the incremental static loading and the creep compliance properties from the 1,000 second response curve for each specimen. A repeated haversine loading was also applied to each specimen in accordance with the VESYS Manual and used to calculate the resilient modulus at the 200th cycle.

The problem of permanent deformation of asphalt layers, which may result in rutting and cause potentially dangerous hydroplaning as well as reduce the service life of the pavement through disintegration of the pavement structure, is a major concern on heavily trafficked asphalt roads. The creep test has been developed into a practical method with which the resistance to permanent deformation of different asphalt mixes can be compared and assessed.

In the creep test, a constant force is applied perpendicularly to the parallel end faces of a cylindrical asphalt specimen. The specimen is placed between two load platens, one of which is fixed and the other, to which the load is applied, is movable in the axial direction as shown in figure 28. Deformation of the specimen in the axial direction, occurring under the influence of the load, is measured by linear variable differential transformers (LVDT) as a function of loading time. After removal of the load, the specimen recovers to some extent, which is also measured against time, beginning at the point the load is removed. During the test the temperature is kept constant.

The results obtained for a particular asphalt mix depend on the chosen test parameters, such as temperature, level of stress applied, preloading conditions, the manner in which load is applied, and the shape and dimensions of the test specimen. It is possible to eliminate the influence of the various test parameters by adopting standardized

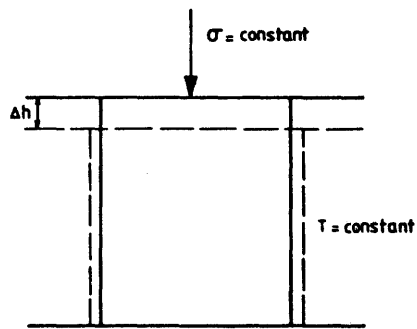


Figure 28a. The principle of the creep test procedure.

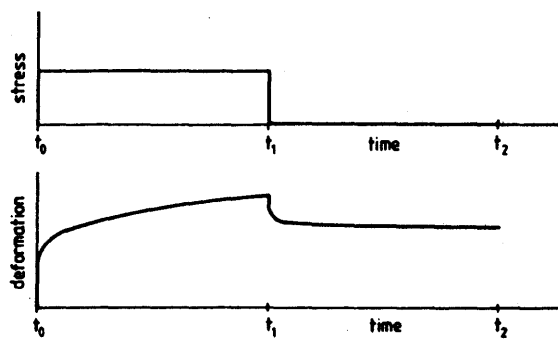


Figure 28b. Qualitative diagram of the stress and total deformation during the creep test.

methods. Three standard temperatures of 40°F (4°C), 70°F (21°C), and 100°F (38°C) were used. A maximum stress level of 20 psi (1.38×10^5 MPa) was used, if the deformation under load began to exceed 2500 microunits of strain, the stress level was reduced by 5 psi (3.45×10^4 MPa). If the deformation again began to exceed 2500 micro strain, the stress level was reduced by another 5 psi. For preload conditioning, three ramp loads for ten minutes each were applied, followed by a 10-minute rest period.

For the creep test five ramp loads were applied for durations of 0.1, 1, 10, 100, and 1000 seconds. Total permanent deformations after two minutes of unload were measured for the 0.1, 1, and 10-second loadings. After the 100-second loading, the specimen was allowed to rest for four minutes and the permanent deformation measured. The 1000-second load was used to measure the creep compliance as well as the permanent deformation measured after a rest of 8 to 12 minutes. A repeated haversine loading at the same stress level was then applied for 200 repetitions. Each load application had a load duration of 0.1 second followed by a rest period of 0.9 second. The recoverable strain measured at the 200th cycle was used to calculate the resilient modulus of the specimen. The testing procedure is outlined in detail in the VESYS Manual (20).

5. VESYS Deformation Parameters

The VESYS structural pavements subsystem uses parameters in the production of permanent deformation. They are called ALPHA and GNU and simply represent mathematical parameters for fitting the relations of permanent strain to cycles of load on a log-log plot.

In developing ALPHA and GNU, researchers (37) decided that it was important to develop a method of representing permanent deformation that was most accurate and sensitive in the region of interest. This region was well past the number of cycles applied during laboratory testing. It was also important to relate the amount of deformation that occurred during a single cycle to the number of previous load cycles so that the permanent strain during any load cycle could be predicted.

The method selected to represent permanent deformation characteristics, ϵ_a , of material for VESYS IIM involves a linear curve-fit on a log-log plot. This line may be defined by its intercept, I, at one load cycle and its slope, S. Thus,

$$\log \epsilon_a = \log I + S \log N \quad \text{Equation 27}$$

or

$$\epsilon_a = IN^S \quad \text{Equation 28}$$

The desired permanent strain due to the N^{th} loading is then

$$\epsilon_p(N) = \epsilon_a(N) - \epsilon_a(N-1) \quad \text{Equation 29}$$

or converting the right side of the equation to a continuous variable

$$\epsilon_p(N) = ISN^{S-1} \quad \text{Equation 30}$$

The resilient or elastic strain, ϵ_r , is essentially a constant after relatively few cycles and is large compared to the permanent strain. Therefore, the fraction of the total strain $F(N)$, that is permanent may be considered to be

$$F(N) = \frac{\epsilon_p(N)}{\epsilon_r(N)} = \frac{\epsilon_p(N)}{\epsilon_r} = \frac{ISN^{S-1}}{\epsilon_r} \quad \text{Equation 31}$$

For convenience, arbitrary definitions were made for mathematical simplification:

$$\mu = IS/\epsilon_r \text{ (GNU)} \quad \text{Equation 32}$$

$$\alpha = I - S \text{ (ALPHA)} \quad \text{Equation 33}$$

As $F(N)$ is the fraction of permanent strain during cycle N , the permanent strain in a compression specimen during cycle N is $F(N)$

multiplied by ϵ_r . The increment of permanent strain, $\Delta\epsilon_a$, may also be calculated during the interval of loading, N_1 to N_2 , by integrating $\epsilon_r F(N)$ as follows:

$$\Delta\epsilon_a = \int_{N_1}^{N_2} \epsilon_r F(N) dN = \frac{\epsilon_r \mu}{1-\alpha} [N_2^{1-\alpha} - N_1^{1-\alpha}] \quad \text{Equation 34}$$

The total height (H) reduction of a specimen would be $H \cdot \Delta\epsilon_a$ during the increments of repetitive load N_1 and N_2 .

Both μ and α are considered by VESYS to be constant for a layer of material. In reality, they are quite stress dependent. Thus μ and α vary with depth in the layer as well as laterally from the center of load.

ALPHA and GNU are difficult parameters to which one may attach physical significance. However, the extensive sensitivity analysis of the VESYS structural subsystem by Rauhut, et al. (37) provided a great step toward understanding the significance of these values. The most important findings in the Rauhut study with respect to this research in terms of ALPHA and GNU are summarized as follows:

1. The ALPHA parameter for asphalt concrete normally occurs within a range of from 0.63 to 0.07.
2. GNU of the surface layer (asphalt concrete) is quite variable and may be as high as 1.5, 2.0 or even higher.
3. ALPHA and GNU are used in VESYS IIM as if they were invariants, but they actually vary with stress, temperature, mix, etc.
4. ALPHA and GNU are very stress-sensitive. Both decrease with increasing deviatoric stress, but at different rates.
5. Temperature should be an important parameter in testing for ALPHA and GNU for the surface layer but it is apparently introduced in VESYS IIM in a different manner. ALPHA and GNU define the fraction of the elastic response to load that will remain when the load is removed. This elastic response is dependent on the stiffness or compliance. For asphalt concrete, a time-temperature shift function revises the master 70°F (21°C) curve to account for actual temperatures. The assumptions of VESYS IIM are that the effects of varying layer stiffness with

temperature will represent the effects of varying permanent deformation with temperature. It is not known whether or not this is a valid assumption for mixtures containing additives. The proper test temperature for ALPHA and GNU is that used for the master creep-compliance curve (70°F).

6. Both ALPHA and GNU are much more heavily dependent on stress level than upon temperature.

7. A low ALPHA or a high GNU indicate increased rutting and vice versa.

8. Although quite variable, a low ALPHA is usually associated with a low GNU.

9. There is virtually no rutting, slope variance, or deterioration for ALPHA greater than 0.90.

6. Measuring ALPHA and GNU

ALPHA and GNU are obtained by conducting incremental static-dynamic load tests on 4-inch (102 mm) diameter by 8-inch (204 mm) tall cylindrical specimens. Since these parameters are sensitive to the in situ state of stress and local environments, they should be determined on specimens subjected to realistic in situ stress states and average moisture contents and temperatures expected in the field. The laboratory creep testing specified by the VESYS Manual and used in this study is realistic in that a triaxial stress state is developed during testing. However, various levels of confining pressure are not accounted for nor are variation in moisture conditions, except for selected specimens tested following Lottman moisture conditioning.

ALPHA and GNU were measured at three temperature levels: 40°F (4°C), 70°F (21°C), and 100°F (38°C). Figure 27 presents the experimental design for the permanent deformation testing.

Straight lines on log-log paper of accumulative strain versus number of load applications were fitted to the data to define the slope, S , and intercept, I . Dynamic, resilient strains were measured at the 200th repetition and were used in the computation of GNU.

7. Results

a. Creep Compliance

The 1,000 second response curve was used to calculate the creep compliance, $D(t)$, at the loading times of 0.03, 0.1, 0.3, 1.3, 10, 30, 100, 300 and 1,000 seconds. The creep compliance, $D(t)$, is defined as:

$$D(t) = \frac{\text{Total strain observed (function of time)}}{\text{Applied stress}} \quad \text{Equation 35}$$

Figures 29 and 30 present the results of creep compliance testing for mixtures bound with blends of Texaco AC-5 and additives. These responses are compared to the AC-20 control mixture in each figure. Figure 29 contains data at 40⁰F (4⁰C) and 100⁰F (38⁰C) while figure 30 contains data at 70⁰F (21⁰C). Figures 31 and 32 present 70⁰F compliance data following Lottman conditioning and accelerated aging at 140⁰F (60⁰C), respectively. The compliance data are tabulated in appendix F.

From the compliance testing results as depicted in figures 29 through 32, the following trends were observed:

1. The addition of Novophalt to AC-5 transforms the compliance characteristics of the blend to those which are statistically the same as the AC-20 control. In essence, this says that although the resistance of the AC-5 to high temperature deformation is greatly improved by adding Novophalt, the low temperature (40⁰F) compliance is also reduced making it essentially the same as the AC-20 control. This indicates a similar susceptibility to fracture.

2. Blends of AC-5 with SBR (Latex), EVA (Elvax), SBS (Kraton) and carbon black all allow the AC-5 to respond with a higher compliance at the low temperature (40⁰F). The more compliant nature of these blends (compared to the AC-20 control mixture) indicates mixtures which are better suited to relieve stresses induced at lower temperatures and thus better resist low temperature or thermally induced cracking.

3. SBS (Kraton) and carbon black blends with AC-5 respond acceptably at 100⁰F. Although their compliances at 100⁰F are

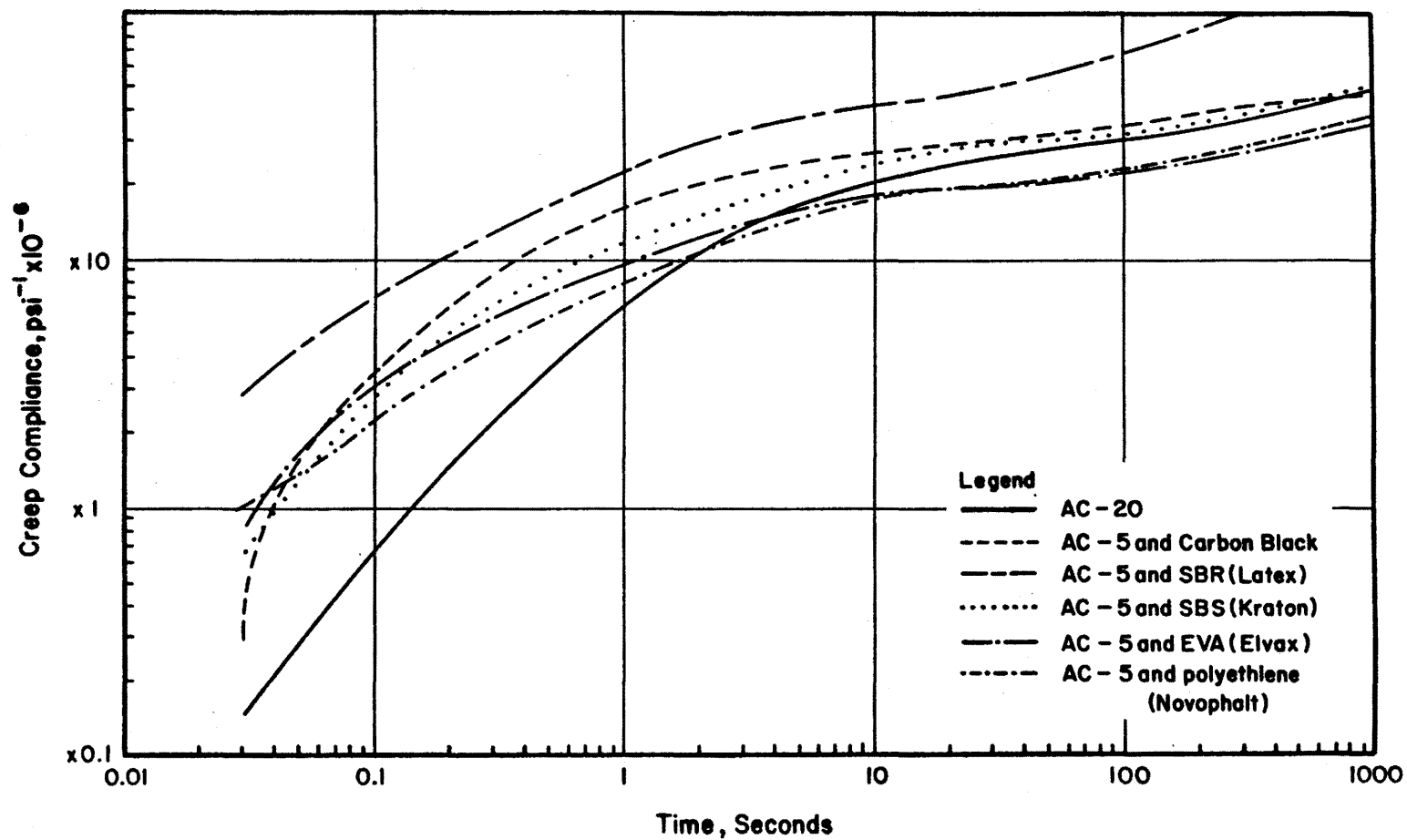


Figure 29. Creep compliance curves at 70°F (21°C) for mixtures containing Texaco asphalts.

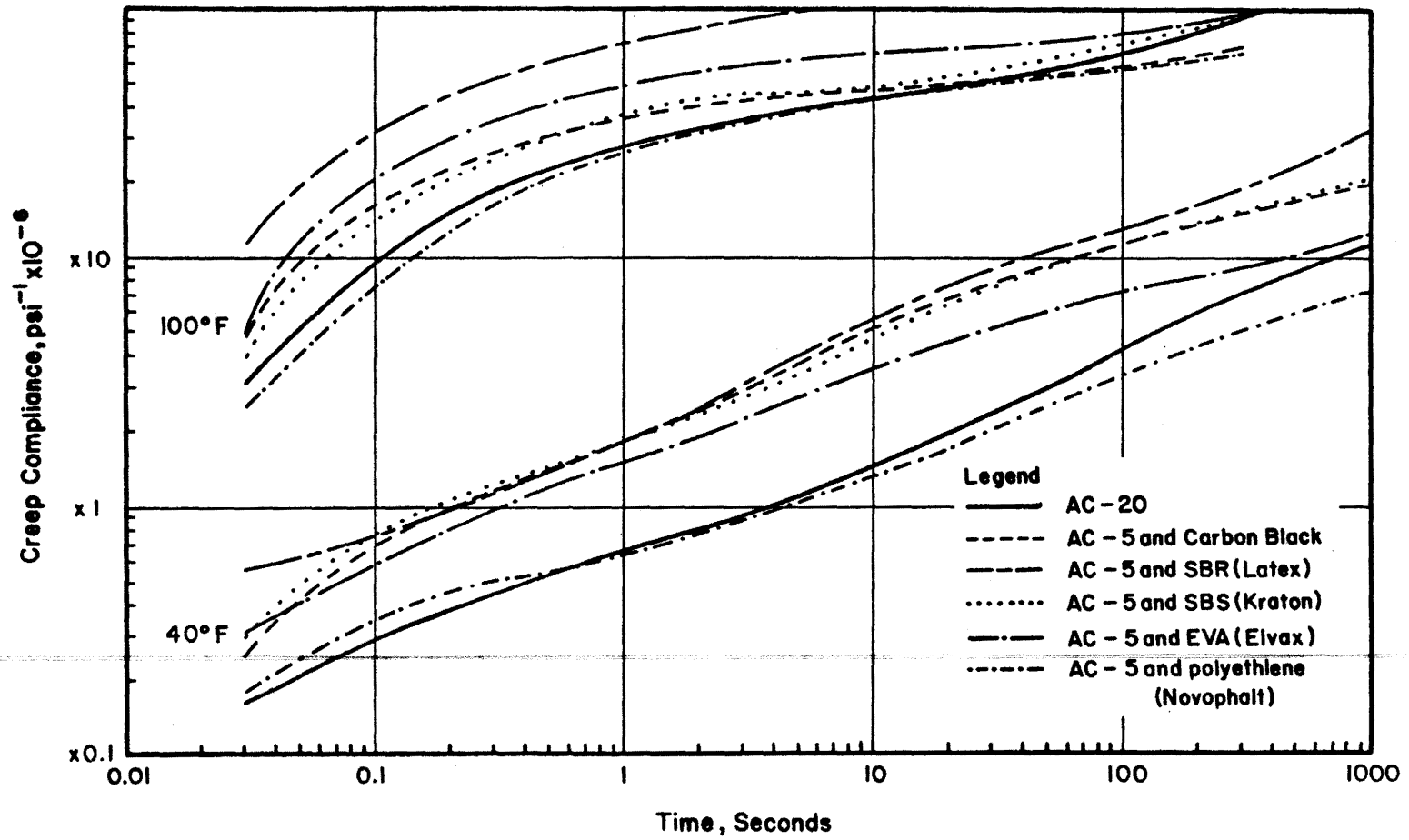


Figure 30. Creep compliance curves at 40°F (4°C) and 100°F (38°C) for mixtures containing Texaco asphalts.

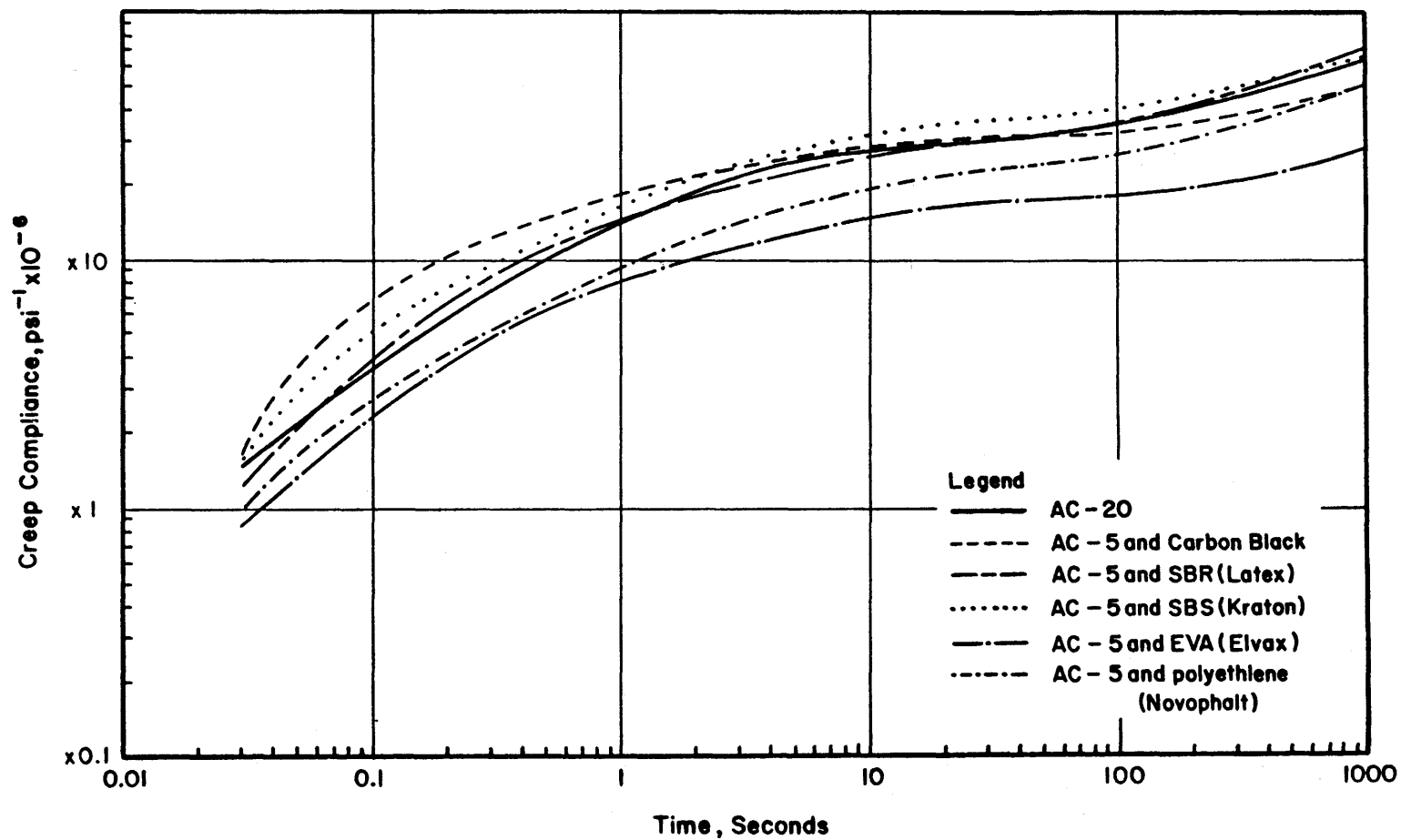


Figure 31. Creep compliance curves at 70°F (21°C) after Lottman moisture conditioning for mixtures containing Texaco asphalt.

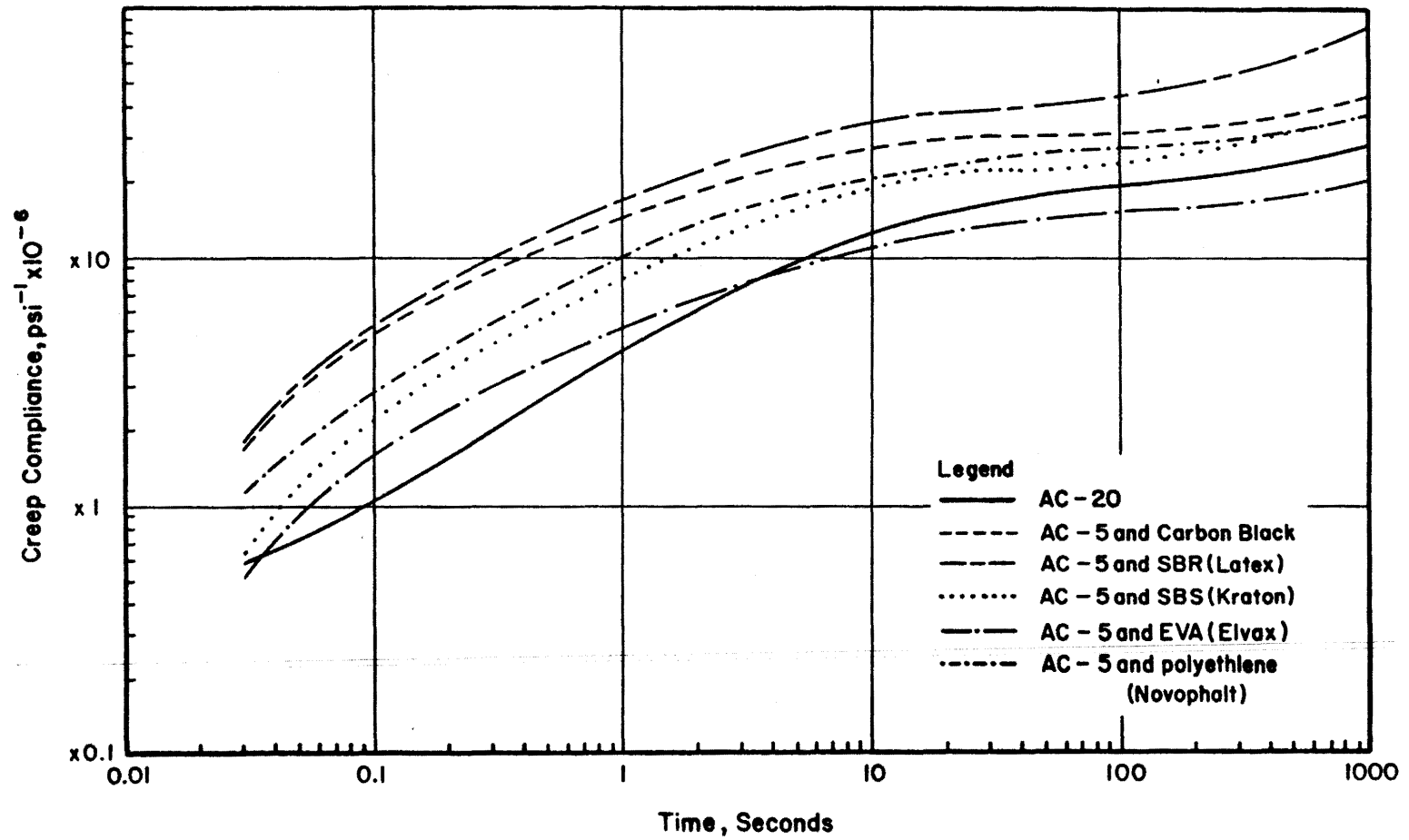


Figure 32. Creep compliance curves at 70°F (21°C) after 7 days at 140°F (60°C) for mixtures containing Texaco asphalt.

significantly higher than those of the control at relatively short load durations (less than 10 seconds), the compliances approach those of the control at long load durations, approaching 1000 seconds.

4. The compliances of the AC-5 and SBR (Latex) or EVA (Elvax) at 100°F are significantly higher than those of the control mixture. This is particularly true of the SBR (Latex) blend. From these data, one would expect a reduced potential for load spreading capabilities and excessive permanent deformation at high pavement service temperatures.

5. The effect of Lottman conditioning on the 70°F (21°C) compliance data was not significant for AC-5 blends with carbon black, polyethylene (Novophalt), SBS (Kraton) and EVA (Elvax). However, the compliances of the AC-20 control mixture were significantly increased (at least at the shorter durations of load) by Lottman conditioning. The compliances of the AC-5 and SBR (Latex) blend showed a significant reduction due to the Lottman conditioning period.

6. A comparison of the 70°F compliance data between normally conditioned specimens and specimens aged for seven days at 140°F reveals no significant difference for any of the mixtures except AC-5 plus EVA (Elvax). The AC-5 and EVA (Elvax) showed a significantly higher compliance before heat aging for load durations of less than 10 seconds. Compliance responses for loading durations of 10 seconds and greater showed no statistical difference.

Based upon figure 29, it may be stated that, generally, EVA (Elvax), SBS (Kraton), SBR (Latex) and carbon black reduce the temperature susceptibility of AC-5 based on the property of mixture compliance. This occurs because the compliances of all mixtures are significantly higher than for the AC-20 control at 40°F (4°C) and the compliances of the AC-5 mixtures converge toward those of the AC-20 at the 100°F (38°C) test temperature. The practical significance of this observation is that such a response is expected of additives which reduce rutting potential at higher temperatures and maintain a compliant (fracture resistant) nature at lower temperatures. The most favorable

responses, based on this criterion, occur with the AC-5 blends with carbon black and SBS (Kraton) followed by the EVA (Elvax) blend.

Creep compliance data for mixtures composed of additive blends of the California Valley asphalt (AR series) and river gravel at 70°F are shown in figure 33. Here the additives were blended with an AR-1000 asphalt and the control mixture was bound with an AR-4000 asphalt. When comparing these compliance data with those of the blends containing Texaco AC-5 asphalt and the AC-20 control, the following observations are made:

1. In general, the compliances are not significantly different between the Texaco and California Valley asphalts at loading duration of less than 10 seconds. However, the compliances are significantly higher at load durations above 10 seconds for the California Valley Asphalts than for Texaco asphalts.

2. The relative responses of some of the asphalt additive blends are apparently significantly affected by the base asphalts as a result of asphalt-additive compatibility. For example, Novophalt responded essentially the same as the AC-20 control, when the Texaco asphalts were compared. However, the Novophalt AR-1000 blend revealed substantially larger compliances at long loading durations (greater than 10 seconds) than the AR-4000 control mixture. This is a dramatic difference between the two data sets (two asphalt sources). The AR-1000 and SBS (Kraton) blends resulted in the highest compliances. Mixture alterations would probably be necessary in order to bring these compliances into an acceptable range (defined for specific climatic and traffic conditions) in order to reduce the potential for unacceptable deformation.

3. The AR-1000 and carbon black blend produced, as was the case with the AC-5 base asphalt, high compliances at the shorter load durations. However, compliances at the longer load durations were lower than the control. This is the response hoped for when reducing time-temperature susceptibility through the addition of modifiers.

4. The AR-1000 and EVA (Elvax) blend responded very nearly like the AR-4000 control over the loading duration range.

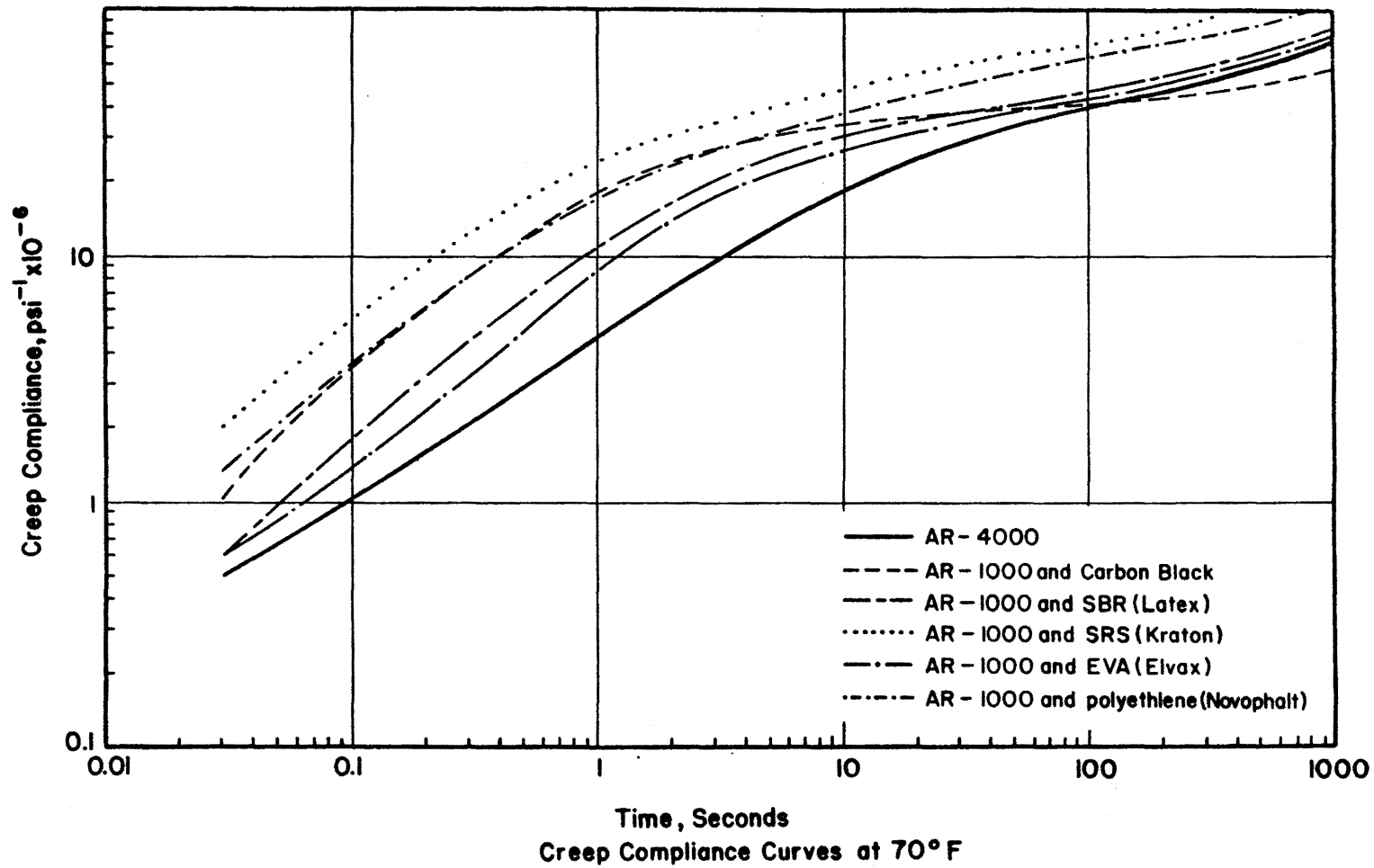


Figure 33. Creep compliance data at 70°F (21°C) for mixtures using California Valley asphalts.

In general, with AR-1000 as the base asphalt, the addition of carbon black most effectively produced the favored response of high compliances at short loading times and lower compliances at longer loading times. All other additives were successful to some degree in maintaining the lower compliances at short load durations (attributable to the soft AC-5 asphalt) and producing stiffer, less compliant mixes at the longer load durations. This indicates lower time-of-loading temperature susceptibility.

b. Permanent Deformation

The total permanent strain at the end of each rest period was plotted on log-log paper as a function of the incremental times of loading: 0.1, 1, 10, 100, and 1000 second. The permanent deformation plots from the incremental static loading tests (performed in accordance with the procedures established in reference 20) are shown in figures 34 through 40.

An analysis of the plots of accumulated strain versus incremental loading time from figures 34 through 40 reveals the following:

1. Mixtures containing AC-5 and SBR (latex) exhibited large deformations during pre-loading (exceeding 2500 micro-strain units) at 70°F (21°C) and at 100°F (38°C), and, in accordance with the VESYS Manual, the level of applied stress was reduced in these cases. Even at the lower level of applied stress, the latex specimens showed the greatest permanent deformation relative to the AC-20 control and the other additives tested.

2. Also at 40°F (4°C), the mixture containing the latex blend exhibited significantly higher deformation than the other five mixtures. Perhaps a reduction in binder content (AC-5 and latex blend) within the mixture or an increase in the amount of latex used in the blend (AC-5 plus latex) is warranted to improve the creep and deformation responses.

3. Polyethylene (Novophalt) exhibited a greater resistance to permanent deformation at 40°F and at 70°F than any other mixtures,

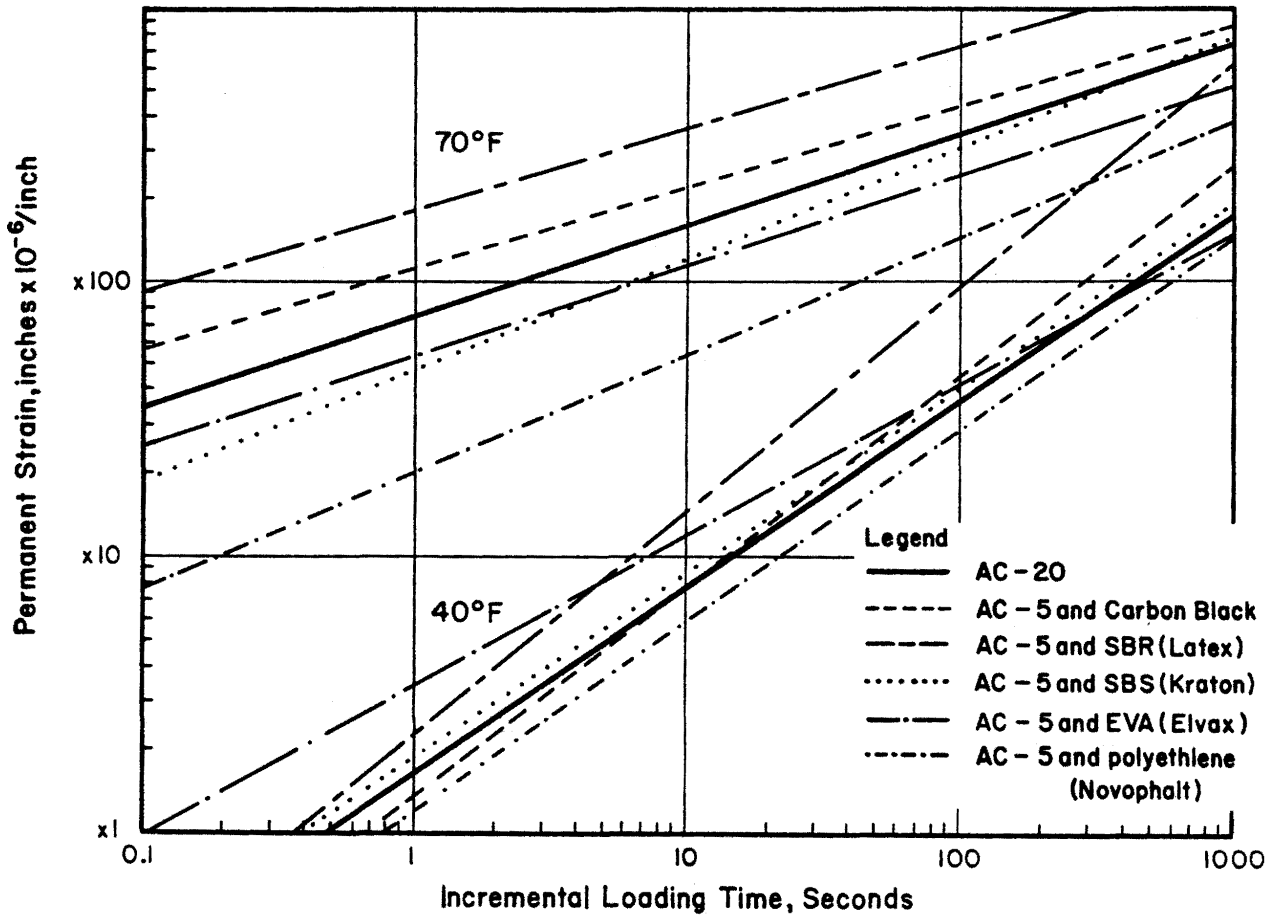


Figure 34. Permanent strain from incremental static loading tests at 40°F (4°C) and 70°F (21°C) for mixtures using Texaco Asphalts.

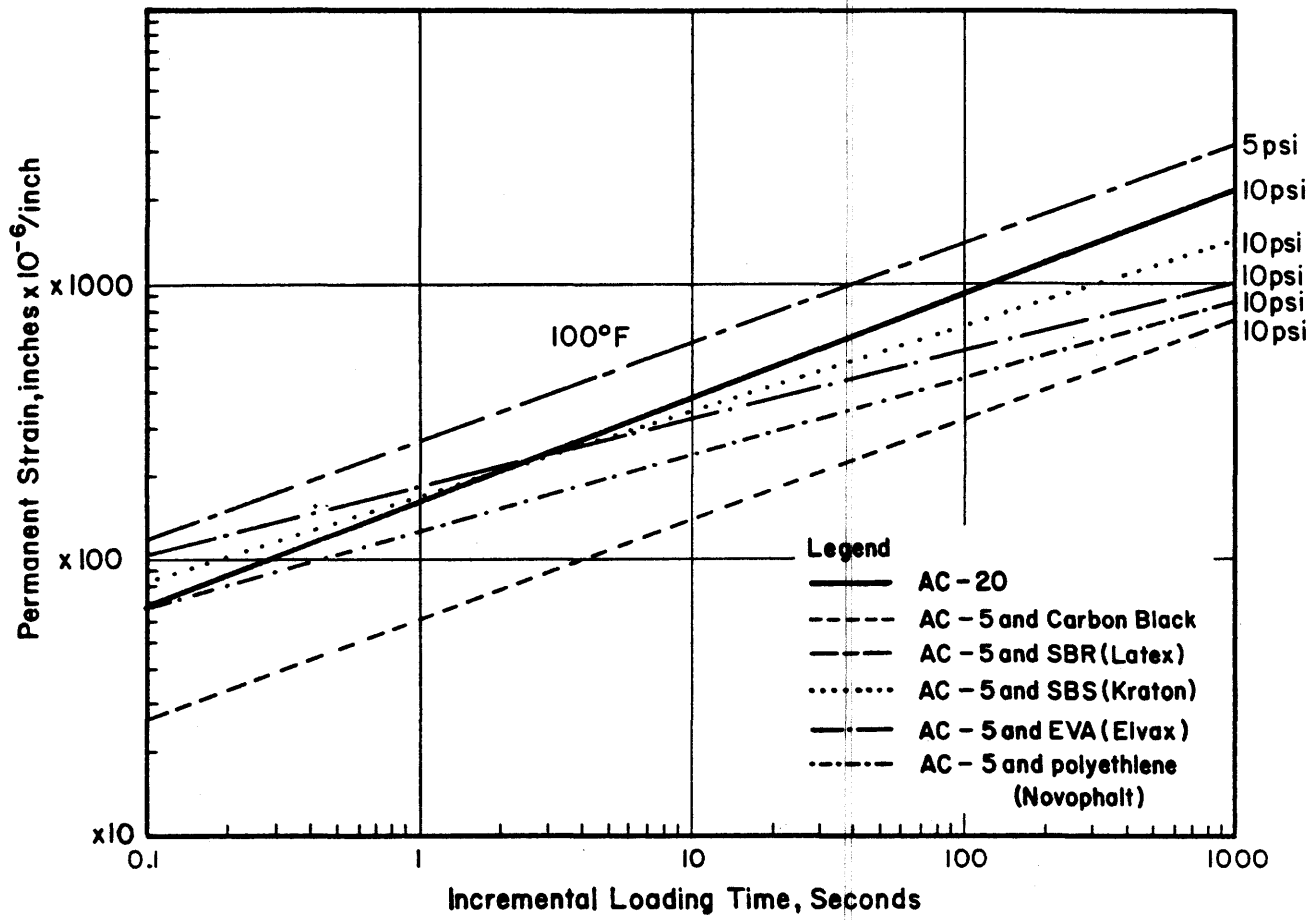


Figure 35. Permanent strain from incremental static loading tests at 100°F (38°C) for mixtures using Texaco asphalts.

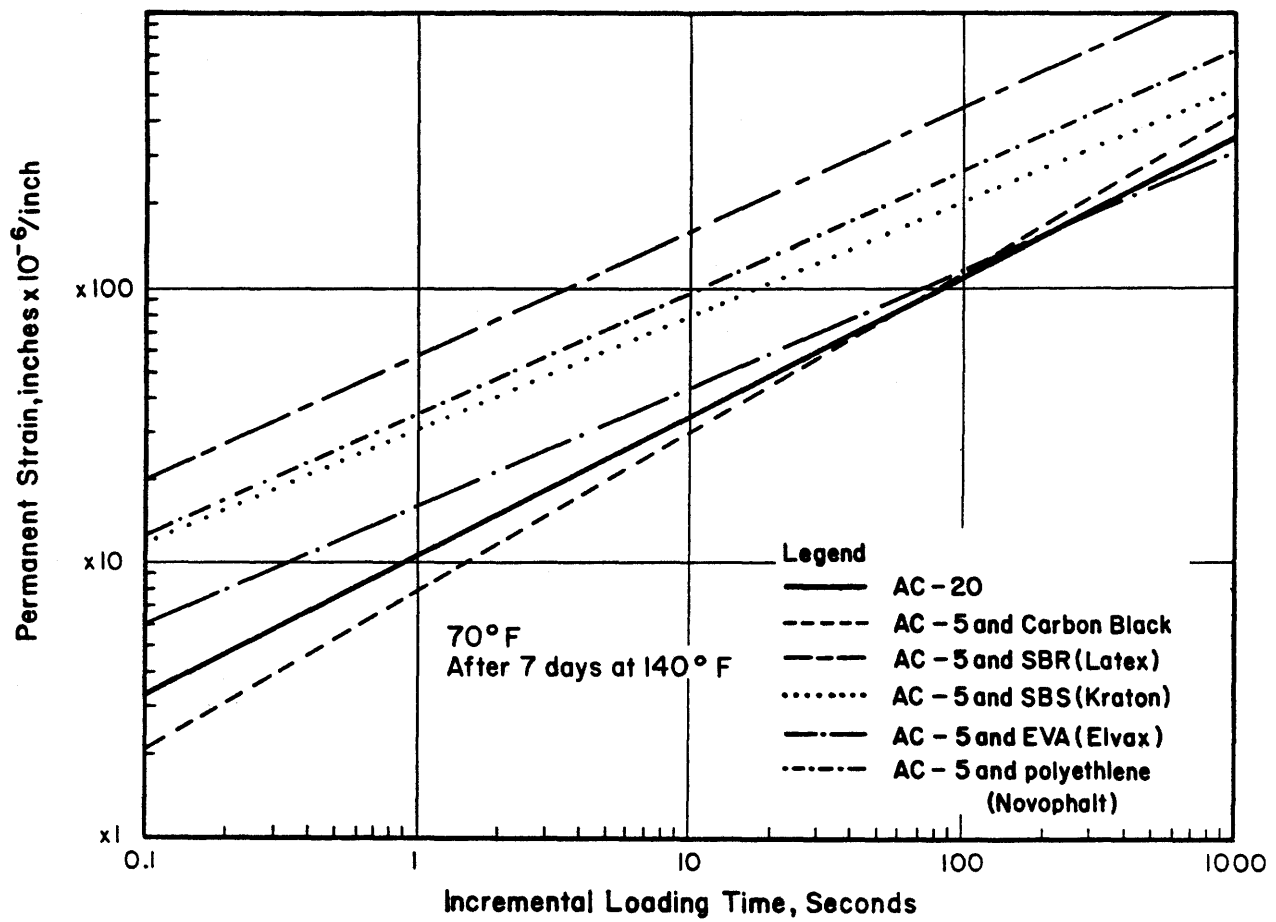


Figure 36. Permanent strain from incremental static loading tests at 70°F (21°C) after 7 days at 140°F (60°C) (all tests at 20 psi) for mixtures using Texaco asphalts.

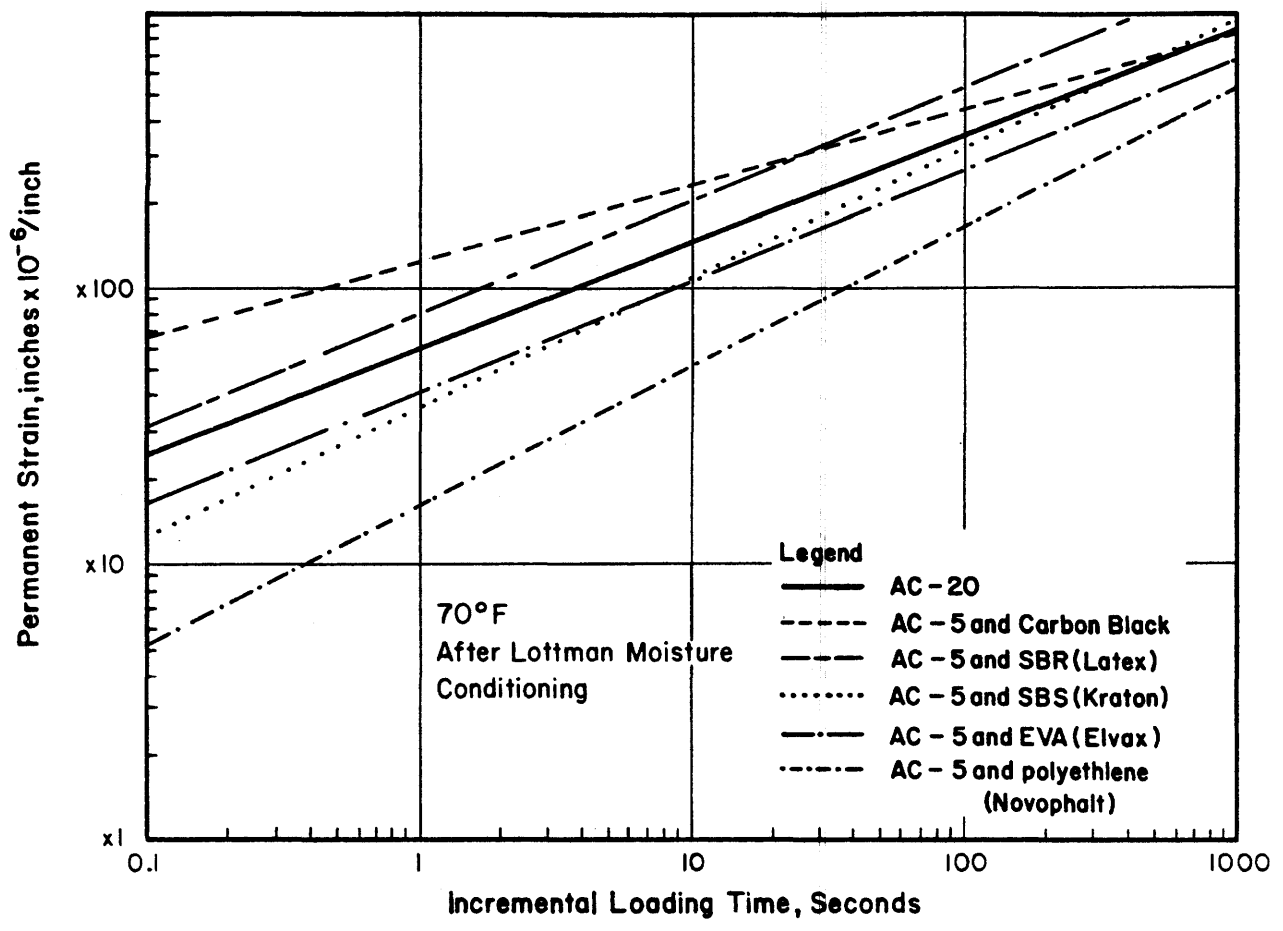


Figure 37. Permanent strain from incremental static loading tests at 70°F (21°C) after one-cycle Lottman for mixtures using Texaco asphalts.

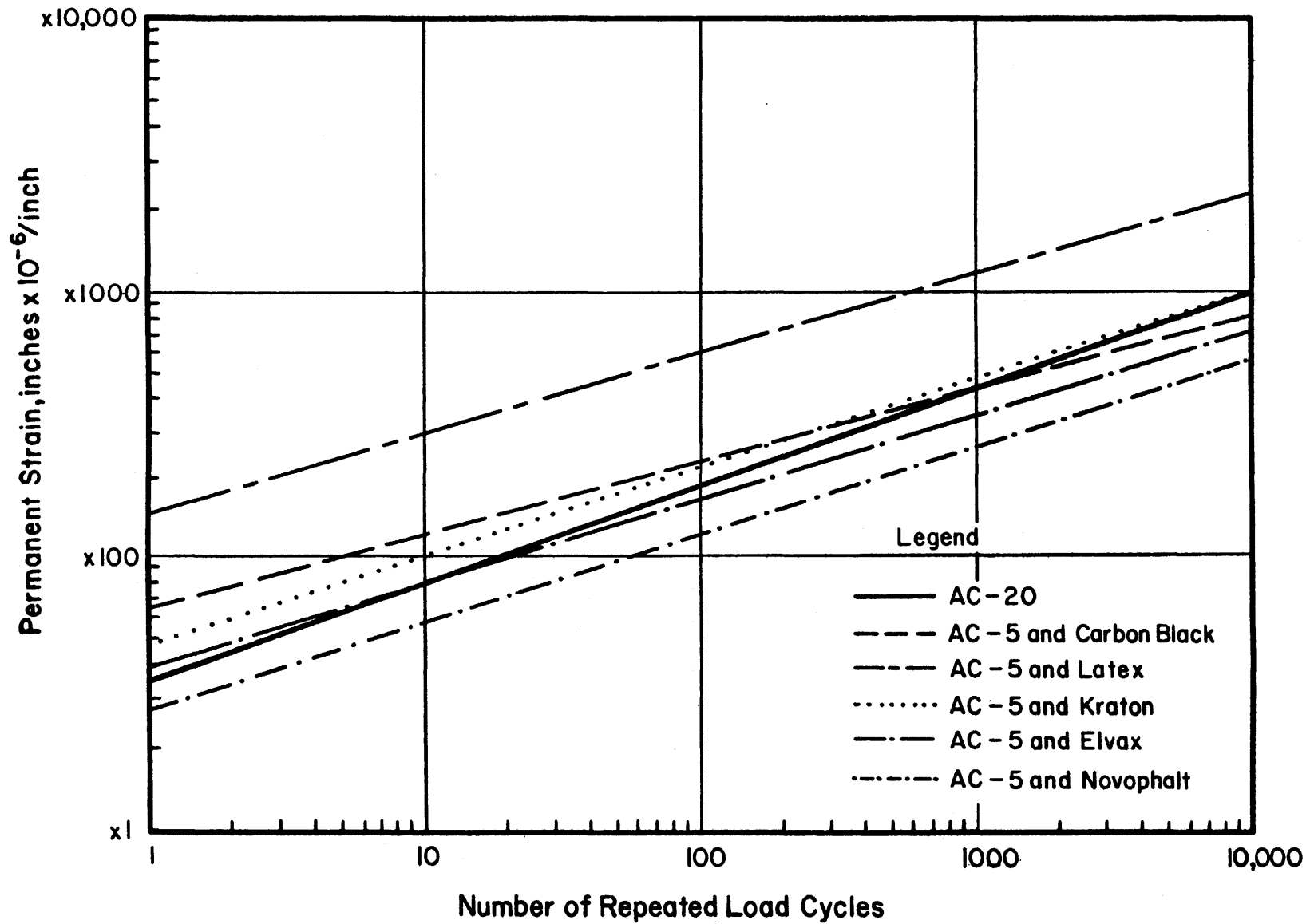


Figure 38. Accumulated strain versus cycles at 100°F (38°C) for additive modified Texaco AC-5.

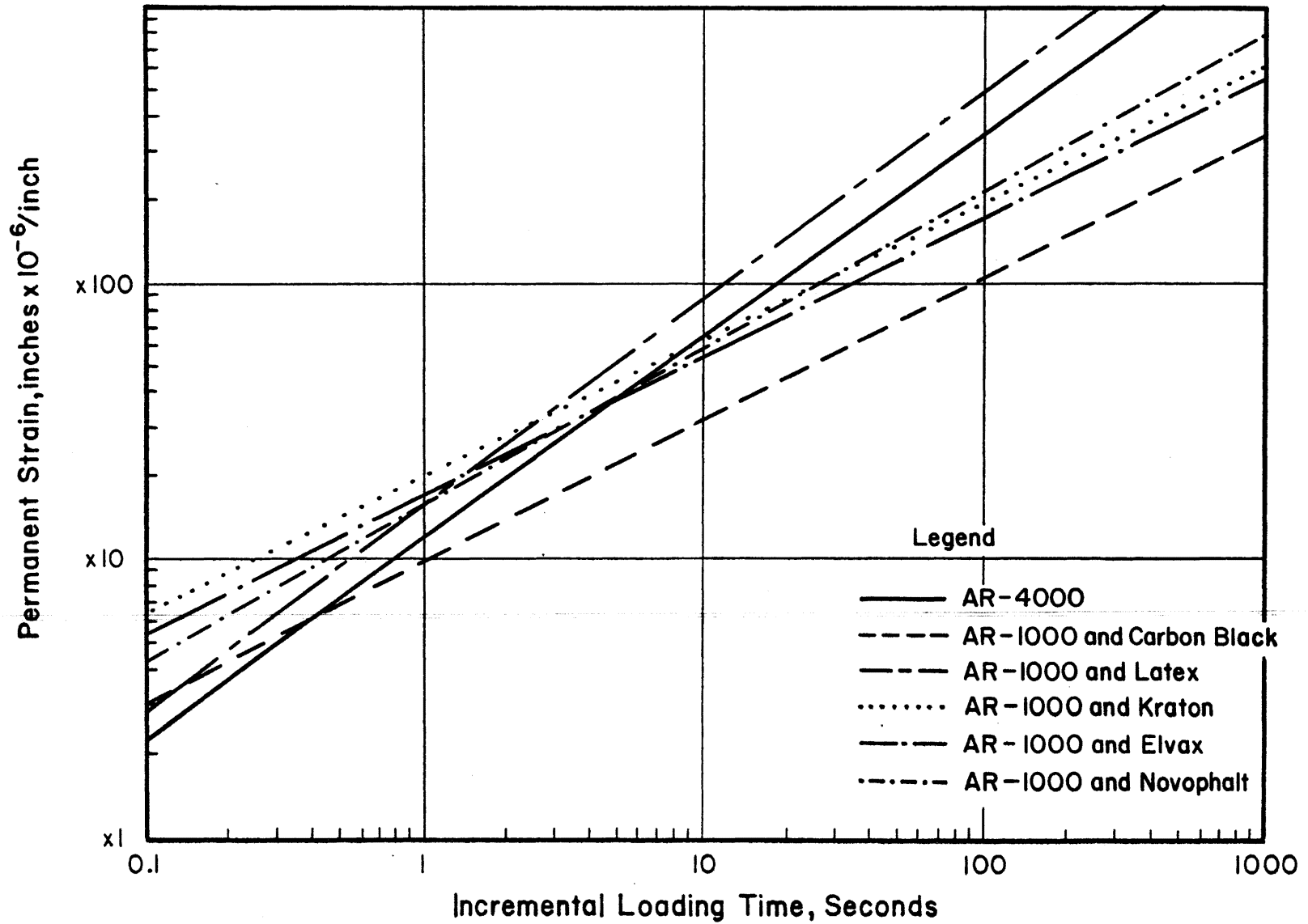


Figure 39. Accumulated strain versus incremental loading time at 70°F (21°C) for additive modified California Valley AR-1000.

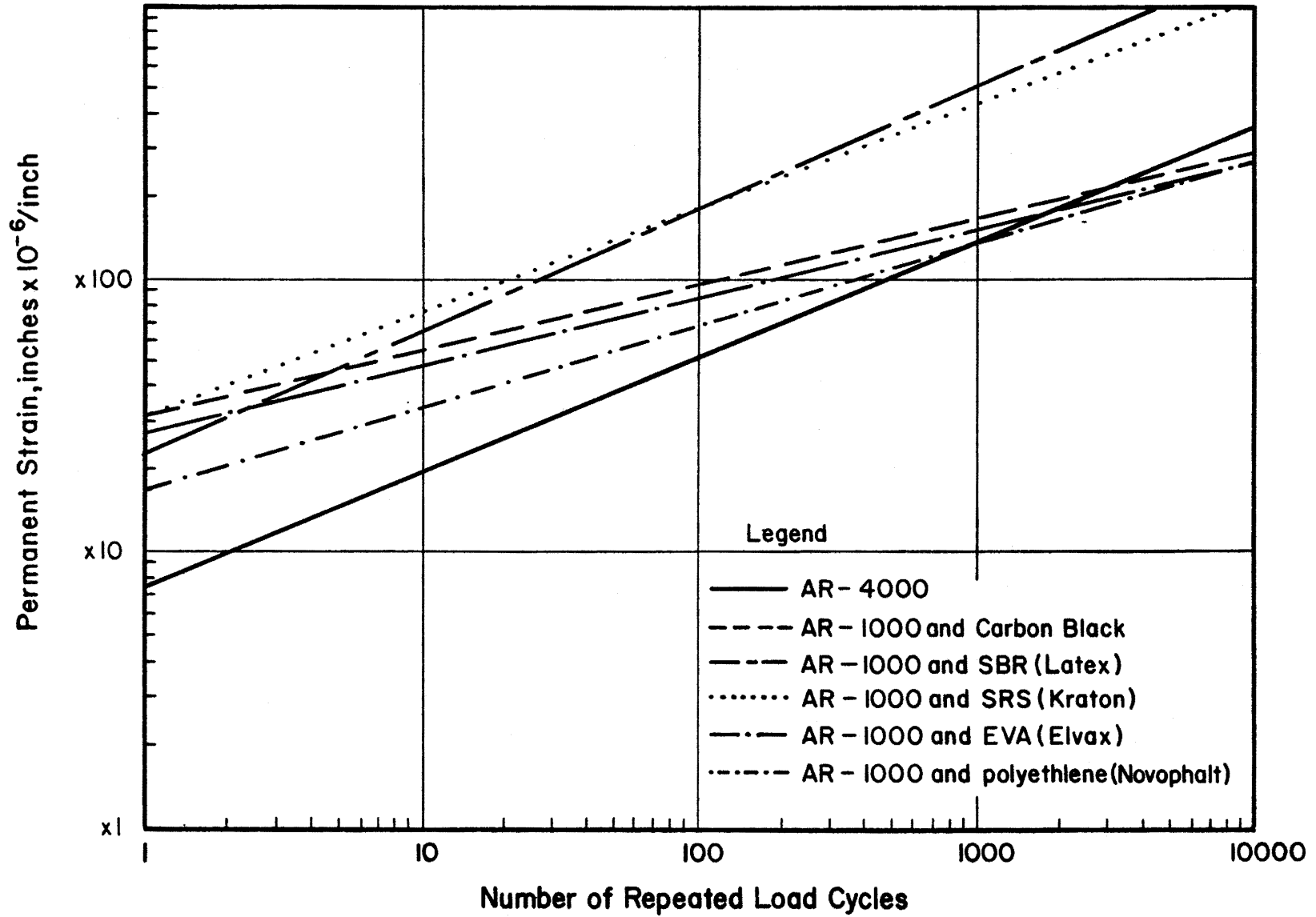


Figure 40. Accumulated strain versus loading cycles at 70°F (21°C) for additive modified California Valley AR-1000.

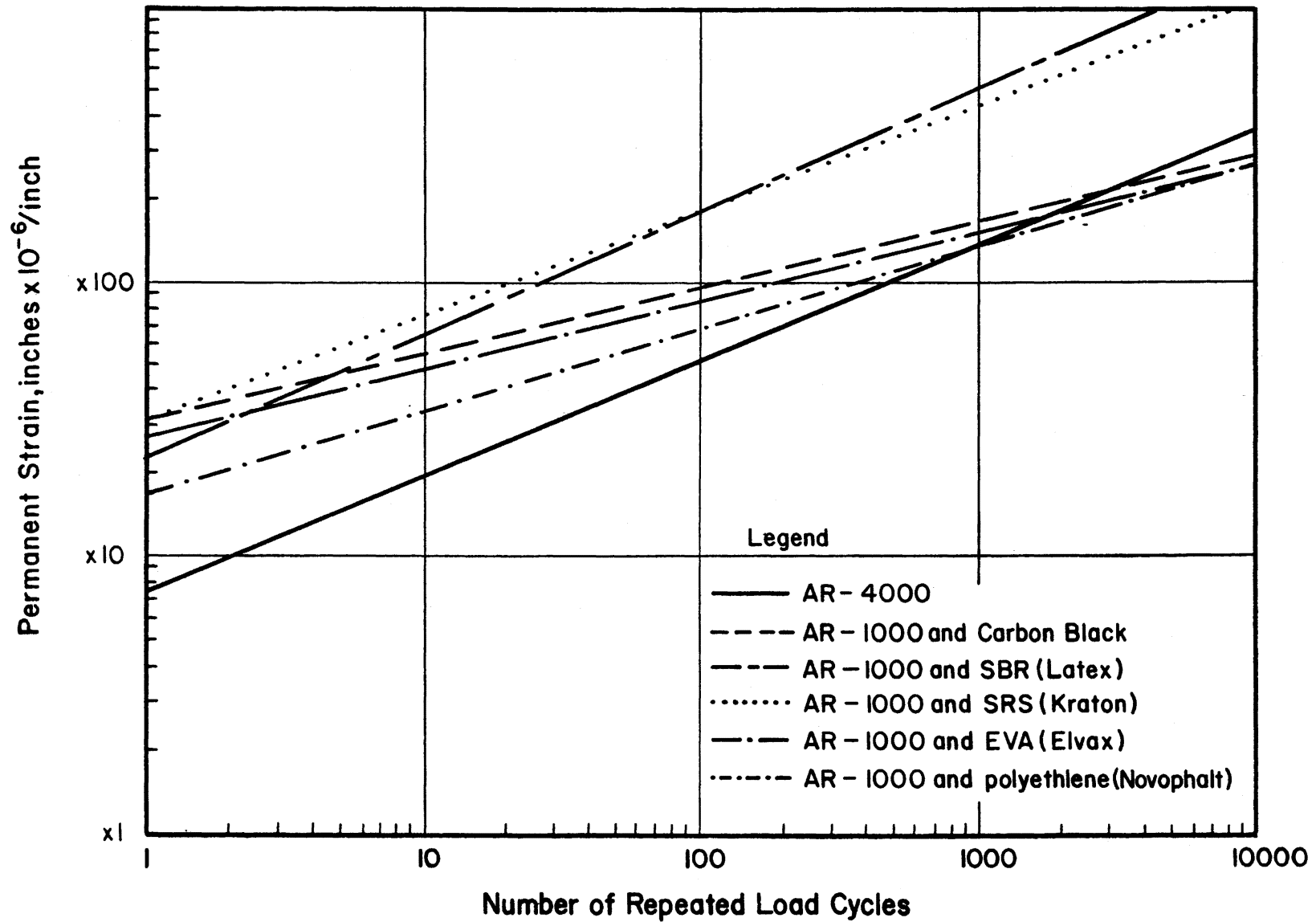


Figure 40. Accumulated strain versus loading cycles at 70°F (21°C) for additive modified California Valley AR-1000.

including the AC-20 control. At 100⁰F, the carbon black blend yielded the least permanent deformation followed closely by Novophalt. However, the slope of the permanent deformation versus time of loading plot for the Novophalt mixture was statistically smaller than slopes for the other mixtures. This fact coupled with the relative position of the plot, with respect to the other mixtures, indicates a greater resistance overall for Novophalt in resisting permanent deformation.

4. It is surmised that the relative positions of the permanent strain versus incremental loading time plots are influenced greatly by the preconditioning procedure. This procedure may not adequately account for material property peculiarities of polymer-modified asphalts. This hypothesis will require further study for evaluation.

5. Mixtures containing EVA (Elvax) and SBS (Kraton) showed permanent deformation responses similar to the AC-20 control.

The effects of heat aging may be evaluated by comparing the results of figures 34 and 36. An analysis of these results yield the following observations:

1. The susceptibility of mixtures to permanent deformation appeared to be significantly affected based on the different intercept values between figures 34 and 36. However, the values of permanent strain at incremental, static loading times of 1000 seconds were not significantly different for mixtures containing blends of AC-5 and SBR (latex) or AC-5 and SBS (Kraton). The mixtures containing AC-5 and carbon black, AC-5 and EVA and the control mixture (AC-20) exhibited statistically significant, though not substantial, reductions in accumulated strain at a loading time of 1000 seconds due to heat aging. The mixture containing carbon black and polyethylene actually demonstrated slightly more susceptibility to deformation following accelerated aging.

2. The visual differences between deformation plots before and after aging were a significantly smaller intercept and a significantly steeper slope for the aged samples. The net result was approximately the same accumulated strain at long loading times. Perhaps this was due to

an initial set caused by 140°F aging which was overcome during long-term creep.

The effects on one-cycle Lottman conditioning are demonstrated by comparing figures 34 and 37. Once again the relative deformation susceptibilities were not markedly altered. In fact, the values of accumulated strain at an incremental static loading time of 1000 seconds were not significantly different between tests for latex, carbon black, the AC-20 control, EVA or SBS. The AC-5 and polyethylene blend showed larger permanent strains (statistically significant though not practically significant) at the incremental loading time of 1000 seconds.

Figure 38 demonstrates the accumulated strain versus repeated load applications for the six mixtures in which the California Valley asphalts were used. These data are recorded at 100°F and can be compared to the data in figure 35. Although the results are somewhat different from those in figure 35, the relative behavior of the additives are similar. At 10,000 loading cycles, the order of resistance to permanent deformation is as follows: (1) Polyethylene (Novophalt), (2) EVA (Elvax), (3) Carbon black, (4) SBS (Kraton), (5) AC-20 and (6) SBR (latex). The mixtures were so weak at 100°F (38°C) that a loading stress of only 5 psi (3.49 x KPa) could be used during the test.

Figures 39 and 40 depict the incremental static and repeated load permanent deformation results, respectively, for the AR-1000, California Valley asphalt. These tests were performed at 70°F (21°C). Based on these results, the following observations are presented:

1. Polyethylene (Novophalt), EVA (Elvax) and carbon black were successful in limiting long-term permanent deformation of the AR-1000 base asphalt to ranges equal to or less than those developed when the AR-4000 binder is used in the mixture.

2. Although the mixture containing SBS (Kraton) responded with high deformation based on the repeated load testing, the responses were similar to other mixtures based on incremental time of loading results. This discrepancy may be due in part to the inadequacy of the incremental static load test to account for rebound time.

3. In general, although some anomalies exist, the results of incremental static load induced permanent deformation and repeated load induced permanent deformation are consistent. However, the results should be evaluated by considering not only the relative position of the plot but also the slope. Slopes of the mixtures containing polyethylene, EVA and carbon black are significantly lower than the other mixtures.

4. Where the differences in deformation responses are affected by the asphalt source, the answer may at least partially lie in asphalt-polymer compatibility. However, in general, the SBR and SBS rubber-modified mixtures responded with the least resistance to permanent deformation while EVA demonstrated a substantial resistance.

In conclusion, although a sensitivity of the additives to asphalt source is strongly inferred from the results of permanent deformation testing, the relative effects of the additives in reducing long term permanent deformation at the higher temperatures are consistent. These may be summarized in table 55.

In general, the polyethylene, carbon black and EVA additives were most successful in preventing permanent deformation.

c. Evaluation of Binder Volume Effects on Compliance and Deformation

Although the mixture design called for a five percent binder content for the latex-AC-5 blends with the river gravel aggregate, the design was re-evaluated for two reasons: first, all other additive mixture designs called for lower binder contents (4.5 to 4.75 percent) and second, the mixtures modified by latex responded as quite susceptible to permanent deformation and exhibited relatively large compliances at high temperature and/or long loading durations. Thus the properties of mixtures containing latex were re-evaluated using 4.5 percent binder.

Figures 41 and 42 compare the compliance and incremental static load deformation data, respectively, for the 4.5 and 5.0 percent blends. From these data one should observe:

1. Reduction of 0.5 percent has a statistically significant effect on compliance as well as accumulated permanent deformation.

Table 55. Relative resistance to permanent deformation at long term load durations.

Binder	When additive is mixed with:	
	AC-5 (Texaco)	AR-1000 (California Valley)
Control	5 (5)*	5 (4)*
Carbon Black (Microfil-8)	2 (3)	1 (3)
EVA (Elvax)	3 (2)	2 (2)
SBR (Latex)	6 (6)	6 (6)
SBS (Kraton)	4 (4)	3 (5)
Polyethylene (Novophalt)	1 (1)	4 (1)

* Results in parentheses are from repeated load versus accumulated strain testing at 70°F (21°C) for Texaco asphalts and 100°F (38°C) for California Valley Asphalt.

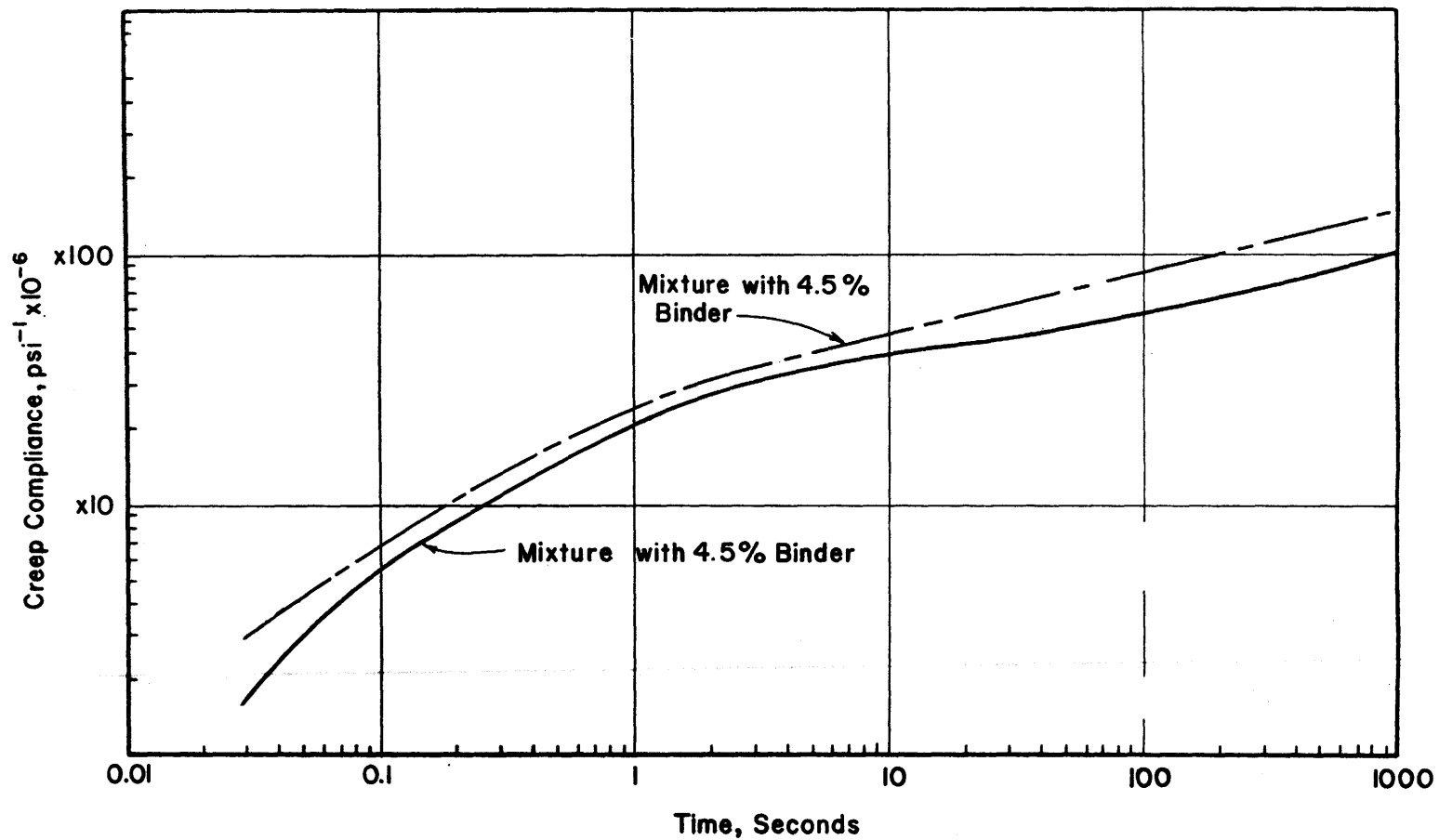


Figure 41. Comparison of creep compliance of mixtures containing 4.5 and 5.0 percent of blends of latex and AC-5.

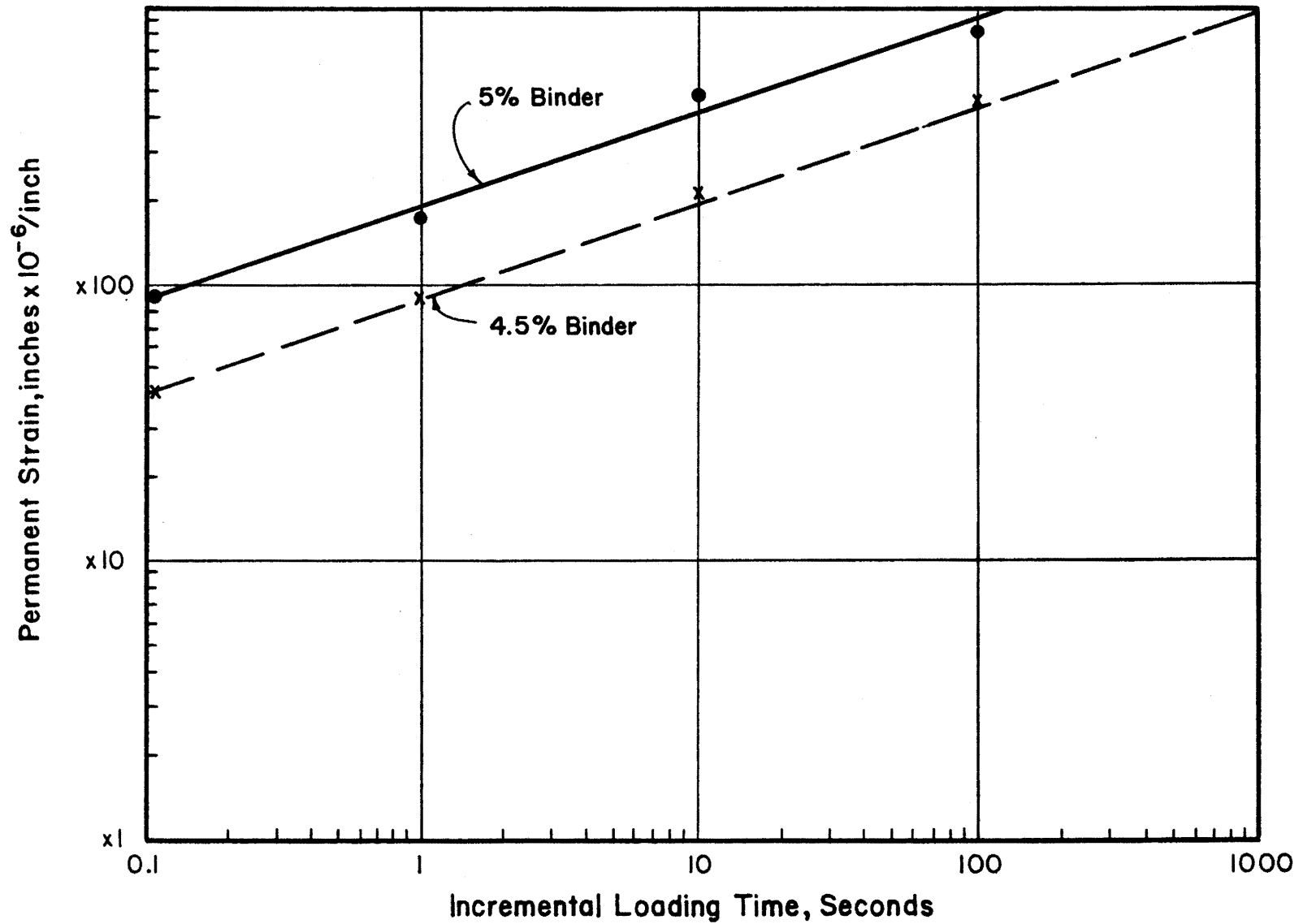


Figure 42. Comparison of incremental loading derived permanent deformation plots for mixtures containing AC-5 and latex (5% binder versus 4.5% binder).

2. In terms of deformation susceptibility, the mixture containing 4.5 percent binder improved dramatically but, relative to other mixtures, still ranked most susceptible to deformation.

3. All mixtures containing AR-1000 and latex blends and tested in permanent deformation were prepared at 4.5 percent binder. In these mixtures, the latex modified asphalt also showed the greatest potential to deform at both 70°F (21°C) and 100°F (38°C). However, the response was not significantly different from the mixtures containing Kraton (SBS).

4. The sensitivity of permanent deformation response and creep compliance to mixture properties such as binder content is illustrated by these data. In-deed minor changes in the binder content may have as great an effect on permanent deformation performance as the additives themselves.

d. VESYS Parameters

The ALPHA (α) and GNU (μ) parameters as explained previously were calculated from accumulated permanent strain versus duration of loading data for five conditions: 40°F (4°C), 70°F (21°C), 100°F (38°C), 70°F following Lottman conditioning and 70°F following aging at 140°F (60°C) for a period of seven days. Results of these tests are presented in table 56.

These results were used in the VESYS computer model to predict permanent deformation responses of the asphalt mixtures containing additives.

The α and μ values computed in table 56 were based on the VESYS procedure for incremental static loading. A comparison of 40, 70 and 100°F data in table 56 indicates an anomaly. The α values in table 56 increase as temperature increases; whereas, one would expect a decrease in α with increasing temperature.

Apparently, the anomaly in α values, table 56, stems from the limitations of incremental static load-induced accumulated strain. At

Table 56. Summary of VESYS permanent deformation parameters: ALPHA and GNU.

Binder	Parameter	Condition of Deformation Test				
		40°F	70°F	100°F	70°F Following Lottman	70°F Following -140°F Aging
AC-20	α	0.34	0.67	0.63	0.62	0.50
	μ	0.076	0.45	0.69	0.25	0.14
AC-5 + Carbon Black	α	0.26	0.70	0.64	0.72	0.43
	μ	0.024	0.41	0.12	0.27	0.021
AC-5 + Latex (SBR)	α	0.19	0.71(0.64)*	0.64	0.59	0.55
	μ	0.021	0.92(0.29)*	0.48	0.19	0.20
AC-5 + Kraton (SBS)	α	0.33	0.61	0.70	0.54	0.59
	μ	0.027	0.23	0.32	0.091	0.17
AC-5 + EVA	α	0.46	0.67	0.76	0.59	0.57
	μ	0.083	0.29	0.22	0.22	0.13
AC-5 + Novophalt (Polyethylene)	α	0.34	0.58	0.73	0.49	0.56
	μ	0.034	0.17	0.38	0.072	0.16

*For a AC-5 and latex blend binder content of 4.5% in lieu of 5.0% binder in mixture.

higher temperatures, a short recovery period between long duration loading cycles is sufficient for recovery. However, at low temperatures, the recovery period is not long enough. Thus the measured accumulated strain at low temperatures may not be accurate as it possibly includes viscoelastic (recoverable) strain not yet recovered due to inadequate recovery time. This may result in steep slopes (low α 's) for 40^oF data relative to 100^oF data. Thus, it is recommended that all α and μ data be derived from repeated load-accumulated strain experiments.

e. Time-Temperature Shift Factors

Although it has been established that, for practical engineering purposes, asphalt concrete can be considered to be linearly viscoelastic, the application of a horizontal shift factor along the log time abscissa to produce a master curve is quite subjective. The value becomes even more subjective when the shift factor is described in terms of BETA. The term BETA is defined as the ratio of the change in $\log_{10} a_T$ over a change in temperature or a temperature interval

$$\text{BETA} = \frac{\Delta(\log_{10} a_T)}{\Delta T} \quad \text{Equation 36}$$

This value assumes a linear relationship between $\log_{10} a_T$ and temperature. This is not the case as the $\log_{10} a_T$ versus temperature curves are nonlinear. The values of BETA which were used in the Structural Design chapter are presented in table 57. These values represent best fit linear approximations of the $\log_{10} a_T$ versus temperature data.

Table 57. Time - temperature shift factors (BETA) selected for VESYS analysis.

Binder	Time - Temperature Shift Factors	
	Warm Climate (BETA-1)	Cool Climate (BETA-2)
AC-20	0.062	0.090
AC-5 + Carbon Black	0.055	0.084
AC-5 + Latex (SBR)	0.054	0.077
AC-5 + Kraton (SBS)	0.052	0.077
AC-5 + EVA	0.066	0.090
AC-5 + Polyethylene (Novophalt)	0.069	0.105

*Note: All the $\log a_T$ versus temperature curves are non-linear, two slopes (BETA) were calculated. The (BETA-1) value is for 70°F to 40°F while the (BETA-2) value is for 70°F to 100°F. The BETA values for the two climates were calculated on the basis of weighted temperatures.

$$^{\circ}\text{C} = (^{\circ}\text{F} - 32)/1.8$$

EVALUATION OF THERMAL CRACKING POTENTIAL

1. Approach

The thermal cracking potential of the binders and mixtures studied was evaluated using three approaches. The first approach was based on traditionally used concepts of limiting stiffness and critical stress. This approach is based totally on binder properties and is reported in Chapter III. The second approach is based on thermal-fatigue cracking and fracture mechanics and the viscous response of the binder in an asphalt concrete matrix. Finally, the indirect tensile strengths over a wide range of temperatures were compared to stresses induced in a pavement. The induced stresses were computed using a viscoelastic slab theory.

2. Thermal Fatigue Analysis

Models for low temperature cracking have been used with varying degrees of success in the more northerly regions of the United States and Canada. In these areas, the temperature drops low enough that it will reach the "fracture temperatures" of the pavement material. This fracture temperature is defined as the temperature at which the developed tensile thermal stress exceeds the tensile strength of the asphalt concrete mixture. However, in many cases transverse cracking may be common even though the pavement has not been subjected to such temperature extremes.

A mechanism to account for the thermally induced transverse cracking of flexible pavements other than the low temperature cracking model mentioned above is thermal fatigue cracking. It was first described by M. Shahin and B. F. McCullough (38) and is defined to be caused by thermal fatigue distress due to daily temperature cycling, which eventually exceeds the fatigue resistance of the asphalt concrete.

Lytton and Shanmagan (39) have developed a computer model based on fracture mechanisms for predicting transverse cracking due to thermal fatigue cracking in asphalt concrete pavements. Basically, the model uses Shahin's and McCullough's revision to Barber's Equations (40) to

compute pavement temperatures based on air temperatures, wind speed and solar radiation; calculates pavement effective moduli and employs the computation of stress intensity factors and fracture mechanics to predict thermal fatigue resistance.

The results of the Lytton-Shanmagan procedure are typically presented as cumulative damage factors. These damage factors were computed for typical climatic conditions in Abilene, Texas, and in Detroit, Michigan. However the damage factor values were inconsistent and are not presented as they may be misleading. The authors believe that inconsistency in the results may be due to the method used to construct the stiffness curves for the additive-asphalt blends. This procedure employs the Van der Poel nomograph which assumes that the additive-asphalt blends behave as traditional bitumens throughout the time-temperature spectrum. This assumption may well be misleading, especially for mixtures, for which the binder to mixture transformation factor used in the Lytton-Shanmagan procedure adds a second variable. In summary the modification of asphalts through the addition of polymers may alter their viscoelastic behavior so as to invalidate use of the Van der Poel assumptions.

3. Thermal Cracking Analysis Based on Mixture Properties

The previous analyses were based on mixture stiffnesses predicted from rheological properties of the binder, and aggregate volumetric properties were accounted for strictly in an empirical manner. The final analysis is based on mixture properties.

The available literature suggests that the fracture strength of asphalt concrete is at its highest level at low temperatures and/or rapid loading rates; but fracture occurs at small strains. In fact Finn (41) defined the limiting strain for asphalt concrete at relatively low temperatures to be approximately 1.0×10^{-3} in/in. This is about one order of magnitude greater than allowable strain levels in fatigue loading.

The critical condition for fracture in asphalt concrete occurs at low temperatures and/or rapid loading rates. It is here that the asphalt behaves in a most brittle manner.

McLeod (42) has used the bitumen stiffness as a fundamental indicator of the asphalt cement characteristics; limits are placed on the bitumen stiffness at a given low temperature to eliminate transverse cracking. McLeod concluded that cracking will not occur if mix stiffness is less than 1×10^6 psi (6.9×10^9 MPa) at 20,000 seconds loading time for the minimum anticipated temperature. Saal (43) used virtually the same approach as McLeod. Saal calculated that the limiting stiffness for asphalt concrete was approximately 715,000 psi (4.93×10^9 MPa) for a loading time of 10^4 seconds and a change in temperature from 32°F (0°C) to 14°F (-10°C).

Monismith, et. al. (44), using the principles of linear viscoelasticity and creep compliance data, computed by numerical methods the stresses at the surface of an asphalt concrete slab subjected to a range of temperature distributions. They showed that in the north central U.S. and in Canada surface stresses in excess of 3,300 psi (2.28×10^7 MPa) could be induced. This far exceeds the fracture strength of any asphalt concrete.

The postulated mechanism for cracking is traditionally based on the concept of induced thermal stresses, which exceed the tensile strength.

$$\sigma(\dot{T}) = \alpha \sum_{T_0}^{T_f} S(\Delta T) \cdot (\Delta T) \quad \text{Equation 37}$$

where $\sigma(\dot{T})$ = accumulated thermal stress for a particular cooling rate T ,
 α = average thermal contraction coefficient over the temperature drop, $T_0 - T_f$,
 T_0, T_f = initial and final temperature and
 $S(\Delta T)$ = stiffness at the midpoint of discrete temperature intervals T over the range of T_0 and T_f , using a loading time corresponding to the time interval for the T change.

Of course, if the predicted thermal stress as a function of temperature exceeds the tensile strength of the mix at that temperature, fracture occurs.

The above relationship clearly illustrates the fact that very stiff mixtures are susceptible to low temperature fracture even if they possess high fracture strength because of the high stresses induced during cooling.

For a selected cooling rate, \dot{T} , temperature drop (cooling rate times period of cooling) and thermal contraction coefficient (approximately equal to 1.5×10^{-6} in/in/ $^{\circ}$ F for asphalt concrete between 30° F, -2° C, and -20° F, -29° C), the only variable affecting $\sigma(\dot{T})$ is $S(\Delta T)$. Stiffness, $S(\Delta T)$, versus temperature was computed for the modified Texaco and California Valley asphalt mixtures, respectively. The stiffnesses were derived from the creep compliance tests and the time temperature shift factor, a , discussed earlier in this chapter. The $S(\Delta T)$ values are for loading rates of 7,200 second which is assumed to approximate a 10° F/hr (5.4° C/hr) temperature drop and is based on field data. This loading rate is simulated in the laboratory in the indirect tensile mode by a stroke rate of 0.02 to 0.01 in/min (0.51 to 1.02 mm/min).

Once the rate and range of temperature drop are fixed, stiffness is the only variable of consequence. Figures 43 and 44 clearly illustrate the effect of stiffness on producing induced stresses within the AC. The plots in figures 43 and 44 are for a cooling rate of 10° F/hr (5.4° C/hr) and a temperature drop of four hours.

4. Discussion of Thermal Cracking Analysis

Based on this analysis the following conclusion are formed:

1. The results of the three methods of analysis are somewhat contradictory. However, in general the softer asphalts (AC-5 and AR-1000), with or without modifiers, performed significantly better than the stiffer, control asphalts.

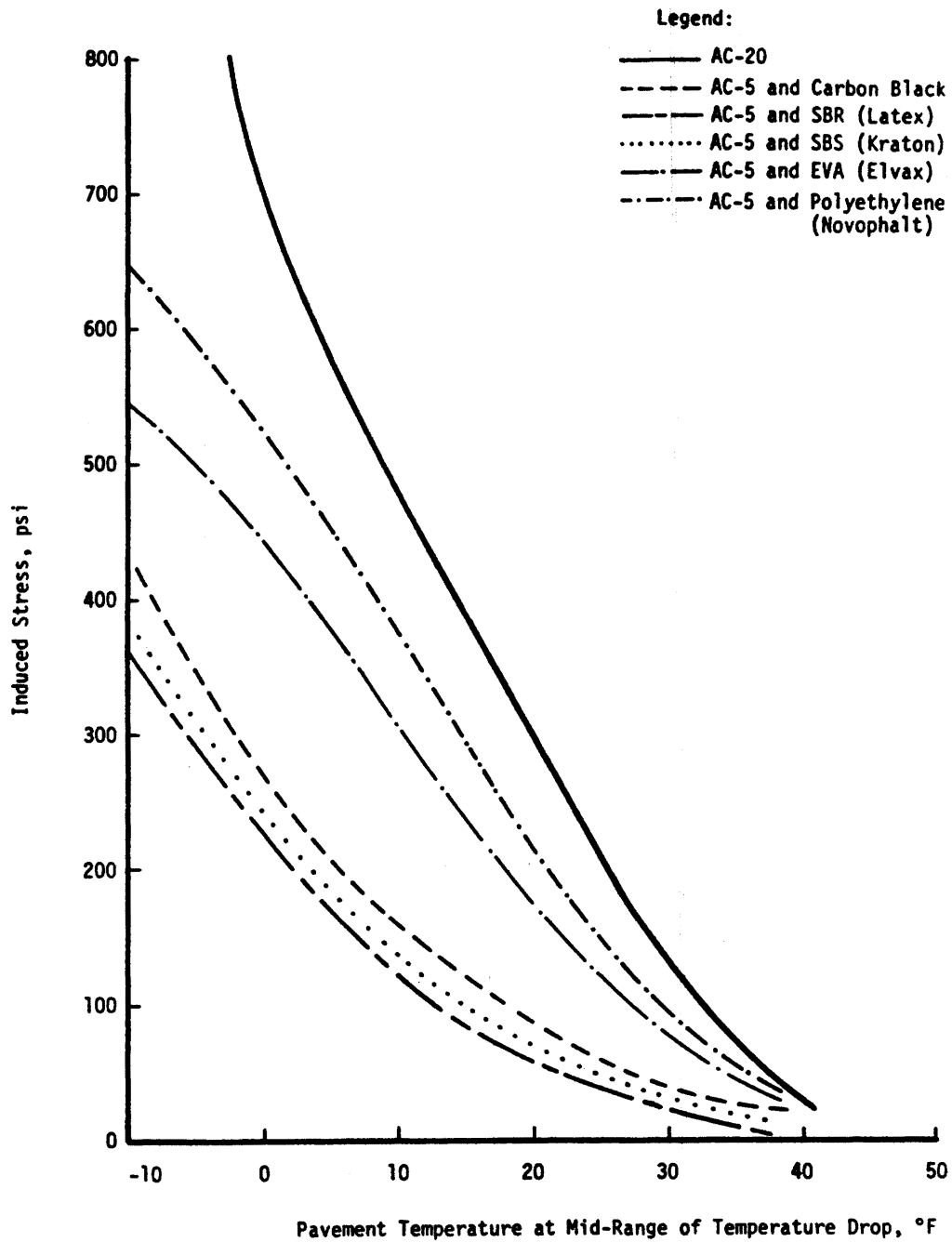


Figure 43. Induced stresses for modified Texaco asphalt mixtures.

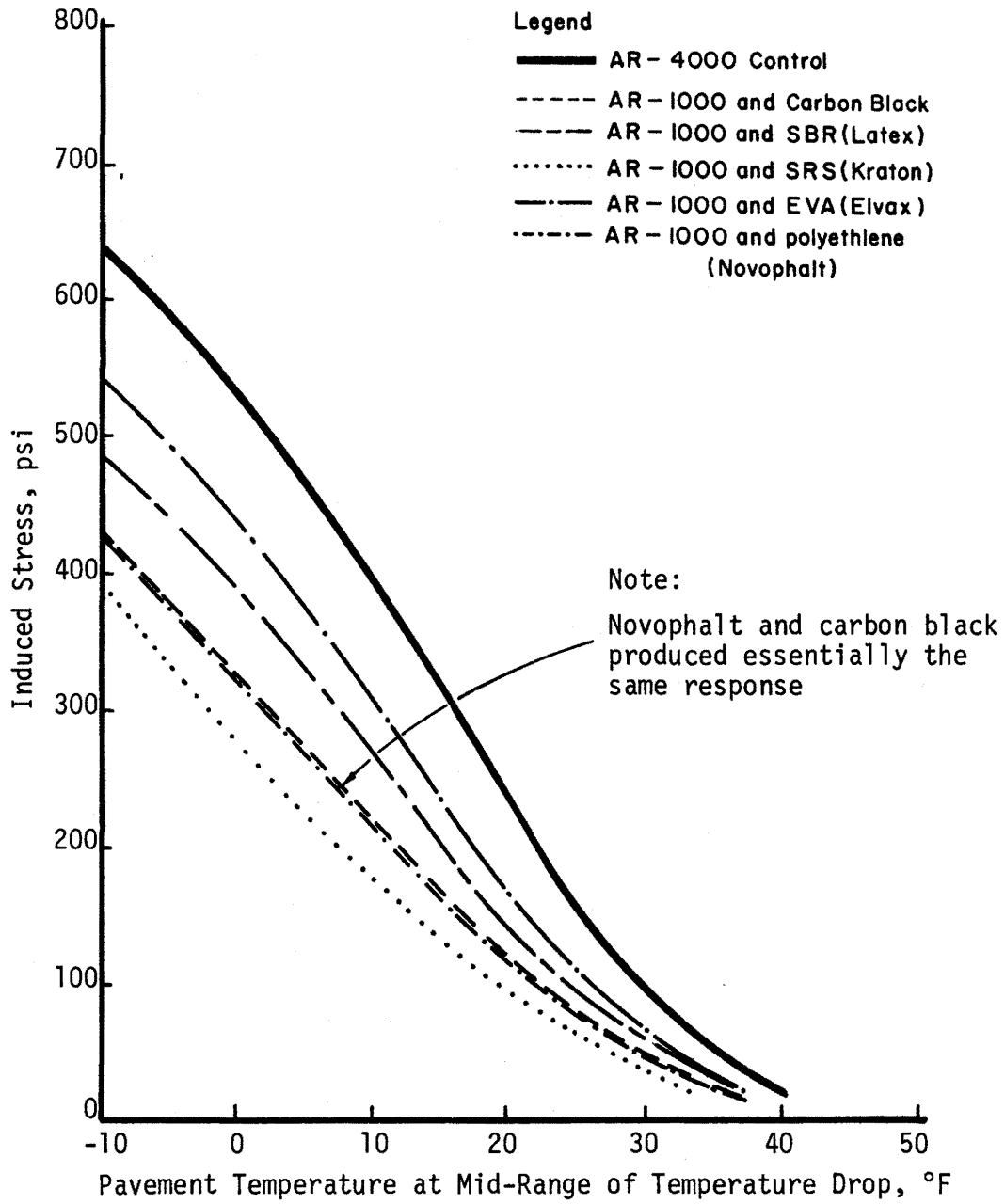


Figure 44. Induced stresses for modified California Valley asphalt mixtures.

2. The thermal cracking analysis based on the creep testing of mixtures revealed substantial differences in S_{mix} versus temperature relationships and in the resulting levels of induced stress. However, indirect tensile data, tables 40 through 43, indicate similar tensile strength versus temperature results among the mixtures. This underscores the importance of insuring relatively low levels of S_{mix} versus temperature for mixtures subjected to rapid thermal temperature drops.

3. The ability of the modifier to produce favorable S_{mix} versus temperature relationships is highly dependent upon asphalt-additive compatibility.

4. Acceptable low temperature performance is a function of the rheological properties of the base asphalt.

The authors believe that the results of the mixture analysis summarized in figures 43 and 44 deserve the most credibility as these are based on stiffnesses actually measured in creep compliance testing at loading rates which simulate those actually occurring in the field. These tests have the best chance of evaluating the response of the additive-modified asphalt; whereas, nomographic solutions based on physical properties of the bulk binder only may be biased as they do not account for aggregate effects and are based on empirical data for asphalt cement (unmodified). With this in mind, the general trend is that all additive-soft asphalt blends significantly reduce thermally induced stresses in the mixture. Polyethylene (Novophalt) appears to be quite susceptible to the base asphalt properties, showing a much more compliant nature with the California Valley asphalt than with the Texaco asphalt.

MODULUS PROPERTIES OF ASPHALT MIXTURES MODIFIED WITH ADDITIVES

1. General

The modulus properties of the materials which make up flexible pavement layers are an indispensable part of most up-to-date structural pavement design techniques. In fact, the most commonly used failure criteria in flexible pavement design are tensile strain in the stiffest layer and vertical compressive strain in the subgrade layer. These

criteria are extremely sensitive to the respective modulus properties of the pavement layers. Thus, the pavement engineer must not only seek an accurate estimate of the modulus but also the proper definition of modulus for the intended purpose.

Of course, viscoelastic materials such as asphalt concrete add another dimension of difficulty to the task of selecting the correct modulus. These materials have modulus properties which are affected by time (duration of loading) and temperature.

Van der Poel (45) has defined the modulus of asphalt cement as stiffness:

$$S(t,T) = \sigma / \epsilon \quad \text{Equation 38}$$

where t = time of loading and T = temperature.

Figure 45 is a simplified illustration of the time of loading dependency of idealized asphalt concrete at a selected temperature. It is easy to trace the change in behavior from an elastic response at short loading times, through a delayed elastic behavior zone and finally to a region where the stiffness is totally a function of the viscous properties of the binder. This representation is helpful in analyzing the creep stiffness data presented previously. Due to the time-temperature superposition of asphalt the abscissa in figure 45 could be changed to temperature if stiffness were measured at a selected duration of loading.

In this study the modulus properties of additive-modified asphalts were measured in the following forms:

1. Diametral resilient modulus, M_R .
2. Creep Stiffness.
3. Dynamic modulus, (measured on 4 in (102 mm) by 8 in (204 mm) cylinders).
4. Flexural modulus.

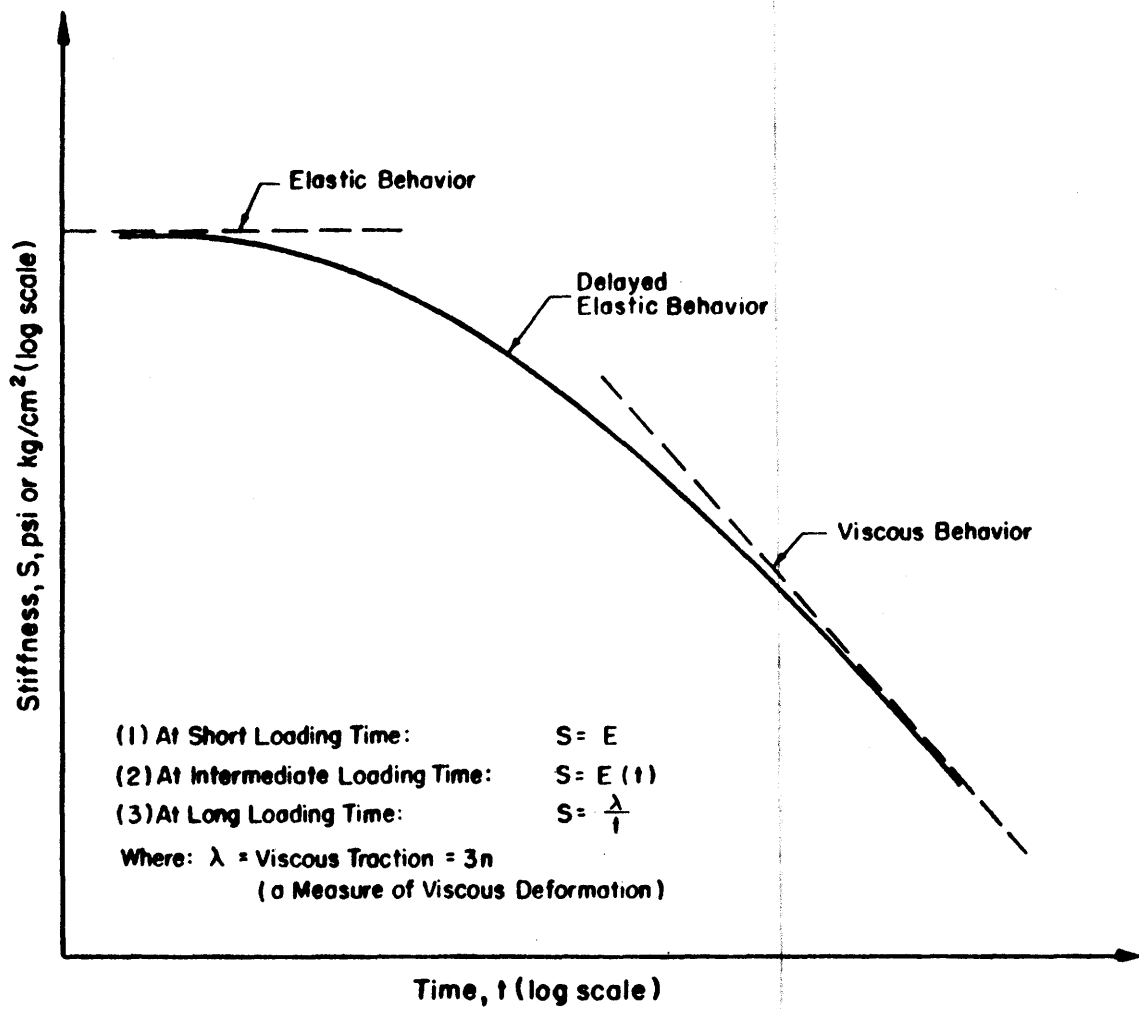


Figure 45. Simplified illustration of components of stiffness: elastic, viscoelastic, and viscous.

2. Resilient Modulus

The resilient moduli, defined as the ratio of induced stress to recoverable strain, were measured by the Mark III device developed by Schmidt (46). The device applies a 0.1-second load pulse once every three seconds across the vertical diameter of a cylindrical specimen (Marshall type specimen) and senses by linear variable transformers the resultant deformation across the horizontal diameter.

The resilient modulus was used throughout this research as a quality assurance measure. Resilient moduli data were recorded from aging studies, water susceptibility studies, and mixture design studies. The results of these data are reported under the section on mixture properties. All resilient modulus specimens were aged for six days at 50°F prior to testing. The 6-day cure period was selected based on an aging study which revealed that the resilient modulus does not appreciably change in the laboratory following six days of curing at 50°F (10°C).

3. Creep Stiffness

The diametral resilient modulus is often subjected to criticism because of the light load used, the conditions of biaxial stressing and the rigid assumptions which must be closely adhered to in order for the cylindrical, diametrically loaded specimen to respond elastically. In order to more precisely establish the modular properties of asphalt mixtures under different conditions of loading and different states of stress, other forms of moduli were computed.

Creep stiffness is simply the inverse of the creep compliance. For purposes of comparison creep stiffness was calculated at 0.1 seconds of load duration at 40°F (4°C), 70°F (21°C) and 100°F (38°C) during the compressive creep test. The resulting values are tabulated in tables 58 and 59, and appendix G.

As expected these moduli do not closely agree with the resilient moduli. However, the same trends are evident as were established with resilient moduli data.

4. Dynamic Modulus

The dynamic modulus is defined as the ratio of repeated stress applied in an unconfined compressive mode to recoverable elastic strain at the 200th load cycle. This test is performed on 4 in (102 mm) by 8 in (204 mm) cylinders as prescribed in the VESYS Manual (20).

The results of dynamic modulus testing for blends of additives with the Texaco asphalts at three temperatures (40 (4°C), 70 (21°C) and 100°F (38°C)) are presented in table 58.

5. Flexural Modulus

The flexural moduli are also presented in table E6, appendix E. The flexural modulus is defined as the modulus of the flexural fatigue beams at the 200th load application. The modulus is more clearly defined as

$$E_{flex.} = \frac{Pa(3\ell^2 - 4a^2)}{48I\Delta} \quad \text{Equation 39}$$

where P = dynamic load applied to deflect the beam (lb),
 a = $(\ell - 4)$ (inches),
 ℓ = reaction span length (in),
 I = specimen moment of inertia (in⁴) and
 Δ = dynamic beam deflection at the center point (in).

6. Discussion of Results of Modulus Testing

Table 58 summarizes the results of dynamic modulus, creep stiffness, resilient modulus and flexural modulus testing for mixtures prepared with Texaco asphalts.

Although the absolute modulus values differ substantially depending on the type of test, the general trend is that the AC-20 mixture is

Table 58. Summary of average dynamic moduli, creep stiffness (0.1 sec.) and resilient moduli from all mixtures fabricated with Texaco asphalt.

Binder	Dynamic Modulus $\text{psix}10^6$			Creep Stiffness $\text{psix}10^6$			Resilient Moduli $\text{psix}10^6$			Flexural Modulus $\text{psix}10^6$	
	40°F	70°F	100°F	40°F	70°F	100°F	40°F	70°F	100°F	34°F	68°F
AC-20	6.11	0.76	0.27	4.00	0.35	0.10	1.75	0.65	0.12	1.28	0.71
AC-5 and Carbon Black	2.54	0.48	0.19	1.42	0.14	0.075	0.90	0.16	0.040	0.97	0.22
AC-5 and EVA (Elvax)	1.96	0.39	0.06	1.81	0.50	0.050	1.10	0.30	0.055	0.99	0.08
AC-5 and SBS (Kraton)	2.13	0.60	0.13	1.33	0.20	0.080	1.20	0.35	0.060	0.91	0.09
AC-5 and SBR (Latex)	3.43	0.74	0.09	1.33	0.25	0.033	1.00	0.18	0.045	0.81	0.12
AC-5 and Polyethylene (Novophalt)	3.38	0.98	0.23	3.33	0.40	0.14	1.25	0.45	0.080	0.90	0.34

stiffest across the temperature range followed by AC-5 mixtures containing polyethylene (Novophalt). Mixtures containing AC-5 and SBS (Kraton), SBR (Latex) and EVA (Elvax) show somewhat similar trends.

At 100°F (38°C), representing a nominal high temperature range, the AC-20 control responds with the highest modulus (considering each type of modulus test) followed by the mixture containing AC-5 and polyethylene (Novophalt). Once again, mixtures containing blends of AC-5 and SBS, SBR, carbon black and EVA are not significantly different based on stiffness at 100°F.

At the nominal low temperature, 40°F (4°C), the results are similar. Once again, the AC-20 control produces the lowest average modulus based on each test type (i.e., diametral, creep and resilient modulus) and the AC-5 polyethylene (Novophalt) blend ranks as second stiffest. There are no significant differences among the other responses.

Although no clearly defined advantages are established for any additive based on these data, the polyethylene (Novophalt) appears to be most beneficial in reducing temperature susceptibility. This is, of course, the beneficial claim of most polymer and/or filler-type additives.

Table 59 summarizes the results of modulus testing for modified California Valley asphalts. The results of the diametral resilient modulus testing are graphically presented in figure 6 of Chapter IV. Based on these results, polyethylene, carbon black and latex all show similar (statistically no difference) effects in improving the temperature susceptibility of the base asphalt (AR-1000). Kraton was slightly, though statistically significantly, less effective. Elvax responded statistically the same as the AR-1000, i.e., no stiffening at the higher temperatures.

Based on creep stiffnesses at a loading time of 0.1 seconds, the AR-4000 control was stiffest by a factor of about 2.5 over the AR-1000 blends with either carbon black, Elvax or Novophalt. The control mixture was 4.5 times stiffer than the Kraton blend and about 60 percent stiffer than the latex blend.

At a loading time of 1000 seconds, the AR-4000 control was essentially the same as AR-1000 blends with either carbon black, Elvax or

Table 59. Summary of resilient moduli and creep stiffnesses (0.1 sec - 1000 sec) for all mixtures fabricated with California Valley asphalt.

Binder	Resilient Modulus, psi x 10 ⁶			Creep Stiffness, psi x 10 ⁶	
	40°F	70°F	100°F	0.1 sec Loading	1000 sec Loading
AR- 4000	1.75	0.80	0.12	0.80	0.014
AR-1000	0.80	0.20	0.02	—	—
AR-1000 and Carbon Black	1.20	0.38	0.07	0.27	0.018
AR-1000 and EVA (Elvax)	0.80	0.20	0.02	0.30	0.013
AR-1000 and SBS (Kraton)	1.00	0.32	0.04	0.18	0.008
AR-1000 and SBR (Latex)	0.95	0.31	0.05	0.53	0.012
AR-1000 and Polyethylene (Novophalt)	1.20	0.40	0.07	0.27	0.009

latex. Blends of AR-1000 and both Kraton and Novophalt were substantially softer. The softness of the AR-1000 and Novophalt blend appears to be a function of asphalt-polymer compatibility.

CHAPTER V

STRUCTURAL EVALUATION

GENERAL

The objective of the structural evaluation phase is to compare the predicted structural performances of the modified asphalt concrete mixtures and of the control mixtures. The VESYS IV computer model (20) was used for the structural analysis. The VESYS model was selected as it provides the ability to evaluate the structural pavement response to repeated loads as well as to static loads (response is a function of the viscoelastic effects).

The request for proposals for this contract also required the development of load equivalencies by which to judge relative performance. Layer equivalencies as well as AASHTO structural coefficient will be presented in this section together with a discussion of their development.

VESYS ANALYSIS

The VESYS model is a probabilistic procedure which uses the following inputs along with their variabilities for computational analysis:

1. Traffic
2. System Geometry
3. Environment
4. Material Properties
5. System Properties
6. System Performance Bounds.

Using these values, the computer program determines the pavement response to a defined wheel load. These responses, are then used as inputs in the calculation of three damage indicators: rut depth, roughness, and cracking. These distress mechanisms are components of the AASHTO equation which predicts pavement performance on the basis of Present Serviceability Index (PSI). When used as a design tool, the

values of rut depth, roughness, cracking, and PSI are compared to allowable criteria. In this case, these results were used to compare the predicted performance of asphalt concrete modified with the additives selected for evaluation in this study.

TRAFFIC

VESYS provides several inputs that describe the expected traffic. They are traffic level, load intensity, configuration, and duration.

SYSTEM GEOMETRY

The pavement cross-sections to be evaluated in the VESYS IV analysis were selected with the aid of a pavement structural subsystem, FPS-BISTRO.

As its name implies, this system is a combination of the Flexible Pavement System (FPS-13) used by the Texas State Department of Highways and Public Transportation (47) and BISTRO, a linear elastic structural analysis program developed by Shell. Initially, trial designs for the materials under consideration were evaluated on the basis of Present Serviceability Index.

The Present Serviceability Index (PSI) is based upon a rating scale that designates the condition of the pavement at any time. A rating of 5.0 indicates a "perfect" pavement; whereas, a rating of 0 indicates an "impassible" pavement. The concept of PSI was developed at the AASHTO Road Test. Here it was found that new pavements had an average PSI of 4.2. Terminal serviceability index is the PSI of a pavement when riding quality has dropped to a certain minimum acceptable level. Values typically used for terminal serviceability indices are 2.0 and 2.5. Serviceability loss over time has been defined by Scrivner (48) as a function of surface curvature index, temperature and the number of 18-kip (80 KN) single-axle loads. Using data from the AASHTO Road Test, Scrivner developed the following relationship:

$$P = 5 - \left(\sqrt{5 - P_1} + 53.6 \frac{NS^2}{\alpha} \right)^2$$

Equation 40

where P is the serviceability index at time t ,
 P_1 is the initial serviceability index immediately after construction or after an overlay,
 N is the total number of 18-kip equivalent single axle loads, in millions, applied during a period for which S is relatively constant,
 $\bar{\alpha}$ is the harmonic mean of daily temperature values above 32°F (0°C), and
 S is the surface curvature index, defined as the difference in deflections of geophones 1 and 2 of the Dynaflect.

Obviously, serviceability loss increases with increased load repetitions, N , and increased surface deflection as reflected by S , and is affected by temperature as accounted for by $\bar{\alpha}$. The effect of $\bar{\alpha}$ on serviceability loss is partially accounted for by an increased susceptibility to fatigue cracking at lower temperatures as well as increased susceptibility to deformation at higher temperatures.

The PSI deteriorates with time (and load repetitions) to a terminal serviceability thereby resulting in the need for an overlay. Program inputs allow for specific values of initial and terminal PSI and minimum time to first overlay. Designs meeting serviceability requirements are then checked against structural failure criteria. The failure criteria include the following:

1. Flexural fatigue at the bottom of the surface course,
2. Permanent deformation at mid-depth of the granular base course,
3. Flexural fatigue at the bottom of stabilized base layers and
4. Permanent deformation at top of subgrade.

A detailed discussion of the above failure criteria may be found in reference 48.

As a result of the FPS-BISTRO screening analysis, the pavement systems presented in table 60 were selected for the detailed VESYS IV analysis. The thicknesses of the asphalt concrete surfaces were selected based on actual laboratory data input from characterization of mixtures using river gravel. The river gravel mixtures resulted in relatively soft mixtures necessitating relatively thick surface layers in order to produce acceptable stress levels within the pavement as evaluated by failure criteria traditionally used in layered elastic evaluations.

Table 60. Summary of pavement geometrics established by FPS-BISTRO for VESYS pavement evaluation.

-
-
- Category 1: Full depth asphalt concrete (AC) pavement with AC layers 8 in., 10 in. and 12.5 in. thick. Subgrade of moderate strength characterized by a stiffness modulus of 30,000 psi.
- Category 2: Conventional pavement system with an AC thickness of 6 in. over a 12 in. base of crushed stone with a stiffness of 40,000 psi. Subgrade of moderate strength characterized by a stiffness modulus of 15,000 psi.
- Category 3: Full depth asphalt concrete (AC) pavement with AC layer of 12.5 in. over weak subgrade characterized by a stiffness modulus of 10,000 psi.
-
-

ENVIRONMENT

The major environmental influences on pavement response are temperature and moisture. Two climatic regions representing a warm climate typical of the southwestern United States and a cool climate typical of the upper mid-west were evaluated in this study. The average monthly air temperatures of these climates are presented in table 61. The pavement analysis system VESYS IV allows one to account for the effects of temperature on the response of the viscoelastic asphalt concrete layer in a variety of ways. In this analysis, dynamic stiffnesses associated with the specific temperature period were used.

The parameters used to predict load associated cracking, K_1 and K_2 , (from phenomenological fatigue curves) and those used to compute accumulated permanent deformation, ALPHA and GNU, are greatly affected by temperature. To account for these effects K_1 , K_2 , ALPHA and GNU values were input for each monthly temperature. The values of ALPHA and GNU were determined at 40, 70 and 100°F (4, 21, and 38°C) for each material and, therefore, values at intermediate temperatures could be approximated by interpolation. Fatigue parameters K_1 and K_2 were determined at 34°F (1°C) and 68°F (20°C). The value of K_1 and K_2 at temperatures above 68°F were calculated using the model established by Rauhut, et. al. (37) which is assumed to be valid for additive-modified asphalts. Fatigue parameters K_1 and K_2 at temperatures between 68°F and 34°F were determined by interpolation. The values of K_1 and K_2 used in the VESYS analysis are presented in appendix E. Values of ALPHA and GNU used in VESYS are presented in appendix F.

The design wheel load was 1/2 of an 18-kip (80 KN) single axle. For an 80 psi (5.52×10^5 MPa) tire pressure, the contact radius of the load is 6-inches (152 mm). Since equivalent axle loads were used, the variance of the load amplitude was set at zero. Load duration, a function of vehicle speed and contact radius, has a tremendous impact on pavement response especially in viscoelastic materials. A value of 0.1 seconds was used to simulate traffic operating in the 55-60 mile-per-hour (88 to 97 Km/hr) speed range.

Table 61. Average monthly air temperatures for the cool and warm climates used in the structural analysis.

Month	Average Monthly Temperature, °F	
	Cool Climate	Warm Climate
January	10	41
February	13	43
March	16	45
April	35	60
May	50	75
June	56	87
July	63	93
August	65	95
September	61	91
October	57	87
November	34	64
December	22	59

The variance of the load duration was set at 0.52×10^{-5} seconds.

MATERIAL CHARACTERIZATION

The parameters used to characterize the pavement materials in VESYS IV are dynamic stiffnesses for each temperature period, ALPHA and GNU values for each temperature period (permanent deformation) and K_1 and K_2 fatigue parameters for each temperature period (flexural fatigue). The values used in this analysis are presented in appendices G, F and E for dynamic stiffness, ALPHA and GNU and K_1 and K_2 values, respectively.

Two pavement system properties are used in the computation of pavement roughness. The value of the correlation coefficient of the roughness model was set at 1.0 while the value of the exponent was 0.058.

SYSTEM PERFORMANCE BOUNDS

System performance bounds define acceptable limits of PSI and account for its variation. The initial serviceability index was chosen as 4.2 with a standard deviation of 0.20. The minimum acceptable level of serviceability was set at 2.5. The minimum acceptable reliability that the PSI was above the failure level was set at 70 percent.

VESYS STRUCTURAL SYSTEM

The structural analysis portion of VESYS IV uses the responses from the layered analysis as input into three damage models. These models are for rut depth, roughness and cracking.

Rut depth is the accumulation of permanent deformation with the increase in the number load applications. It is a function of the general moving load deflection response, the number of previous repetitions and the system permanent deformation properties.

Roughness of the pavement is measured by the slope variance of the pavement surface. Slope variance is actually the statistical variance of the longitudinal pavement elevation. It is a function of the magnitude

and variability of rut depth, the variation in the primary deflection response and system roughness properties.

The dimensionless cracking damage index is a measure of the amount of fatigue life remaining in the pavement. When this index reaches a value of 1.0, the surface pavement layer cracks at the bottom. The cracking damage index is a function of the number of load repetitions, the mean and variance of the general radial strain response at a given temperature and the mean and variance of the fatigue properties of the pavement.

Each of these distresses are calculated at certain specified intervals within the life of the pavement. Following each interval the distress parameters are input in the following AASHTO equation predicting PSI:

$$PSI' = PSI - 1.91 (\log(1+SV)) - 0.001 C - 1.38(RT)^2 \quad \text{Equation 41}$$

where PSI' is present serviceability index after a given number of load applications,
PSI is initial serviceability index,
SV is slope variance (millionth radians),
C is area cracked (sq. ft./1000 sq. ft.) and
RT is rut depth (in).

RESULTS OF VESYS ANALYSIS

Results of the VESYS IV Analysis for Category 1, full depth asphalt concrete pavements, are summarized in tables 62 through 65. Tables 62 through 64 present the results for full-depth asphalt concrete of 8, 10 and 12.5-inches over a moderately stiff subgrade (modulus = 30,000 psi) for both cool and warm climates. Table 65 is for the 12.5-inch full-depth construction over a soft subgrade (10,000 psi modulus). Table 66 presents the results of a conventional pavement where the asphalt concrete surface is either bound with the Texaco AC-20 control or an additive plus the Texaco AC-5. Both cool and warm climates are evaluated in the tables.

Table 62. Pavement performance summary from VESYS IV analysis for 8-inch full-depth asphalt concrete pavements over moderate strength subgrade in both cool and warm climates.

Binder	Performance Summary			
	Damage Index after 20 years	Percent Cracking after 20 years**	Rut Depth after 20 years	Years Required for PSI to Fall below 2.0
AC-20	11.86(3.55)*	100 after 6 yrs. (100)	1.48(2.21)	4-5(3-4)
AC-5 and Carbon Black	4.79(0.21)	100 after 15 yrs. (0)	2.34(2.54)	3-4(2-3)
AC-5 and EVA (Elvax)	0.02(0.005)	0(0)	0.63(0.69)	2.18 after 20 yrs.
AC-5 and SBS (Kraton)	0.09(0.02)	0(0)	1.28(1.64)	6-7(5-6)
AC-5 and SBR (Latex)	0.21(0.04)	0(0)	4.53(8.45)	1-2(<1)
AC-5 and Polyethylene (Novophalt)	2.39(0.03)	99(0)	1.01(1.18)	9-10(8-9)

*First value is for cool climate. The value in parentheses is for warm climate.

** Percent of wheel path area.

Table 63. Pavement performance summary from VESYS IV analysis for 10-inch full-depth asphalt concrete pavements over moderate strength subgrade in both cool and warm climates.

Binder	Performance Summary			
	Damage Index after 20 years	Percent Cracking after 20 years**	Rut Depth after 20 years	Years Required for PSI to Fall below 2.0
AC-20	5.40(1.23)*	100 after 13 yrs. (30)	1.21(1.82)	6-7(4-5)
AC-5 and Carbon Black	2.18(0.08)	96(0)	2.02(2.22)	3-4(3-4)
AC-5 and EVA (Elvax)	0.01(0.001)	0(0)	0.58(0.60)	2.4(2.3) both after 20 yrs.
AC-5 and SBS (Kraton)	0.04(0.004)	0(0)	1.16(1.40)	8-9(6-7)
AC-5 and SBR (Latex)	0.10(0.01)	0(0)	4.00(7.30)	1-2(<1)
AC-5 and Polyethylene (Novophalt)	0.91(0.01)	5.4(0)	0.90(1.01)	13-14(11-12)

*First value is for cool climate. The value in parentheses is for warm climate.

** Percent of wheel path area.

Table 64. Pavement performance summary from VESYS IV analysis for 12.5-inch full-depth asphalt concrete pavements over moderate strength subgrade in both cool and warm climates.

Binder	Performance Summary			
	Damage Index after 20 years	Percent Cracking after 20 years**	Rut Depth after 20 years	Years Required for PSI to Fall below 2.0
AC-20	2.26(0.40)*	97(0)	0.99(1.34)	10-11(6-7)
AC-5 and Carbon Black	0.88(0.03)	4(0)	1.65(1.79)	5-6(4-5)
AC-5 and EVA (Elvax)	0.002(0.0003)	0(0)	0.52(0.41)	2.57 after 20 yrs.(3.01 after 20 yrs.)
AC-5 and SBS (Kraton)	0.01(0.001)	0(0)	1.04(1.17)	10-11(8-9)
AC-5 and SBR (Latex)	0.04(0.004)	0(0)	3.44(6.07)	2-3(1-2)
AC-5 and Polyethylene (Novophalt)	0.03(0.003)	0(0)	0.77(0.71)	17-18(19-20)

*First value is for cool climate. The value in parentheses is for warm climate.

** Percent of wheel path area.

Table 65. Pavement performance summary from VESYS IV analysis for 12.5-inch full-depth asphalt concrete pavements over soft subgrade in warm climate.

Binder	Performance Summary			
	Damage Index after 20 years	Percent Cracking after 20 years*	Rut Depth after 20 years	Years Required for PSI to Fall below 2.0
AC-20	4.72	100 after 15 yrs.	1.87	3-4
AC-5 and Carbon Black	2.24	97	2.67	2-3
AC-5 and EVA (Elvax)	0.004	0	0.61	2.22 after 20 yrs.
AC-5 and SBS (Kraton)	0.04	0	1.64	3-4
AC-5 and SBR (Latex)	0.15	0	4.47	1-2
AC-5 and Polyethylene (Novophalt)	0.79	2	1.31	5-6

* Percent of wheel path area.

Table 66. Pavement performance summary from VESYS IV analysis for conventional asphalt concrete pavements (6 inches of AC over 12 inches of crushed stone base).

Binder	Performance Summary			
	Damage Index after 20 years	Percent Cracking after 20 years**	Rut Depth after 20 years	Years Required for PSI to Fall below 2.0
AC-20	10.88(7.75)*	100 after 7 yrs. (100 after 9 yrs.)	1.37(2.15)	6-7(3-4)
AC-5 and Carbon Black	2.70(0.24)	100(0.24)	1.94(2.09)	5-6(4-5)
AC-5 and EVA (Elvax)	0(0)	0(0)	0.54(0.61)	2.85 after >20 yrs. (2.50 after 20 yrs.)
AC-5 and SBS (Kraton)	0.05(0.02)	0(0)	0.98(1.33)	14-15(8-9)
AC-5 and SBR (Latex)	0.07(0.06)	0(0)	3.58(6.84)	2-3(1-2)
AC-5 and Polyethylene (Novophalt)	1.7(0.06)	76(0)	0.86(0.99)	15-16(12-13)

*First value is for cool climate. The value in parentheses is for warm climate.

** Percent of wheel path area.

In every case, the aggregate is the river gravel described in appendix D. The resulting mixtures are generally quite susceptible to rutting due to the relatively low level of internal friction developed within the aggregate matrix. Obviously, such a system is highly sensitive to binder properties. It was for this reason that the river gravel system was selected.

The traffic level for each pavement system is representative of a moderately heavily traveled State highway with 445-18 kip (80 KN) single axle load equivalents per day or 3,248,500-18 kip single axle load equivalents in a 20 year life. The traffic was assumed to be uniformly distributed on both a daily and seasonal basis.

Based on the results tabulated in tables 62 through 66 the following trends are presented.

1. For every pavement category and for each climate and for each condition within a pavement category, the predicted fatigue life of the pavements containing the asphalt-additives were significantly superior to the control mixture containing AC-20. These results are quantified in columns two and three of tables 62 through 66.

2. The blend of AC-5 and EVA (Elvax 150) produced the mixtures with the best fatigue performance in every case.

3. The predicted fatigue performance of mixtures containing SBS (Kraton TR60-8774) and SBR (Ultrapave Latex) were not significantly different and were a close second to the EVA modified mixtures. In general, mixtures modified with polyethylene (Novophalt) were significantly more susceptible to fatigue cracking than mixtures containing the copolymers EVA, SBS or SBR. However, the polyethylene modified mixtures performed substantially superior to the carbon black modified mixtures.

4. The river gravel aggregate makes each mixture highly susceptible to permanent deformation. However, based on the rut depth prediction (column four of tables 62 through 66), the relative abilities of the additives to resist permanent deformation are, from least susceptible to rutting to most susceptible to rutting:

- (a) AC-5 and EVA (Elvax)
- (b) AC-5 and Polyethylene (Novophalt)
- (c) AC-5 and SBS (Kraton)
- (d) AC-20 Control
- (e) AC-5 and Carbon Black
- (f) AC-5 and SBR

5. The AASHTO present serviceability (PSI) equation is highly sensitive to roughness or slope variance and rutting (depth of ruts in the wheel path). The PSI is not greatly sensitive to cracking. Column five in tables 62 through 66 shows the period of time required for the PSI to fall below 2.0. To maintain a high level of serviceability, a pavement layer must successfully distribute vertical compressive stresses, so that they are not capable of damaging subsequent layers, and resist deformation through the mobilization shear resistance. Based on the PSI serviceability function, the binders are rated from best to poorest as follows:

- (a) AC-5 and EVA (Elvax)
- (b) AC-5 and polyethylene (Novophalt)
- (c) AC-5 and SBS (Kraton)
- (d) AC-20
- (e) AC-5 and carbon black
- (f) AC-5 and SBR (latex)

VESYS analyses for the California Valley asphalts were not performed as flexural fatigue testing was not accomplished for mixtures containing California Valley asphalts.

AASHTO STRUCTURAL COEFFICIENTS

1. General

Clearly the development of realistic AASHTO structural layer coefficients is a formidable task. In the first place, these empirical coefficients which are the results of the AASHTO factorial experiments vary across a wide range. Secondly, the AASHTO Interim Guide (49), which is the design manual for the AASHTO pavement design method, provides no

guidance for selecting structural coefficients for materials different from those used in the Road Test.

In order to estimate AASHTO structural coefficients, a method must be developed which (1) is linked to the original AASHTO factorial experiments in terms of a performance related concept of pavement evaluation and (2) is based on some rational means of pavement evaluation.

The fundamental serviceability-performance equation developed at the AASHTO Road Test is the the basis for developing structural coefficients.

$$\log N = \log \rho + \frac{G}{\beta} \quad \text{Equation 42}$$

where N = number of load repetitions,

ρ and β = functions of load type, load magnitude and pavement structure and

G = a damage function marked by loss in serviceability.

The structural coefficients developed for the AASHTO factorial experiments are used to develop the structural number, SN, which is in turn used to compute ρ and β . For a given type of loading at the Road Study the performance of the pavement section was influenced solely by the structural number,

$$SN = a_1 D_1 + a_2 D_2 + a_3 D_3, \quad \text{Equation 43}$$

where D_1, D_2, D_3 = layer thickness and

a_1, a_2, a_3 = layer structural coefficients of the asphalt concrete surface, granular base and subbase respectively.

The problem of establishing realistic structural coefficients becomes even more perplexing when one considers the sensitivity of the performance equation to the surface and base structural coefficients. This is clearly illustrated in terms of the a_2 by Darter and Devos (50). Darter and Devos used the special base study of the Road Test to estimate structural coefficients of the bituminous bases. This was done by comparing the performance of the various bases to the standard crushed

stone base whose a_2 was established at 0.14. Based on this analysis, the range of practical significance in a_2 for the various bases was 0.11 to 0.35. Darter and Devos evaluated the effects on the performance life of low volume roads of this range of a_2 values. The variation in performance life for one selected cross section was from less than one to well in excess of 20 years. A similar analysis was performed over a realistic variation in a_1 values due to seasonal and temperature changes as determined by Van Til, et. al. (51). This analysis revealed a comparable sensitivity of the performance equation to a_1 values ranging from 0.30 to 0.50. Thus, it is evident that the method selected to determine a_j 's must be sensitive and well thought out.

2. Criteria for Establishing Structural Coefficients

It is necessary to select a response from within the pavement structure to use as a basis of comparison when establishing structural coefficients. Three responses are generally considered in structural pavement analysis: (1) surface deflection, (2) maximum tensile strain in the bottom of the asphalt concrete and (3) vertical compressive strain.

Each of these responses was carefully evaluated as to its ability to estimate serviceability. Although the use of any one or all of the responses in establishing comparative criteria may be justified, the response of vertical deformation at the top of the subgrade was selected for the comparative analysis for several reasons. First, vertical subgrade deformation is directly correlated with performance, particularly in terms of riding quality. This point was verified by Jung and Phang (52) who studied the performance of pavement design in Ontario. Jung and Phang used layered elastic theory to arrive at stresses, strains and deformation within the pavement structure in hopes of establishing a distress mechanism that would provide a practical design criterion. Through this process of testing different cases, it was finally discovered that only the vertical deformation on the top of the subgrade emerged as the parameter which could be made to remain constant for a certain level of performance within each traffic or load class. This

discovery pointed in the same direction as the results of previous research on the Brampton Road Test (46).

Second, vertical subgrade deformation has been shown by layered elastic theory to correlate well with performance loss in the AASHO Road Test. In fact, it has been shown to correlate better than maximum tensile strain in the bottom of the surface asphalt concrete layer.

Third, the AASHTO equation for serviceability, was developed statistically as a means to correlate the present serviceability rating, PSR (a subjective performance rating from 0 to 5, where 0 is impassible and 5 is perfect), to physical pavement distress parameters. Obviously, the serviceability is primarily sensitive to slope variance and is relatively quite insensitive to cracking, patching and rut depth. Mechanically, the criterion most closely related to slope variance is vertical subgrade deformation.

3. Approach

Little and Epps (53) developed AASHTO structural coefficients for recycled pavement materials. They modeled the AASHO Road Test sections using stress sensitive layered elastic method and determined the resulting subgrade deformation which Little showed to be highly correlated to the serviceability history of the pavements as illustrated by the following relationship.

$$N_{18(2.5)} = 0.098 e^{-3.39 \ln W_s} \quad \text{Equation 44}$$

where $N_{18(2.5)}$ is the number of 18 kip single axle loads to reduce the pavement serviceability to 2.5 and

W_s is subgrade deformation.

Little and Epps (53) used the above relationship together with the layered elastic analysis to determine W_s for various combinations of pavement layers in Loop 4 of the AASHTO Test Road. The effect of substituting a recycled layer for the asphalt concrete surface actually used at the Road Test was evaluated by substituting the stiffness versus

temperature relationship of the recycled layer for that of the control in the layered analysis to compute W_s and then predict $N_{18(2.5)}$.

Then the traditional AASHTO performance equation, based on structural number, was used to predict the structural coefficient, a_j , by allowing a_j to vary until the number of design axle loads as predicted by the W_s relationship could be matched.

This approach was also considered for use in predicting structural coefficients for the modified mixtures in this study. However, as this approach depends only on stiffness it does not directly account for permanent deformation or fatigue-cracking potential.

The method selected to develop the AASHTO structural coefficient employed the results of the VESYS IV structural analysis. The VESYS IV analysis predicts the changes in serviceability in the form of the present serviceability index (PSI) over the life of the pavements.

The methodology for predicting the structural coefficients using the VESYS IV output was as follows. First, VESYS IV was used to predict the number of 18 kip (80 KN) single axle equivalents to lower the PSI to 2.0 for the specific pavement geometric and climatic conditions in question. In the VESYS IV model, the PSI is predicted using the regression model developed from Road Test data (equation 41).

Second, the general AASHTO Road Test performance equation (equation 42) was used to predict the structural coefficient of the asphalt concrete surface, a_1 , which yields the same number of 18 kip single axle applications as predicted by VESYS IV to achieve a $PSI = 2.0$. This methodology is based on the weighted parameters of slope variance, permanent deformation and fatigue cracking. The relative importance of each parameter is based on equation 41.

4. Results of AASHTO Structural Coefficient Analysis

AASHTO structural coefficients were evaluated for the structural and climatic conditions presented in table 67. Based on the results of table 67, the following observations are presented:

1. As suggested in the introductory section, structural coefficients are not material properties and hence their values are dramatically

Table 67. AASHTO structural coefficients computed from results of the VESYS IV analysis.

Binder	Structural Coefficients				
	Full Depth Pavement			Conventional Pavement (3-layer)	
	8 in.	10 in.	12.5 in.	Warm Climate	Cool Climate
AC-20	0.40	0.31	0.28	0.22	0.28
AC-5 and Carbon Black	0.37	0.30	0.26	0.24	0.25
AC-5 and EVA (Elvax)	0.50	0.40	0.34	0.41	0.46
AC-5 and SBS (Kraton)	0.42	0.35	0.28	0.30	0.34
AC-5 and SBR (Latex)	0.34	0.29	0.22	0.14	0.20
AC-5 and Polyethylene (Novophalt)	0.44	0.38	0.31	0.33	0.35

affected by pavement structural geometrics, loading conditions, temperatures and material selections for the surrounding layers.

2. The structural coefficients for modified Texaco asphalts blended with river gravel aggregate are relatively low (compared to the 0.44 average value determined at the Road Test for hot-mix asphalt concrete surfaces). This is expected due to the high rutting potential of mixtures prepared with this rounded aggregate with low internal friction and hence low shear resistance.

3. The substantial reduction in a_1 values due to AC layer thickness increases is due to the greater accumulation of permanent deformation in the thicker layers, increasing rut depths and reducing serviceability levels more rapidly.

4. The a_1 values reflect the same relative performances of the additives with the Texaco asphalt as previously discussed based on permanent deformation, roughness (slope variance) and present serviceability index. Since AASHTO structural coefficients are so heavily weighted to roughness (equation 41), it is not surprising that additives which improve high temperature stiffness and resist permanent deformation produce the highest structural coefficients. Thus the success of the additives in producing high a_1 values when mixed with the Texaco AC-5 are listed from most successful to least successful:

- (a) EVA (Elvax)
- (b) Polyethylene (Novophalt)
- (c) SBS (Kraton)
- (d) AC-20, control
- (e) Carbon black and
- (f) SBR (Latex).

One would, of course, expect different results for the modified California Valley asphalt mixtures based on characterization of their creep stiffness and resilient modulus versus temperature.

5. Structural coefficients, a_j 's, can be used in the AASHTO performance model to predict relative performance life. However, these values, like other AASHTO coefficients are not thickness equivalencies and should never be used as such.

6. The effects of aging were not evaluated in the analysis. These effects may be of considerable consequence and require further study.

THICKNESS EQUIVALENCY FACTORS

1. General

The use of thickness equivalency factors is discouraged for asphalt bound surface materials where rutting is a probability. The thickness equivalency concept assumes that a determined thickness of one material can be substituted for a unit thickness of the standard material and still provide an equivalent load distributing function. This function is simply to successfully distribute vertical compressive stresses and thus protect the vulnerable, underlying weaker layers (i.e., subgrade). Obviously, the concept disregards rutting in the asphalt layer but indirectly accounts for roughness induced by overstressing the weaker, underlying layers.

The concept of load-spreading capability assumes that stiffer layers distribute vertical stresses more effectively than softer layers through more efficient mobilization of shear stresses. A quick review of the partial differential equation of elastic equilibrium would demonstrate that a more efficient reduction in vertical stresses results in a greater mobilization of shear stresses. Thus, the layer equivalency concept assumes adequate shear resistance (resistance to permanent deformation) in all materials analyzed. This is not always a good assumption.

2. Determination of Thickness Equivalencies Based on Stiffness

The Odemark transformation has long been used to transform multiple layer pavements into an equivalent one layer system. The Odemark transformation is used as follows:

$$h_e = h_1 (E_1/E_s)^n + h_2 (E_2/E_s)^n + h_3 (E_3/E_s)^n \quad \text{Equation 45}$$

where h_e is the equivalent thickness of the upper three layers (1, 2 and 3) of elastic moduli E_1 , E_2 and E_3 in terms of the less stiff subgrade modulus, E_s . This technique has often been used to transform a layered system into a one layer system in which the one-layer Boussinesq solution can be used to evaluate stresses, strain and deformation at depth h_e . The value n in the Odemark transformation was suggested by Odemark to be 0.33. Further, Lytton (54), Alam and Little (55) have found that the value can indeed vary but that 0.33 is a very good approximation.

Thickness equivalency ratios were evaluated for the modified Texaco and California Valley asphalt mixtures based on the mixture stiffnesses at selected temperatures. At a selected temperature, the equivalency factor was derived as follows:

$$\text{Thickness Equivalency Ratios} = \sqrt[3]{\frac{E_i}{E_{\text{control}}}} \quad \text{Equation 46}$$

where E_i is the stiffness of the modified asphalt and E_{control} is the stiffness of the control asphalt.

Table 68 presents the equivalency ratios or factors based on diametral and axial resilient modulus testing. These values represent an approximation of the relative contribution to the material in question to the ability of a pavement layer to distribute vertical compressive stresses and hence limit subgrade deformation. In the case of the Texaco asphalts, the control is the AC-20 mixture. In the case of the California Valley asphalt, the AR-4000 mixture is the control. For example, in table 68, at 50°F (10°C) one inch of the AC-5 and carbon black mixture is equivalent to 0.80 inches of the AC-20 control mixture.

From table 68, the diametrally and axially determined resilient moduli produce different values, absolutely and relatively. Table 69 is a ranking of the ability of the additive blends to distribute vertical stresses. The ranking is from most effective to least effective.

Table 68. Thickness equivalency factors computed based on stiffness.

<u>Binder</u>	Thickness Equivalency Ratios Based on Resilient Modulus Determined by the					
	<u>Diametral Method</u>			<u>Axial Cylindrical Method</u>		
	50°F	60°F	70°F	50°F	60°F	70°F
TEXACO AC						
AC-20 (Control)	1.0	1.0	1.0	1.0	1.0	1.0
AC-5 and Carbon Black	0.80	0.70	0.67	0.80	0.82	0.86
AC-5 and EVA (Elvax)	0.85	0.78	0.81	0.96	0.98	0.98
AC-5 and SBS (Kraton)	0.88	0.83	0.85	0.84	0.88	0.92
AC-5 and SBR (Latex)	0.81	0.73	0.67	0.73	0.77	0.79
AC-5 and Polyethylene (Novophalt)	0.92	0.87	0.91	1.02	1.04	1.08
AC-5	0.81	0.73	0.71	--	--	--
CALIFORNIA VALLEY AC						
AR-4000	1.0	1.0	1.0	1.0	1.0	1.0
AR-1000 and Carbon Black	0.89	0.84	0.78	--	--	--
AR-1000 and EVA (Elvax)	0.82	0.67	0.63	--	--	--
AR-1000 and SBS (Kraton)	0.85	0.80	0.72	--	--	--
AR-1000 and SBR (Latex)	0.85	0.80	0.72	--	--	--
AR-1000 and Polyethylene (Novophalt)	0.89	0.84	0.78	--	--	--
AR-1000	0.82	0.67	0.63	--	--	--

Table 69. Relative ability of the various additives to distribute vertical stresses and protect the subgrade based on the equivalent thickness analysis.

Texaco asphalts		California Valley asphalts
Diametral	Axial	Diametral
AC-20	AC-5 and polyethylene (Novophalt)	AR-4000
AC-5 and polyethylene (Novophalt)	AC-20	AR-1000 and polyethylene (Novophalt)
AC-5 and SBS (Kraton)	AC-5 and EVA (Elvax) black	AR-1000 and carbon black
AC-5 and EVA (Elvax)	AC-5 and SBS (Kraton) (Kraton)	AR-1000 and SBS
AC-5 and SBR (latex)	AC-5 and carbon black (latex)	AR-1000 and SBR
AC-5 and carbon black	AC-5 and SBR (latex)	AR-1000 and EVA (Elvax)

MECHANO-LATTICE ANALYSIS

1. General

The mechano-lattice analysis was developed by W. O. Yandell (56) to analytically investigate non-elastic and sequence dependent constitutive properties of pavement materials. The solution technique enables simulation of translating loads for any Poisson's ratio and constitutive properties. This enables the manifestation of rolling resistance and non-symmetric stress patterns to be demonstrated.

Initial work with the mechano-lattice approach demonstrated the build up of residual horizontal stresses and permanent horizontal material movements in, for example, repeatedly rolled elasto-plastic pavement structures.

In 1979 the mechano-lattice technique was developed into the simulation of a three dimensional, multi-layered, elasto-plastic pavement repeatedly transversed by a rolling wheel load.

The mechano-lattice analysis uses a finite element system consisting of 28 links. Stiffness factors of the links are calculated on the assumption that the element simulates an equal-sized cube of homogenous elastic material with a particular Young's Modulus and Poisson's ratio. With a fixed Young's Modulus used for calculating stiffness factors of each link, one can use an assembly of the elements to simulate a linear elastic material. But when the Young's Modulus used for calculating the load-deflection behavior of each link is made a function of the load itself or, of the sense of loading in that link, non-linear and elasto-plastic behavior can be simulated. The unloading modulus is a calculation expedient and allows elasto-plasticity to be simulated.

The computer program performs a complex task after each load cycle. A length-load calculation is made in which the forces at each joint emanating from their attached links are resolved into vertical, longitudinal and lateral components. The joint is then moved in a damped manner in the direction of the unbalanced forces. The process is continued until all out of balance forces on free joints become insignificant. After convergence and after stresses have been

calculated, the element in the residual condition is used as the initial condition for the next simulated wheel pass, and the process is repeated. The foregoing techniques can be used to simulate the behavior of elastic perfectly plastic and non-plastic energy absorbing material.

2. MATERIAL CHARACTERIZATION

Concisely stated, the mechano-lattice approach simulates translating loads on a three dimensional pavement structure for any Poisson's ratio and constitutive equations. It can simulate repeated rolling action of a tire on an elasto-plastic pavement. Residual stresses and strains are calculated and both rutting and flexural fatigue are evaluated considering the effects of residual stresses.

A series of laboratory tests are required to characterize the elasto-plastic properties of the different pavement layers. These tests include:

1. Poisson's ratio,
2. Elastic modulus or resilient modulus and
3. Repeated load triaxial creep test.

These properties are determined for each pavement layer.

3. PAVEMENT SIMULATION

The pavement simulated in this analysis consists of four-inches of asphalt concrete, twelve-inches of crushed limestone base and a stiff clay subgrade. The repeated load creep and stiffness values for the base and subgrade layers are identical to those used in the VESYS analysis for these materials. The mechano-lattice approach computes deformation within each layer of the system.

The simulated pavement was subjected to a 9000 pound single wheel load. Load applications were repeated sequentially until one million cycles were simulated.

The asphalt concrete investigated in the analysis consisted of AC-20 and river gravel and AC-5 (modified with either polyethylene, latex, SBS or EVA) and river gravel. The repeated load deformation properties used

in this analysis are presented in Chapter IV and the resilient moduli used materials are presented in table 58.

4. MECHANO-LATTICE RESULTS

Table 70 summarizes the results of the mechano-lattice analysis. The rutting predictions show that deformation potential is significantly less for the AC-5 modified asphalt than for the AC-20 control mixture for the two pavement temperatures analyzed. The first pavement temperature is 70°F (21°C); the second is 100°F (38°F).

A flexural fatigue cracking analysis was performed at 70°F (21°C). The results indicate that flexural fatigue occurs not due to transient tensile flexural stresses but due to residual tensile flexural stresses. Transient tensile flexural stresses are traditionally used together with phenomenological fatigue acceptance criteria such as that shown in figure 15 to predict fatigue cracking. However, the effects of residual stresses due to sequential loading cannot be accounted for in traditional procedures, i.e., layered elastic or quasi-viscoelastic (VESYS). The mechano-lattice approach demonstrates that in each case residual tensile flexural stresses at the top of the pavement induce flexural fatigue cracking. Residual stresses prestress the bottom of the pavement layer directly under the wheel load. Since the effect of these residual stresses cumulatively builds, the transient stresses at the bottom of the pavement and directly under the wheel load decrease due to increased prestressing and residual stresses (tension) at the top of the pavement increase, leading to cracking at the top.

The relatively long fatigue lives of the AC-5 modified materials (compared to the AC-20 control mixtures) are due to an interaction of favorable fatigue behavior, figures 15 and 16, and the compliant nature of the material.

Mechano-lattice analyses were not performed at 32°F (0°C) due to the lack of repeated load deformation data at this low temperature. However, one would predict that the impressive fatigue test results, figure 16, together with the more compliant nature of the AC-5 modified asphalts at

Table 70. Summary of mechano-lattice analysis of modified Texaco
asphalts.

Straight Edge Rutting in Inches

<u>Temp., °F</u>	<u>AC-20</u>	<u>AC-5 & PE</u>	<u>AC-5 & CB</u>	<u>AC-5 & EVA</u>	<u>AC-5 & SBS</u>
70	0.260	0.072	0.059	0.062	0.080
100	0.270	0.158	0.160	0.135	0.270

Fatigue Cracking (70°F)

<u>Parameter</u>	<u>AC-20</u>	<u>AC-5 & PE</u>	<u>AC-5 & CB</u>	<u>AC-5 & EVA</u>	<u>AC-5 & SBS</u>
Transient Stress, psi, at Failure	1.25×10^{-5}	1.8×10^{-5}	1.5×10^{-5}	1.6×10^{-5}	5.0×10^{-5}
Residual Stress, psi, at Failure	2.0×10^{-4}	1.2×10^{-4}	1.0×10^{-4}	3.0×10^{-4}	2.5×10^{-4}
Mode of Failure	cracking at top	cracking at top	cracking at top	cracking at top	cracking at top
Load Application to Failure, 18 Kip Equivalent	30,000	400,000	500,000	4,000,000	1,500,000

Note: 1 psi = 6894 Pa
1 in = 25.4 mm
1°C = 5/9 (°F-32)

32⁰F than the AC-20 control would lead to superior relative lives for the modified AC-5 mixtures.

CHAPTER VI

EVALUATION AND IMPLEMENTATION OF RESULTS

MIXTURE DESIGN AND CHARACTERIZATION

1. General

The current state of the art in mixture design very possibly does not afford the sensitivity necessary to optimize binder content when additive modified asphalts are used. Currently used mixture design concepts, such as Marshall, Hveem and the Texas Method (a version of the Hveem procedure), base optimum binder content on volumetric considerations (i.e., VMA, air voids, voids filled with asphalt, etc.) and stability measurements. However, no true material properties are determined such as elastic modulus, relaxation modulus, tensile strength, compressive strength, etc. It is necessary that fundamental material properties be determined in order to realistically approximate performance.

Fortunately, concerted efforts (Sponsored by the National Cooperative Highway Research Program and by the Texas State Department of Highways) are underway to develop mixture design/analysis schemes which will provide material properties and hence a more fundamentally based link to predicted performance. These new procedures will most certainly not abandon the basic volumetric concepts necessary to insure durability (impermeability) and stability (enough air voids to prevent plastic flow and/or flushing). The new techniques will complement the basic concepts by providing the potential to assess the effects of small variations in binder content on the various performance phases of the asphalt concrete. Since the critical link is the inability of the plant to produce mixtures within the tolerance levels shown to be optimal, perhaps the greatest benefit from the new techniques will be their ability to analyze and compare potential additives for specific applications.

Based on the results of this study and the nature of the additives studied, the authors applaud the aggressive move to develop more fundamentally based and sensitive mixture design concepts. Asphalt

additives, especially the additives studied here, polymers and a microfiller, alter the temperature-time sensitivity of the asphalt cement and, in turn, the asphalt concrete. This alteration in temperature-time sensitivity alters the behavior of the binder in various climatic and traffic conditions. To take full advantage of this altered binder behavior, it is necessary to design the mixture as precisely as possible, accounting for the traffic and climatic conditions to which it will be subjected. Once again, the practical limitation is that mix plants cannot achieve the tolerance levels which may be identified by more sophisticated mixture design techniques. However, the improved testing techniques can offer a guide in determining what level of time-temperature sensitivity is acceptable for specific traffic and climatic conditions and for the mixture production tolerance levels associated with the mix plant to be used.

The authors believe that the sensitivity of additive-modified asphalt mixtures to selected climatic and traffic conditions is exemplified in this study. For example, the SBS (Kraton) and SBR (Latex) additives which performed well in resisting controlled strain fatigue but relatively poorly in terms of resisting permanent deformation (at least with the river gravel aggregate used in this study), may perform very well as designed in a cool climate but may require a slightly lower binder content (4.5 percent in lieu of 5.0 percent) or better designed aggregate to perform acceptably in a warmer climate. This, of course, assumes that acceptable void content parameters can be achieved over the suggested range in binder contents. In the case of the mixtures containing latex and Kraton, acceptable void contents were achieved over the binder content range of 4.5 to 5.0 percent. While it may be misleading to rank performance of additive-modified mixtures where binder contents were selected solely by traditional mix design methods, the practical limitations of production will no doubt dictate that traditional mixture limits based on void contents and volumetric considerations be used. The goal is then to select the best additive for the specific situation with the understanding that design criteria limitations exist and that these limitations are based on practical

production tolerances. With this in mind, several tests have proved worthwhile in this study as material characterization techniques. The results of these tests were ultimately used to predict pavement performance. These tests include:

<u>Test</u>	<u>Purpose</u>
Creep Compliance	Characterize deformation (total, recoverable and irrecoverable) under a constant stress level as a function of temperature and time of loading. Predict rutting and fracture potential.
Permanent Deformation	Characterize the permanent accumulated strain as a function of time of loading or number of loading repetitions and temperature. Predict rutting potential.
Resilient Modulus (axial compressive and diametral)	Characterize the load distributing capability of the mixture under moving wheel loads as a function of temperature. Predict development of fatigue cracking and roughness.
Flexural (controlled stress) beam fatigue and controlled strain fatigue	Predict resistance to load-induced fatigue cracking.
Indirect tensile tests	Predict resistance to thermal fracture.

Based on the results of this study, the authors believe that the creep compliance test, diametral resilient modulus test versus temperature, indirect tension test and perhaps repeated load permanent deformation testing provide the most reliable and valuable materials testing for mixture design and evaluation.

2. Suggested Mixture Design/Evaluation Approach

a. Initial Mixture Design

The initial step in mixture design must include a procedure which effectively accounts for the fundamental concepts of void content and stability. Currently used methods, Marshall and Hveem, are acceptable.

The concepts of determining proper mixing and compaction temperatures must be accounted for in the initial mixture design as discussed in this section. The initial design procedure will probably be the only method used to insure adequate mixture stability. The authors recommend the Marshall Stability test as it is more sensitive to binder characteristics.

b. Resistance to Permanent Deformation

The resistance of a mixture to excessive deformation is due as much to aggregate as to deficiencies in binder content or binder rheology. The effects of the binder (content and binder rheology) as well as the aggregate type and gradation can be effectively assessed by the creep compliance test, as has been demonstrated in this study.

Compliance testing for 1000 seconds at 40, 70 and 100°F (4, 21 and 38°C) should provide the data necessary to evaluate relative effects of binder content on deformation potential and stiffness at long load durations which can be directly related to thermally induced stresses and/or fracture potential.

Acceptance and/or rejection criteria for permanent deformation can be established by using the rather simple Shell procedure (57) which predicts the amount of permanent deformation as a function of the material property, mixture stiffness. The technique used to determine mixture stiffness as a function of duration of loading or number of loading cycles and temperature is explained in (57).

The creep modulus can also effectively be used to predict relative acceptability of modified asphalt mixtures to thermally induced fracture. This is based on the concept that the stiffness modulus of the mixture is directly related to the level of stress induced in the pavement through thermal cycling. The objective would be to design a mixture which would provide the lowest acceptable mixture stiffness at the design temperature (duration of load). The lowest acceptable mixture stiffness may be defined from creep compliance data as the level of mixture stiffness (reciprocal of compliance) that will not induce

excessive thermal stresses for the environmental conditions in question and yet will provide adequate resistance to permanent deformation.

c. Diametral Resilient Modulus

The diametral resilient modulus, such as developed by Schmidt, is of acceptable accuracy to account for relative binder variations. The diametral test should be performed over a range of temperature of at least 40⁰F (4⁰C) to 100⁰F (38⁰C). Achieving an acceptable level of resilient modulus over the temperature range defined will allow one to select the mixture design with the greatest reliability against flexural fatigue cracking and overstressing the weaker base, subbase and subgrade materials.

A procedure developed by Little (58) predicts acceptable levels of resilient modulus versus temperature necessary to resist overstressing underlying layers and to resist flexural fatigue cracking.

d. Indirect Tensile Test (IDT)

The indirect tensile strength of asphalt mixtures at long loading durations (i.e., 0.02 in/min, 0.51 mm/min, stroke rate) and at low temperatures can be compared to induced stresses due to thermal variations to evaluate the relative susceptibility of mixtures to thermal cracking. This procedure is discussed in the section on "Evaluation of Thermal Cracking Potential," Chapter IV.

e. Additive Evaluation/Selection

The procedure suggested to actually evaluate an additive or select a particular additive from a list of candidates is outlined below.

Step 1: Screen the candidate additives based on the penetration viscosity numbers (PVN's). The tests required to determine PVN's will be performed on blends of additives and asphalts recommended by the manufacturer. The additives producing

the most favorable PVN's for the specific climatic region in question will be selected for mixture evaluation.

Step 2: Use traditional mixture design techniques to identify the optimum or target voids and binder content. The authors suggest the Marshall method because of its sensitivity to binder properties.

Step 3: Fabricate traditional sized (Hveem or Marshall size) specimens for diametral resilient modulus testing over a temperature range of from 0°F (-18°C) to 100°F (38°C). Specimens should be fabricated over a range of binder contents and air void contents which reflects those expected based on the mix plant tolerances. The acceptance criterion (explained previously) should be developed for specific pavement structures, climates and traffic conditions.

Step 4: The diametral resilient modulus specimens fabricated in Step 3 and tested nondestructively should now be tested in indirect tension at 0°F (-18°C) and 32°F (0°C) as a minimum to determine the tensile strength of the mixtures.

Step 5: Creep compliance, diametral resilient modulus and indirect tensile tests should be performed over the range of void contents and binder contents dictated by the target design values and the tolerance ranges expected in plant production. These results must be evaluated against acceptance criteria in order to either select the best additive for the specific traffic, pavement structure and climatic conditions or the predict expected performance levels for the additive selected.

The development of acceptance criteria is beyond the scope of this report. However, the general methodology has either been presented or referenced.

METHODS OF ADDITION

Methods of incorporating the additives into asphalt were not specifically addressed in this study. Contacts with highway department and contractor personnel indicate that the preferred method is to combine the asphalt and additive(s) prior to arrival at the mix plant site. This would provide good dispersion of the additive and would not interrupt normal mixing plant operations. It should be pointed out that tank trucks have no positive agitation capability and certain additives, such as polyethylene and carbon black, may separate from the asphalt during hot storage. Therefore, preblending may not always be possible.

Felsing, Inc. the supplier of Novophalt, has developed a high shear blending apparatus capable of modifying asphalt at the plant site without delaying plant operations. If storage of modified asphalt is necessary, the apparatus is furnished with an integral surge tank which is equipped for remixing as required.

During the course of this work, a private company (59) has developed a proprietary dispersing agent for carbon black which holds it in suspension in hot asphalt for periods up to 2 weeks. Two field trials have been installed in Texas (17) using preblended carbon black with drum plants in 3-inch hot mix asphalt concrete pavements.

Latex (70 percent SBR and 30 percent water) is often added in drum mix plants just downstream from the asphalt inlet or in batch plants shortly after the addition of the asphalt and a brief mixing period. In either case, the relatively small quantity of water is flashed away without consequence (apparently). Additional work is being performed at Texas A&M University to investigate differences in mixing efficiency when the latex is added in the plant or preblended with the asphalt cement.

Prolonged hot storage of modified asphalts can cause degradation of quality other than physical separation of the asphalt and the additive. Laboratory tests and field experience has shown that block copolymers (SBS) and latex (SBR) will "breakdown" and exhibit a significant decrease in viscosity upon prolonged hot storage or exposure to excessive heat. These "reactions" are without doubt dependent upon the chemical composition of the additive as well as the asphalt. Additional study

will be required to define safe limits for storage periods and temperatures. Additive manufacturers should provide this information to their customers.

MIXING AND COMPACTION TEMPERATURES

According to the Asphalt Institute (TAI), there are certain binder viscosities that should be used for optimum mixing (170 centistokes) and compaction (280 centistokes) of asphalt concrete mixtures. All of the additives addressed in this study produce a significant increase in the 150°C (300°F) viscosity of the original asphalt. Even when a softer-than-usual grade of asphalt is used with the additive, the 150°C viscosity of the blend may be greater than that of the usual grade asphalt. Therefore, in order to assure suitable mixing and adequate compaction time, it may be necessary to increase the plant temperature. Field experience with the additives studied herein has shown that the increase in temperature is necessary to achieve good compaction (17); however, optimum mixing and compaction temperatures are not simply a function of the viscosity of the binder when asphalt additives are used. These optimum temperatures need to be determined. Viscosity-temperature data for these modified binders can be used as a guide; but, apparently, only field experience can be used to make final decisions.

SPECIAL REQUIREMENTS ASSOCIATED WITH ADDITIVES

The use of specific additives under certain circumstances presents special needs regarding equipment and logistics. Most refineries or asphalt distributors are not presently equipped to properly mix additives into their asphalt products. Therefore, when an additive is specified, special processing is necessary either at the asphalt distribution point or at the mix plant site.

When carbon black is used in conjunction with a batch plant, preweighed polyethylene bags are introduced directly into the pug mill. The polyethylene melts and the carbon black is dispersed into the mix. However, when a drum mix plant is employed, the carbon black must be

preblended with the asphalt cement or "blown" into the drum just downstream from the asphalt inlet. Preblended carbon black in hot-stored asphalt will "settle out" (specific gravity of carbon black is 1.7) if not treated with special dispersing agents (17). Blowing of the carbon black into the drum plant requires special conveying and metering equipment; and there is a high probability of losing much of the carbon black in the stack gases.

Styrene-butadiene rubber (latex) can either be preblended with asphalt or added in the plant. Addition of latex in a plant (drum mix or batch) is usually accomplished after addition of the asphalt. In either case, special equipment is necessary to measure and transfer the latex. At least one highway district in Texas requires the addition of latex after introduction of the asphalt and initial coating of the aggregate when porous aggregates are used. This is an attempt to avoid loss in effectiveness of the relatively expensive additive by minimizing the quantity of latex that is absorbed into the aggregate.

Obviously, preblending of additives in asphalt will minimize changes in mix plant operations. However, this blending operation, whether at the refinery or asphalt the distribution point, requires special equipment. If the asphalt producer does not have blending capabilities, special arrangements must be made which could involve shipment of the asphalt to a blending facility before final shipment to the plant site.

APPROXIMATE COSTS FOR ADDITIVES

Costs of the additives examined herein are influenced by the cost of crude oil as is the cost of asphalt cement. Currently, the price for the polymers ranges from 0.80 to 1.00 dollars per pound and for the carbon black, about 0.50 dollars per pound. This translates into a cost increase of about 4.00 to 9.00 dollars per ton of hot mixed asphalt concrete, depending on the dosage of the additive. Based on an in-place cost of 35.00 dollars per ton of hot mixed asphalt concrete, the additives would increase the paving cost by about 10 to 25 percent. In other words, assuming an average pavement life of 15 years, an additive would need to increase pavement life by 2 to 4 years to be cost effective

or decrease maintenance costs accordingly. Based on the laboratory test results reported herein, the polymer and microfiller additives studied can be reasonably expected to provide cost effective pavement performance.

CHAPTER VII

CONCLUSIONS AND RECOMMENDATIONS

CONCLUSIONS

Preliminary work on this research study included an extensive review of published data on a host of asphalt additives and admixtures. Those additives offering the most promise in reducing both cracking (normally associated with temperature less than 70⁰F) and rutting (normally associated with temperatures above 90⁰F) appeared to be those capable of lowering the temperature susceptibility of the binder. Typically, a softer than usual asphalt is used with these additives. The soft asphalt provides flexibility at the lower temperatures and the additive increases the viscosity at higher temperatures to reduce the potential for permanent deformation. From both costs and physical properties standpoints, certain types of polymers and carbon black appeared to be the most promising. Five additives were selected and evaluated in a logical sequence of laboratory tests. The effects of these additives on rheological and physicochemical properties of asphalt cement and on mixture stability, stiffness, tensile properties, and resistance to fatigue and thermal cracking, plastic deformation and moisture damage were assessed. These data were used with predictive computer models to estimate the effects of the additives on pavement performance parameters such as cracking, rutting, and roughness. Based on results of these tests and review of the available literature on asphalt additives, the following conclusions and recommendations are offered.

1. Traditional mixture design procedures, such as the Marshall, Hveem and Texas methods are acceptable for determining target binder contents for asphalt mixtures. However, small variations in binder content such as those associated with mix plant tolerance limitations may cause significant variations in mixture performance. These variations for modified mixtures may well be greater than for traditional, unmodified mixtures. Identification of the ranges in performance affected by small variations in binder content and/or void contents

should be identified by mixture characterization. Development of a characterization procedure is part of this study and is summarized in Chapter VI.

2. Each additive studied demonstrated the ability to substantially alter the temperature susceptibility of asphalt concrete mixtures. The degree of alteration is highly dependent upon the chemical composition of the asphalt cement.

3. The ability of additives to alter the mechanical properties of asphalt concrete is reflected in the predicted performance of the pavement systems which incorporate modified asphalt concrete layers. Although each additive tested showed a potential to reduce temperature susceptibility of the base asphalt, no additive appeared to be a panacea. The task of selecting the best additive for a specific combination of climatic, pavement structure and traffic condition is formidable.

4. Although certain binder and mixture properties appeared to be sensitive to compatibility between the asphalt and the additives, overall, the mixture properties demonstrated an ability for each additive to alter temperature susceptibility in a generally favorable manner.

5. Flexural fatigue response at 68°F (20°C) of mixtures containing AC-5 plus an additive was superior to the control mixture which contained AC-20 with no additive. Accelerated aging of test specimens containing additives resulted in a significant decrease in fatigue life; the control specimens, however, exhibited better fatigue properties after aging.

6. Controlled displacement fatigue testing at 34°F (1°C) demonstrated that mixtures containing AC-5 plus an additive gave better resistance to crack propagation than control mixtures containing AC-20. The "solubilized" additives, EVA, SBR and SBS, showed evidence of improving the distribution of tensile stresses within the mixture. Practically, this could result in retarding crack propagation as manifested by resistance to cracking in asphalt concrete overlays.

7. In a limited study of crack healing, the mixtures containing the soft asphalt (AC-5) plus an additive gave better responses than those containing the control asphalt (AC-20). The practical significance of

improved healing potential could be substantially improved flexural fatigue lives of asphalt concrete pavements.

8. Creep/permanent deformation testing showed that, at high temperatures, all the additives except latex produced equal or better performance than the AC-20 control mixture. (The binder content of the latex mixture was apparently in excess of the true optimum.) At low temperature, all the additives in AC-5 except polyethylene produced equal or better performance than the AC-20 control mixture.

9. Indirect tension test results showed that, at the lower temperatures and higher loading rates, the additives increased mixture tensile strength over that of the control mixtures. Elongation to failure was generally increased by the additives. This is indicative of improved resistance to traffic induced cracking at low temperatures. At the higher temperatures and lower loading rates, the additives did not appreciably affect the mixture tensile properties as measured by the indirect tension test.

10. The additives increased Marshall stability of mixtures when added to AC-5 (or AR-1000) but not up to that of mixtures containing AC-20 (or AR-4000) with no additive. This should not discourage the use of these additives with asphalts softer than the usual paving grade, particularly if low temperature cracking is a concern.

11. Hveem stability of mixtures was not significantly altered by the additives. Although Hveem stability is quite sensitive to changes in binder quantity, it is not very sensitive to changes in rheological properties of the binder properties.

12. At low temperatures (less than 32⁰F or 0⁰C), the additives had little effect on consistency of the asphalt cements. This was reflected in the diametral resilient moduli (stiffness) of the mixtures. Resilient moduli of AC-5 (or AR-1000) mixtures above 60⁰F (16⁰C) were generally increased by the additives but not up to that of the AC-20 (or AR-4000) mixtures without additives. Although the load spreading ability of asphalt concrete containing a soft asphalt is increased when these additives are employed, the pavement thickness should not be reduced.

13. The additives had little effect on moisture susceptibility of the mixtures made using the materials included in this study.

14. Standard asphalt extraction methods to determine binder content of paving mixtures are unsuitable when polymers or carbon black are used as these materials are insoluble or only partly soluble in standard solvents.

15. Long term aging characteristics of modified binders are substantially different, physically but not chemically, from the unmodified asphalts. Short term aging characteristics, as measured by standard tests, do not manifest an appreciable difference.

16. The five additives studied were selected because of their potential to reduce rutting and cracking. Each additive proved to be successful to some degree in improving properties on at least one end of the performance spectrum. However, no additive proved to be a panacea. Thus, the need for an additive selection procedure based on traffic conditions, pavement structure and climatic conditions is again emphasized. To rank the additives according to relative capabilities is a difficult task as sensitivity to the base asphalt played a significant role. In general, the most effective additives in reducing rutting were EVA, polyethylene and SBS (Kraton) for the Texaco (AC-5) asphalt. For the California Valley asphalt carbon black, polyethylene, and EVA performed most effectively and without significant difference. In terms of reduction of flexural fatigue cracking the most successful additives were, in order, EVA, SBS (Kraton) and SBR (latex) and polyethylene which demonstrated essentially equal performance.

RECOMMENDATIONS

1. Future research efforts to evaluate asphalt additives should include a segment to investigate the long-term effects of compatibility with asphalt cement. This study showed no appreciable problem associated with compatibility and short-term mixture properties, however, long-term mixture properties were not evaluated. Since noncompatible products do not form a homogeneous blend, the two phases of the binder may age differently and have deleterious effects upon a pavement structure.

Evidence of potential long-term aging problems were indicated during the binder study.

2. Satisfactory methods for extracting modified binders from paving mixtures should be developed. A suitable procedure is necessary for quality assurance regarding binder and additive contents.

REFERENCES

1. Anderson, D. I., Wiley, M. L., Force-Ductility An Asphalt Performance Indicator, AAPT, Vol. 45, 1976.
2. Benson, J. R., Tentative Standard Method of Test for Toughness and Tenacity of Rubberized Asphalts, Bituminous Consultants, Denver, Colorado, February, 1955.
3. Young, F. D., Deme, I., Burgess, R. A. and Kopvillem, D., St. Anne Test Road-Construction Summary and Performance After Two Years Service, Proceeding CTAA, 1969.
4. Burgess, Kopvillem, R.A. and Young, F. D., St. Anne Test Road-Relationship Between Predicted Fracture Temperature and Low Temperature Field Performance, Proceeding AAPT, 1971.
5. Kandhal, P. S., Low Temperature Shrinkage Cracking of Pavements in Pennsylvania, Proceedings AAPT, 1978.
6. Hills, J. F., Predicting the Fracture of Asphalt Mixes by Thermal Stresses, Journal Institute Petroleum, 1974.
7. Sor, K., Laboratory Testing of Solar Laglugel Treated Asphalt Mixes, Report Number 82-5031, Shime1 and Sor Testing Laboratories, Inc., East Hanover, New Jersey, September 23, 1982.
8. Petersen, J. C., Quantitative Method Using Differential Infrared Spectrometry for the Determination of Compound Types Absorbing in the Carbonyl Region in Asphalts, Analytical Chemistry, 47, 112 (1975).
9. Petersen, J. C. and Plancher, H., Quantitative Determination of Carboxylic Acids and Their Salts and Anhydrides in Asphalts by Selective Chemical Reactions and Differential Infrared Spectrometry, Analytical Chemistry, 53, 786 (1981).
10. Petersen, J. C., Quantitative Functional Group Analysis of Asphalts Using Differential Infrared Spectrometry and Selective Chemical Reactions - Theory and Application, Prepared for presentation at the 65th Annual Meeting, Transportation Research Board, Washington, D.C., January 13-17, 1986, and subsequent publication.
11. Schmidt, R. J., Laboratory Measurement of the Durability of Paving Asphalts, ASTM-Special Technical Publication No. 532, 79, (1973).
12. Rush, S. G., Theory of Liquid Viscosity, Chem. Rev., 62, 513, (1962).
13. Hershfelder, J. D., Curtiss, C. F. and Bird, R. B., Molecular Theory of Gases and Liquids, John Wiley and Sons, Inc., 1954, p. 625.

14. Moavenzadeh, F. and Stander, R. R., On Flow of Asphalt, Highway Research Record, No. 178, Washington, D.C., (1967).
15. Nadkarni, V. M., Shenoy, A. V. and Mathew, J., Thermomechanical Behavior of Modified Asphalts, Ind. Eng. Chem. Prod. Res. Div., 24, 478, (1985).
16. Gietz, R. H., Mineral Fines Effect on Asphalt Viscosity, Materials Office Report 164, Washington State Department of Transportation, Olympia, Washington, April 1980.
17. Button, J.W. Little, D. N., Asphalt Additives for Increased Pavement Flexibility, Report 471-1F, Texas Transportation Institute, Texas A&M University, November 1986.
18. Lottman, R.P., Laboratory Test Method for Predicting Moisture-Induced Damage to Asphalt Concrete, Transportation Research Record 843, Transportation Research Board, National Research Council, Washington, D.C., 1982.
19. Epps, J. A. and Monismith, C. L., Fatigue of Asphalt Concrete Mixtures - Summary of Existing Information, Fatigue of Compacted Bituminous Aggregate Mixtures, American Society for Testing and Materials, Special Technical Publication No. 508, 1972.
20. Kenis, W. J., Predictive Design Procedures, VESYS Users Manual, Report No. FHWA-RD-77-154, January 1978.
21. Button, J. W., Epps, J. A., and Gallaway, B. M., Tests Results on Laboratory Standard Asphalt, Aggregate and Mixtures, Research Brief No. 1, Materials Division, Texas Transportation Institute, Texas A&M University, January 1977.
22. Button, J. W., Epps, J. A., Little, D. N., and Gallaway, B. M., Influence of Asphalt Temperature Susceptibility on Pavement Construction and Performance, NCHRP Report 268, National Cooperative Highway Research Program, Transportation Research Board, December, 1983.
23. Majidzadeh, K., Kauffman and Sarat, C., Analysis of Fatigue of Paving Mixtures from a Fracture Mechanics Viewpoint, ASTM Special Technical Publication No. 508, 1972.
24. Majidzadeh, K. and Ramsamooj, D., Applications of Fracture Mechanics for Improved Design of Bituminous Concrete, FHWA Report FHWA-RD-76-91, June 1976.
25. Germann, P. F. and Lytton, R. L., Methodology for Predicting the Reflection Cracking Life of Asphalt Concrete Overlays, Report No. TT-2-8-75-207-5, Texas Transportation Institute, College Station, Texas, 1977.

26. Irwin, G. R., Analysis of Stresses and Strains Near the Tip of a Crack Transversing a Plate, Transaction of ASME, Journal of Applied Mechanics, Volume 24, 1957.
27. Rice, J. R. and Johnson, M. A., The Role of Large Crack Tip Geometry Changes in Plane Strain Fracture, Inelastic Behavior of Solids, Kanninen Ed., McGraw Hill, 1970.
28. Lytton, R. L. and Jayawickrama, P., Reinforcing Grids for Asphalt Overlays, Texas Transportation Institute, Texas A&M University, February, 1985.
29. Schapery, R. A., A Theory of Crack Growth in Visco-Elastic Media, Report MM 2764-73-1, Mechanics and Materials Research Center, Texas A&M University, 1973.
30. Van Dijk, W., Practical Fatigue Characterization of Bituminous Mixes, Proceedings Association of Asphalt Paving Technologists, Volume 44, 1975.
31. Finn, F. N., Factors Involved in the Design of Asphaltic Pavement Surfaces, NCHRP Report 39, 1982.
32. Santucci, L. E., Thickness Design Procedure for Asphalt and Emulsified Asphalt Mixes, Proceedings of Fourth International Conference Structural Design of Asphalt Pavements, University of Michigan, 1977, p. 434.
33. Pickett, D. E., et. al., Extension and Replacement of Asphalt Cement by Sulfur, Report FHWA-RD-78-95, March 1978.
34. Little, D. N., Balbissi, A. H., Gregory, C. and Richey, B., "Engineering Characterization of Sulphlex Binder," FHWA Report FHWA/RD-85/032, March 1986.
35. Pickett, D. L. and Lytton, R. L., "Laboratory Evaluation of Selected Fabrics for Reinforcement of Asphalt Concrete Overlays," Report No. TTI-2-8-80-261-1, Texas Transportation Institute, College Station, Texas, 1983.
36. Jud, K., Kausch, H. H. and Williams, J.G., "Fracture Mechanics Studies of Crack Healing and Welding of Polymers," Journal of Materials Science, Volume 16, No. 1, pp. 204-210, 1981.
37. Rauhut, J. B. and Kennedy, T. W., "Characterizing Fatigue Life for Asphalt Concrete Pavements," Paper Presented to Transportation Research Board, Washington, D.C., 1983.

38. Shahin, Mohamed, Y. and Frank McCullough, B., "Prediction of Low-Temperature and Thermal-Fatigue Cracking in Flexible Pavements," Research Report No. 123-14, Highway Design Division Texas Highway Department, Texas Transportation Institute, Texas A&M University, Center for Highway Research, The University of Texas at Austin, August 1972, 225 p.
39. Lytton, R. L. and Shanmugham, Ulpala., "Analysis and Design of Pavements to Resist Thermal Cracking Using Fracture Mechanics," Proceedings of Fifth International Conference - Structural Design of Asphalt Pavements, Delft, 1982.
40. Barber, E. S., "Calculation of Maximum Pavement Temperature from Weather Reports," Highway Research Board Bulletin 168, Washington, D.C., 1957, pp. 1-8.
41. Finn, F. N., "Factors Involved in the Design of Asphaltic Pavement Surfaces," NCHRP Report No. 39, 1967.
42. McLeod, N. W., "Reduction in Transverse Pavement Cracking by Use of Softer Asphalt Cements," Highway Research Board Western Meeting, Denver, Colorado, 1968.
43. Saal, R. N. J., "Physical Properties of Asphaltic Bitumen; Surface Phenomena, Thermal and Electrical Properties, Etc.," Properties of Asphaltic Bitumen, Elsevier, 1950.
44. Monismith, C. L., Secor, G. A. and Secor, K. R., "Temperature-Induced Stresses and Deformation in Asphalt Concrete," Proceedings, Association of Asphalt Paving Technologists, 1965.
45. Van de Poel, C., "A General System Describing the Viscoelastic Properties of Bitumens and the Relation to Routine Test Data," Shell Bitumen Reprint No. 9, Shell Laboratorium - Koninklijke, 1954.
46. Schmidt, R. J., "Laboratory Measurement of the Durability of Paving Asphalts," ASTM-Special Technical Publication No. 532, 79, 1973.
47. Scrivner, F. H., Moore, W. M., McFarland, W. F. and Carey, G. R., "A Systems Approach to the Flexible Pavement Design Problem," Research Report 32-11, Texas Transportation Institute, 1968.
48. Scrivner, F. H. and McFarland, W. F., "Texas Tries a Flexible Pavement Design System," Texas Transportation Research, Volume 6, No. 3, July 1970.
49. American Association of State Highway Officials, AASHTO Interim Guide for Design of Pavement Structures-1972, Washington, D.C., 1972.

50. Darter, M. I. and Devos, A. J., "Structural Analysis of Asphaltic Cold Mixtures Used in Pavement Bases," FHWA-IL-UI-171, Department of Civil Engineering, University of Illinois, Urbana, Illinois, August 1977.
51. Van Til, C. J., et. al., "Evaluation of AASHO Interim Guides for Design of Pavement Structures," National Cooperative Highway Research Program Report 128, Washington, D.C., 1972.
52. Jung, F. W. and Phang, W. A., "Elastic Layer Analysis Related to Performance in Flexible Pavement Design," Engineering Research and Development Branch, Research and Development Division, Ministry of Transportation and Communication, Ontario, Canada (March 1974).
53. Little, D. L. and Epps, J. A., "Certain Structural Characteristics of Recycled Pavement Materials," AAPT, Vol. 49, 1980.
54. Lytton, R. L. and Michalak, C. H., "Flexible Pavement Deflection Equation Using Elastic Moduli and Field Measurements," Research Report 207-7F, Texas Transportation Institute, 1979.
55. Alam, S. M., Little, D. N. and Ledbetter, W. B., "Evaluation of Flyash Test Sites Using a Simplified Elastic Theory Model and Field Measurements," Research Report 240-47, Texas Transportation Institute, 1984.
56. Yandell, W.O., "The Prediction of Behavior of Elasto-Plastic Roads During Rolling Using the Mechano-Lattice Analogy and Results of Cyclic Load Materials Tests", Highway Research Record No. 374, 1971.
57. "Developments of Asphalt Aggregate Mixture Analysis System," NCHRP Project 9-6(1), Request for Proposals, January 1986.
58. Little, D. N. and Mahboub, K., "Improved Asphalt Concrete Mixture Design/Analysis System for Texas - Interim Report," Submitted to Texas State Department of Highways and Public Transportation, July 1986.
59. Unpublished data from Mono-Chem Corporation, Atlanta, Texas, 1984.

APPENDIX A: PENETRATION-VISCOSITY DATA AND PHOTOMICROGRAPHS
FOR ASPHALT-ADDITIVE BLENDS

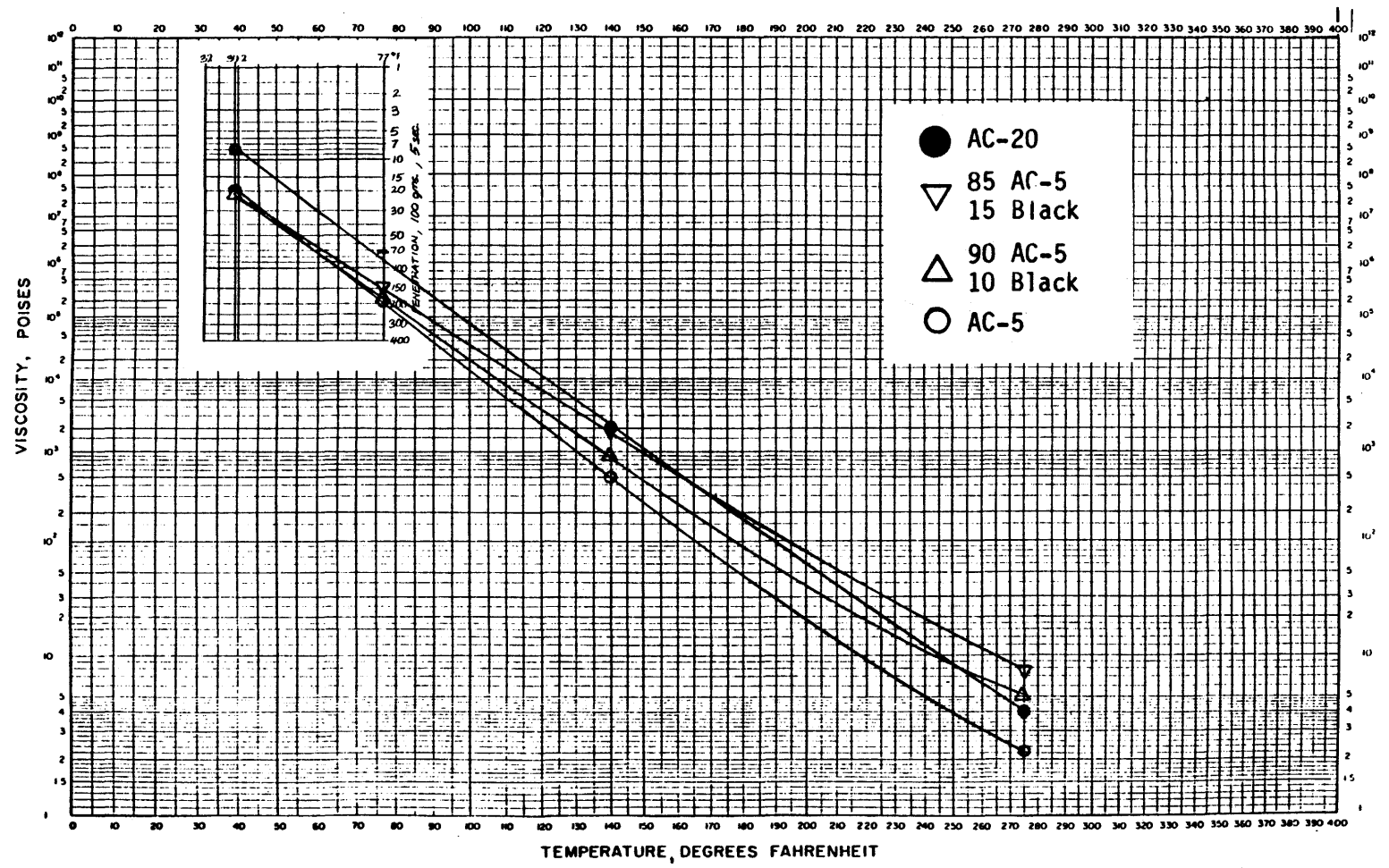


Figure A1. Blends of Texaco AC-5 and Microfil 8.

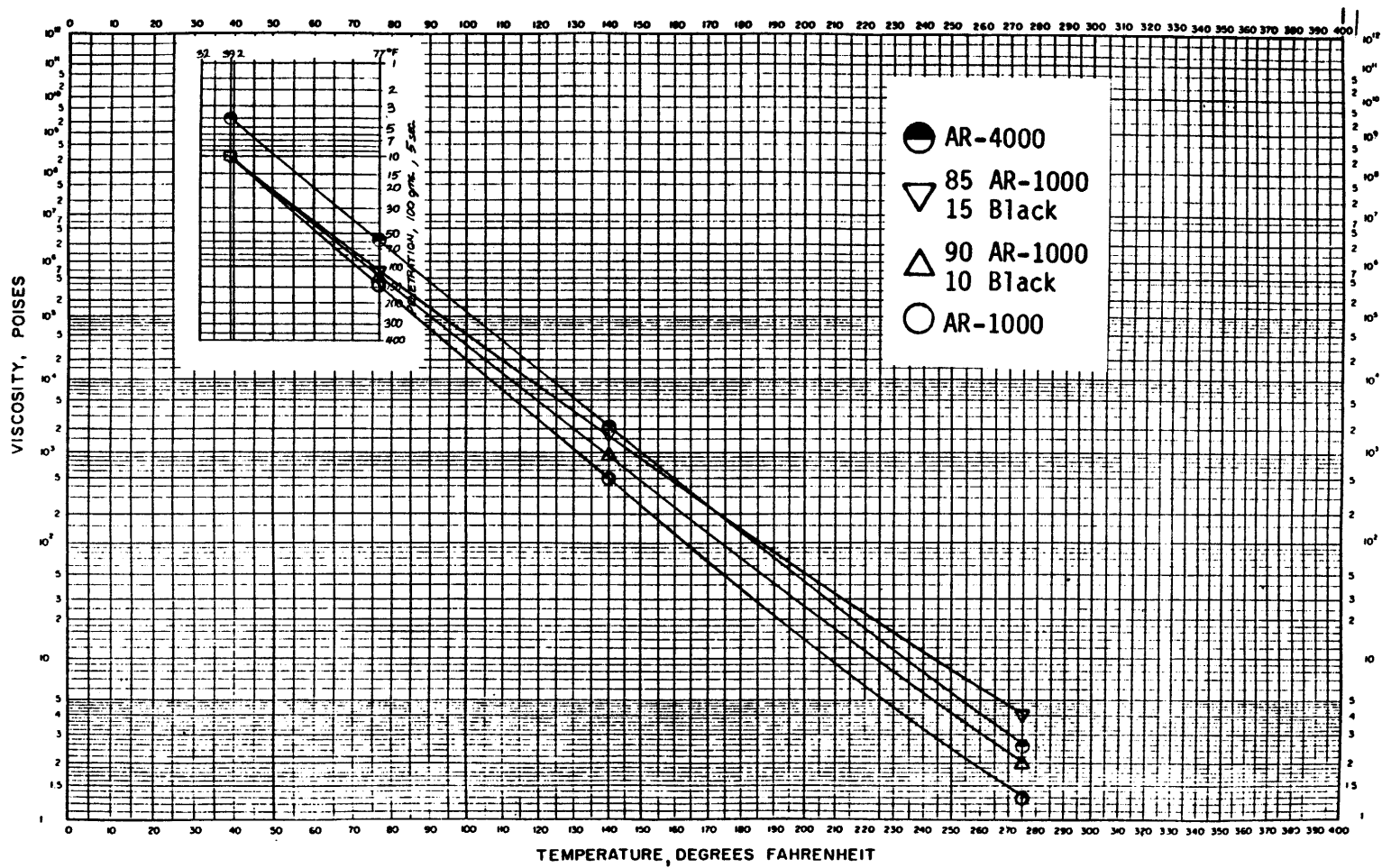


Figure A2. Blends of San Joaquin Valley AR-1000 and Microfil 8.

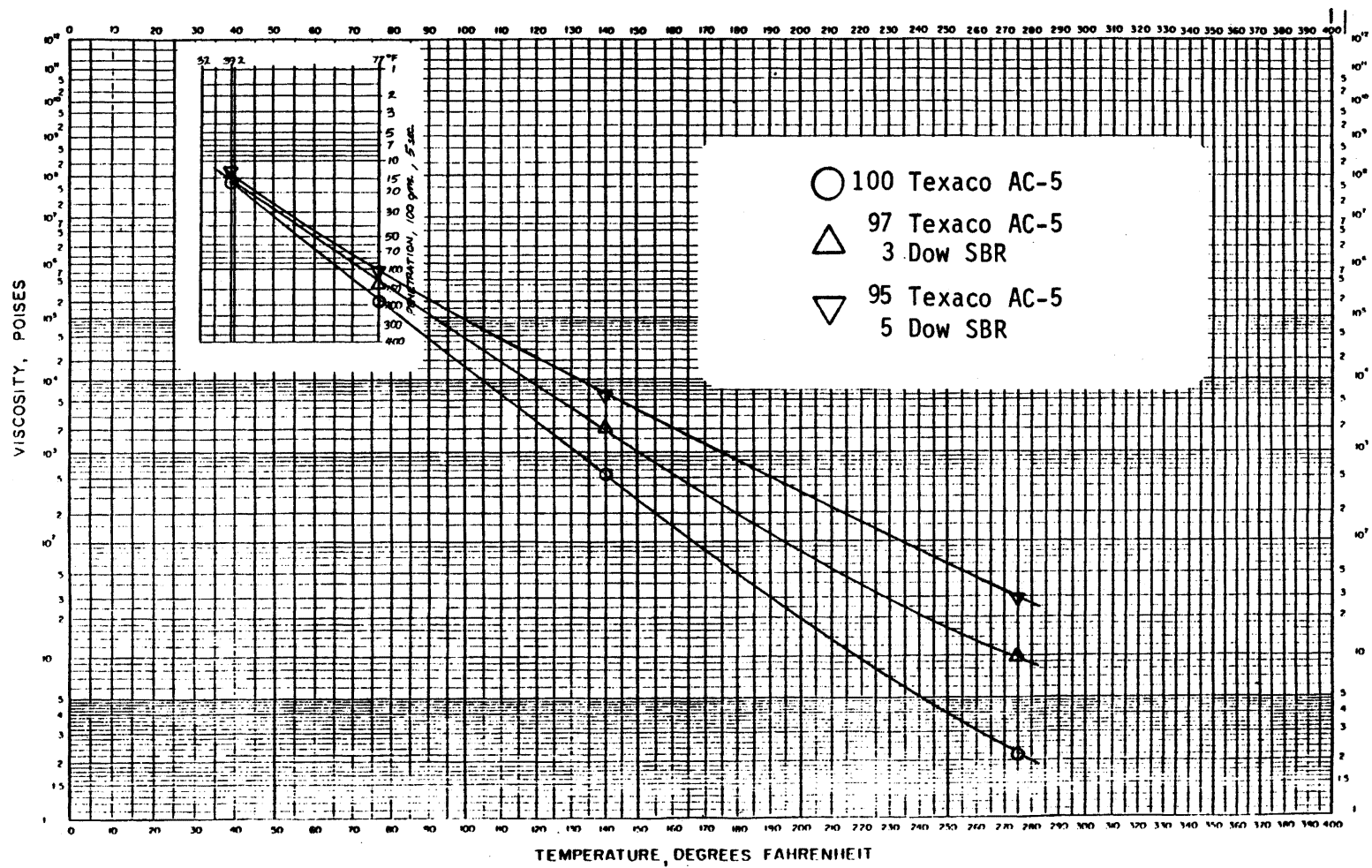


Figure A3. Penetration and viscosity versus temperature for Texaco AC-5, and dispersions of SBR latex.

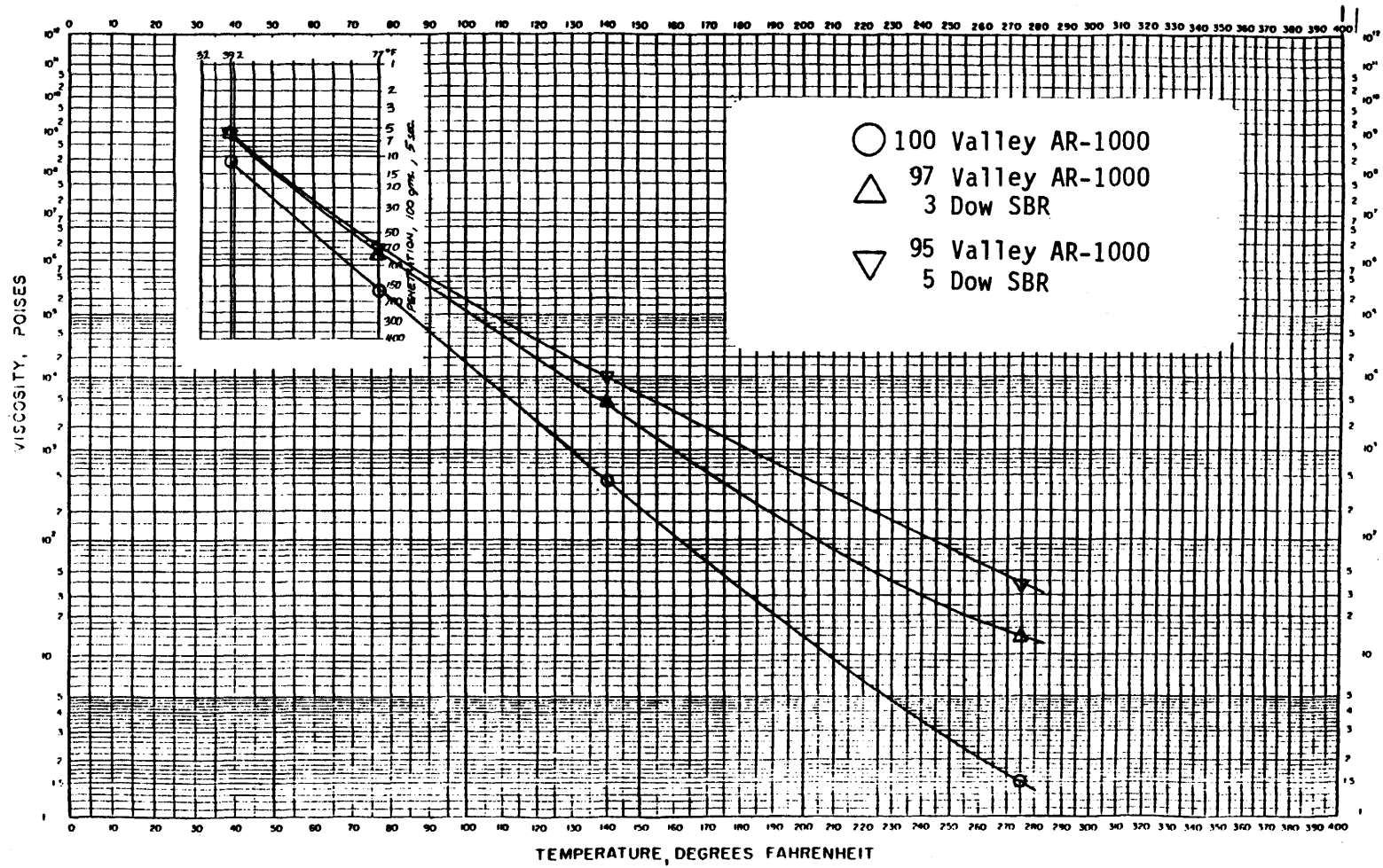


Figure A4. Penetration and viscosity versus temperature for San Joaquin Valley AR-1000, and dispersions of SBR latex.

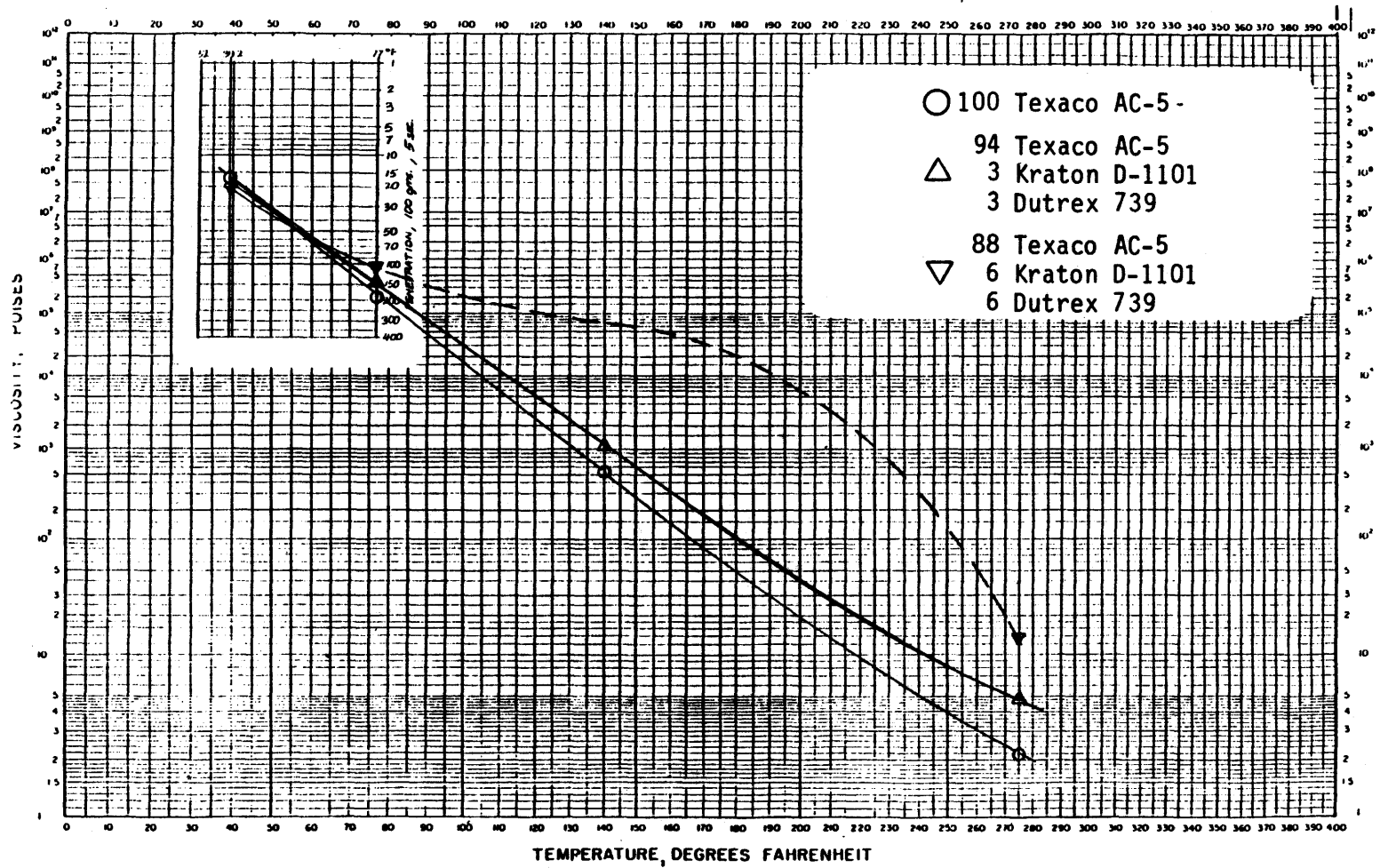


Figure A5. Penetration and viscosity versus temperature for Texaco AC-5, and solutions of S-B-S thermoplastic rubber.

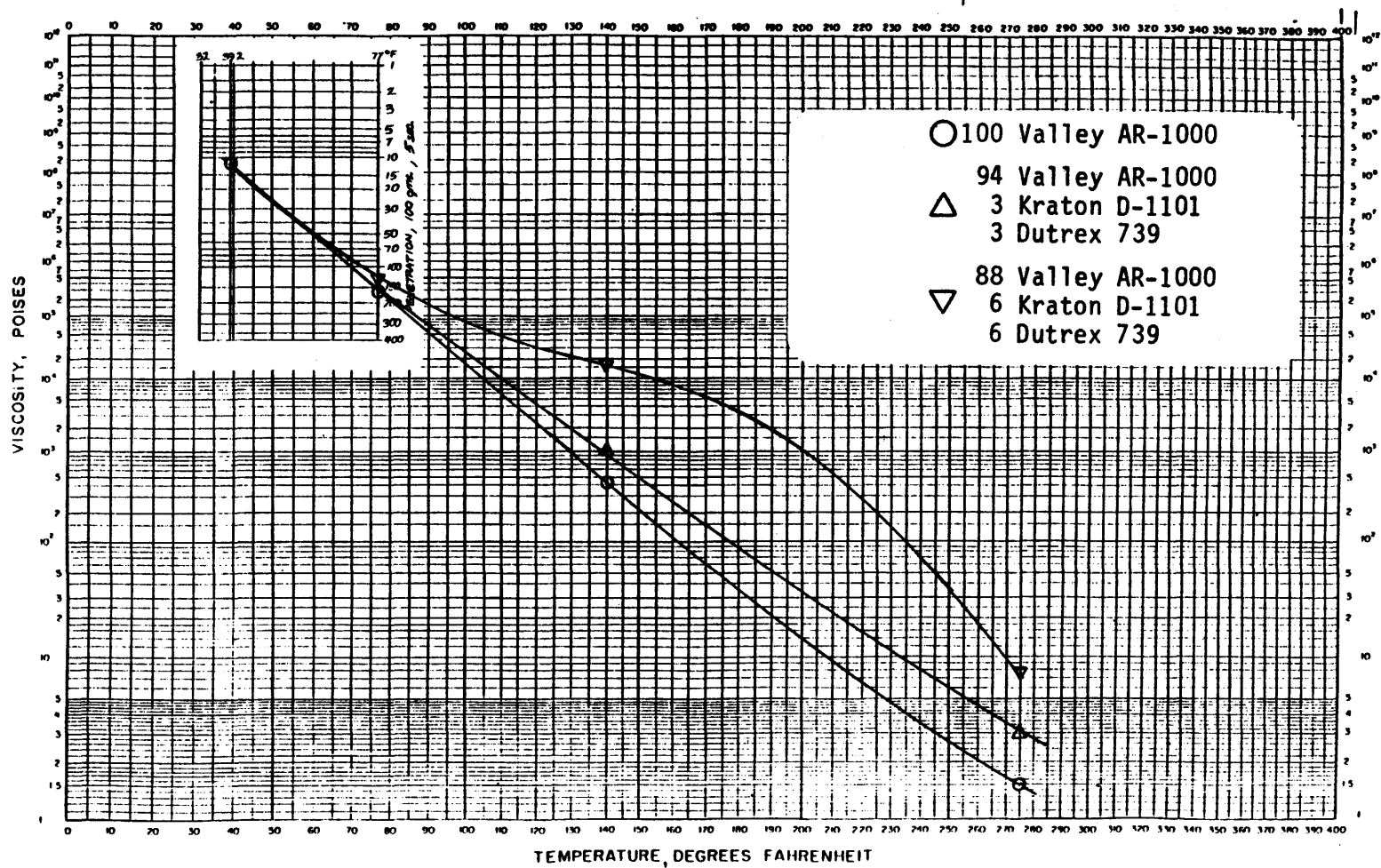


Figure A6. Penetration and viscosity versus temperature for San Joaquin Valley AR-1000, and solutions of S-B-S thermoplastic rubber.

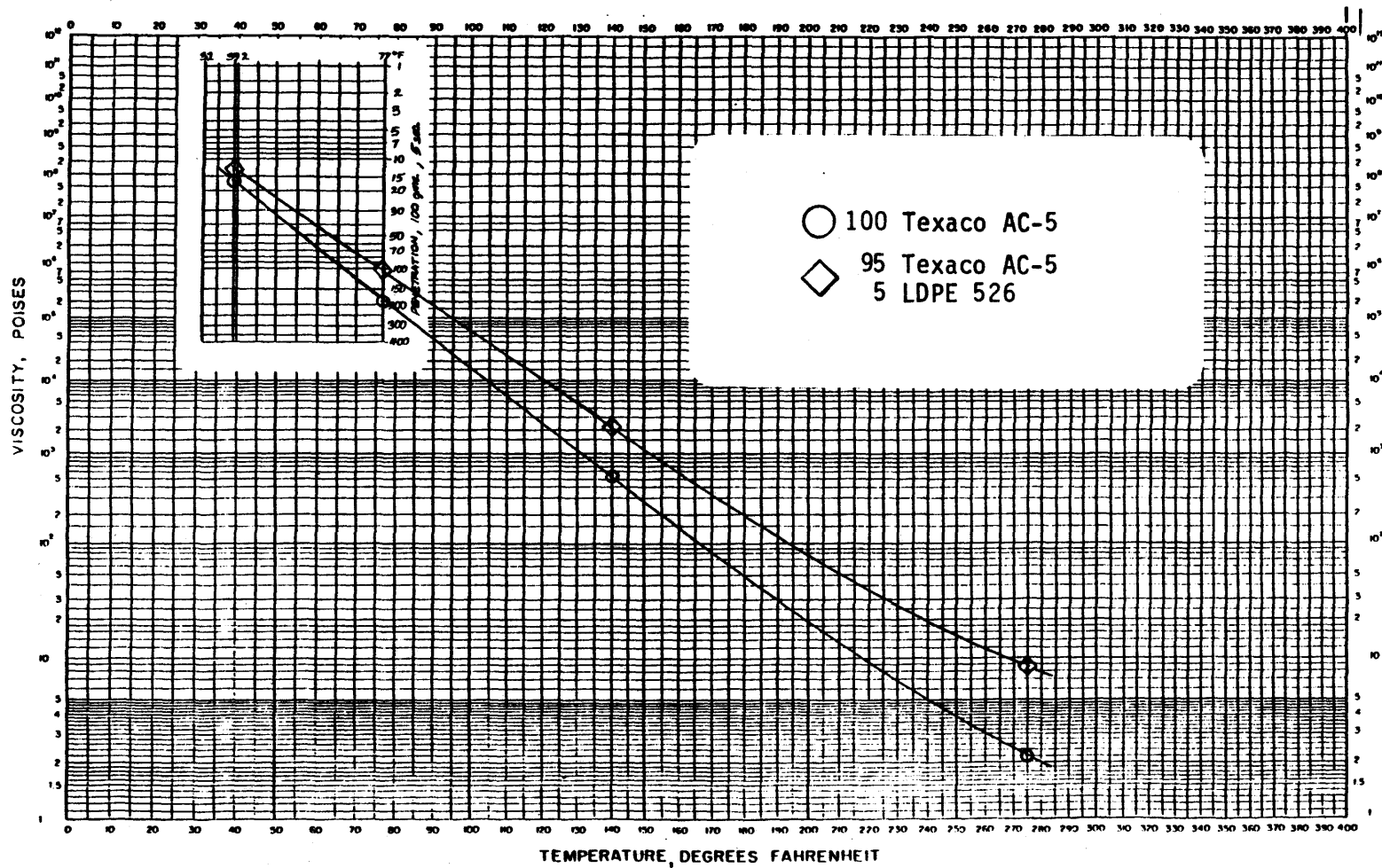


Figure A7. Penetration and viscosity versus temperature for Texaco AC-5, and dispersion containing 5% LDPE 526.

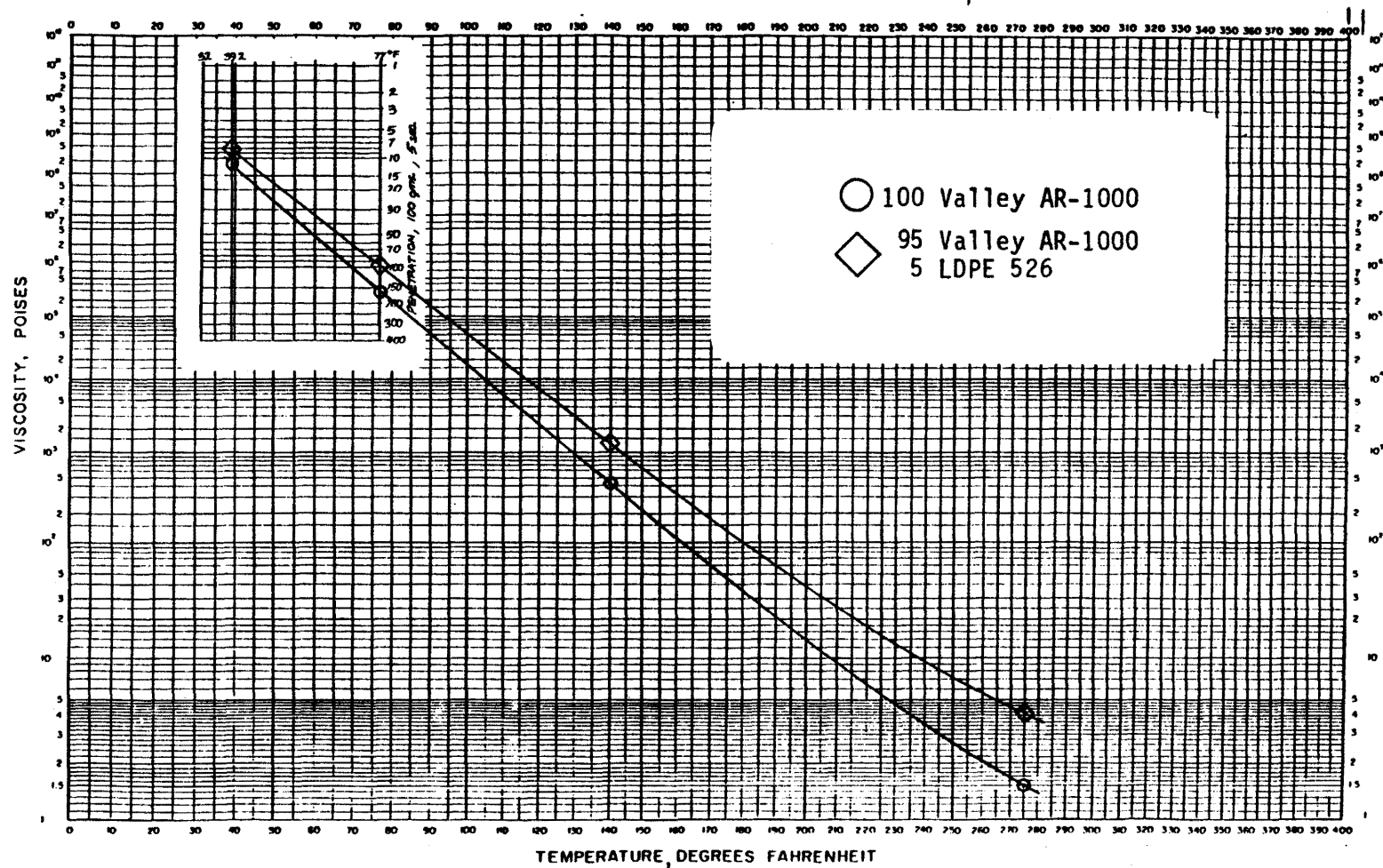


Figure A8. Penetration and viscosity versus temperature for San Joaquin Valley AR-1000, and dispersion containing 5% LDPE 526.

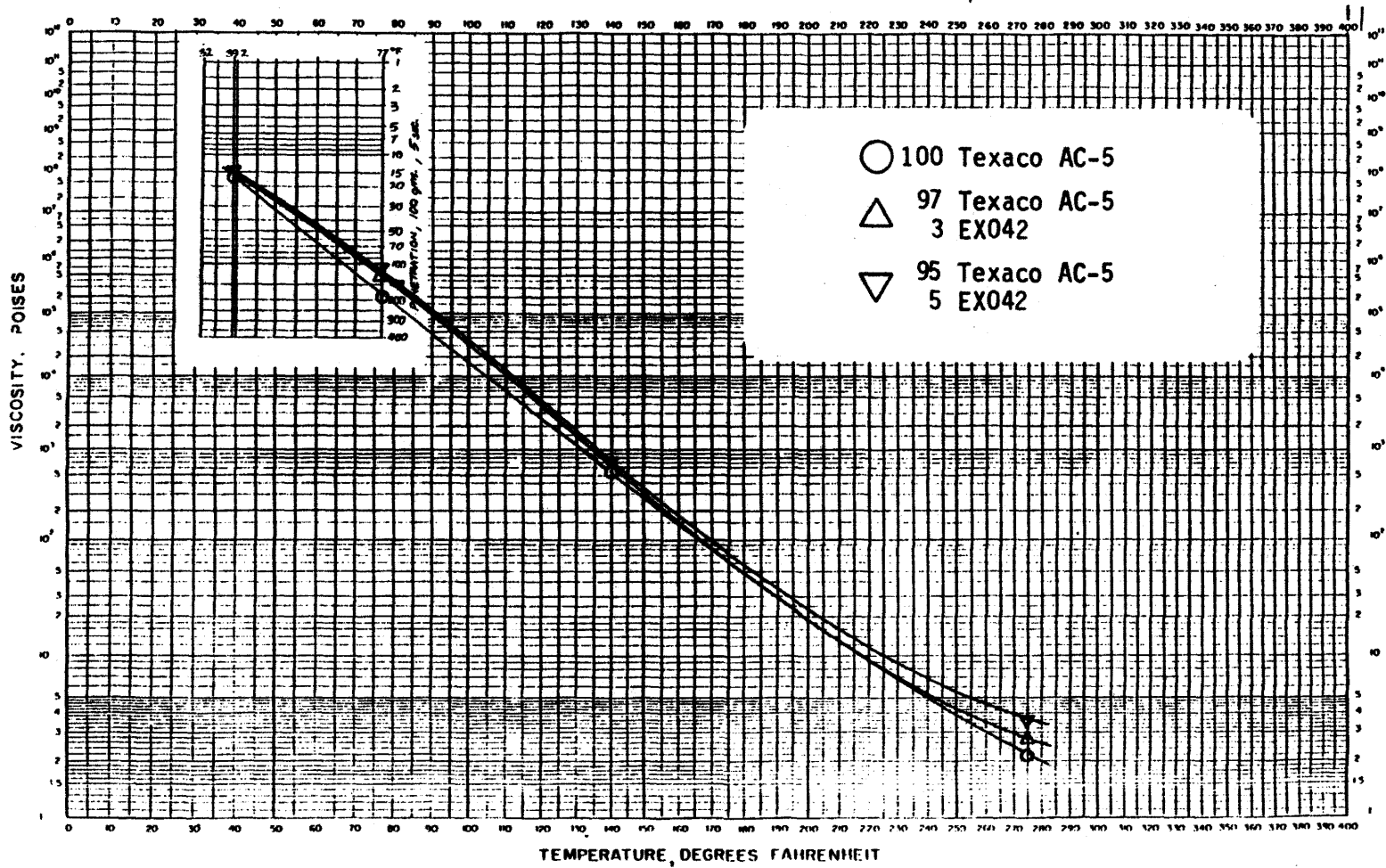


Figure A9. Penetration and viscosity versus temperature for Texaco AC-5, and blends with EVA resin EX042.

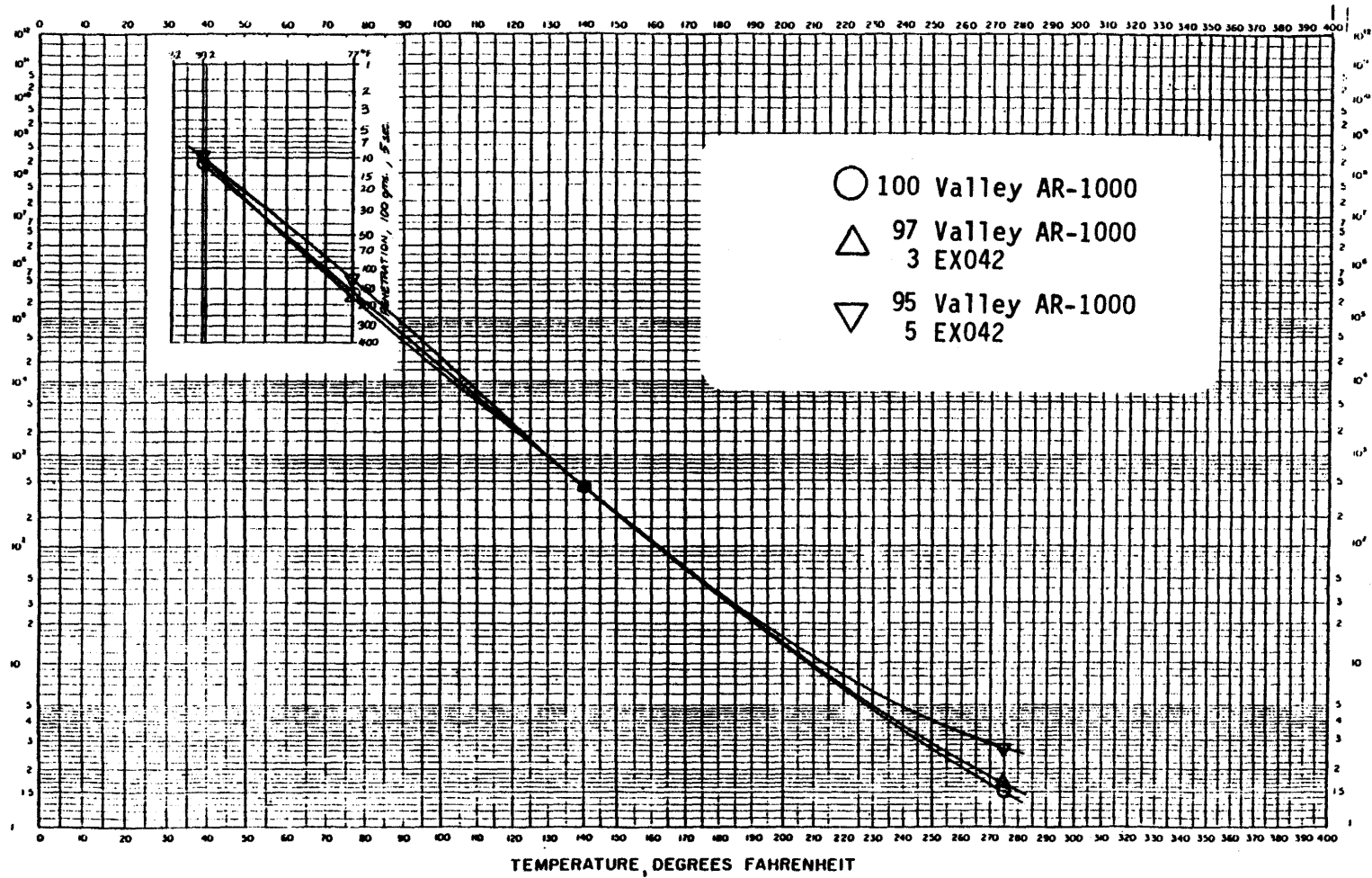


Figure A10. Penetration and viscosity versus temperature for San Joaquin Valley AR-1000, and blends with EVA resin EX042.

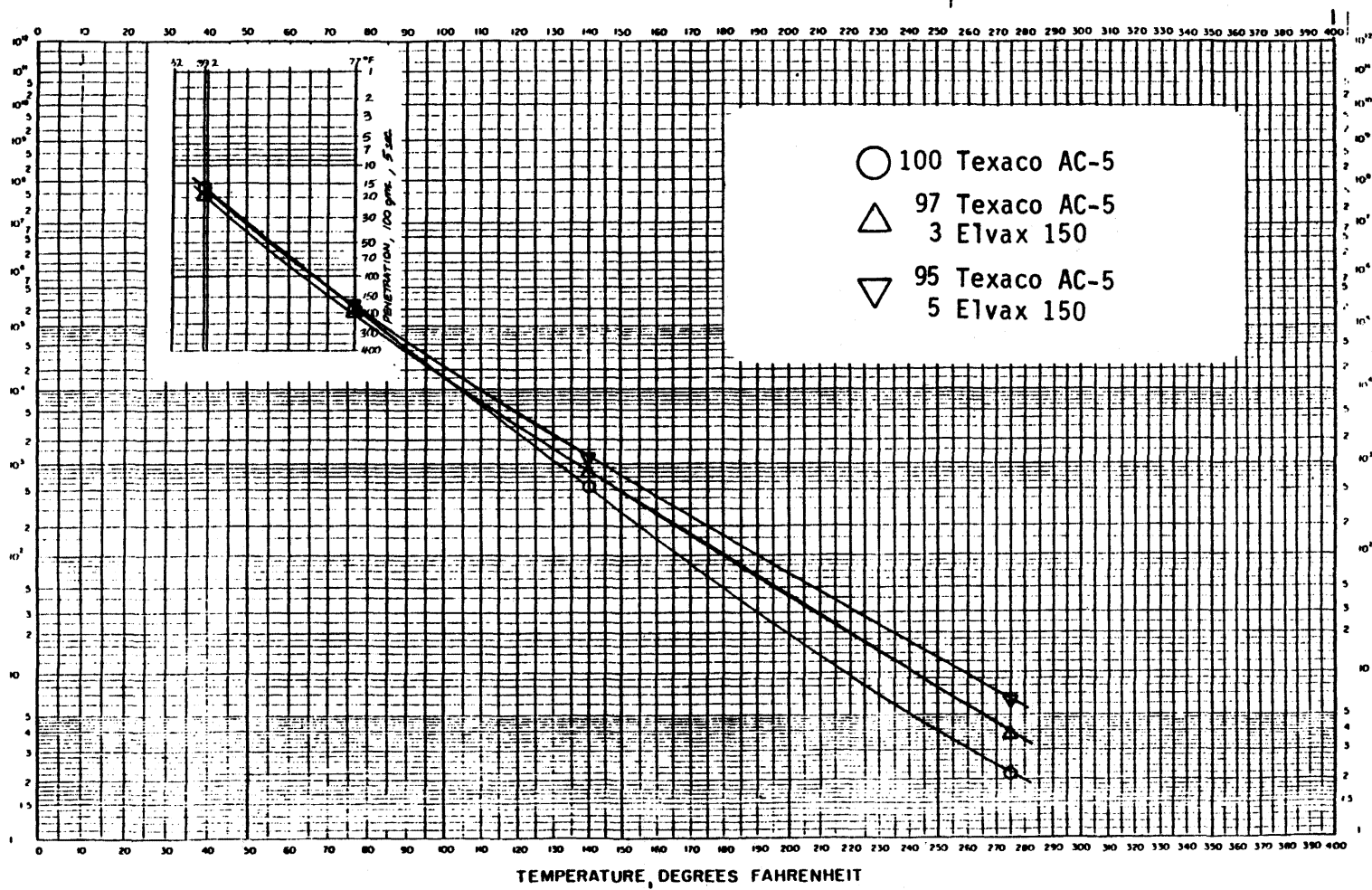


Figure A11. Penetration and viscosity versus temperature for Texaco AC-5, and blends with EVA resin ELVAX 150.

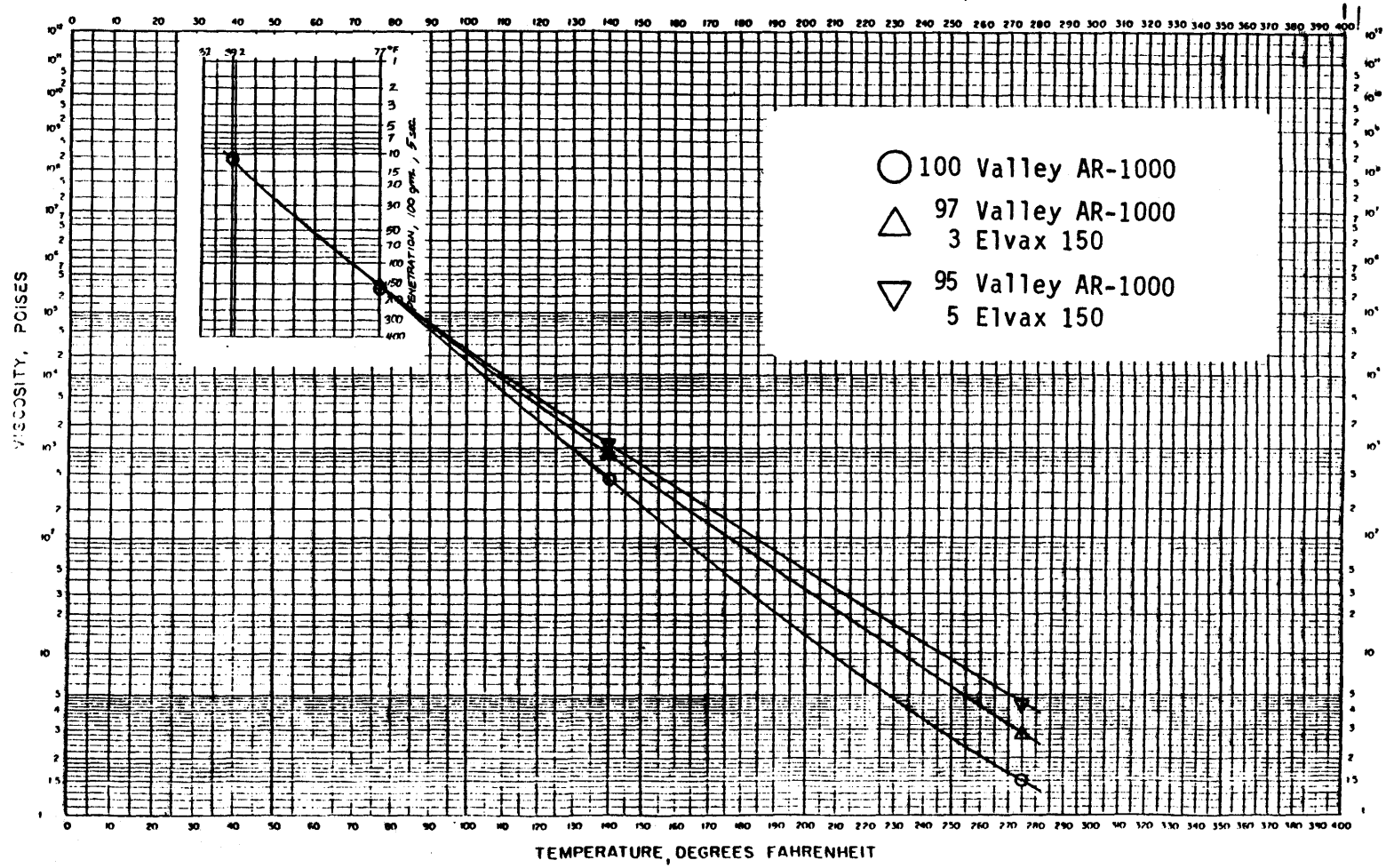
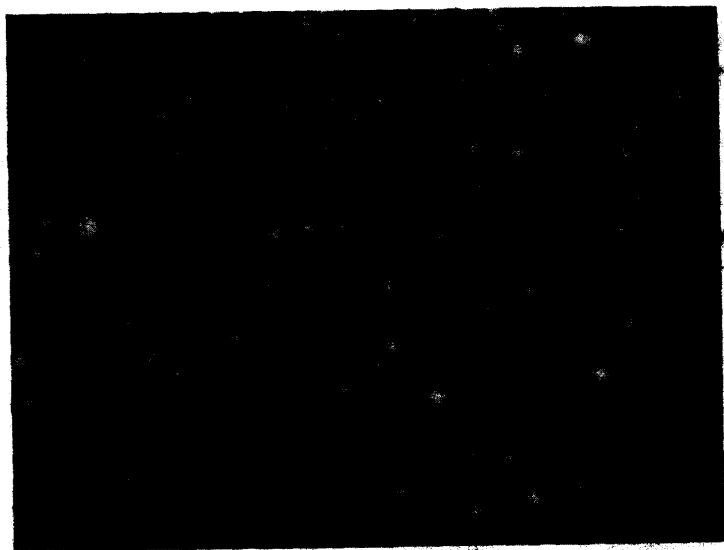


Figure A12. Penetration and viscosity versus temperature for San Joaquin Valley AR-1000, and blends with EVA resin ELVAX 150.

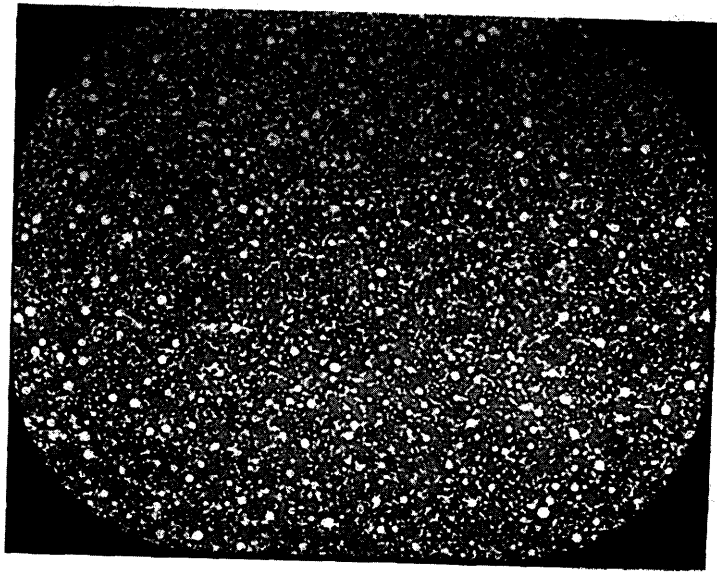


(a)
After one pass through Vicosator



(b)
After five passes through Vicosator

Figure A13. Photomicrographs of Serial No. 49 laboratory dispersion of 5% Dow low-density polyethylene 526 (density 0.919, Melt Index 1.0) in Texaco AC-10 asphalt. One scale division = 10 μm or 0.0004 in.

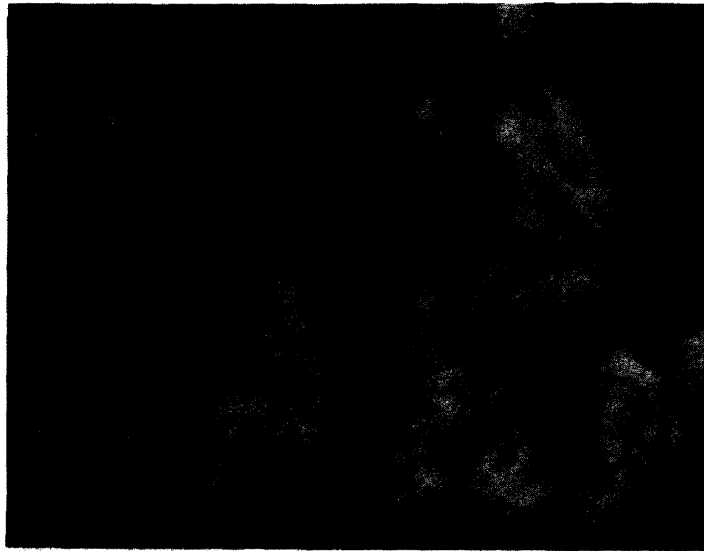


(a)
After one pass through Vicosator

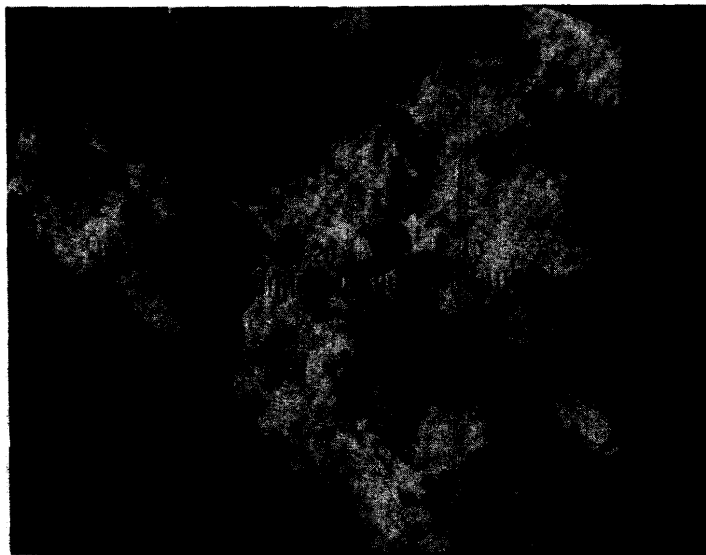


(b)
After five passes through Vicosator

Figure A14. Photomicrographs of Serial No. 50 laboratory dispersion of 5% Dow low-density polyethylene 527 (density 0.921, Melt Index 2.9) in Texaco AC-10 asphalt. One scale division = 10 μm or 0.0004 in.

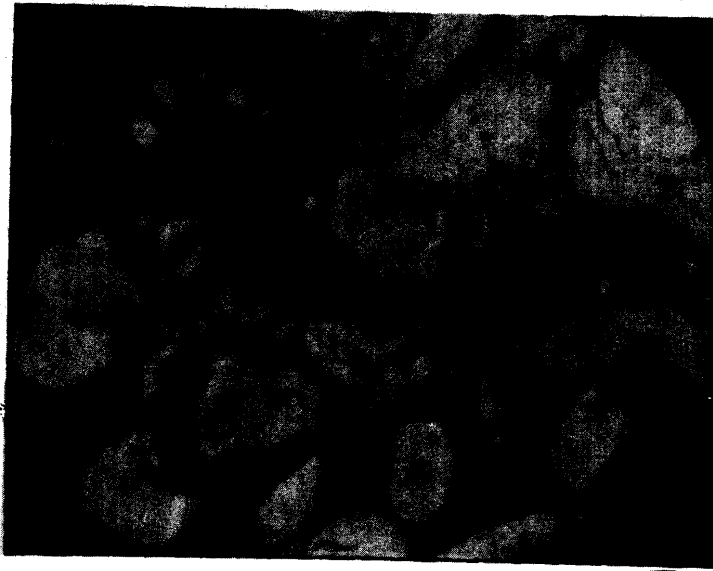


(a)
After two passes through Vicosator

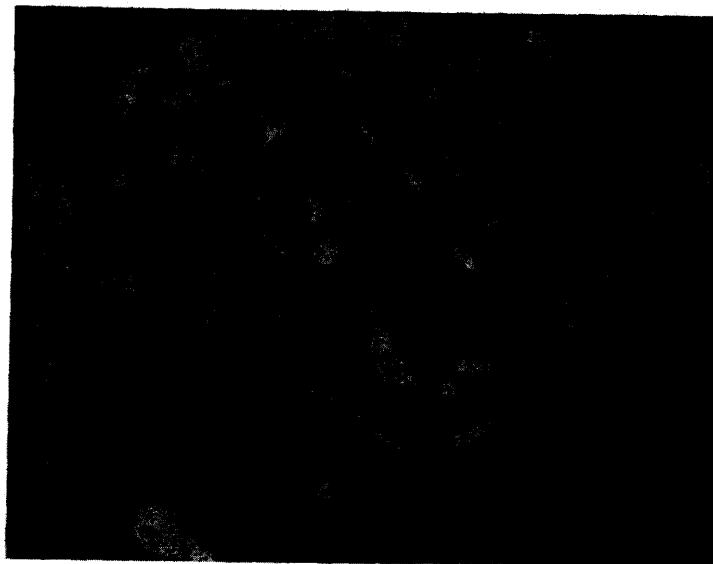


(b)
After six passes through Vicosator

Figure A15. Photomicrographs of Serial No. 51 laboratory dispersion of 5% Dow high-density polyethylene 69065P (density 0.961, Melt Index 0.60) in Texaco AC-10 asphalt. One scale division = 10 μm or 0.0004 in.



(a)
After one pass through Vicosator

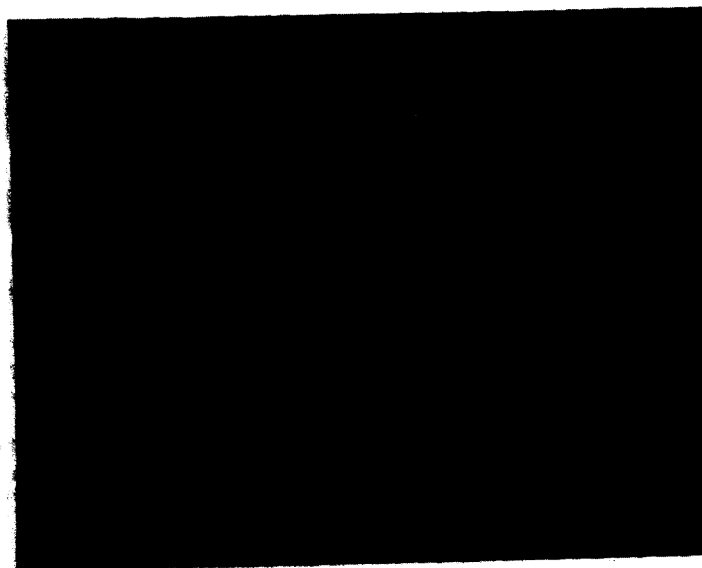


(b)
After five passes through Vicosator

Figure A16. Photomicrographs of Serial No. 52 laboratory dispersion of 5% Dow linear-low-density polyethylene 2045 (density 0.920, Melt Index 1.0) in Texaco AC-10 asphalt. One scale division = 10 μm or 0.0004 in.



(a)
After one pass through Vicosator



(b)
After five passes through Vicosator

Figure A17. Photomicrographs of Serial No. 53 laboratory dispersion of 5% Dow high-molecular-weight-low-density polyethylene 880 (density 0.932, Melt Index 0.45, contains 2.6% carbon black) in Texaco AC-10 asphalt. One scale division = 10 μ m or 0.0004 in.

APPENDIX B: RELATION BETWEEN VISCOSITY AND
COHESIVE ENERGY DENSITY

Kirkwood, et. al. (B1) have discussed two phenomena that contribute to viscosity. They include the original Newtonian momentum transfer, which is referred to as shear viscosity and they include an intermolecular interaction term, which is referred to as bulk viscosity. Momentum transfer contributes but molecular interactions are very large and principally determine the viscous properties. The Kirkwood approach requires several simplifications in order to apply it to even simple liquids. Application to asphalt is impossible. Another attempt to relate molecular interactions to viscosity was discussed by Eyring (B2). Eyring relates viscosity to energy required to form molecular size holes in a liquid as the liquid flows. After some simplifications, viscosity can be related to heat of vaporization as shown below:

$$\eta = \frac{Nh}{v} e^{EVAP/2.45 RT} \quad \text{Equation 47}$$

where N = Avogadro's number
 h = Planck's constant
 v = molar volume
 Evap = heat of vaporization
 R = gas constant
 T = temperature.

Evap is the energy required to evaporate a liquid to the extent there are no molecular interactions. Evap of a fluid is related to the cohesive energy density, E/V, at any temperature as follows:

$$E/V = Evap + \int_T^{B.P} Cp dT \quad \text{Equation 48}$$

where Cp = heat capacity and
 BP = boiling point.

Another way of comparing viscosity to cohesive energy density is through the thermodynamic equation of state (B3).

Unit analysis shows that the cohesive energy density, E/V , has the same units as pressure. On a molecular scale, this implies that a pressure is produced between two imaginary planes in a liquid by attractive molecular forces. In terms of units, it is perhaps more informative to express viscosity in terms of joules meter⁻² sec rather than pascal-sec.

REFERENCES FOR APPENDIX B

- B1. Kirkwood, J. G., Buff, F. P. and Green M, S., "The Statistical Mechanical Theory of Transport Processes", Journal of Chemistry and Physics, 17, 988, 1949.
- B2. Moavenzadeh, F. and Stander, R. R., "On Flow of Asphalt", Highway Research Record No. 178, 1967.
- B3. Barton, A. F. M., "Internal Pressure - A Fundamental Liquid Property", Journal of Chem. Ed., 48, 156, 1971.

APPENDIX C: ELASTICITY TEMPERATURE SUSCEPTIBILITY

The ultimate but presently unachievable goal is to interpret viscoelastic data in terms of molecular interactions. This would be of practical interest to the asphalt engineer in predicting performance over a wide temperature range. Asphalt and polymer elastic modulus temperature dependencies may be similar.

Asphalt has been interpreted as having polymer characteristics and thus continuous borrowing of formulas from polymer science occurs, as is done here. Young's modulus, E , expressed in terms of temperature, T , for a cross-linked rubber is given below (C1).

$$E = nRT \left[\left(\frac{L}{L_u} \right)^2 + \frac{L_u}{L} \right] \quad \text{Equation 49}$$

where n = molar network concentration,

R = gas constant and

L/L_u = ratio of stretched length to original length.

The argument for the applicability of this equation to asphalts is rooted in the concept that dipole-dipole interactions in asphalt are similar to cross linking in polymers. One major difference would probably be temperature dependence of elastic properties. Asphalts associate and dissociate as the temperature changes. In contrast, polymers increase in vibration with temperature increase but exhibit little change in association. Therefore, caution should be exercised in applying polymer equations to asphalt data. Polymers appear to have a linear elastic temperature susceptibility; whereas, the data for asphalt would support an exponential temperature dependency for the elastic component.

REFERENCES FOR APPENDIX C

C1. Tobolsky, A. V., Properties and Structures of Polymers, John Wiley and Sons, p. 23, 1960.

APPENDIX D. MISCELLANEOUS MIXTURE MATERIAL PROPERTIES

Table D1. Individual aggregate gradations for washed pea gravel, washed sand, field sand, and limestone crusher fines.

Sieve Size	Washed Pea Gravel	Washed Sand	Field Sand	Limestone Crusher Fines
	Percent retained	Percent retained	Percent retained	Percent retained
#4	65.6	0.3	1.4	0.1
#8	31.6	13.1	1.1	6.2
#16	1.6	17.7	1.0	18.4
#30	0.4	18.4	0.4	16.1
#50	0	35.4	1.1	11.7
#100	0	11.9	44.8	10.4
#200	0	0.7	28.5	7.1
-#200	0.8	2.5	21.7	30.0
Percentage of each aggregate used in blend	50%	30%	10%	10%

Table D2. Bulk specific gravity, apparent specific gravity, and percent absorption for the pea gravel and combined fines.

	Pea Gravel	Pea Gravel	Combined Fines (washed sand, field sand, limestone fines)
Bulk Specific Gravity	2.575	2.529	2.584
Apparent (maximum) specific gravity	2.658	2.640	2.642
Absorption, percent	1.22	1.68	0.86

Table D3. Mixing and molding temperatures.

	Mixing Temperature (°F)	Molding Temperature (°F)
AC-20	305	275
AC-5	285	266
AC-5 + 15% Carbon Black	341	317
AC-5 + 5% Latex	340	320
AC-5 + 5% Kraton D	340	310
AC-5 + 5% Elvax 150	335	290
AC-5 + 5% Novophalt	345	290

Table D4. Results of Marshall mix designs.

	<u>Asphalt Content, percent</u>	<u>Air Void Content, percent</u>	<u>Marshall Stability, lbs</u>	<u>Marshall Flow</u>	<u>Voids in Mineral Aggregate, percent</u>
River Gravel and Texaco Asphalt (50 Blow)					
AC-20 (Control)	4.5	3.2	1700	6	12
5% Latex + AC-5	5.0 (4.5)*	4.9	1200	6	13
5% Kraton + AC-5	4.5	4.7	1500	6	13
5% Novophalt + AC-5	4.6	5.0	1500	6	13
5% Elvax + AC-5	4.5	4.7	1400	5	13
15% Car. Black + AC-5	4.75	5.0	1400	6	13
AC-10	4.6	4.9	1300	6	13
AC-5	4.6	4.8	900	8	13
River Gravel and San Joaquin Valley Asphalt (50 Blow)					
AR4000 (Control)	4.6	5.0	1200	7	12
5% Latex + AR1000	4.5	5.7	800	7	12
5% Kraton + AR1000	4.5	5.0	900	6	13
5% Novophalt + AR1000	4.5	4.7	1100	6	12
5% Elvax + 5% AR1000	4.5	5.2	700	7	13
15% Car. Black + AR1000	4.7	7.1	1000	6	14
AR2000	4.5	5.4	1000	6	13
AR1000	4.5	4.5	700	6	12
Crushed Limestone and Texaco Asphalt (75 Blow)					
AC-20 (Control)	4.5	4.0	3100	8	-
5% Latex + AC-5	4.5	4.0	2600	8	-
5% Kraton + AC-5	4.5	4.0	2900	10	-
5% Novophalt + AC-5	-	-	-	-	-
5% Elvax + AC-5	4.5	3.0	2400	8	-
15% Car. Black + AC-5	4.7	4.4	3000	9	-

* Later changed to 4.5 percent and used in subsequent tests.

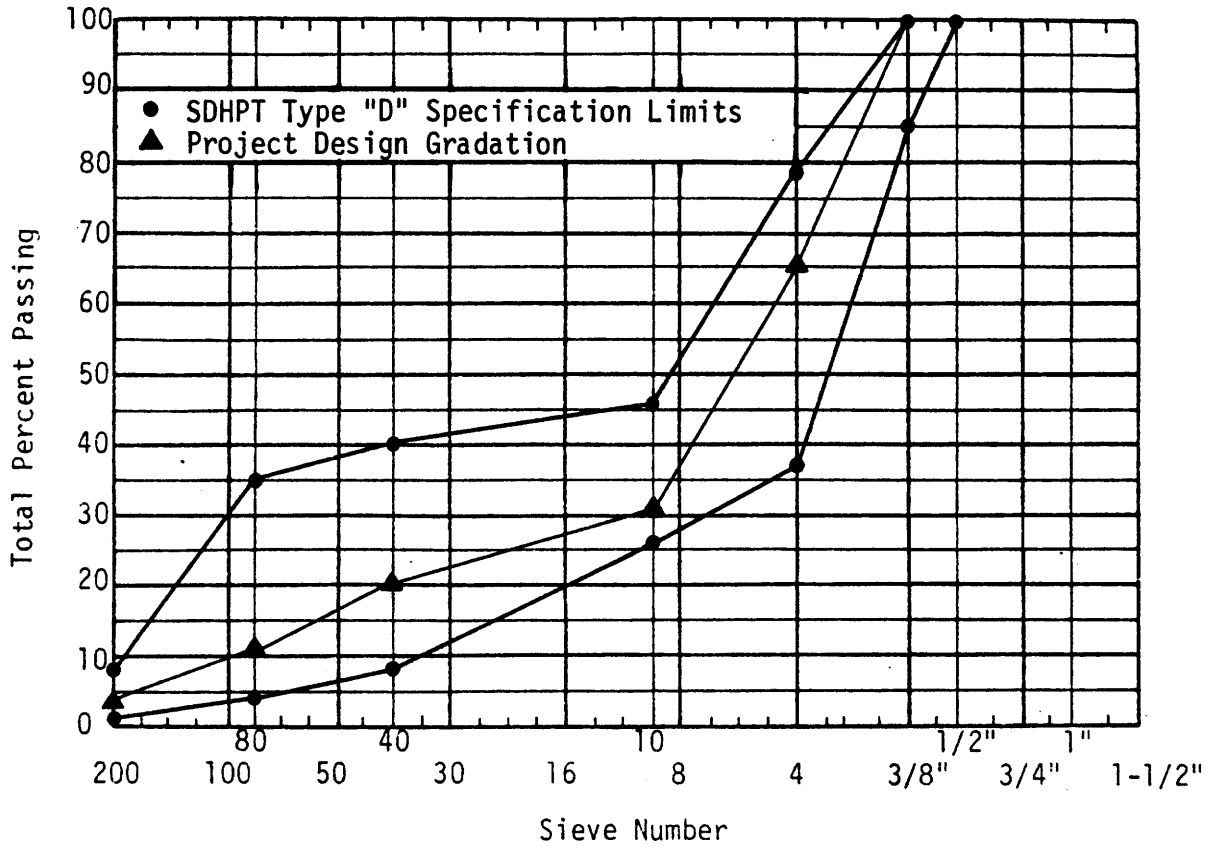


Figure D1. Design gradation specification limits for pea gravel aggregate.

APPENDIX E: BACKGROUND INFORMATION ON
FRACTURE AND FATIGUE

FRACTURE MECHANICS

1. The J-Integral

The energy line integral, J, is defined for the two-dimensional case for either elastic or elastic-plastic behavior as follows:

$$J = \int_{\Gamma^*} (w dy - T \frac{\partial u}{\partial y} ds) \quad \text{Equation 50}$$

where w is strain energy density, Γ^* is a close contour followed counterclockwise in surrounding an area in a stressed solid, T is the tension vector perpendicular to Γ^* , u is the incremental distance in the y direction and ds is an element of Γ^* . For a closed curve, Γ^* , Rice (E1) has shown that

$$J = \int_{\Gamma^*} (w dy - T \frac{\partial u}{\partial x} ds) = 0 \quad \text{Equation 51}$$

From a more physical viewpoint, J may be interpreted as the potential energy difference between two identically loaded bodies having incrementally different crack sizes or

$$J = \frac{1}{B} \left(\frac{du}{da} \right) \quad \text{Equation 52}$$

where u is the potential energy and B is thickness. In other words, J is a generalized relation for the energy release due to crack propagation, which may be valid even if there is appreciable crack tip plasticity.

The usefulness of the J integral lies in the fact that the conditions of specimen size and thickness need not be as stringent as in the case of the critical stress intensity factor, K_{IC} . The requirements for limited plasticity can be dropped when using the J integral. In principle this allows determination of J_{IC} from a small specimen; and, thus, K_{IC} for actual pavement geometries may be predicted from small laboratory specimens.

The J integral was used in this research to analyze results of controlled displacement fatigue testing. The rationale was that the amount of energy released by a specific material per unit area of crack extension will be the same regardless of the size of the specimen. Thus, the J integral provides a method of computation of energy release rate from small specimens that may have some plastic deformation. These energy release rates may be compared to those calculated from three-dimensional field conditions where the plastic zone is very small compared to the confining area which results in an elastic response.

The overlay test, developed at Texas A&M, was selected for the great majority of testing in the fracture mechanics-based study. The fabrication procedure for the beam specimens used in this test is identical to that used in beam fatigue testing. This relatively large specimen size allows the use of typical mixture aggregate gradations. The overlay tester was calibrated to apply a maximum ram displacement of 0.045 in for specimens tested at 77°F (25°C) in a manner illustrated schematically in figure E1. The oscillating horizontal movement was designed to simulate the opening and closing of pavement cracks produced by thermal contraction and expansion of pavement materials.

A loading rate of one cycle per ten seconds was used throughout most of the test program. The load and displacement values were monitored and recorded on any X-Y plotter as illustrated in figure E2. The change in crack length with each loading cycle was visually measured. The area within the load-displacement loops was used to measure the energy required to cause crack propagation and thus to compute the J integral. Note the shaded area in figure E2 which represents the energy dissipation as the crack grows from cycle N to cycle N + 1.

The cyclic loading and unloading which occurs in the overlay test suggests that the J integral cannot be used. This is because the path independence of the J integral has been shown only using deformation theory of plasticity which does not allow for unloading.

For this analysis the definition of the J-integral has been modified by including the effects of unloading as:

$$J^* = \frac{1}{B} \left(\frac{\partial u^*}{\partial a} \right)$$

Equation 53

where u^* reflects the energy released by the material and includes the effects of unloading. The J^* integral for cyclic loading is analogous to the J integral for monotonic loading. The J^* integral should be suitable in a comparative analysis of energy release rates among various asphalt binders.

Reference E1 provides a more complete explanation of the fracture mechanics based controlled displacement fatigue testing. Reference E1 also describes a detailed study which evaluated the effects of specimen size, displacement magnitudes and displacement rates on the fracture parameters determined from overlay testing.

The Paris equation was the form of the regression model used to evaluate controlled displacement fatigue data. Since the J^* parameter was introduced by Balbissi (E2) to account for the cyclic type of loading in these controlled displacement applications, the Paris equation is defined as follows:

$$dC/dN = A^* (J^*)^{n^*}$$

Equation 54

where the $*$ terms differentiate the cyclic loading parameters from traditional monotonic loading parameters.

2. Method of Evaluation Using Fracture Mechanics

The primary objective of controlled displacement, fracture mechanics based on testing is to evaluate the potential of modified asphalt concrete mixtures to resist fracture due to controlled displacement cyclic fatigue. This type of cycling occurs due to thermal cycling or other contraction induced displacement.

Figure E3 shows the typical form of a dc/dN versus J^* regression plot. An upward shift in this line represents a material possessing more brittle behavior and, of course, a more ductile material will plot below the control curve in figure E3. In the displacement control mode, which was used in this study, the slope of the regression line indicates how

sensitive the material is to crack growth. A steep slope is an indication of rapid reduction in crack growth rate, dc/dN , as the test continues. This may be due to several effects:

1. A brittle material exhibits a rapid crack growth in the early cycles, leaving a small uncracked ligament behind. In the displacement control mode, the smaller the size of uncracked ligament, the slower is the crack growth rate.

2. A ductile material may exhibit some crack growth in early cycling due to low stiffness and the presence of voids. However, due to the ductile nature of the material, a significant crack blunting occurs which inhibits the crack growth rate. Generally, ductile materials exhibit relatively small n^* values compared to brittle materials which means that the crack growth is insensitive to fatigue and slow throughout the test.

Figure E4 illustrates the distinctively different behavior typical of brittle and ductile materials. In this figure, crack length is plotted as a function of load cycle.

Controlled displacement fracture test results are contrary to the results that would be obtained from fatigue-fracture tests conducted in a load control mode. The large n -values in the load control case would be an indication of the rate at which crack growth increases. Also, the results are plotted in a manner similar to figure E4, except the start and the end of the test is reversed.

As a result, in the application of J^* parameter, the interpretation of the fatigue-fracture behavior cannot be made solely on the basis of either the "intercept," A^* , or the "slope," n^* , of the Paris equation:

$$\log dc/dN = \log A^* + n^* \log J^* \quad \text{Equation 55}$$

A combined form of parameters A and n , in Paris' law, was suggested by Lytton and Pickett (E3) which accounts for the effects of both parameters in fatigue-fracture behavior. In this approach the term $(n^* + \log A^*)$ is defined to be a measure of resistance to crack growth. The term $(n^* + \log A^*)$ is the logarithmic value of crack speed ($\log dc/dN$) when the numerical value of J^* is equal to 10. We will refer to this

term as "crack speed index." This parameter always will be negative; the more negative it is, the more crack resistant the material is.

In this research, the modified form of the Paris Law was used to express crack growth rates under controlled displacement. Based on the crack length and the energy required to open the crack a specified displacement, two regression equations were developed: (1) the crack length, c , versus number of load applications, N , and (2) the energy to cause the predetermined displacement, u , versus crack length. The coefficient of determination of these regression relationships were all above 0.9. The regression equations were then differentiated once to obtain da/dN and J^* . The values of A^* and n^* were determined from the regression equations.

A second method was also used to interpret the controlled displacement fatigue data. This method assumes linearly elastic behavior. Thus the form of the Paris Law employing this stress intensity factor was used. Lytton and Jayawickrama (E4) have developed a procedure for analyzing the beam fatigue data in order to develop this

$$da/dN = A \Delta K^n \quad \text{Equation 56}$$

relationship.

The magnitude of the opening displacement for the controlled displacement fatigue testing was 0.045 inches (1.14 mm) for the 77°F (25°C) testing (all mixtures). At 33°F (1°C) the 0.045 in displacement would fail the samples in one loading cycle. A cyclic displacement of 0.015 in (0.38 mm) was selected for testing at 33°F.

REFERENCES FOR APPENDIX E

- E1. Rice, J. A., "A Path Dependent Integral and the Approximate of Strain Concentration by Notches and Cracks", Journal of Applied Mechanics, 35, 1968.

- E2. Little, D. N., Balbissi, A. H., Gregory, C. and Richey, B., "Engineering Characterization of Sulphlex Binders", FHWA Report FHWA/RD-85/032, March, 1986.
- E3. Pickett, D. L. and Lytton, R. L., "Laboratory Evaluation of Selected Fabrics for Reinforcement of Asphalt Concrete Overlays", Report No. TTI-2-8-80-261-1, Texas Transportation Institute, 1983.
- E4. Lytton, R. L. and Jayawickarama, P., "Reinforcing Grids for Asphalt Overlays", Texas Transportation Institute Report, February, 1985.

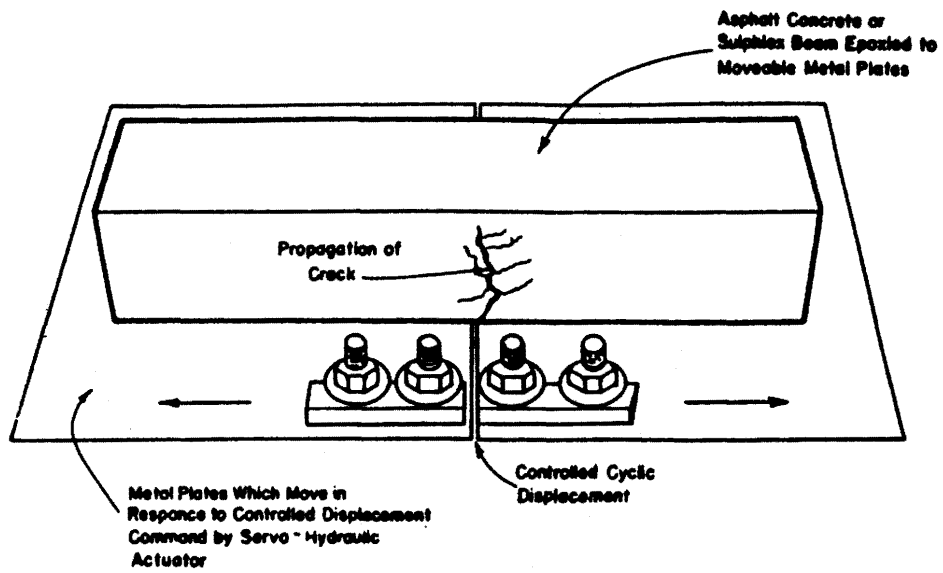


Figure E1. Schematic of overlay tester.

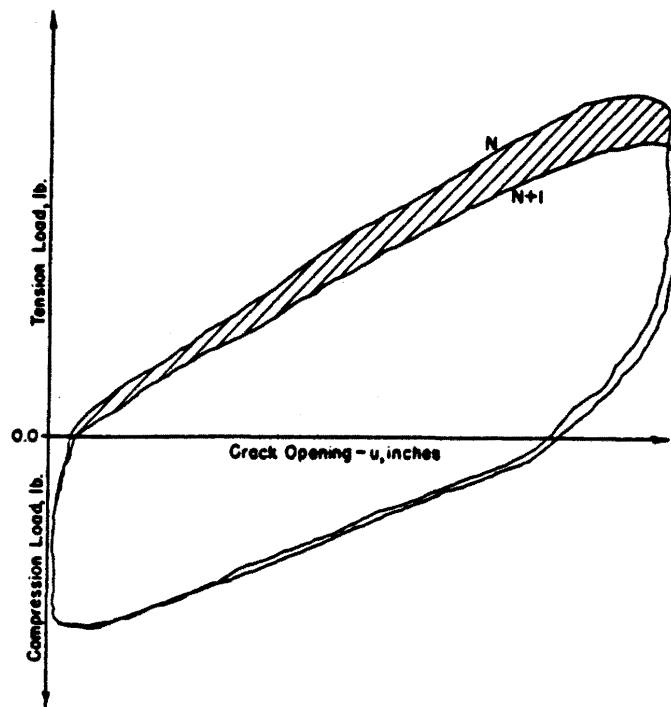


Figure E2. Displacement response in overlay tester recorded on X-Y plotter.

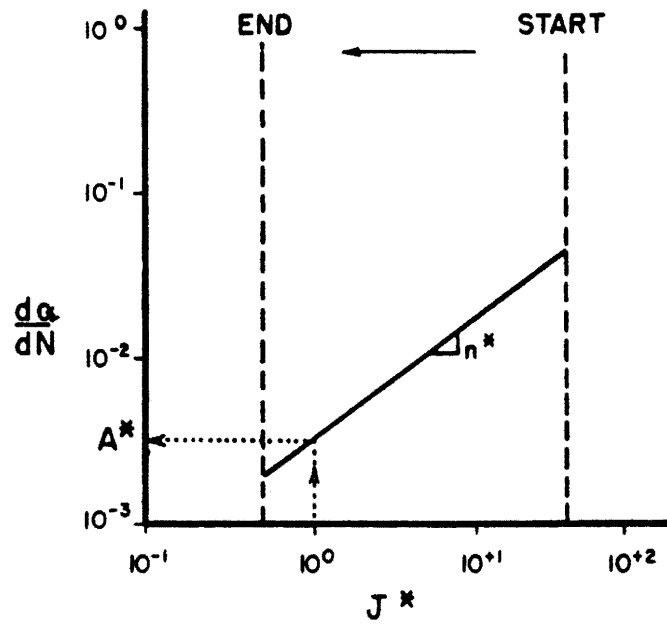


Figure E3. dc/dN versus J^* , general trend for a controlled displacement test.

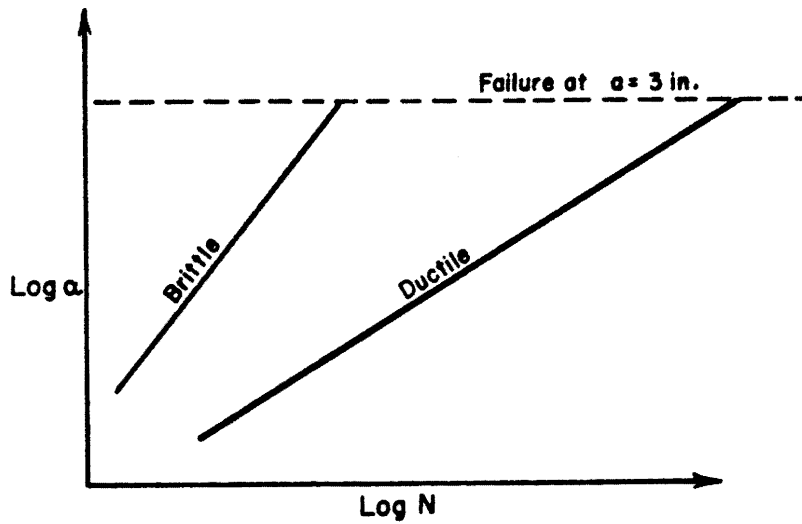


Figure E4. Crack length, a , versus displacement cycle number, N , for brittle and ductile mixtures.

Table E1. Fatigue factors K_1 and K_2 at 34°F and 68°F.

Binder Used in Mixtures	34°F			68°F		
	K_1	Shifted K_1	K_2	K_1	Shifted K_1	K_2
AC-20	1.81×10^{-12}	1.81×10^{-11}	3.72	4.70×10^{-6}	4.70×10^{-5}	2.63
AC-5 and Carbon Black	2.56×10^{-17}	2.56×10^{-16}	5.78	2.62×10^{-6}	2.62×10^{-5}	2.84
AC-5 and Latex	7.84×10^{-11}	7.84×10^{-10}	4.16	3.63×10^{-5}	3.63×10^{-4}	3.04
AC-5 and Kraton	9.76×10^{-13}	9.76×10^{-12}	4.73	1.64×10^{-5}	1.64×10^{-4}	3.12
AC-5 and Elvax	1.93×10^{-10}	1.93×10^{-9}	4.00	1.28×10^{-7}	1.28×10^{-6}	3.92
AC-5 and Novophalt	7.18×10^{-17}	7.18×10^{-16}	5.91	2.33×10^{-8}	2.33×10^{-7}	3.38

Table E2. K_1 values for cool climate VESYS analysis.

Temperature °F	Values of K_1					
	AC-20	AC-5 + Carbon Black	AC-5 + Latex	AC-5 + Kraton	AC-5 + Elvax	AC-5 + Novophalt
10	0.18×10^{-10}	0.26×10^{-15}	0.78×10^{-9}	0.98×10^{-11}	0.19×10^{-8}	0.72×10^{-15}
13	0.18×10^{-10}	0.26×10^{-15}	0.78×10^{-9}	0.98×10^{-11}	0.19×10^{-8}	0.72×10^{-15}
16	0.18×10^{-10}	0.26×10^{-15}	0.78×10^{-9}	0.98×10^{-11}	0.19×10^{-8}	0.72×10^{-15}
35	0.27×10^{-10}	0.76×10^{-15}	0.11×10^{-8}	0.15×10^{-10}	0.23×10^{-8}	0.16×10^{-14}
50	0.19×10^{-7}	0.35×10^{-9}	0.34×10^{-6}	0.22×10^{-7}	0.41×10^{-7}	0.39×10^{-10}
56	0.26×10^{-6}	0.22×10^{-7}	0.35×10^{-5}	0.40×10^{-6}	0.13×10^{-6}	0.96×10^{-9}
63	0.51×10^{-5}	0.16×10^{-5}	0.50×10^{-4}	0.12×10^{-4}	0.48×10^{-6}	0.27×10^{-7}
65	0.12×10^{-4}	0.51×10^{-5}	0.11×10^{-3}	0.33×10^{-4}	0.70×10^{-6}	0.65×10^{-7}
61	0.22×10^{-5}	0.50×10^{-6}	0.24×10^{-4}	0.45×10^{-5}	0.33×10^{-6}	0.11×10^{-7}
57	0.40×10^{-6}	0.42×10^{-7}	0.50×10^{-5}	0.64×10^{-6}	0.15×10^{-6}	0.16×10^{-8}
34	0.18×10^{-10}	0.26×10^{-15}	0.78×10^{-9}	0.98×10^{-11}	0.19×10^{-8}	0.72×10^{-15}
22	0.18×10^{-10}	0.26×10^{-15}	0.78×10^{-9}	0.98×10^{-11}	0.19×10^{-8}	0.72×10^{-5}

Table E3. K_2 values for cool climate VESYS analysis.

Temperature °F	Values of K_2					
	AC-20	AC-5 + Carbon Black	AC-5 + Latex	AC-5 + Kraton	AC-5 + Elvax	AC-5 + Novophalt
10	3.72	5.78	4.16	4.73	4.00	5.91
13	3.72	5.78	4.16	4.73	4.00	5.91
16	3.72	5.78	4.16	4.73	4.00	5.91
35	3.65	5.62	4.09	4.63	3.98	5.77
50	3.19	4.35	3.60	3.93	3.95	4.67
56	3.00	3.85	3.42	3.67	3.94	4.24
63	2.79	3.25	3.19	3.35	3.92	3.73
65	2.72	3.10	3.13	3.25	3.92	3.58
61	2.85	3.45	3.25	3.45	3.93	3.88
57	2.98	3.77	3.38	3.62	3.94	4.16
34	3.69	5.70	4.12	4.68	3.99	5.83
22	3.72	5.78	4.16	4.73	4.00	5.91

Table E4. K_1 for hot climate VESYS analysis.

Temperature °F	Values of K_1					
	AC-20	AC-5 + Carbon Black	AC-5 + Latex	AC-5 + Kraton	AC-5 + Elvax	AC-5 + Novophalt
41	0.37×10^{-9}	0.25×10^{-12}	0.11×10^{-7}	0.27×10^{-9}	0.73×10^{-8}	0.14×10^{-12}
43	0.89×10^{-9}	0.14×10^{-11}	0.24×10^7	0.72×10^{-9}	0.11×10^{-7}	0.55×10^{-12}
45	0.16×10^{-8}	0.79×10^{-11}	0.52×10^{-7}	0.19×10^{-8}	0.16×10^{-7}	0.20×10^{-11}
60	0.11×10^{-5}	0.27×10^{-6}	0.16×10^{-4}	0.27×10^{-5}	0.27×10^{-6}	0.68×10^{-8}
75	0.36×10^{-4}	0.26×10^{-4}	0.36×10^{-3}	0.16×10^{-3}	0.13×10^{-5}	0.23×10^{-6}
87	0.36×10^{-4}	0.26×10^{-4}	0.36×10^{-3}	0.16×10^{-3}	0.13×10^{-5}	0.23×10^{-6}
93	0.36×10^{-4}	0.26×10^{-4}	0.36×10^{-3}	0.16×10^{-3}	0.13×10^{-5}	0.23×10^{-6}
95	0.36×10^{-4}	0.26×10^{-4}	0.36×10^{-3}	0.16×10^{-3}	0.13×10^{-5}	0.23×10^{-6}
91	0.36×10^{-4}	0.26×10^{-4}	0.36×10^{-3}	0.16×10^{-3}	0.13×10^{-5}	0.23×10^{-6}
87	0.36×10^{-4}	0.26×10^{-4}	0.36×10^{-3}	0.16×10^{-3}	0.13×10^{-5}	0.23×10^{-6}
64	0.63×10^{-5}	0.29×10^{-5}	0.74×10^{-4}	0.20×10^{-4}	0.58×10^{-6}	0.42×10^{-7}
59	0.78×10^{-6}	0.15×10^{-6}	0.11×10^{-4}	0.17×10^{-5}	0.22×10^{-6}	0.42×10^{-8}

Table E5. K_2 for hot climate VESYS analysis.

Temperature °F	K_2 (Exp) After Shift Factors					
	AC-20	AC-5 + Carbon Black	AC-5 + Latex	AC-5 + Kraton	AC-5 + Elvax	AC-5 + Novophalt
41	3.48	5.10	3.90	4.35	3.97	5.32
43	3.40	4.95	3.83	4.26	3.97	5.18
45	3.34	4.78	3.77	4.17	3.97	5.02
60	2.88	3.52	3.28	3.48	3.93	3.95
75	2.63	2.84	3.04	3.12	3.92	3.38
87	2.63	2.84	3.04	3.12	3.92	3.38
93	2.63	2.84	3.04	3.12	3.92	3.38
95	2.63	2.84	3.04	3.12	3.92	3.38
91	2.63	2.84	3.04	3.12	3.92	3.38
87	2.63	2.84	3.04	3.12	3.92	3.38
64	2.75	3.18	3.16	3.30	3.92	3.65
59	2.90	3.60	3.32	3.53	3.93	4.02

Table E6. Summary of flexural moduli computed from the controlled stress flexural beam fatigue test.

Temperature, °F	Binder	Load, lb.	Flexural Modulus, psi	
68	AC-20	150	683,827	
		250	1,367,655	
		250	586,137	
		250	539,864	
		350	446,790	
		350	698,110	
		350	638,272	
		350	744,651	
		450	683,862	
		Average		709,908
		AC-5 and Carbon Black	120	239,352
			120	289,620
			140	203,086
			140	159,568
			150	341,913
			200	95,640
			200	197,256
			200	212,758
		250	443,244	
		Average		220,271
		AC-5 and Latex (SBR)	189	68,439
			189	117,170
			189	121,510
			270	89,948
			270	146,463
			338	183,079
			459	51,660
			472	98,381
		540	187,393	
		Average		118,227
		AC-5 and Kraton (SBS)	189	109,359
			189	88,669
			270	80,311
	270		104,151	
	270		93,696	
	338		80,311	
	338		104,107	
	338		62,464	
	Average		90,384	
	AC-5 and EVA	189	102,524	
		211	107,521	
		216	93,736	
		270	74,957	
		270	66,139	
		270	60,776	
		338	70,272	
		371	67,217	
		371	61,840	
	Average		78,331	
	AC-5 and Polyethylene (Novophalt)	140	310,494	
		140	297,860	
		250	306,861	
		250	398,920	
		250	227,954	
		300	478,704	
		350	240,140	
		350	438,030	
	Average		337,370	

Table E6. (Continued).

Temperature, °F	Binder	Load, lb.	Flexural Modulus, psi
34	AC-20	600	911,817
		600	420,817
		700	1,116,976
		700	893,581
		700	827,390
		800	1,021,235
		800	851,029
		800	729,454
		900	1,276,544
		900	617,503
		900	526,021
			Average 785,034
	AC-5 and Carbon Black	338	545,734
		400	1,091,467
		420	1,018,703
		420	1,222,444
		500	1,039,492
		620	902,280
		675	1,473,481
		720	657,799
		780	752,206
	AC-5 and Latex (SBR)	350	1,175,426
		420	1,146,041
		500	704,172
		540	615,477
		675	1,052,486
		760	694,344
		800	444,191
		840	636,001
			Average 808,517
	AC-5 and Kraton (SBS)	540	689,334
		540	907,018
		621	861,667
		675	1,227,900
		675	1,281,288
		675	1,016,194
		675	982,321
		700	789,032
		729	1,178,785
		800	631,221
		800	485,587
			Average 913,668
	AC-5 and EVA	567	1,206,334
		621	1,043,071
		675	1,683,978
		675	982,321
		675	841,989
		800	601,167
		800	548,892
		800	664,448
		810	1,309,761
	AC-5 and Polyethylene (Novophalt)	580	1,012,881
		675	1,052,486
		675	1,178,784
		720	781,137
		760	942,323
		800	991,919
		800	771,493
		820	790,780
		880	565,761
			Average 898,618

Table E7. Basic flexural beam fatigue data for Texaco AC-20.

Temperature, °F	Sample No.	Stress Level, psi	200th Cycle Bending Strain	Cycles to Failure Predicted	Cycles to Failure Actual
34	1	440	0.000293	0	1
	2	440	0.000310	0	1
	3	440	0.000275	0	1
	4	200	0.000200	113	200
	5	200	0.000236	60	75
	6	200	0.000133	520	596
	7	150	0.000100	1539	1000
	8	150	0.000126	645	900
	9	150	0.000150	330	460
	10	100	0.000067	7100	9000
	11	100	0.000091	2200	3000
68	1	83	.000097	171662	455331
	2	138	.000081	277438	136201
	3	138	.000205	24000	25375
	4	138	.000205	24000	27275
	5	192	.000347	6012	9660
	6	192	.000222	19471	7945
	7	192	.000243	15379	17985
	8	192	.000208	23078	17286
	9	83	.000189	29802	44137
	10	248	.000292	9516	7151

Table E8. Basic flexural beam fatigue data for Texaco AC-5 and carbon black.

Temperature, °F	Sample No.	Stress Level, psi	200th Cycle Bending Strain	Cycles to Failure Predicted	Actual
34	1	186	.000274	9970	49280
	2	371	.000203	56525	30605
	3	275	.000213	42632	77109
	4	231	.000152	298257	130113
	5	341	.000305	5422	1408
	6	396	.000485	367	434
	7	429	.000460	502	357
	8	231	.000183	103943	256854
	9	220	.000162	205371	180527
68	1	110	.000450	8209	6389
	2	110	.000417	10174	6112
	3	77	.000306	24529	29404
	4	77	.000389	12374	16808
	5	82	.000194	88420	44368
	6	66	.000222	60545	75302
	7	110	.000928	1053	1580
	8	66	.000183	103987	438758
	9	138	.000250	43346	14407

Table E9. Basic flexural beam fatigue data for Texaco AC-5 and SBR (latex).

Temperature, °F	Sample No.	Stress Level, psi	200th Cycle Bending Strain	Cycles to Failure Predicted	Actual
34	1	371	.000284	43982	15461
	2	297	.000389	11944	37181
	3	275	.000315	28800	22105
	4	192	.000132	1070087	729035
	5	231	.000162	451121	931260
	6	418	.000485	4759	8026
	7	462	.000586	2179	1091
	8	440	.000799	600	601
68	1	104	.001226	24988	236846
	2	104	.000716	127809	151147
	3	104	.000690	142727	143999
	4	148	.001332	19401	26507
	5	148	.000818	85218	58215
	6	136	.000818	85218	42122
	7	297	.001279	21960	7868
	8	252	.003944	720	744
	9	260	.002132	4658	2411

Table E10. Basic flexural beam fatigue data for Texaco AC-5 and Novophalt (polyethylene).

Temperature, °F	Sample No.	Stress Level, psi	200th Cycle Bending Strain	Cycles to Failure Predicted	Actual
34	1	371	.000284	63954	221858
	2	371	.000254	124934	198480
	3	440	.000358	16512	3044
	4	440	.000460	3740	2544
	5	451	.000460	3740	4313
	6	418	.000358	16512	27912
	7	396	.000409	7501	12222
	8	319	.000254	124934	48005
	9	484	.000690	341	404
68	1	138	.000361	9771	8457
	2	138	.000278	23699	10560
	3	138	.000486	3581	5780
	4	77	.000200	72040	123475
	5	77	.000208	62610	112092
	6	165	.000278	23699	19209
	7	192	.000647	1371	1980
	8	192	.000354	10434	4665

Table E11. Basic flexural beam fatigue data for Texaco AC-5 and EVA (Elvax).

Temperature, °F	Sample No.	Stress Level, psi	200th Cycle Bending Strain	Cycles to Failure Predicted	Cycles to Failure Actual
34	1	371	.000177	183296	6282
	2	371	.000305	21285	93113
	3	371	.000355	11499	30581
	4	445	.000274	32423	22549
	5	312	.000208	97035	303907
	6	342	.000264	37743	279921
	7	440	.000590	1519	375
	8	440	.000647	1056	620
	9	440	.000534	2265	2425
68	1	148	.001599	11313	9316
	2	148	.001812	6930	12682
	3	148	.001972	4977	7664
	4	119	.001023	65021	110964
	5	116	.000869	122847	75680
	6	104	.000818	155754	128497
	7	186	.002132	3668	3804
	8	204	.002452	2122	1794
	9	204	.002665	1531	868

Table E12. Basic flexural beam fatigue data for Texaco AC-5 and SBS (Kraton).

Temperature, °F	Sample No.	Stress Level, psi	200th Cycle Bending Strain	Cycles to Failure Predicted	Actual
34	1	371	.000244	116057	83211
	2	371	.000233	141918	16563
	3	371	.000294	47446	22399
	4	371	.000305	40421	56156
	5	400	.000274	66511	10800
	6	297	.000347	21757	368643
	7	297	.000264	79607	465646
	8	342	.000319	32267	373650
	9	440	.000562	2239	2781
	10	440	.000731	648	254
	11	385	.000393	12083	2426
68	1	186	.001865	5443	4894
	2	186	.001439	12237	4074
	3	186	.002398	2484	3440
	4	104	.000767	87199	36163
	5	104	.000946	45308	209287
	6	148	.001492	10923	10249
	7	148	.001151	24591	28043
	8	148	.001279	17675	20796

APPENDIX F: DEFORMATION PARAMETERS

Table F1. Average creep compliance from 1000 second creep test.

Test Temperature, °F	Sample ID	Creep Compliance ($\text{psi}^{-1} \times 10^{-6}$) at Load Duration Given Below in Seconds									
		0.03	0.1	0.3	1	3	10	30	100	300	1000
40	AC-20	0.16	0.31	0.44	0.64	0.94	1.45	2.55	4.35	7.10	11.90
	Carbon Black	0.25	0.74	1.15	1.85	2.95	4.85	7.40	11.0	15.0	21.0
	Latex	0.547	0.781	1.13	1.96	3.24	5.54	9.79	13.75	20.9	33.9
	Kraton	0.31	0.814	1.285	1.97	3.045	4.845	7.375	11.25	15.90	21.70
	Elvax	0.297	0.648	0.967	1.55	2.24	3.46	4.96	7.08	9.26	12.47
	Novophalt	0.18	0.367	0.50	0.65	0.91	1.35	2.08	3.16	4.90	7.69
70	AC-20	0.156	0.625	2.34	6.17	13.95	21.7	26.4	32.3	38.35	49.9
	Carbon Black	0.312	3.2	8.83	16.5	22.9	28.2	30.85	35.15	39.55	47.3
	Latex	2.92	7.12	13.9	23.6	33.5	43.2	60.15	78.3	100.8	147.5
	Kraton	0.86	2.92	6.74	12.3	18.05	24.45	30.05	34.8	41.5	52.25
	Elvax	0.86	2.78	5.86	10.0	14.15	18.6	21.65	25.75	30.35	36.25
	Novophalt	1.05	2.30	4.57	8.09	12.45	17.6	21.85	26.75	31.75	39.15
100	AC-20	3.12	9.37	18.8	29.6	37.5	45.3	53.1	68.7	95.3	175
	Carbon Black	5.16	13.4	27.5	36.7	42.8	47.8	52.45	60.0	67.8	81.5
	Latex	10.94	31.9	48.45	72.5	92.6	121.5	162	244.5	418	700
	Kraton	3.90	14.05	25.3	37.2	43.25	52.75	60.75	73.70	96.70	148.4
	Elvax	5.0	21.5	35.0	46.5	54.0	64.0	71.0	81.0	97.5	120.0
	Novophalt	2.5	8.15	17.5	27.0	36.0	44.5	51.0	58.5	68.5	93.0

* Additives blended with AC-5

Table F2. Average creep compliance from 1000 second creep test on specimens tested at 70°F.

Sample ID	Treatment	Creep Compliance ($\text{psi}^{-1} \times 10^{-6}$) at Load Duration Given Below in Seconds									
		0.03	0.1	0.3	1	3	10	30	100	300	1000
AC-20	Heat Aged for 7 Days at 140°F	0.66	1.02	1.99	4.02	7.30	12.15	16.6	20.65	24.05	28.2
Carbon Black		1.76	4.80	9.06	15.45	21.90	27.70	31.5	34.85	38.5	43.45
Latex		1.88	5.55	10.23	17.90	26.0	34.20	40.05	48.05	58.30	79.45
Kraton		0.90	2.50	4.45	8.40	13.30	18.90	22.95	26.95	30.90	36.35
Elvax		0.55	1.57	2.96	5.08	7.70	10.80	13.20	15.65	17.60	20.10
Novophalt		1.09	3.12	5.58	9.91	14.80	20.15	24.05	27.95	32.30	37.85
AC-20		Over Cycle Lottman Conditioning	1.48	3.75	7.42	14.1	21.0	27.95	33.05	39.20	47.70
Carbon Black	1.64		6.72	11.95	19.80	24.35	28.75	31.60	35.95	40.95	50.75
Latex	1.25		3.98	8.43	14.4	20.85	26.85	31.8	38.20	47.75	68.45
Kraton	1.56		5.0	9.40	16.70	23.90	31.65	37.50	44.50	54.0	67.5
Elvax	0.86		2.34	4.88	8.20	11.65	14.90	17.40	19.50	22.15	28.20
Novophalt	1.09		2.93	5.78	9.94	14.28	19.50	24.20	29.75	36.55	48.70

Table F3. Average creep compliance from 1000 second creep test on specimens at 70°F
(California Valley asphalt).

Sample ID	Creep Compliance ($\text{psi}^{-1} \times 10^{-6}$) at Load Duration Given Below in Seconds*									
	0.03	0.1	0.3	1	3	10	30	100	300	1000
AR-4000	0.78	1.25	2.19	4.69	9.32	19.0	29.4	40.2	52.10	73.2
AR-1000 + 15% Carbon Black	1.02	3.67	8.81	18.75	28.05	35.4	39.85	44.45	49.4	56.3
AR-1000 + 5% Latex	0.62	1.88	4.54	11.1	20.4	30.7	38.0	47.20	59.90	85.5
AR-1000 + 5% Kraton	2.03	5.68	12.1	24.8	37.6	50.8	60.3	73.2	91.3	130.8
AR-1000 + 5% Elvax	0.62	1.35	3.28	9.12	18.6	27.5	34.2	44.8	56.8	78.8
AR-1000 + 5% Novophalt	1.32	3.75	8.04	16.8	28.6	41.6	51.6	63.8	80.2	113.7

* All samples run at 20 psi except Elvax @ 15 psi

Table F4. Average permanent strain from the incremental static compression test at 40°F. All tests at 20 psi applied stress.

Sample ID	Permanent Strain (inch x 10 ⁻⁶ /inch) After Load Duration Given Below				
	0.1 sec.	1 sec.	10 sec.	100 sec.	1000 sec.
AC-20	*	*	7.8	39.0	165.0
AC-5 + 15% Carbon Black	*	*	6.88	67.0	225.0
AC-5 + 5% Latex	*	*	13.1	111.5	501.0
AC-5 + 5% Kraton	*	*	9.4	27.4	188.0
AC-5 + 5% Elvax	1.40	2.97	9.7	41.75	127.0
AC-5 + 5% Novophalt	*	1.25	7.50	31.10	104.2

*Deformation too small to measure.

Table F5. Average permanent strain from the incremental static compression test at 70°F. All tests at 20 psi applied stress except for latex. Results of only one test are shown for latex at 10 psi applied stress.

Sample ID	Permanent Strain (inch x 10 ⁻⁶ /inch) After Load Duration Given Below				
	0.1 sec.	1 sec.	10 sec.	100 sec.	1000 sec.
AC-20	27.0	98.0	141.1	336	716.6
AC-5 + 15% Carbon Black	19.5	101.6	281.4	519.3	834.4
AC-5 + 5% Latex	93.8	159.0	562.0	656.0	1480.0
AC-5 + 5% Kraton	*	28.9	139.0	295.0	722.5
AC-5 + 5% Elvax	26.6	66.6	95.4	228.0	504.0
AC-5 + 5% Novophalt	*	*	54.7	142.8	375.0

*Deformation too small to measure.

Table F6. Average permanent strain from the incremental static compression test at 100°F. All tests at 10 psi applied stress except for latex, which was tested at 5 psi. Results of only one test each for AC-20 and carbon black are shown.

Sample ID	Permanent Strain (inch x 10 ⁻⁶ /inch) After Load Duration Given Below				
	0.1 sec.	1 sec.	10 sec.	100 sec.	1000 sec.
AC-20	65.6	209.0	419.0	809.0	2260.0
AC-5 + 15% Carbon Black	28.1	37.5	156.0	334.0	766.0
AC-5 + 5% Latex	120.0	275.0	628.0	1415.0	2980.0
AC-5 + 5% Kraton	84.4	178.5	334.0	630.0	1570.0
AC-5 + 5% Elvax	110.5	185.0	352.5	515.0	1140.0
AC-5 + 5% Novophalt	69.5	140.0	265.0	425.0	890.0

Table F7. Average permanent strain from the incremental static test at 70°F after specimens were subjected to one cycle Lottman moisture conditioning. All tests at 20 psi applied stress.

Sample ID	Permanent Strain (inch x 10 ⁻⁶ /inch) After Load Duration Given Below				
	0.1 sec.	1 sec.	10 sec.	100 sec.	1000 sec.
AC-20	5.47	58.55	154.0	325.0	899.0
AC-5 + 15% Carbon Black	5.00	131.50	274.0	443.5	851.50
AC-5 + 5% Latex	25.55	82.80	229.50	523.50	1300.0
AC-5 + 5% Kraton	*	31.30	127.50	330.0	959.5
AC-5 + 5% Elvax	12.50	51.60	152.50	290.0	516.5
AC-5 + 5% Novophalt	*	10.18	61.75	184.50	533.0

*Deformation too small to measure.

Table F8. Average permanent strain from the incremental static test at 70°F after specimens were heat aged at 140°F for 7 days. All tests at 20 psi.

Sample ID	Permanent Strain (inch x 10 ⁻⁶ /inch) After Load Duration Given Below				
	0.1 sec.	1 sec.	10 sec.	100 sec.	1000 sec.
AC-20	*	5.47	49.70	138.0	249.5
AC-5 + 15% Carbon Black	*	4.68	57.80	140.0	326.5
AC-5 + 5% Latex	7.82	57.80	187.50	453.0	1211.5
AC-5 + 5% Kraton	6.25	31.25	108.0	228.0	424.0
AC-5 + 5% Elvax	1.88	17.65	54.4	117.0	211.0
AC-5 + 5% Novophalt	*	34.35	128.8	269.5	501.50

*Deformation too small to measure.

Table F9. Average permanent strain from the incremental static test at 70°F (California Valley asphalt).

Sample ID	Permanent Strain (inch x 10 ⁻⁶ inch) After Load Duration Given Below**				
	0.1 sec.	1 sec.	10 sec.	100 sec.	1000 sec.
AR-4000	*	10.9	188	437.5	1064.5
AR-1000 + 15% Carbon Black	8.6	89.1	224	407.5	731.5
AR-1000 + 5% Latex	7.8	104	368	826.5	1810
AR-1000 + 5% Kraton	43.8	189	438	797	1770
AR-1000 + 5% Elvax	37.5	138	328	788	2190
AR-1000 + 5% Novophalt	15.6	129.8	357	740.5	1390
AR-1000 + 5% Novophalt	*	51.6	282.5	720	1955

* Additives blended with AC-5

** All samples run at 20 psi except Elvax @ 15 psi

Table F10. Average accumulated strain for repeated load tests at 70°F
(California Valley asphalt).

Sample ID	Accumulated Strain After Number of Repetitive Cycles (Average) ($\times 10^{-6}$) For Number of Cycles Given Below					
	1	10	100	200	1000	10,000
AR-4000	4.69	25.8	108.5	141.9	195.5	282.5
AR-1000 + 15% + Carbon Black	19.55	102.30	188.5	209.5	2545.5	407.0
AR-1000 + 5% + Latex	15.6	93.5	220.5	262.5	399.0	967
AR-1000 + 5% + Kraton	31.2	131.0	253.0	294.0	450.0	912.0
AR-1000 + 5% + Elvax	17.95	70.25	153.35	179.1	--	333.5
AR-1000 + 5% + Novophalt	9.38	56.2	156	180	212	244

*All samples run at 20 psi except Elvax @ 15 psi

Table F11. GNU μ values for hot climate VESYS analysis.

Temperature °F	Values of GNU (μ)						
	AC-20	Carbon Black	Latex		Kraton	Elvax	Novophalt
41	0.09	0.04	0.03	0.05	0.04	0.09	0.04
43	0.12	0.06	0.05	0.11	0.05	0.10	0.05
45	0.14	0.09	0.07	0.17	0.06	0.12	0.06
60	0.32	0.28	0.20	0.62	0.16	0.22	0.12
75	0.45	0.41	0.29	0.92	0.23	0.29	0.17
87	0.45	0.41	0.29	0.92	0.23	0.29	0.17
93	0.45	0.41	0.29	0.92	0.23	0.29	0.17
95	0.45	0.41	0.29	0.92	0.23	0.29	0.17
91	0.45	0.41	0.29	0.92	0.23	0.29	0.17
87	0.45	0.41	0.29	0.92	0.23	0.29	0.17
64	0.38	0.33	0.22	0.74	0.19	0.25	0.14
59	0.31	0.27	0.19	0.59	0.16	0.21	0.12

Table F12. Alpha values for hot climate VESYS analysis.

Temperature °F	Values of Alpha						
	AC-20	Carbon Black	Latex		Kraton	Elvax	Novophalt
41	0.35	0.27	0.20	0.21	0.34	0.47	0.35
43	0.37	0.30	0.24	0.24	0.36	0.48	0.36
45	0.40	0.33	0.26	0.28	0.38	0.49	0.38
60	0.56	0.55	0.49	0.54	0.52	0.60	0.50
75	0.67	0.70	0.64	0.71	0.61	0.67	0.58
87	0.67	0.70	0.64	0.71	0.61	0.67	0.58
93	0.67	0.70	0.64	0.71	0.61	0.67	0.58
95	0.67	0.70	0.64	0.71	0.61	0.67	0.58
91	0.67	0.70	0.64	0.71	0.61	0.67	0.58
87	0.67	0.70	0.64	0.71	0.61	0.67	0.58
64	0.61	0.61	0.55	0.61	0.55	0.63	0.53
59	0.55	0.54	0.47	0.52	0.51	0.59	0.49

Table F13. GNU μ values for cool climate VESYS analysis.

Temperature °F	Values of GNU (μ)						
	AC-20	Carbon Black	Latex	Kraton	Elvax	Novophalt	
10	0.08	0.02	0.03	0.03	0.03	0.08	0.03
13	0.08	0.02	0.03	0.03	0.03	0.08	0.03
16	0.08	0.02	0.03	0.03	0.03	0.08	0.03
35	0.08	0.02	0.03	0.03	0.03	0.08	0.03
50	0.20	0.15	0.11	0.32	0.10	0.15	0.08
56	0.28	0.23	0.46	0.50	0.14	0.19	0.11
63	0.36	0.32	0.23	0.71	0.18	0.24	0.14
65	0.39	0.35	0.24	0.77	0.20	0.25	0.14
61	0.34	0.29	0.21	0.65	0.17	0.23	0.13
57	0.29	0.24	0.17	0.53	0.14	0.20	0.11
34	0.08	0.02	0.03	0.03	0.03	0.08	0.03
22	0.08	0.02	0.03	0.03	0.03	0.08	0.03

Table F14. Alpha values for cold climate VESYS analysis.

Temperature °F	Values of Alpha						
	AC-20	Carbon Black	Latex		Kraton	Elvax	Novophalt
10	0.34	0.26	0.19	0.19	0.33	0.46	0.34
13	0.34	0.26	0.19	0.19	0.33	0.46	0.34
16	0.34	0.26	0.19	0.19	0.33	0.46	0.34
35	0.34	0.26	0.19	0.19	0.33	0.46	0.34
50	0.45	0.41	0.34	0.36	0.42	0.53	0.42
56	0.52	0.49	0.43	0.46	0.48	0.57	0.47
63	0.59	0.60	0.53	0.59	0.54	0.62	0.52
65	0.62	0.63	0.56	0.62	0.56	0.64	0.54
61	0.57	0.57	0.50	0.55	0.53	0.61	0.51
57	0.53	0.51	0.44	0.48	0.49	0.58	0.48
34	0.34	0.26	0.19	0.19	0.33	0.46	0.34
22	0.34	0.26	0.19	0.19	0.33	0.46	0.34

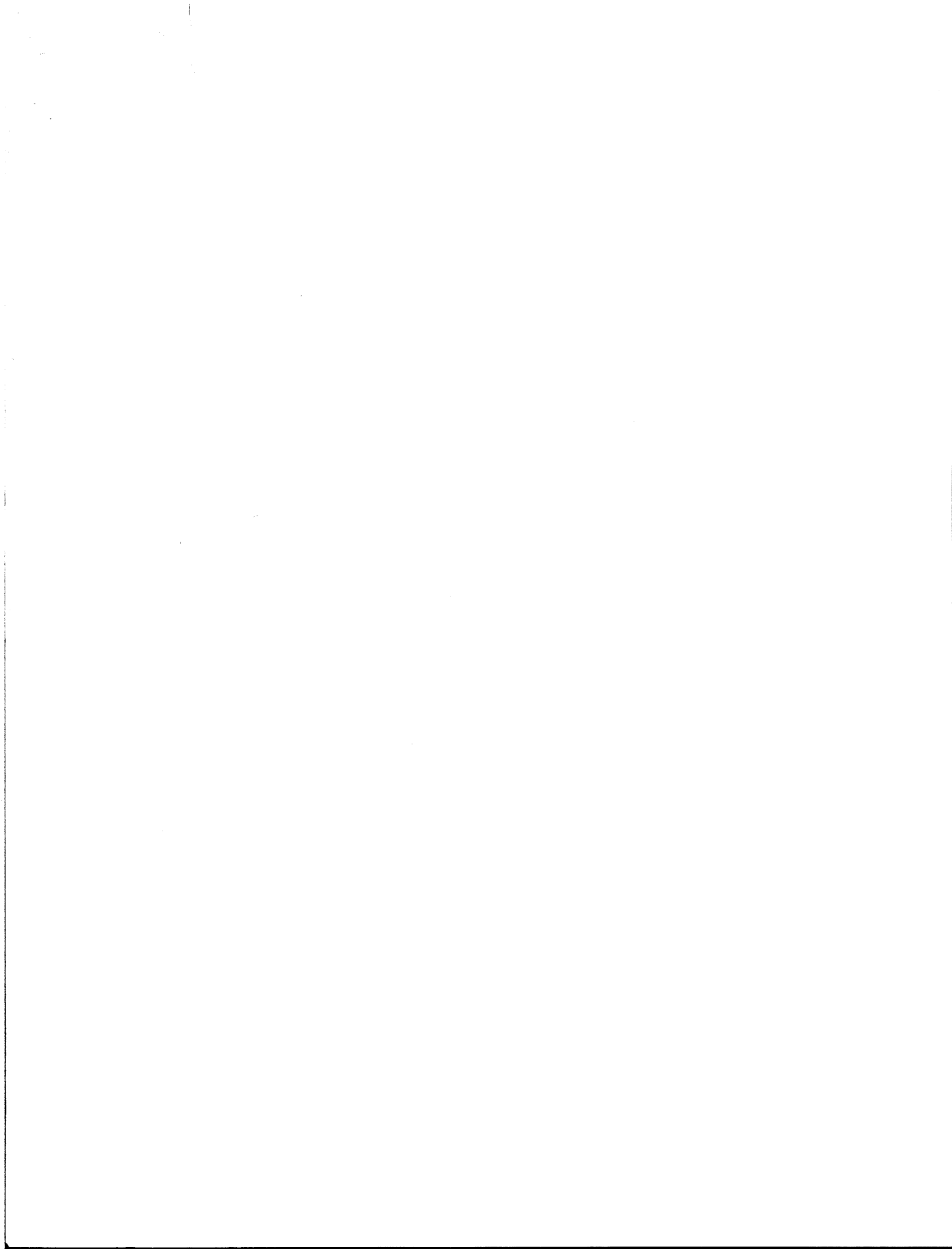
APPENDIX G: RESILIENT MODULUS DATA

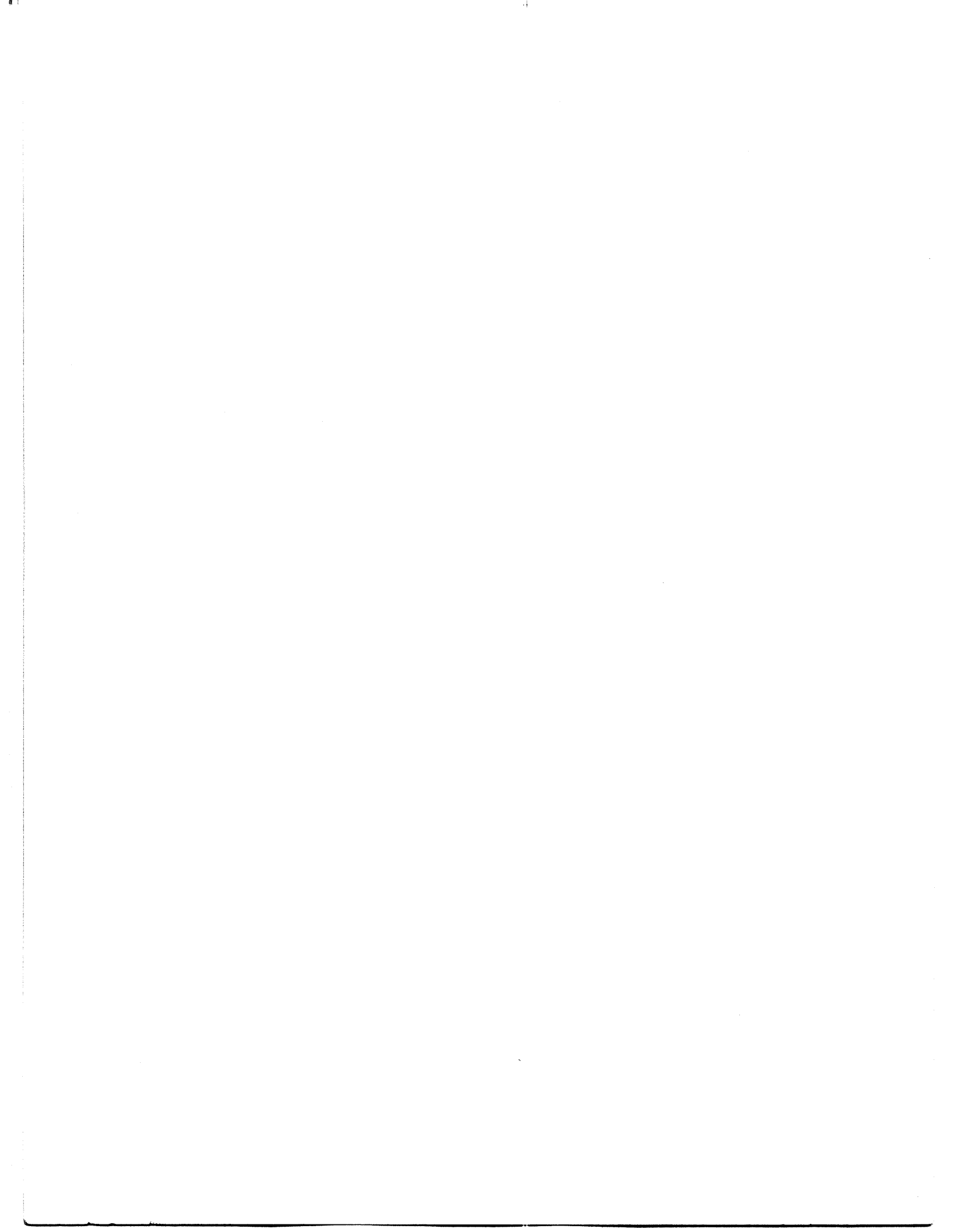
Table G1. Resilient moduli in psi for cool climate VESYS analysis.

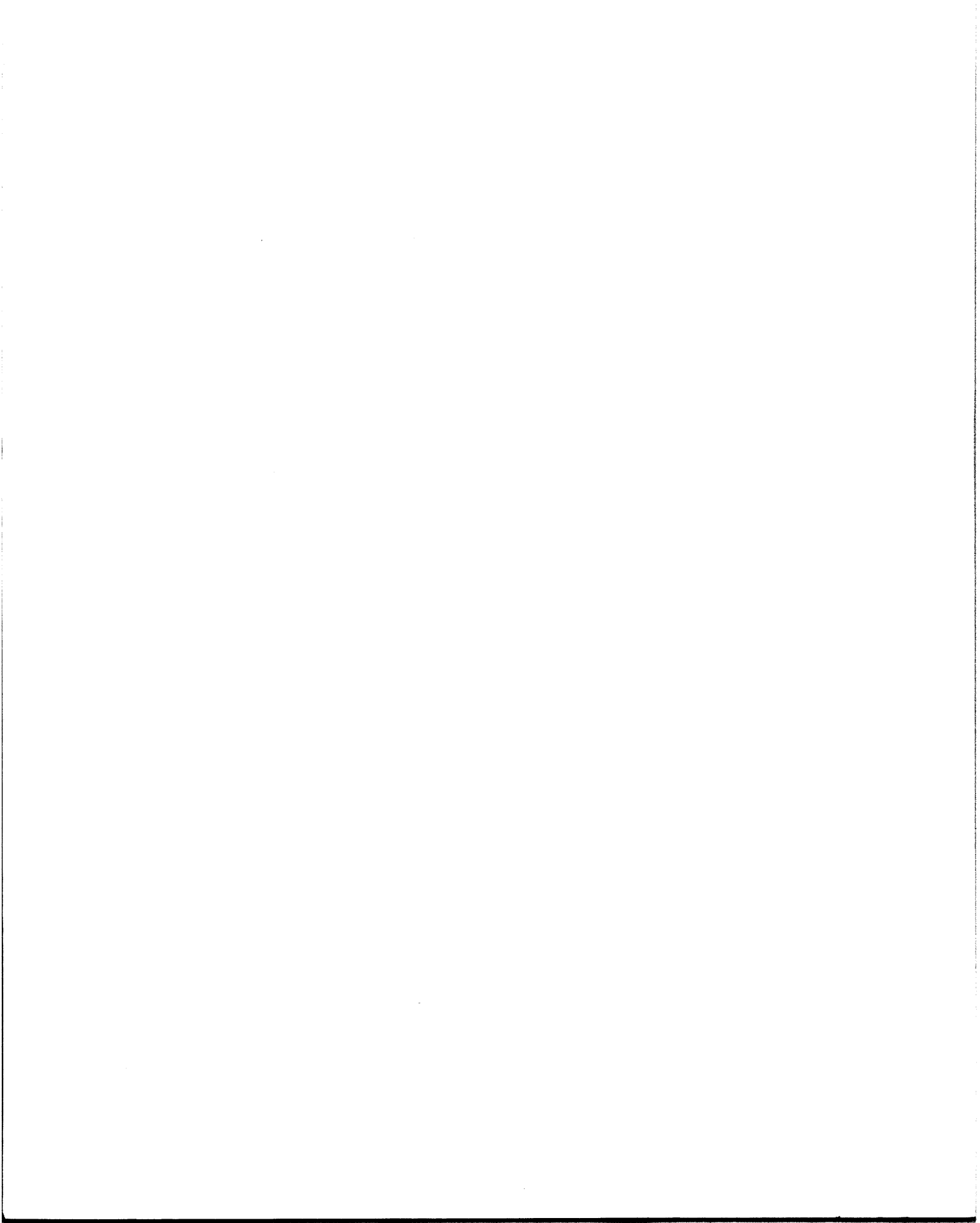
Temperature, °F	Resilient Modulus, psi					
	AC-20	AC-5 & Carbon Black	AC-5 & Latex	AC-5 & Kraton	AC-5 & Elvax	AC-5 & Novophalt
10	6,109,000	2,541,000	1,958,000	2,134,000	3,431,000	3,378,000
13	6,109,000	2,541,000	1,958,000	2,134,000	3,431,000	3,378,000
16	6,109,000	2,541,000	1,958,000	2,134,000	3,431,000	3,378,000
35	6,109,000	2,541,000	1,958,000	2,134,000	3,431,000	3,378,000
50	2,700,000	1,330,000	1,110,000	1,480,000	2,200,000	2,330,000
56	1,800,000	950,000	790,000	1,140,000	1,630,000	1,840,000
63	1,150,000	660,000	522,000	830,000	1,130,000	1,350,000
65	1,000,000	600,000	470,000	750,000	1,000,000	1,250,000
61	1,300,000	730,000	590,000	910,000	1,250,000	1,480,000
57	1,680,000	900,000	740,000	1,080,000	1,550,000	1,780,000
34	6,109,000	2,451,000	1,958,000	2,134,000	3,431,000	3,378,000
22	6,109,000	2,541,000	1,958,000	2,134,000	3,431,000	3,378,000

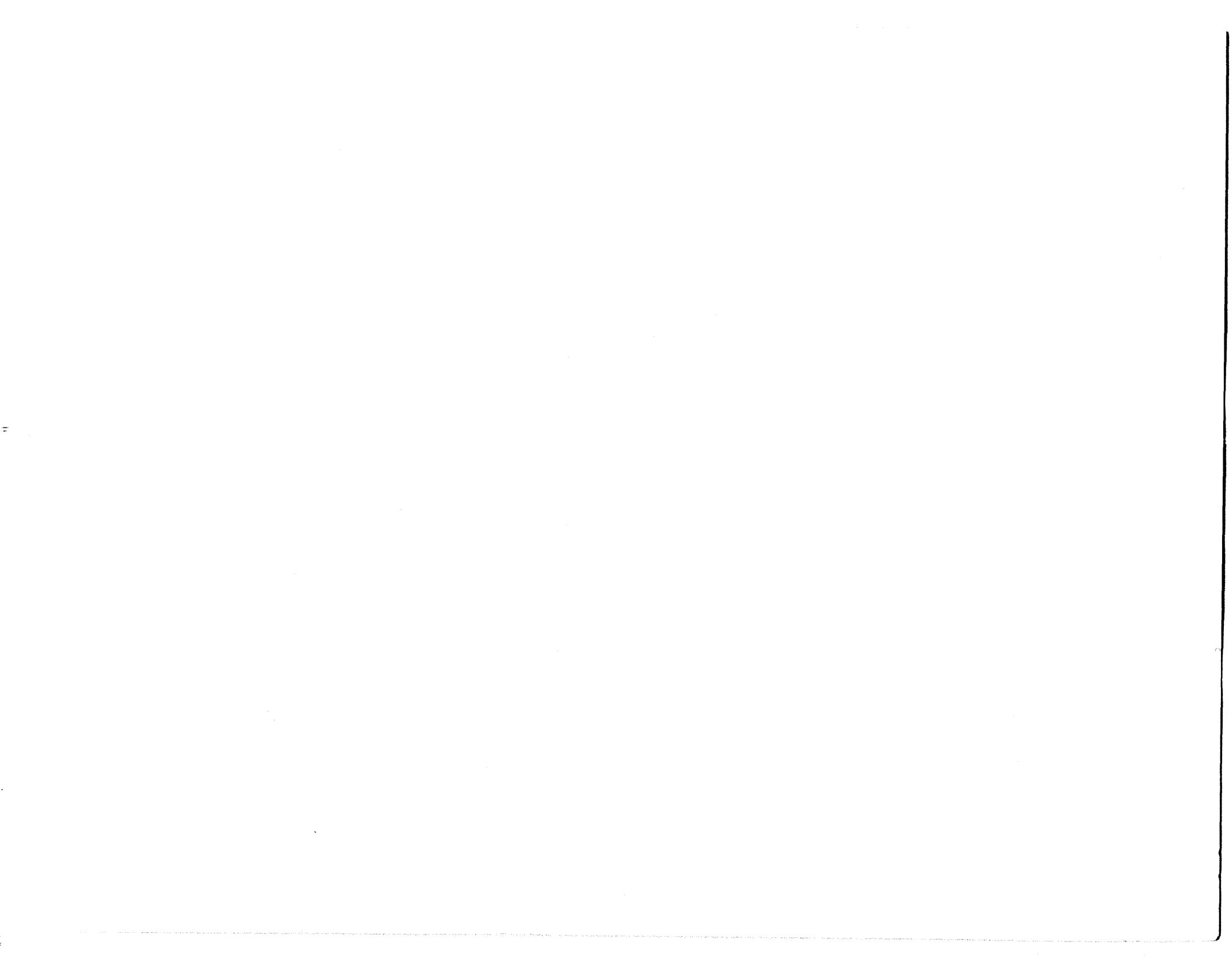
Table G2. M_R (psi) values for hot climate VESYS analysis.

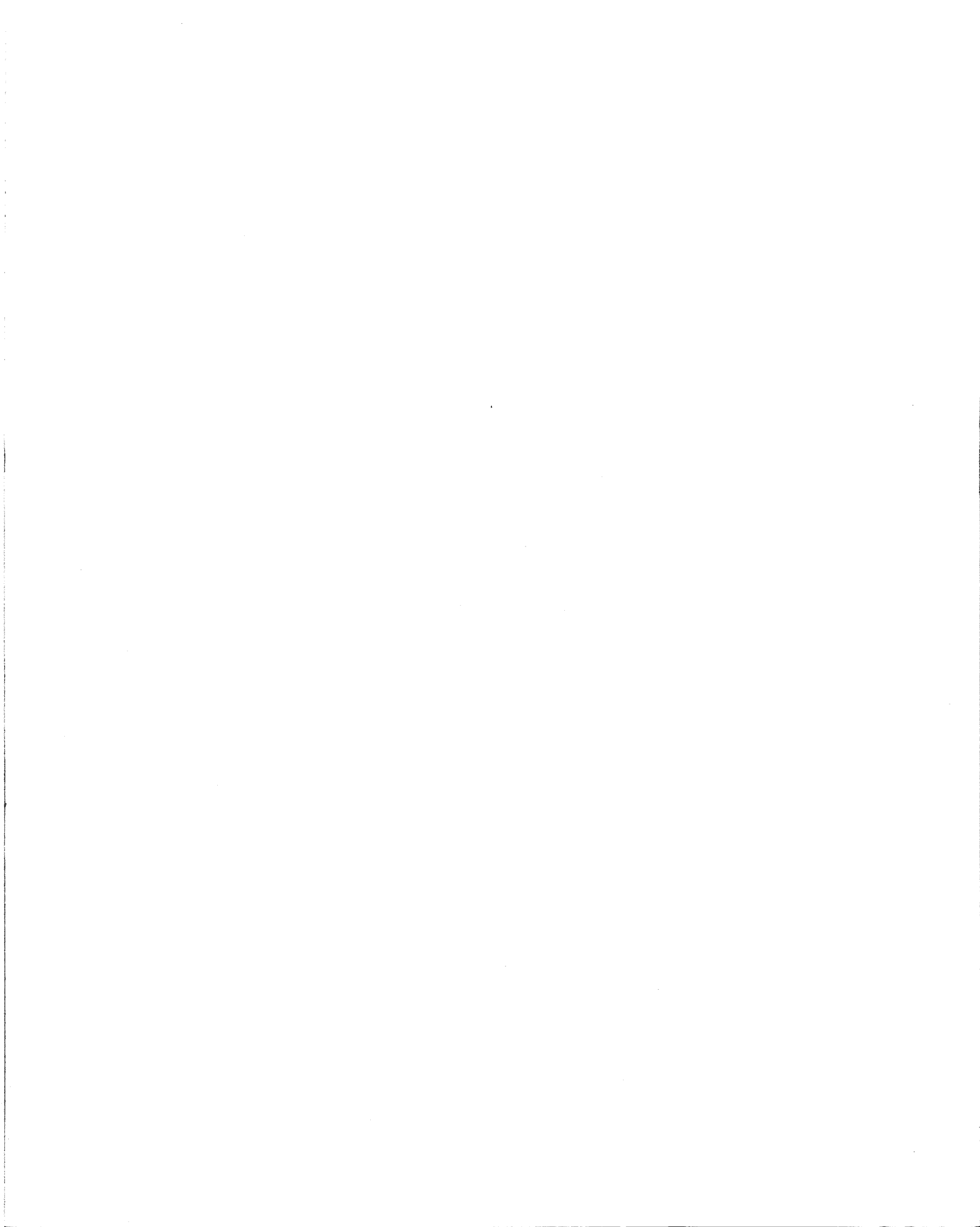
Temperature °F	Values of M_R (psi)					
	AC-20	AC-5 + Carbon Black	AC-5 + Latex	AC-5 + Kraton	AC-5 + Elvax	AC-5 + Novophalt
41	5,500,000	2,350,000	1,850,000	2,050,000	3,250,000	3,250,000
43	4,700,000	2,050,000	1,650,000	1,900,000	3,000,000	3,000,000
45	3,900,000	1,800,000	1,470,000	1,780,000	2,720,000	2,800,000
60	1,390,000	770,000	630,000	950,000	1,320,000	1,550,000
75	600,000	390,000	262,000	470,000	570,000	800,000
87	370,000	253,000	130,000	261,000	270,000	460,000
93	310,000	215,000	93,000	188,000	172,000	342,000
95	295,000	207,000	82,000	165,000	145,000	310,000
91	330,000	228,000	105,000	210,000	205,000	380,000
87	370,000	253,000	131,000	261,000	270,000	460,000
64	1,090,000	630,000	500,000	790,000	1,080,000	1,300,000
59	1,450,000	810,000	660,000	1,000,000	1,400,000	1,610,000











FEDERALLY COORDINATED PROGRAM (FCP) OF HIGHWAY RESEARCH, DEVELOPMENT, AND TECHNOLOGY

The Offices of Research, Development, and Technology (RD&T) of the Federal Highway Administration (FHWA) are responsible for a broad research, development, and technology transfer program. This program is accomplished using numerous methods of funding and management. The efforts include work done in-house by RD&T staff, contracts using administrative funds, and a Federal-aid program conducted by or through State highway or transportation agencies, which include the Highway Planning and Research (HP&R) program, the National Cooperative Highway Research Program (NCHRP) managed by the Transportation Research Board, and the one-half of one percent training program conducted by the National Highway Institute.

The FCP is a carefully selected group of projects, separated into broad categories, formulated to use research, development, and technology transfer resources to obtain solutions to urgent national highway problems.

The diagonal double stripe on the cover of this report represents a highway. It is color-coded to identify the FCP category to which the report's subject pertains. A red stripe indicates category 1, dark blue for category 2, light blue for category 3, brown for category 4, gray for category 5, and green for category 9.

FCP Category Descriptions

1. Highway Design and Operation for Safety

Safety RD&T addresses problems associated with the responsibilities of the FHWA under the Highway Safety Act. It includes investigation of appropriate design standards, roadside hardware, traffic control devices, and collection or analysis of physical and scientific data for the formulation of improved safety regulations to better protect all motorists, bicycles, and pedestrians.

2. Traffic Control and Management

Traffic RD&T is concerned with increasing the operational efficiency of existing highways by advancing technology and balancing the demand-capacity relationship through traffic management techniques such as bus and carpool preferential treatment, coordinated signal timing, motorist information, and rerouting of traffic.

3. Highway Operations

This category addresses preserving the Nation's highways, natural resources, and community attributes. It includes activities in physical

maintenance, traffic services for maintenance zoning, management of human resources and equipment, and identification of highway elements that affect the quality of the human environment. The goals of projects within this category are to maximize operational efficiency and safety to the traveling public while conserving resources and reducing adverse highway and traffic impacts through protections and enhancement of environmental features.

4. Pavement Design, Construction, and Management

Pavement RD&T is concerned with pavement design and rehabilitation methods and procedures, construction technology, recycled highway materials, improved pavement binders, and improved pavement management. The goals will emphasize improvements to highway performance over the network's life cycle, thus extending maintenance-free operation and maximizing benefits. Specific areas of effort will include material characterizations, pavement damage predictions, methods to minimize local pavement defects, quality control specifications, long-term pavement monitoring, and life cycle cost analyses.

5. Structural Design and Hydraulics

Structural RD&T is concerned with furthering the latest technological advances in structural and hydraulic designs, fabrication processes, and construction techniques to provide safe, efficient highway structures at reasonable costs. This category deals with bridge superstructures, earth structures, foundations, culverts, river mechanics, and hydraulics. In addition, it includes material aspects of structures (metal and concrete) along with their protection from corrosive or degrading environments.

9. RD&T Management and Coordination

Activities in this category include fundamental work for new concepts and system characterization before the investigation reaches a point where it is incorporated within other categories of the FCP. Concepts on the feasibility of new technology for highway safety are included in this category. RD&T reports not within other FCP projects will be published as Category 9 projects.

